CHARACTERIZATION AND IDENTIFICATION OF A

GALACTURONOSYLTRANSFERASE INVOLVED IN PECTIN BIOSYNTHESIS

by

JASON DWIGHT STERLING

(Under the Direction of Debra Mohnen)

ABSTRACT

Pectins are a class of acidic, plant cell wall polysaccharides that contain (1,4)-linked α-D-galactopyranosyluronic acid (D-Gal*p*A) as part of their backbone structure. Pectin is involved in the regulation of plant growth and development, the elucidation of plant defense responses, and the maintenance of plant cell adhesion. While a significant amount of published information is available on the structure and function of pectin in the plant cell wall, relatively little is known about pectin biosynthesis. This study centers around the characterization and identification of an α-1,4-galacturonosyltransferase (GalAT) involved in the biosynthesis of the backbone structures of pectin. The subcellular localization of a GalAT was determined by sucrose density gradient centrifugation of pea epicotyl membranes. GalAT activity was found to co-fractionate with Golgi-resident latent UDPase activity. Treatment of Golgi vesicles with Proteinase K in the absence of detergent showed that intact Golgi membranes from pea protected GalAT activity from proteolytic degradation. These results show that pectin biosynthesis occurs in the Golgi apparatus and that the pea GalAT has its catalytic site facing the Golgi lumen. A radioactive assay was developed to assay GalAT activity. The assay uses cetylpyridinium chloride-treated filters to separate unincorporated UDP-D-[^{14}C]Gal*p*A from radioactive products formed during the GalAT reaction. The versatility of this assay was demonstrated by its ability to rapidly and

accurately measure GalAT activity in multiple chromatography fractions during the partial purification of a GalAT from tobacco (*Nicotiana tabacum* L. cv. Samsun) and *Arabidopsis thaliana* (cv. Columbia). Using a new detergent solubilization technique and a combination of SP-Sepharose, Reactive Yellow 3, and UDP-agarose chromatography, GalAT activity was purified 17-fold from solubilized Arabidopsis membranes. The partially purified fraction was digested with sequencing-grade trypsin and the released peptides were analyzed by liquid chromatography-tandem mass spectrometry. Peptide analysis revealed the presence of two proteins (JS33 and JS36) with sequence similarity to other glycosyltransferases. Truncated versions of these genes lacking their N-terminal transmembrane domain were cloned into a vector containing an N-terminal signal sequence designed for secretion of the recombinant proteins. Both gene constructs were transiently and stably expressed in human embryonic kidney (HEK) 293 cells. Preliminary transient transfection experiments indicated that GalAT activity was detectable in media from HEK293 cells transiently expressing the JS36 gene construct providing evidence that JS36 encoded a putative GalAT. Inactive, recombinant proteins were detected in cell lysates from stable HEK293 lines expressing either JS33 or JS36. Database analysis indicates that JS33 and JS36 are part of a 25 member gene family in Arabidopsis. Mutation of two members of this putative GalAT gene family gives phenotypes that are similar to previously characterized pectin mutants. Further research needs to be conducted to determine what role(s) these genes play in pectin biosynthesis.

INDEX WORDS: Galacturonosyltransferase, pectin, glycosyltransferase, Golgi apparatus, *Arabidopsis thaliana*, *Pisum sativum*, galacturonic acid, assay, cetylpyridinium chloride, plant cell wall, heterologous expression,

multiple antigenic peptide, sucrose gradient, biosynthesis, CAZy family 8, gene family.

CHARACTERIZATION AND IDENTIFICATION OF A GALACTURONOSYLTRANSFERASE INVOLVED IN PECTIN BIOSYNTHESIS

by

JASON DWIGHT STERLING

B.S., McGill University, Canada, 1996

A Dissertation Submitted to the Graduate Faculty of The University of Georgia in Partial Fulfillment of the Requirements for the Degree

DOCTOR OF PHILOSOPHY

ATHENS, GEORGIA

2004

CHARACTERIZATION AND IDENTIFICATION OF A GALACTURONOSYLTRANSFERASE INVOLVED IN PECTIN BIOSYNTHESIS

by

JASON DWIGHT STERLING

Major Professor: Debra Mohnen

Committee: Alan Darvill
Russell Malmberg
Kelley Moremen
Michael Pierce

Electronic Version Approved:

Maureen Grasso
Dean of the Graduate School
The University of Georgia
December 2004

DEDICATION

I dedicate this dissertation to my family (Suzanne, Tyrone, and T-man), the most important thing in my life. I would not have been able to do it without you.

ACKNOWLEDGEMENTS

I would like to thank Dr. Debra Mohnen for her guidance and support throughout my graduate school career and for the being the best mentor a graduate student could ever have. I would also like to thank Dr. Kelley Moremen, Dr. Michael Pierce, Dr. Alan Darvill, Dr. Russell Malmberg, and Dr. Carl Bergmann for being great committee members, for providing guidance when I had questions about my research and for never letting me settle for "I don't know".

I am extremely grateful to all the members of the Mohnen lab, past and present, that made lab life so much fun over the years. I also thank all of the undergraduate students that have ever worked with me on my graduate research.

I would like to thank Dr. Malcolm O'Neill for generously providing the figures on pectin structure used in Chapter 1. I would also like to thank Dr. Debra Mohnen for providing some of the tables used in the Biosynthesis section of Chapter 1.

The research presented in the thesis would not have been possible without materials generously provided by members of the CCRC, including Stefan Eberhard (for providing the initial Arabidopsis tissue cultures), Dr. Carl Bergmann (Chapter 2), Dr. Maor Bar-Peled (Chapter 4), Dr. Kelley Moremen (Chapter 4), and Dr. Michael Pierce (Chapter 4).

The research presented in Chapter 2 was conducted with the assistance of Lorena Norambuena from the University of Chile, Santiago, Chile. We also thank Dr. Malcolm O'Neill for the critical reading of Chapter 2.

The research presented in Chapter 4 would not have been possible without the guidance of April Harper, Leslie Stanton, Intaek Lee, Dr. Steve Mast, Dr. Alison Vandersall-Nairn, and Dr. Michael Hahn.

TABLE OF CONTENTS

Page

ACKNOWLEDGEMENTS v

INTRODUCTION 1

CHAPTER

1 LITERATURE REVIEW: PECTIN STRUCTURE, FUNCTION, AND BIOSYNTHESIS 4

Introduction 5

Structure 6

Pectin in the Primary Wall 21

Pectin Function 36

Biosynthesis 42

Conclusions and Relevance 109

2 THE CATALYTIC SITE OF THE PECTIN BIOSYNTHETIC ENZYME α-(1,4)-GALACTURONOSYLTRANSFERASE (GALAT) IS LOCATED IN THE LUMEN OF THE GOLGI 112

Abstract 113

Introduction 114

Materials and Methods 115

Results 122

Discussion 139

3 DEVELOPMENT OF A FILTER ASSAY FOR MEASURING HOMOGALACTURONAN:α-(1,4)-GALACTURONOSYLTRANSFERASE ACTIVITY 145

Abstract 146

Introduction 147

Materials and Methods 149

Results 153

Discussion 159

4 IDENTIFICATION AND HETEROLOGOUS EXPRESSION OF TWO PROPOSED GALACTURONOSYLTRANSFERASES FROM *ARABIDOPSIS THALIANA* .161

Abstract 162

Introduction 164

Materials and Methods 165

Results 177

Discussion 220

CONCLUSION 229

REFERENCES 231

INTRODUCTION

All plant cells are surrounded by a complex extracellular matrix known as the plant cell wall. The plant cell wall defines overall cell shape and provides each cell with mechanical strength and a protective barrier against environmental hazards. The cell wall is the first line of defense against pathogen attack and is a repository for a variety of biologically active molecules involved in plant cell signaling. The plant cell wall also has nutritive value and is the main source of dietary fiber found in plant-based foods.

Structural analysis of plant cell walls indicates that they can be subdivided into two types: primary and secondary cell walls. The secondary cell wall surrounds cells that differentiate to perform specialized structural support functions within the plant and generally contain lignin. In contrast, the primary cell wall surrounds cells in elongating, meristematic and succulent regions of the plant, and is the first type of wall laid down by all plant cells.

The primary cell wall is mainly composed of polysaccharides (~90%) and these polysaccharides have been divided into three main types: cellulose, hemicelluloses, and pectin. An in-depth review on what is currently known about pectin structure, function and biosynthesis is presented in Chapter 1. In brief, pectins are a diverse group of acidic polysaccharides found almost exclusively in plant primary walls. They comprise between 10-30% of the primary walls of plants, and are involved in the regulation of plant cell growth and development, the elicitation of plant defense responses, and the maintenance of cell-cell adhesion. Furthermore, pectins are used extensively in the food and cosmetic industries as a gelling and stabilizing agent, and as a dietary supplement to aid in the prevention of high cholesterol and cancer. While much is known about pectin structure and function within the plant, relatively little is known about how

plant cells make pectin, including the site(s) of synthesis and the plant genes that encode pectin biosynthetic enzymes.

Research presented in this dissertation is aimed at increasing our understanding of how pectin is synthesized. The research centers around a pectin glycosyltransferase known as α-1,4-galacturonosyltransferase (GalAT). GalATs are involved in the synthesis of approximately 70% of the backbone structures of pectin. They catalyze the addition of D-Gal*p*A from UDP-D-Gal*p*A onto the non-reducing ends of oligomeric or polymeric pectin acceptors. The first study was aimed at determining the site of pectin biosynthesis within the plant cell. The subcellular location of a homogalacturonan GalAT from pea epicotyl membranes was determined by sucrose density gradient centrifugation (Chapter 2).

The results from this study indicate that the pea GalAT is a Golgi-localized enzyme that has its catalytic site facing the Golgi lumen. These results extend previous *in vivo* labeling and immunocytochemical studies (using antibodies against pectin epitopes) by demonstrating that a pectin biosynthetic glycosyltransferase functions in the Golgi lumen. The study also implicates the Golgi as the initial site of pectin biosynthesis and allows us to design a model for pectin biosynthesis *in vivo*.

The second study was aimed at identifying putative GalAT genes from thale cress (*Arabidopsis thaliana*). GalAT activity was partially purified from solubilized Arabidopsis membranes with the aid of a newly developed GalAT activity assay presented in Chapter 3. This assay uses filters coated with cetylpyridinium chloride to separate unincorporated UDP-D-[^{14}C]Gal*p*A from radioactive products generated during the GalAT reaction. The assay also greatly simplifies the process of identifying GalAT activity in multiple chromatography fractions.

Detergent-solubilized GalAT activity was purified 17-fold using a combination of SP-Sepharose, Reactive Yellow 3, and UDP-agarose chromatography (Chapter 4). Trypsin digestion of the most purified GalAT-containing fraction yielded peptides that were analyzed by liquid chromatography-tandem mass spectrometry. Two proteins (JS33 and JS36) were identified that had conserved domains found in other glycosyltransferases. Truncated versions of these genes lacking their N-terminal transmembrane domain were cloned into a vector containing an N-terminal signal sequence (for secretion of the recombinant proteins) and heterologously expressed in human embryonic kidney (HEK) 293 cells. JS36 was shown to possess GalAT activity in media from HEK293 cells in a preliminary transient transfection experiment, providing further evidence for the identification of a putative GalAT gene from Arabidopsis.

In addition, BLAST analysis of the Arabidopsis genome reveal that JS33 and JS36 are part of a 25 member gene family in Arabidopsis. Mutants in two members of the gene family (*qua1* and *parvus*) display phenotypes consistent with those observed in other pectin structure mutant plants. Future experiments aimed at determining the function of JS33 and JS36, and their role in pectin biosynthesis, are also discussed.

CHAPTER 1

LITERATURE REVIEW: PECTIN STRUCTURE, FUNCTION, AND BIOSYNTHESIS

INTRODUCTION

All plant cells are surrounded by an extracellular matrix known as the plant cell wall (Bacic et al., 1988; Brett and Waldron, 1990). Cell walls are divided into two types based on their structure and the developmental state of the cell. The primary cell wall is the first type of wall that is laid down by all plant cells. It surrounds meristematic, undifferentiated cells and cells of succulent tissues of the plant (McNeil et al., 1984; Albersheim et al., 1996). Plant cells that undergo further differentiation may also produce a secondary wall (Bacic et al., 1988). Secondary cell wall formation is most commonly associated with lignin deposition during xylem differentiation (Fukuda, 1996; Mellerowicz et al., 2001), but certain cell types, for example cotton fibers, may also lay down a specialized unlignified secondary cell wall (Delmer, 1999).

The primary cell wall is composed almost entirely of polysaccharides (90%; McNeil et al., 1984). These polysaccharides have been classified into three major categories: cellulose, hemicelluloses, and pectins (Bacic et al., 1988). Pectins are a class of plant cell wall polysaccharides that contain (1,4)-linked α-D-galactopyranosyluronic acid (D-Gal*p*A) as part of their backbone structure (O'Neill et al., 1990). They are a major component (~30%) of the primary walls of dicots, non-graminaceous monocots and gymnosperms (type I primary walls) and are present in lesser amounts (~10%) in the primary walls of plants of the grass or *Poaceae* family (type II primary walls; Carpita and Gibeaut, 1993; Mohnen, 1999). Pectic polysaccharides have also been detected in lycophyte, pteridophyte, and (to a lesser extent) bryophyte cell walls (Matsunaga et al., 2004), suggesting that they have persisted throughout plant evolution (O'Neill et al., 2004). Studies conducted on pectin structure, function and biosynthesis have focused on pectins found in primary cell walls due to their natural abundance

and ease of extraction (McNeil et al., 1984; O'Neill et al., 1990; McCann and Roberts, 1991; Carpita and Gibeaut, 1993; Albersheim et al., 1996).

Pectins are the most structurally complex of all the plant cell wall polysaccharides (Mohnen, 2002; O'Neill et al., 2004). The fine structure of pectins has proven to be important to plant homeostasis as slight alterations in pectin structure have been shown to cause severe phenotypes in wildtype and mutant plants (O'Neill et al., 2001; Iwai et al., 2002; Jones et al., 2003). It has been hypothesized that pectin biosynthesis will require the coordinated action of over 100 proteins (Mohnen, 2002). Now, after over 70 years of pectin research, genes thought to be involved in pectin biosynthesis are finally being discovered.

There have been several new developments in pectin research since the last major reviews on pectin were published (Ridley et al., 2001; Mohnen, 2002). This review expands on what is currently known about pectin structure, function, and biosynthesis including progress made on the localization of pectin epitopes within the wall, the characterization of pectin mutants, and the identification of several genes involved in pectin biosynthesis.

STRUCTURE

The structure of pectic polysaccharides has been exhaustively studied (reviewed in O'Neill et al., 1990; Ridley et al., 2001; O'Neill et al., 2004). Pectic polysaccharides can be released from primary cell walls by sequential aqueous buffer extractions (Zablackis et al., 1995; Schols et al., 1995a; Nakamura et al., 2001), acid hydrolysis (Nothnagel et al., 1983; Cardoso et al., 2002), or by treating cell walls with pectinolytic enzymes (McNeil et al., 1980; McNeil et al., 1984; York et al., 1986; Stevenson et al., 1988; O'Neill et al., 1990; Ishii and Matsunaga, 1996). Analysis of pectic polysaccharides released from plant primary cell walls has demonstrated that pectin is composed of three main types of polysaccharides: homogalacturonan (HGA),

rhamnogalacturonan I (RG-I) and substituted galacturonans (SGA) such as rhamnogalacturonan II (RG-II; York et al., 1986; O'Neill et al., 1990). While the elucidation of the composition and linkages of the glycosyl residues that make up pectin has been difficult, techniques involving 2D NMR (Vidal et al., 2000; Rodriguez-Carvajal et al., 2003), mass spectrometry (Ishii et al., 1999; Vidal et al., 2000), molecular modeling (Rodriguez-Carvajal et al., 2003), and the use of well characterized *endo*- and *exo*glycanases (McNeil et al., 1980; Lerouge et al., 1993; An et al., 1994a; Vidal et al., 2000; Ishii et al., 2001a; Nakamura et al., 2002a) have greatly enhanced our understanding of the fine structures of pectin in the wall.

Homogalacturonan

Homogalacturonan (HGA) is a linear polymer of (1,4)-linked α-D-Gal*p*A (Figure 1.1). Cell wall analysis of sycamore (*Acer pseudoplatanus*) suspension-cultured cells (O'Neill et al., 1990; Mohnen et al., 1996) and leaves of *Arabidopsis thaliana* (Zablackis et al., 1995) shows that HGA comprises roughly 24% of the primary wall. The exact size of HGA in the wall is not known, although polymers consisting of 30-200 Gal*p*A residues have been reported (Nothnagel et al., 1983; Carpita and Gibeaut, 1993; Willats et al., 2001). HGA may be methylated at *O*-6 (Mort et al., 1993) and may contain acetyl esters at *O*-2 or *O*-3 (Ishii, 1997; Pauly and Scheller, 2000; Willats et al., 2001a). The degree and pattern of methylation and/or acetylation of HGA chains has not been completely elucidated, possibly due to the heterogeneity of HGA polymers or to changes in methylation/acetylation during the extraction of HGA from the wall (O'Neill et al., 1990; Pauly and Scheller, 2000; Willats et al., 2001a). Studies on HGA fragments released from cell wall residues by Driselase (a commercial mixture of fungal *endo*- and *exo*polysaccharidases; (Brown and Fry, 1993; Ishii, 1997; Needs et al., 1998) and on the

Figure 1.1. Structure of HGA. HGA is a linear polymer of (1,4)-linked α-D-Gal*p*A that may be methylated at *O*-6 or acetylated at *O*-2 or *O*-3. Taken from Ridley et al., (2001).

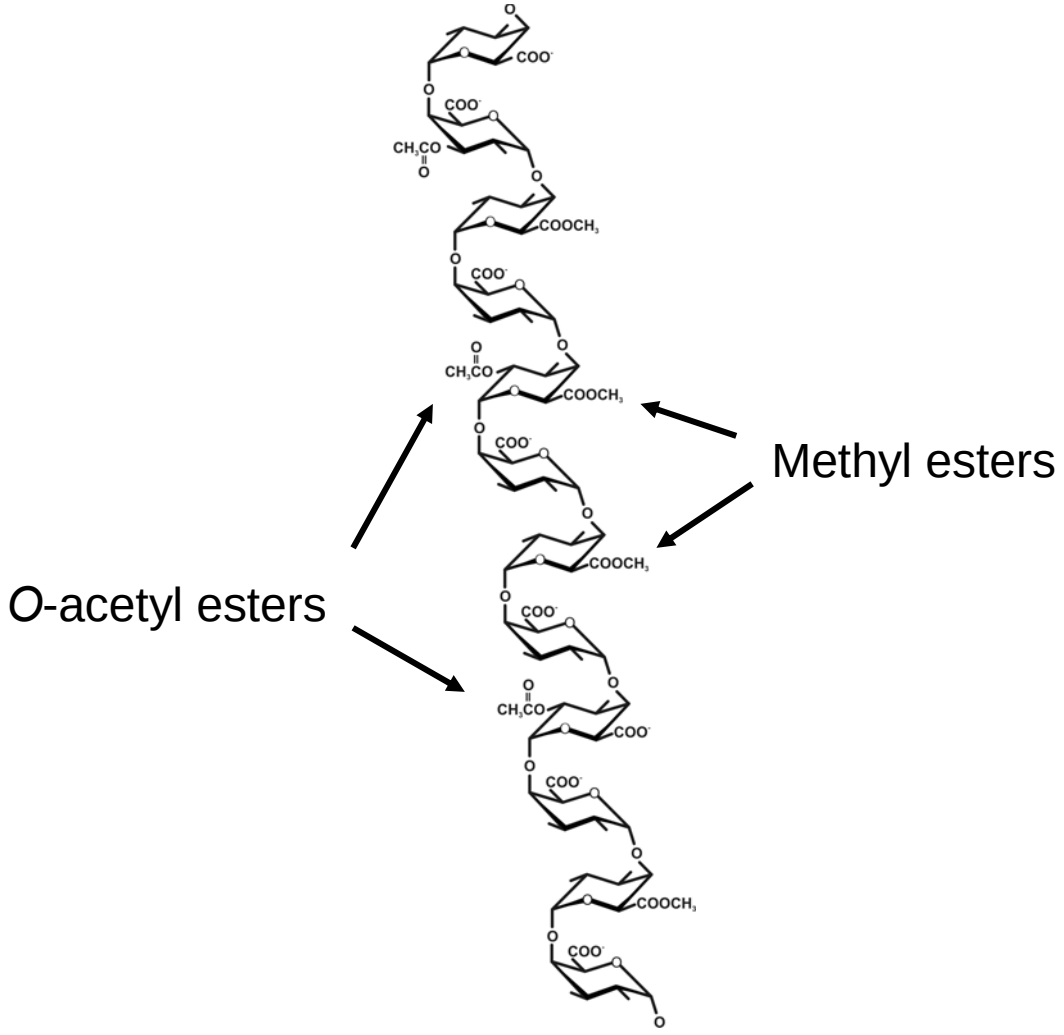

changes in apparent molecular weight of pectins treated with pectinesterases (Lee et al., 2003), suggest that HGA may contain other as yet unidentified esters. Techniques are currently being developed which may enable the determination of methylation and acetylation patterns of HGA (Willats and Knox, 1999a; Clausen et al., 2003; Goubet et al., 2003).

HGA chains can form ionic crosslinks in the presence of Ca^{2+}

Unesterified HGA chains can form ionic crosslinks in the presence of Ca^{2+} (Kohn, 1975; Jarvis, 1984). The properties of Ca^{2+} crosslinked HGA has been extensively studied *in vitro*, as Ca^{2+}-HGA gels are used extensively in the food industry as thickening and stabilizing agents (Thakur et al., 1997). Ca^{2+} crosslinked HGA is also thought to play an important role in plant cell adhesion, as treatment of plant tissues with Ca^{2+} chelating agents solubilizes some of the pectic polysaccharides from the wall and releases individual plant cells (McCann and Roberts, 1991; McCartney and Knox, 2002; Jarvis et al., 2003).

The binding of two Ca^{2+} crosslinked HGA molecules is thought to require HGA chains that have a degree of polymerization of at least 7 Gal*p*A residues (Thakur et al., 1997), with optimal binding occurring between HGA chains that are at least 14 residues in length (Jarvis, 1984). The two chains are thought to form an "egg-box" structure, such as those described for the Ca^{2+}-induced gelation of alginates (Kohn, 1975). Molecular modeling studies suggest that Ca^{2+} crosslinked HGA chains have a 2-fold helical conformation and are likely oriented in an anti-parallel orientation (Braccini et al., 1999; Braccini and Perez, 2001). The specific orientations of Ca^{2+} crosslinked HGA chains within the cell wall are unknown. Studies in this area are further complicated by the fact that highly methylesterified HGA chains can form gels *in vitro* in the presence of high solute concentrations at low pH (Jarvis, 1984; Tibbits et al., 1998). While these conditions may not be suitable for gel formation within the primary wall, the

formation of intermediate gels composed of both highly methylesterified and unesterified HGA chains is possible *in vitro* (Jarvis, 1984). The elucidation of the specific structures of crosslinked HGA chains in the wall will be integral to our understanding of their involvement in plant cell adhesion.

Rhamnogalacturonan I

Rhamnogalacturonan I (RG-I) is a branched polysaccharide that has a repeating disaccharide backbone of [→4)-α-D-Gal*p*A-(1→2)-α-L-rhamnopyranose-(1→] (Figure 1.2; McNeil et al., 1980). The exact length of the backbone of RG-I is not known, but lengths of up to 100 disaccharide repeats have been reported (An et al., 1994; Albersheim et al., 1996). D-Gal*p*A residues in RG-I may be acetylated at either *O*-2 or *O*-3 (McNeil et al., 1980; Lerouge et al., 1993; Ishii, 1997; Pauly and Scheller, 2000); however, the extent and pattern of acetylation is unknown. RG-I comprises between 7-14% of the primary walls of suspension cultured sycamore cells (Mohnen et al., 1996) and 11% of the walls of Arabidopsis leaves (Zablackis et al., 1995).

Rhamnopyranosyl (L-Rha*p*) residues on RG-I may be substituted at *O*-4 with mono- or oligosaccharide chains (McNeil et al., 1984; O'Neill et al., 1990; Mohnen, 1999). The side chains of RG-I have been characterized from Douglas fir (*Pseudotsuga menziesii*; O'Neill et al., 1990), soybean (*Glycine max*; Nakamura et al., 2001), suspension-cultured sycamore (McNeil et al., 1980; Lerouge et al., 1993; An et al., 1994), apple (*Malus x domestica*; Schols et al., 1995), lemon (*Citrus limon*; Ros et al., 1998), olive (*Olea europaea*; Cardoso et al., 2002), maize (*Zea mays*; O'Neill et al., 1990), sugar beet (*Beta vulgaris*; Renard et al., 1999), and Arabidopsis leaves (Zablackis et al., 1995). Results from these studies have shown that there is a substantial amount of heterogeneity concerning the size and abundance of side branching on RG-I isolated

Figure 1.2. Representative structure of RG-I and its side branches. The backbone of RG-I is composed of the disaccharide repeat [→4)-α-D-Gal*p*A-(1→2)-α-L-Rha*p*-(1→]. Representative structures of the most commonly found side branches of RG-I are shown, including A) (1,5)-linked α-L-arabinans, B) branched α-L-arabinans, C) (1,4)-linked β-D-galactans, and D) type I and E) type II arabinogalactans. The location and density of the side chains on RG-I molecules is not known. F) β-D-Glc*p*A is found (1,3)-linked to 2% of the backbone D-Gal*p*A residues from sugar beet walls (Renard et al., 1999). The figure was generously provided by M.A. O'Neill (CCRC) and adapted for this chapter.

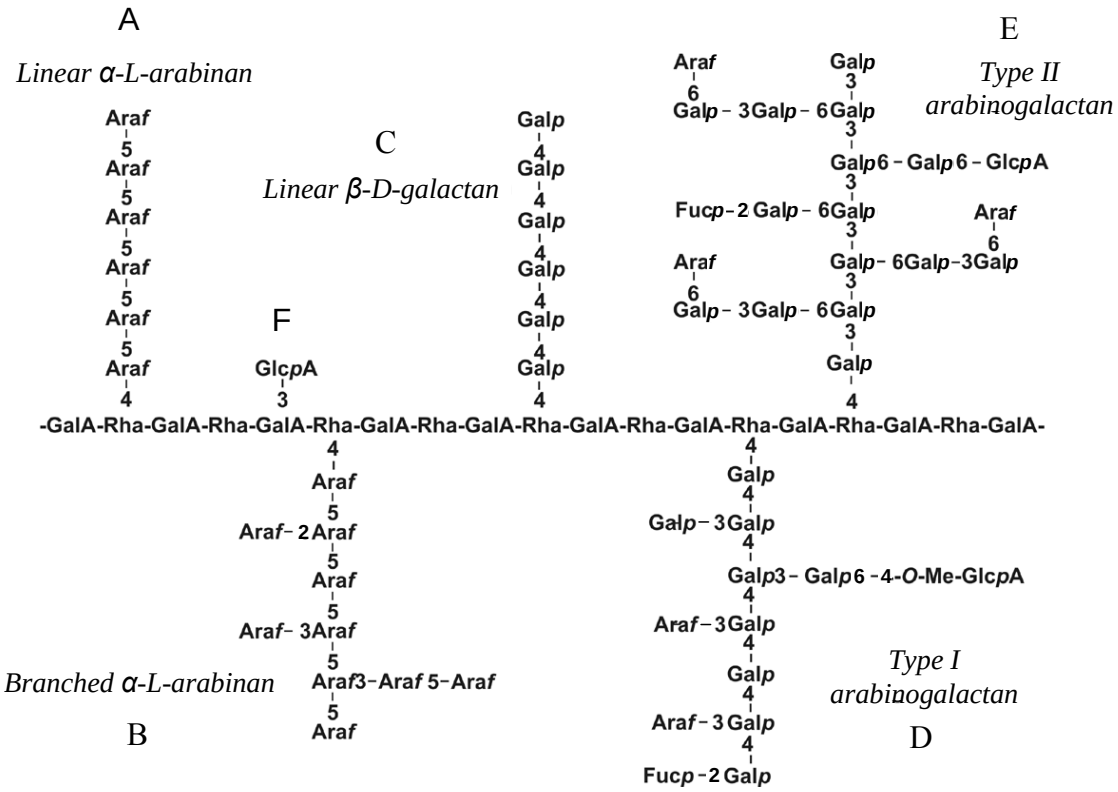

from different tissue sources (Thomas et al., 1989; O'Neill et al., 1990; Lerouge et al., 1993; Schols et al., 1995a; Mohnen, 1999). It has also been suggested that the appearance of specific side branches of RG-I may be temporally, spatially and developmentally regulated (Willats and Knox, 1999a; Willats et al., 2001a; McCartney et al., 2003; Majewska-Sawka et al., 2004; Willats et al., 2004).

Roughly 20-80% of the L-Rha*p* residues in the backbone of RG-I are substituted with arabinan, galactan, or arabinogalactan side chains (Figure 1.2) that may range from 1 to over 50 residues in length (Lerouge et al., 1993; Zablackis et al., 1995; Schols et al., 1995a). Arabinans are composed of linear chains of (1,5)-linked α-L-arabinofuranose (Ara*f*; Figure 1.2, A) that may be branched at *O*-2 or *O*-3 with additional L-Ara*f* residues (Figure 1.2, B; Lau et al., 1987). Linear galactans of (1,4)-linked β-D-galactopyranosyl (D-Gal*p*; Figure 1.2, C) residues are also found on RG-I (Aspinall et al., 1967; Aspinall, 1980; Lau et al., 1987; Nakamura et al., 2001)

Arabinogalactans have been subdivided in two categories based on the structure of the galactan chain (Carpita and Gibeaut, 1993). Type I arabinogalactans (Figure 1.2, D) are composed of a (1,4)-linked β-D-galactan backbone that may be further substituted with (1,3)-linked α-L-Ara*f* and (1,3)-linked β-D-Gal*p* residues or chains (O'Neill et al., 1990). Type II arabinogalactans (Figure 1.2, E) have a backbone composed of (1,3)-linked β-D-galactan that may be substituted with short (1,3)-, (1,6)-, or mixed (1,3;1,6)-linked β-D-galactan chains (O'Neill et al., 1990; An et al., 1994a; Mohnen, 1999). The exact composition of type I and type II arabinogalactan is not known, although terminal (1,2)-linked α-L-fucopyranosyl (L-Fuc*p*), (1,4)- or (1,6)-linked β-D-glucopyranosyluronic acid (D-Glc*p*A), (1,6)-linked 4-*O*-methyl β-D-Glc*p*A, and (1,3)- or (1,6)-linked α-L-Ara*f* may also be found in the side chains of RG-I (O'Neill et al., 1990; Carpita and Gibeaut, 1993; An et al., 1994; Albersheim et al., 1996; Mohnen, 1999).

Type II arabinogalactans are also associated with arabinogalactan proteins (AGPs); however, it is commonly accepted that these polysaccharides are indeed present as side chains of RG-I (McNeil et al., 1984; Bacic et al., 1988; Mohnen, 1999).

Other substitutions on RG-I side chains are known to occur. For example, L-Ara*f* and D-Gal*p* residues may also contain ferulic or coumaric acid (Ishii, 1997a), and in the walls of sugar beet 2% of the D-Gal*p*A backbone residues are substituted with D-Glc*p*A (Figure 1.2, F; Renard et al., 1999). The exact roles these different side chains play in RG-I function has not yet been elucidated, although certain tissues have been found to be enriched in RG-I molecules that have specific side chains (Schols et al., 1995a; Ros et al., 1998; Cardoso et al., 2002; Nakamura et al., 2002a).

Substituted galacturonans

Some polymers of HGA are substituted with mono- or oligosaccharide side branches. These branched HGA polysaccharides are collectively known as substituted galacturonans (SGAs). To date, there are only three types of SGA polysaccharides known to exist in primary cell walls: xylogalacturonan (XGA), apiogalacturonan (AGA) and rhamnogalacturonan II (RG-II).

Xylogalacturonan

XGA has been isolated from pine (*Pinus mugo*) pollen (Bouveng, 1965), carrot (*Daucus carota*) callus (Kikuchi et al., 1996), soybean cotyledons (Nakamura et al., 2002a), cocoa (*Theobroma cacao*) beans (Redgwell and Hansen, 2000), pea (*Pisum sativum*) hulls (Le Goff et al., 2001), and the fruits of watermelon (*Citrullus lanatus*; Yu and Mort, 1996), lemon (Ros et al., 1998), and apple (Schols et al., 1995a). XGA has a backbone of (1,4)-linked α-D-Gal*p*A that is substituted at *O*-3 with β-D-xylopyranosyl residues (D-Xyl*p*; Figure 1.3, A; O'Neill et al.,

Figure 1.3. The structures of xylogalacturonan (XGA) and apiogalacturonan (AGA). Both XGA and AGA have backbones composed of HGA [(1,4)-linked α-D-Gal*p*A]. A) D-Gal*p*A residues in XGA are substituted at the *O*-3 with β-D-Xyl*p* residues. B) D-Gal*p*A is substituted at either *O*-2 or *O*-3 with β-D-Api*f* or [β-D-Api*f*-(1→3')-β-D-Api*f*-(1→] in AGA. D-Api*f* side chains are shown linked only to the *O*-2 of D-Gal*p*A residues for simplicity. Figure was generously provided by M.A. O'Neill (CCRC).

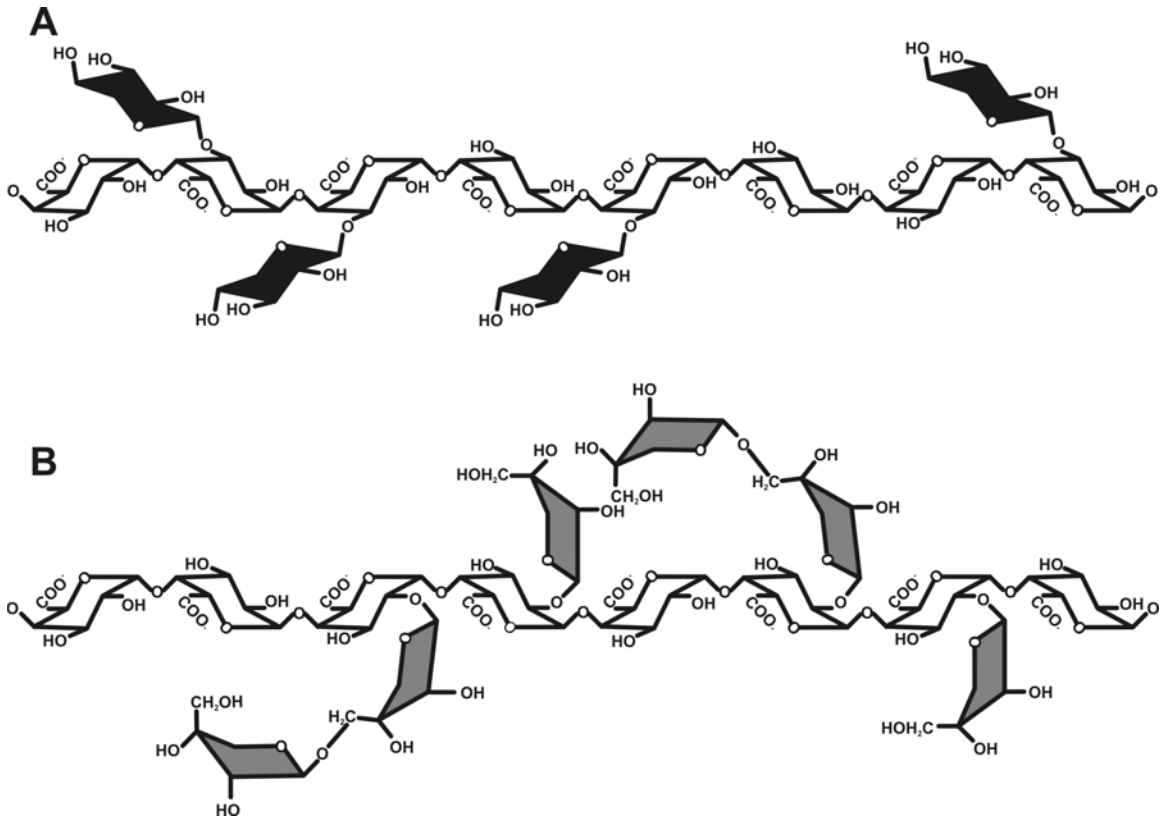

1990; Schols et al., 1995; Kikuchi et al., 1996; Yu and Mort, 1996). The degree of D-Xyl*p* branching on XGA is not known.

Nakamura et al. (2002) found that polygalacturonase treatment of hot-water soluble, soybean cotyledon polysaccharides that had previously had their arabinan and galactan chains removed by treatment with an α-(1,3)-L-arabinosidase and a β-(1,4)-D-galactosidase, respectively (Nakamura et al., 2001), yielded two oligosaccharides rich in D-Xyl*p* and D-Gal*p*A. Linkage analysis revealed the presence of terminal, 4-, and 3,4-linked Gal*p*A and terminal, 4-, and 2,4-linked D-Xyl*p*. Although treatment of these oligosaccharides with an β-(1,4)-D-xylosidase released some D-Xyl*p* residues from the oligosaccharides, the authors were unable to prove that 4- or 2,4-linked D-Xyl*p* were indeed attached to D-Gal*p*A (Nakamura et al., 2002a).

Apiogalacturonan

Apiogalacturonan (AGA; Figure 1.3, B) has been isolated from the cell walls of only a limited number of plants species, for example duckweed (*Lemna minor* L; Golovchenko et al., 2002). It has a linear backbone of HGA that can be substituted at the *O*-2 or *O*-3 with β-D-apiofuranose (D-Api*f*) or [β-D-Api*f*-(1→3')-β-D-Api*f*-(1→] (Cheng and Kindel, 1997; Ridley et al., 2001; Golovchenko et al., 2002). Whether AGA is a component of the cell walls of different plant species, or has special functions in aquatic monocots like duckweed, has yet to be addressed.

Rhamnogalacturonan II

The structure of RG-II is by far the most complicated of any of the primary cell wall polysaccharides (Figure 1.4). It is composed of 13 different monosaccharides in over 20 different linkages (O'Neill et al., 1997). Many of the sugars that make up RG-II are unusual, such as 2-keto-3-deoxy-D-*manno*-octulopyranosyluronic acid (D-Kdo*p*) and 3-deoxy-D-*lyxo*-2-

Figure 1.4. Currently accepted structure of rhamnogalacturonan II. The backbone of RG-II is composed of at least 7 (1,4)-linked α-D-Gal*p*A residues and contains four highly conserved side chains named A-D. Species specific variations in the terminal glycosyl residues of side chain B are shown (Whitcombe et al., 1995; Pellerin et al., 1996; Matsunaga et al., 2004) as well as changes in RG-II structure that occur in the Arabidopsis mutant *mur1* (Zablackis et al., 1996) and the mutant of *Nicotiana plumbaginifolia*, *nolac-H18* (Iwai et al., 2002). Taken from O'Neill et al. (2004).

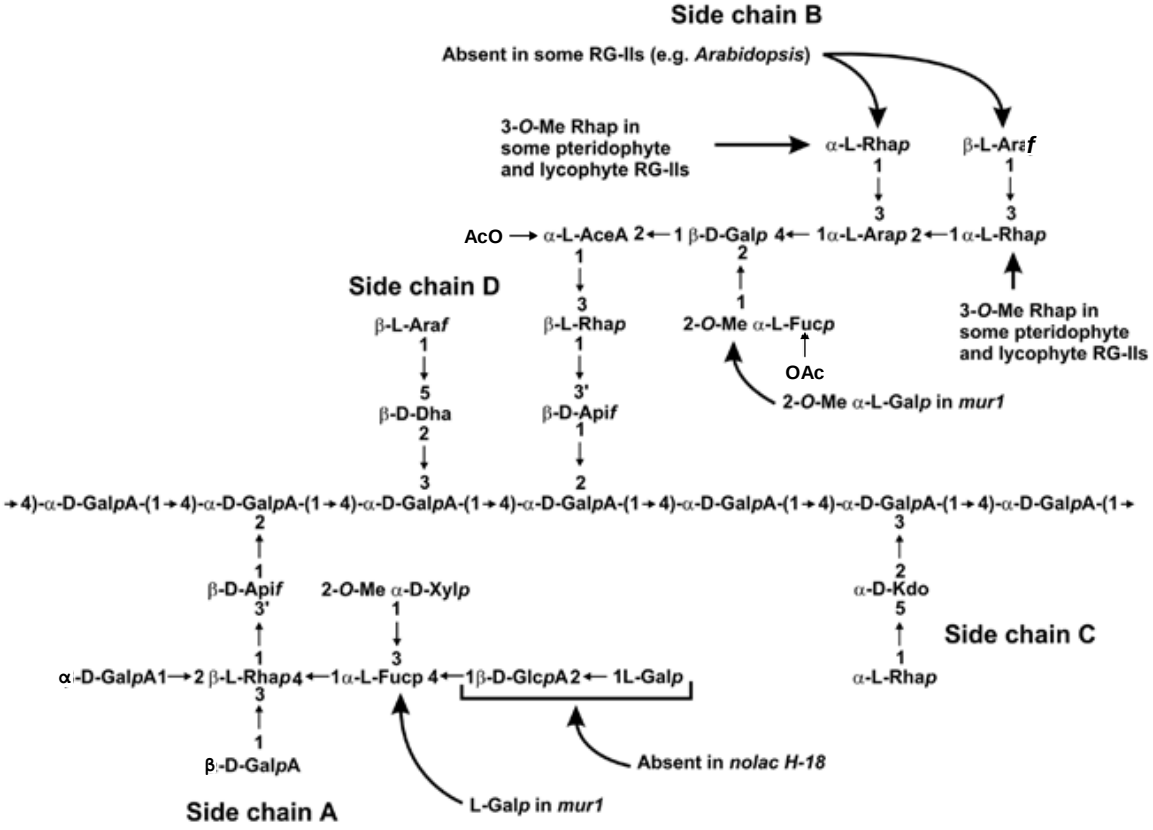

heptulopyranosylaric acid (D-Dha*p*). Some sugars, such as L-aceric acid (3-*C*-carboxy-5-deoxy-L-xylofuranose; L-Ace*f*A) are specific for RG-II and are not found anywhere else in nature. There is some evidence that the HGA backbone of RG-II contain methylesters (Pellerin et al., 1996) and that acetylesters may be present on the 2-*O*-methyl L-Fuc*p* and L-Ace*f*A residues of side chain B (Whitcombe et al., 1995; Glushka et al., 2003); however, the exact pattern of methyl- and/or acetylation has not yet been determined and may be dependent on the original source of RG-II (Whitcombe et al., 1995; Glushka et al., 2003). RG-II accounts for 1-4% of the walls of dicots, non-graminaceous monocots and gymnosperms (O'Neill et al., 1990; Mohnen et al., 1996), 0.2-2% of the walls of lycophytes and pteridophytes (Matsunaga et al., 2004; O'Neill et al., 2004), less that 0.1% of the walls of grasses (Thomas et al., 1989; O'Neill et al., 1990), and can barely be detected in the walls of bryophytes (Matsunaga et al., 2004).

RG-II has a backbone of at least 7 (1,4)-linked α-D-Gal*p*A residues (O'Neill et al., 1996) and is surprisingly resistant to microbial and fungal glycosidases and glycanases, such as those found in commercial preparations (i.e. Pectinol AC and Driselase; Stevenson et al., 1988; Ishii and Matsunaga, 1996). RG-II can be released from primary walls by *endo*polygalacturonase (EPGase) treatment (York et al., 1986) or by buffer extraction followed by EPGase treatment (Thomas et al., 1989; Ishii et al., 2001a). Structural characterization of the side chains of RG-II was done mainly by partial acid hydrolysis of purified RG-II, followed by analysis of the released oligosaccharides using a combination of mass spectrometry (MS) and nuclear magnetic resonance (NMR) techniques (Spellman et al., 1983a; Thomas et al., 1989; Puvanesarajah et al., 1991; Whitcombe et al., 1995; Pellerin et al., 1996).

It is currently believed that RG-II consists of 4 distinct side branches named A-D. Evidence for the attachment sites of these side branches to the backbone of RG-II has been

obtained by periodate oxidation (Puvanesarajah et al., 1991) and by selectively cleaving $NaBH_4$-reduced RG-II with a cell free extract from *Penicillium daleae* that is known to contain RG-II-degrading glycanases (Vidal et al., 2000). Recent studies using 2D NMR have confirmed some of these results (Rodriguez-Carvajal et al., 2003) and have allowed for the further refinement of RG-II structure (Reuhs et al., 2004). These studies have led to a consensus structure of RG-II (Figure 1.4; O'Neill et al., 2004). However, the inability to unequivocally assign all of the peaks from 2D NMR experiments that correspond to backbone D-Gal*p*A residues and to residues that are directly attached to D-Gal*p*A (Vidal et al., 2000; Ridley et al., 2001; Rodriguez-Carvajal et al., 2003) may require that this currently accepted RG-II structure be further refined in the future. For example, it is currently believed that L-Ara*f* may be linked to backbone D-Gal*p*A residues on RG-II (Thomas et al., 1989; Pellerin et al., 1996; Matsunaga et al., 2004) and may even constitute a new side chain (Rodriguez-Carvajal et al., 2003).

RG-II has been isolated from a number of different tissue sources, including sycamore (Darvill et al., 1978; Whitcombe et al., 1995), sugar beet (Ishii and Matsunaga, 1996), potato (*Solanum tuberosum*; Ishii, 1997), pea (O'Neill et al., 1996), rice (*Oryza sativa*; Thomas et al., 1989), radish (*Raphanus sativus*; Kobayashi et al., 1996), Arabidopsis (Zablackis et al., 1995), and red wine (Vidal et al., 2000). Glycosyl composition and linkage analysis have shown that the structure of RG-II is highly conserved amongst plant species. The discovery of conserved RG-II structures in the cell walls of lesser plants (e.g. lycophytes and pteridophytes; Matsunaga et al., 2004) has led to the proposal that RG-II may have been required for the evolution of land plants (Matsunaga et al., 2004; O'Neill et al., 2004).

Structural differences in glycosyl composition of RG-II isolated from different plant species are found only on the residues attached to the *O*-2 and/or *O*-3 of the L-Ara*p* residue of

side chain B (Figure 1.4; Thomas et al., 1989; Whitcombe et al., 1995; Pellerin et al., 1996; Vidal et al., 2000; Matsunaga et al., 2004). The L-Ara*p* is not substituted in species such as sugar beet (Ishii and Matsunaga, 1996) and contains (1,2)-linked α-L-Rha*p* in Arabidopsis (Glushka et al., 2003) and rice (Thomas et al., 1989). RG-II from red wine has α-L-Rha*p* and [β-L-Ara*f*-(1→2)-α-L-Rha*p*-(1→] linked to the *O*-3 and *O*-2 of the L-Ara*p* residue, respectively (Pellerin et al., 1996). Only the disaccharide is found attached to the *O*-2 of the L-Ara*p* residue in RG-II from sycamore (Whitcombe et al., 1995), while RG-II isolated from some lycophytes and pteridophytes may contain 3-*O*-methyl β-D-Rha*p* linked to the *O*-3 and/or *O*-2 of the L-Ara*p* residue (Matsunaga et al., 2004). The functions of the different substitutions on the L-Ara*p* residue of side chain B are unknown, as they do not seem to have any effect on the function of RG-II *in vivo* (O'Neill et al., 2004).

RG-II molecules can dimerize in the presence of boron

RG-II isolated from the primary walls of a number of different tissue sources is predominantly (~95%) in the form of a dimer crosslinked by a 1:2 borate-diol ester (Figure 1.5; Ishii and Matsunaga, 1996; Kobayashi et al., 1996; O'Neill et al., 1996; Pellerin et al., 1996). The presence of dimeric RG-II (dRG-II) complexed by borate di-esters has been confirmed in all plant species in which RG-II has been isolated, including the cell walls of lycophytes and pteridophytes (Matsunaga et al., 2004; O'Neill et al., 2004). The approximate molecular weight of monomeric RG-II (mRG-II) and dRG-II are 5 and 10 kDa, respectively (O'Neill et al., 1996; Pellerin et al., 1996; Matsunaga et al., 2004). The relative proportion of dRG-II:mRG-II isolated from walls depends on the plant source (O'Neill et al., 1996; Matsunaga et al., 2004), but the characteristics of RG-II dimerization are the same across plant species. This suggests that the

Figure 1.5. Rhamnogalacturonan molecules dimerize in the presence of boron. A) Two rhamnogalacturonan II (RG-II) molecules can form a dimer crosslinked by a 1:2 borate-diol ester in the presence of boron. Linkage occurs only on L-Api*f* residues found on side chain A of RG-II. B) Boron involved in the crosslink is chiral and so two stereoisomers of dRG-II are possible. Adapted from O'Neill et al. (2004).

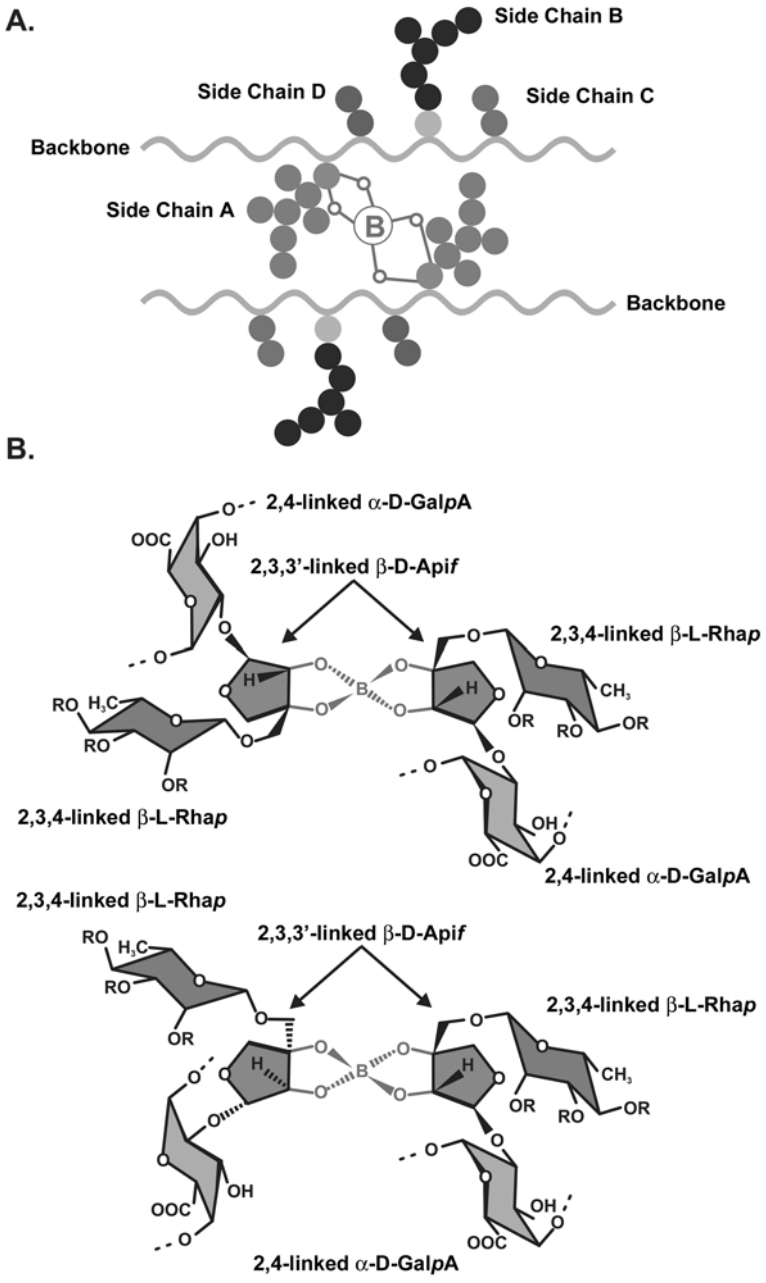

chemical properties of RG-II are the same irrespective of the tissue source and the differences in side chain B structure (O'Neill et al., 1996; Ishii et al., 1999; Matsunaga et al., 2004).

The formation of dRG-II from mRG-II in the presence of boron occurs spontaneously *in vitro* at an optimum pH of 3-4 without the addition of any exogenous proteins (O'Neill et al., 1996; Ishii et al., 1999). The addition of di- and trivalent cations with an ionic radii >1.0, such as Pb^{2+}, Sr^{2+}, Ba^{2+}, La^{3+}, and Ce^{3+}, greatly increases the rate of dimer formation (O'Neill et al., 1996; Ishii et al., 1999). Ca^{2+} also increases this rate, but to a much lesser extent than that of the larger cations (Ridley et al., 2001). Conversely, incubation of dRG-II at pH 1-3 in the absence of boron causes its conversion into mRG-II (Ishii and Matsunaga, 1996; Kobayashi et al., 1996; O'Neill et al., 1996). Glycosyl composition and linkage analysis of *in vitro* synthesized mRG-II or dRG-II are identical, except for the presence of 2,3,3'-linked L-Api*f* found in dRG-II molecules (O'Neill et al., 1996), providing evidence that the site of borate di-ester cross-linking of RG-II is on L-Api*f* residues (Ishii et al., 1999). Selective labeling of derivatives from dRG-II demonstrates that only the L-Api*f* residues on side chain A (Figure 1.5, A) participate in RG-II dimerization (Ishii et al., 1999). Two diastereoisomers of dRG-II are possible due to the fact that the boron molecule involved in the crosslink is chiral (Figure 1.5, B; O'Neill et al., 2004). Further research needs to be conducted to determine which of these stereoisomers is commonly found in nature.

PECTIN IN THE PRIMARY WALL

HGA, RG-I, and RG-II may be covalently linked in the primary cell wall

There is compelling evidence that HGA, RG-I and RG-II may be covalently linked in the primary walls of plant cells (Thomas et al., 1989). HGA, RG-I and RG-II can be isolated as a high molecular complex (>100 kDa) by extracting primary walls with aqueous buffers (O'Neill et

al., 1990; Ishii et al., 2001a; Reuhs et al., 2004). Saponification of this complex followed by enzymic digestion with purified EPGases causes the release of HGA oligosaccharides (oligogalacturonides or OGAs) and RG-II from the remaining high molecular weight material, which consists mainly of RG-I (McNeil et al., 1980; York et al., 1986; O'Neill et al., 1990; Lerouge et al., 1993; O'Neill et al., 1997). Ishii et al. (2001a) found that treatment of the original high molecular weight complex for one hour with 1 N HCl (a treatment that is known to strip boron from dRG-II *in vitro*) changed its elution profile following size exclusion chromatography. Incubation of the acid-treated material for 16 h in a buffer containing boric acid and lead acetate at pH 7.3 (conditions known to cause the formation of dRG-II from mRG-II *in vitro*), caused the acid-treated pectin to elute at the same retention time as the original high molecular weight complex. These results suggest that RG-II dimerization can change the molecular weight distribution of the high molecular weight pectin complex and provides further evidence that pectic polysaccharides may be covalently linked in the wall.

Evidence that RG-II may be covalently linked to HGA stems from the observation that the lengths of the HGA backbones on EPGase-released RG-II molecules are heterogeneous (Whitcombe et al., 1995; Pellerin et al., 1996; Vidal et al., 2000). Partial acid hydrolysis of RG-II from sycamore (Whitcombe et al., 1995) and from red wine (Pellerin et al., 1996) releases RG-II side chains and OGAs of degrees of polymerization of 7-15 (Ishii et al., 1999) with the average length being between 7 and 9 D-Gal*p*A residues for sycamore and red wine RG-II, respectively (O'Neill et al., 1996). This variation in the length of the RG-II backbones is most likely the result of the incomplete hydrolysis of RG-II from the high molecular weight complex by EPGase (Whitcombe et al., 1995; Ishii et al., 1999) or the incomplete digestion of cell wall polysaccharides during the fermentation of red wine (Pellerin et al., 1996). Furthermore,

treatment of sycamore RG-II with a purified *exo*polygalacturonase (*exo*PGase) releases D-Gal*p*A residues from RG-II (Whitcombe et al., 1995), suggesting that RG-II molecules have (1,4)-linked α-D-Gal*p*A residues attached to their backbones that are accessible to *exo*PGase.

The high molecular weight material that remains following treatment of buffer-soluble pectic polysaccharides with EPGase is composed mainly of RG-I (McNeil et al., 1980; York et al., 1986). Lerouge et al. (1993) conducted glycosyl composition analysis of this fraction from sycamore suspension-cultured cells and found that the molar ratios of D-Gal*p*A and L-Rha*p* varied in several RG-I preparations. Treatment of these RG-I preparations with *exo*PGase released D-Gal*p*A as the only monosaccharide and resulted in RG-I fractions that had equimolar ratios of D-Gal*p*A:L-Rha*p*. These results suggested that (1,4)-linked α-D-Gal*p*A residues were covalently attached to RG-I molecules.

Further evidence of a covalent attachment between HGA and RG-I was demonstrated using a hot-water soluble polysaccharide fraction from defatted soybean cotyledons (Nakamura et al., 2002a). Treatment of this fraction with a mixture of purified pectinolytic enzymes [(1,3)-α-L-arabinosidase, (1,5)-α-L-*endo*arabinanase, (1,4)-β-D-galactosidase and (1,4)-β-D-*endo*galactanase, EPGase, and a rhamnogalacturonan α-D-galactopyranosyluronohydolase] released oligosaccharides that, upon separation by anion exchange chromatography, had varying ratios of L-Rha*p*:D-Gal*p*A (ranging from 2.7 to 10.4). Fast atom bombardment (FAB) MS analysis of these oligosaccharides suggested the presence of L-Rha*p* residues within short stretches of (1,4)-linked α-D-Gal*p*A chains; however, the relative placement of these L-Rha*p* residues could not be determined due to the low abundance of fragmentation ions during analysis.

Structural analysis of fragments released by enzymic digestion of RG-I from the high molecular weight complex from soybean walls revealed the presence of segments of XGA

(Nakamura et al., 2002, 2002a). XGA fragments associated with RG-I molecules have also been detected in extracts from apple (Schols et al., 1995a), lemon (Ros et al., 1998), pea (Le Goff et al., 2001) and sugar beet (Ishii and Matsunaga, 2001). It is unknown at this time whether or not the association between RG-I and XGA is due to a covalent interaction, or is simply caused by the natural propensity of pectic polysaccharides to aggregate in solution (Mort et al., 1991).

Evidence for the presence of other covalent linkages between pectic polysaccharides

HGA, RG-I and RG-II may also be held in the wall by other types of covalent linkages. Approximately 50% of the pectic polysaccharides found in primary walls are solubilized by treatment with aqueous buffers or purified EPGase (O'Neill et al., 1990; Zablackis et al., 1995; Ishii and Matsunaga, 2001; Reuhs et al., 2004). The remaining pectic material can be solubilized from walls by treating them with mild alkali, a procedure known to break ester linkages and to solubilize neutral hemicelluloses, such as xyloglucan (York et al., 1986; Zablackis et al., 1995).

Cold alkali treatment of a commercially available fractionated pectin powder (FPP) from citrus peels caused the high molecular weight component of this fraction to migrate as uniformly sized OGAs on polyacrylamide gels (Jackson et al., 2004). OGA formation was not due to β-elimination as an increase in A_{232} was not observed following base treatment. These OGAs were not produced by treating FPP with a purified EPGase alone or in combination with a pectin methylesterase; however, cold alkali followed by EPGase treatment of FPP caused its complete degradation. These results suggested that the OGAs present in FPP were resistant to EPGase treatment and that this resistance was not due to *O*-6 methylation. Driselase treatment of cell wall material from spinach (*Spinacia oleracea*), carrot, rose (*Rosa* sp. 'Paul's Scarlet'), and tall fescue (*Festuca arundinacea*) suspension cultured cells (Brown and Fry, 1993) and from carrot root (Needs et al., 1998) also released OGAs that possessed unidentified esters that were resistant

to pectinolytic degradation. The structures of these esters, and of those found in FPP, have yet to be described.

Pectin methylesterases (PEs) are enzymes that remove methyl groups from pectin molecules (Micheli, 2001). It has been suggested that another function of pectinesterases may be to covalently link pectic polysaccharides in the wall (Lee et al., 2003). Treatment of citrus pectin with a purified pectinesterase (PE) *in vitro* caused it to migrate as a higher molecular weight complex on size exclusion columns (Lee et al., 2003), suggesting that PEs may be able to catalyze reactions that increase the molecular weight of pectin molecules in the wall.

Ferulic and coumaric esters have been found attached to L-Ara*f* and D-Gal*p* residues from Driselase-treated walls of spinach suspension-cultured cells and sugar beet pulp (Fry, 1982; Ishii, 1994). These esters could allow pectic molecules to crosslink to other cell wall components by oxidative coupling (Ishii, 1997a); however, evidence for such crosslinked components has yet to be demonstrated.

Mild alkali treatment of suspension-cultured rose cells released a polysaccharide complex containing both pectin and xyloglucan molecules (Thompson and Fry, 2000). These molecules co-eluted on anion exchange columns, even though xyloglucan itself contains no acidic residues. Furthermore, it has been demonstrated that a membrane-enriched fraction from pea synthesized a galactan that could be solubilized by treating the radioactive products with pectin- or xyloglucan-degrading enzymes (Abdel-Massih et al., 2003). Both of these studies suggest that pectin and xyloglucan are associated in the wall, although data describing the nature of this attachment has yet to be presented.

Simplified model of pectin in the wall

Several models describing the association of pectic polysaccharides within the primary wall have been presented (Keegstra et al., 1973; McCann and Roberts, 1991; Carpita and Gibeaut, 1993). The first models depicted pectic polysaccharides crosslinked to each other and to other cell wall components through covalent linkages (Keegstra et al., 1973). The basis for this model was derived from the fact that 1) pectins isolated from the wall by chemical or enzymic methods co-chromatographed on ion exchange and size exclusion columns with xyloglucan polymers (Keegstra et al., 1973; Thompson and Fry, 2000), 2) that EPGase treatment of wall material allowed the release of higher amounts of cell wall proteins following protease digestion than untreated walls (Keegstra et al., 1973), and 3) that associations between RG-I and AGPs are possible as both molecules contain type II arabinogalactans (McNeil et al., 1984; Bacic et al., 1988; Carpita et al., 2001). The validity of this model was questioned when glycosyl composition and linkage analysis of cell wall material failed to demonstrate the presence of covalent crosslinks between pectin and other wall components (McCann and Roberts, 1991; Carpita et al., 2001). Furthermore, electron microscopy of CDTA or Na_2CO_3 extracted walls revealed an independent, crosslinked network of cellulose and hemicellulose polysaccharides (McCann and Roberts, 1991), suggesting that pectins in the wall formed an independent, gel-like matrix that could be extracted from the other cell wall components.

Recent structural analysis of the wall has revealed the presence of covalent crosslinks between specific classes of pectic polysaccharides (Spellman et al., 1983; Whitcombe et al., 1995; Pellerin et al., 1996; Ishii and Matsunaga, 2001; Nakamura et al., 2002, 2002a). Based on these observations, newer models for the association of pectic polysaccharides within the wall have been presented (Carpita and Gibeaut, 1993; Willats et al., 2001; Nakamura et al., 2002a;

Vincken et al., 2003). Most models of pectin in the wall depict it as stretches of RG-I covalently attached to polymers of HGA in an alternating pattern (Carpita and Gibeaut, 1993; Nakamura et al., 2002). However, one model suggests that pectic polysaccharides are composed of large RG-I polymers that have side branches of HGA, RG-II, XGA, arabinans, galactans and arabinogalactans (Vincken et al., 2003). These authors go on to suggest that associations between RG-I polymers occur in areas of overlapping regions of HGA and RG-II side branches, and that these overlapping regions are the primary sites of Ca^{2+} and boron crosslinking of pectic polysaccharides, respectively.

Glycosyl composition and linkage analysis of RG-I polymers from sycamore (McNeil et al., 1980; York et al., 1986; O'Neill et al., 1990; Lerouge et al., 1993; An et al., 1994; An et al., 1994a), soybean (Nakamura et al., 2001; Nakamura et al., 2002a), cocoa (Redgwell and Hansen, 2000), rice (Thomas et al., 1989), lemon (Ros et al., 1998), Douglas fir (O'Neill et al., 1990), sugar beet (Renard et al., 1999; Ishii and Matsunaga, 2001), apple (Schols et al., 1995a), pea (Le Goff et al., 2001), and Arabidopsis (Zablackis et al., 1995) failed to provide any evidence for the existence of D-Gal*p*A residues attached as side chains to the backbone of RG-I. Therefore, a new model of the association of pectic polysaccharides in the wall based on current structural data is presented (Figure 1.6).

The covalent attachment of HGA to either RG-I or RG-II polymers has been demonstrated (Figure 1.6, A; Lerouge et al., 1993; Ishii and Matsunaga, 2001; Nakamura et al., 2002a; Reuhs et al., 2004). The high molecular weight of pectins extracted from the wall suggests that HGA stretches link several RG-I and RG-II molecules either as independent polymers (Figure 1.6, A) or to each other (Figure 1.6, B). The possibility also exists that

Figure 1.6. Model of the association of pectic polysaccharides in the primary cell wall. A) Recent structural analyses of primary cell wall polysaccharides provide evidence for the covalent attachment of HGA to independent polymers of RG-I and RG-II. Pectin isolated from the cell wall is composed of a high molecular weight complex of all three pectic polysaccharides. B) It is not known whether this complex is composed of HGA, RG-I and RG-II polymers covalently attached to each other in a random or ordered fashion, or C) if the RG-I:HGA and RG-II:HGA molecules are separate pectic species that associate in the wall due to intermolecular attractions.

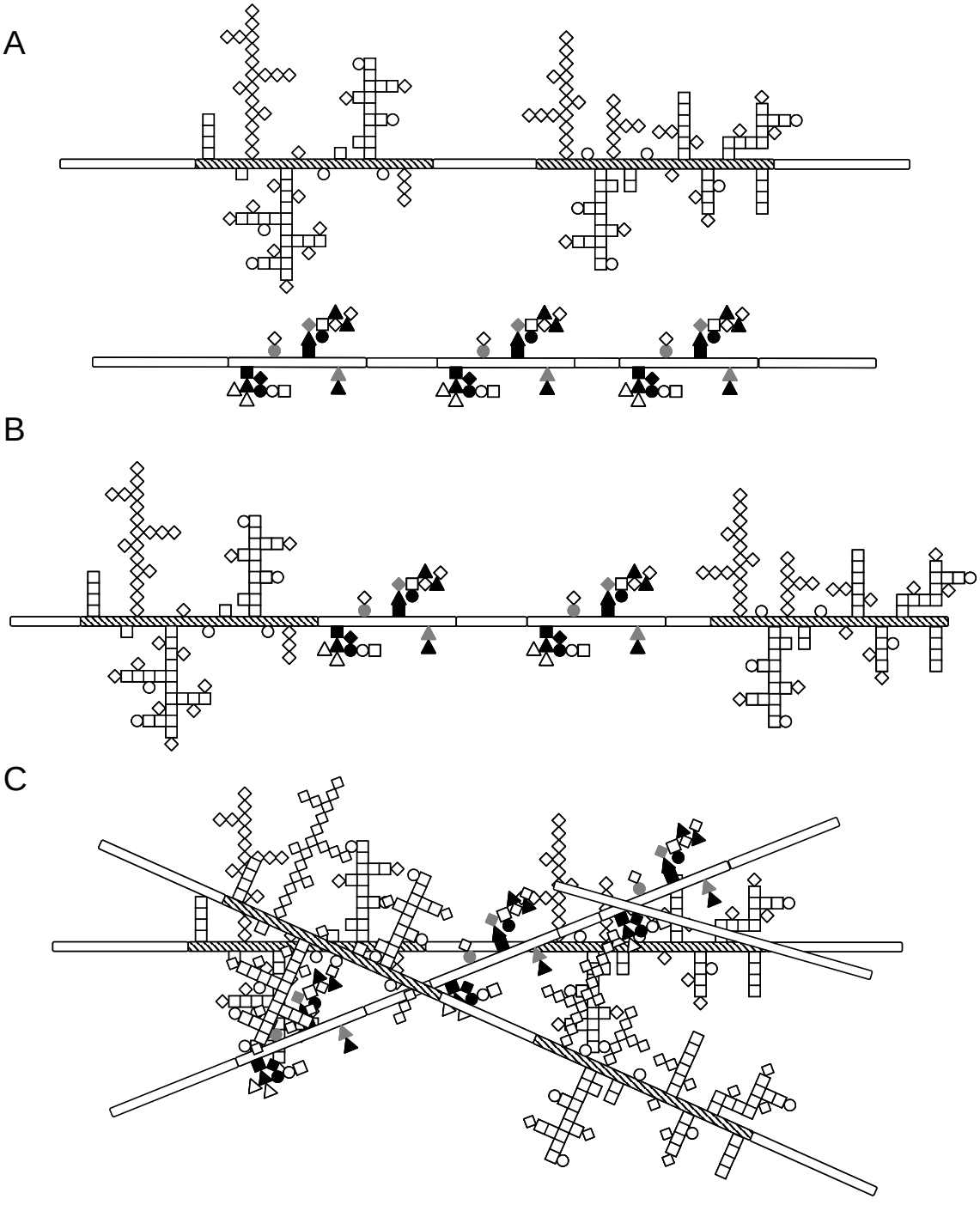
A
B
C
Legend:
△GalA
◇Ara
▲Rha
◆Xyl
▲Kdo
◆AceA
HGA
○GlcA
□Gal
●Fuc
■Api
●Dha
RGI

independent RG-I:HGA and RG-II:HGA polymers form the high molecular weight complex due to ionic or other intermolecular interactions, such as Ca^{2+} crosslinking or hydrogen bonding (Figure 1.6, C; Mort et al., 1991; Tibbits et al., 1998; Braccini et al., 1999; Braccini and Perez, 2001). Further research into the structure of pectic polysaccharides *in muro* is required before accurate models describing pectin function and biosynthesis can be designed.

Location of pectin epitopes in the primary wall

One of the reasons that it has been difficult to design accurate models of pectin structure in the wall is that pectic polysaccharides are heterogeneous and specific pectin populations can be isolated from the walls of different tissues (Thomas et al., 1989; O'Neill et al., 1990; Oxenboll Sorensen et al., 2000; Nakamura et al., 2001). Furthermore, it has been shown that the presence of pectic polysaccharides in the wall may be developmentally (McCartney et al., 2003), spatially (Willats et al., 2001a), and temporally (McCartney and Knox, 2002) regulated. Differences in pectic polysaccharide expression may also occur within the walls of individual plant cells (Orfila and Knox, 2000).

Immunocytochemistry using antibodies generated against purified pectin fragments (Knox et al., 1990; Willats et al., 1999b; Willats et al., 2004) or isolated by screening phage display libraries (Williams et al., 1996; Willats et al., 1999) has increased our understanding of the distribution of pectic polysaccharides in the primary wall. Antibodies such as LM5 (Jones et al., 1997) and LM6 (Willats et al., 1998) have been well characterized and bind to specific side chains of RG-I (Table 1.1). JIM5, JIM7, LM7, and PAM1 all bind to HGA chains with differing degrees of *O*-6 methylesterification (Knox et al., 1990; Willats et al., 2000), while LM8 and CCRC-R1 are thought to bind to XGA and RG-II, respectively. The exact pectic epitope(s) recognized by these latter antibodies is still largely unknown. Synthesis and/or

Table 1.1. Monoclonal antibodies that bind to specific regions on pectic polysaccharides.

Antibody[a]	Recognized Epitope	Pectic polysaccharide	References
PAM1 (Fab)	>30 non-esterified GalA residues	HGA	(Willats et al., 1999)
JIM5 (mAb)	Low methylesterified pectin[b] 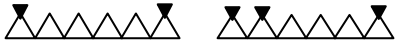	HGA	(Knox et al., 1990; Willats et al., 2000)
JIM7 (mAb)	High methylesterified pectin[b] 	HGA	(Knox et al., 1990; Willats et al., 2000)
LM7 (mAb)	Base or fungal PE treated pectin[b] 	HGA	(Willats et al., 2001a)
LM5 (mAb)	four (1,4)-linked β-D-Gal*p* residues	RG-I	(Jones et al., 1997)
LM6 (mAb)	five (1→5)-linked α-L-Ara*f* residues	RG-I/AGP[e]	(Willats et al., 1998)
LM8 (mAb)	Xyl*p*:Gal*p*A = 0.60-0.95[c]	XGA	(Willats et al., 2004)
CCRC-R1 (Fab)	Unknown[d]	RG-II	(Williams et al., 1996)

[a]Antibodies are either phage display (Fab) or hybridoma monoclonal antibodies (mAb).
[b]The synthetic methyl hexagalacturonates listed have been shown to compete for binding of the designated antibody to pectic polysaccharides (Clausen et al., 2003). △, (1,4)-linked α-D-Gal*p*A; ▼, O-6 methyl group.
[c]LM8 binding to pea testae XGA is inhibited by XGA molecules that have a D-Xylp:D-GalpA ratio greater than 0.60.
[d]CCRC-R1 binding to RG-II is strongly inhibited by RG-II molecules.
[e]Recent, unpublished evidence suggests that LM6 may also bind arabinogalactan proteins (http://www.bmb.leeds.ac.uk/staff/jpk/antibodies.htm).

purification of well-defined pectic structures coupled with immunodot binding and competitive enzyme-linked immunoabsorbant assays (ELISAs) will aid in the determination of the specific epitope(s) that these antibodies recognize (Willats and Knox, 1999a; Clausen et al., 2003). The antibodies listed in Table 1.1 have been extensively used to analyze the cell- and tissue-dependent distribution of specific pectin epitopes during different developmental stages of the plant life cycle and have given new insight into the potential roles that pectin may play in the wall and in the plant (McCann and Roberts, 1991; Willats et al., 2001).

The degree and pattern of methylesterified HGA seems to be spatially and developmentally regulated (Willats et al., 2001). Analysis of the cell walls of tissues from plants such as pea (Willats et al., 2001a), sugar beet (Majewska-Sawka et al., 2002; Majewska-Sawka et al., 2004), carrot (Willats et al., 1999b), clover (*Trifolium pratense* L.; Lynch and Staehelin, 1992), Arabidopsis (Dolan et al., 1997; Willats et al., 1999), potato (Bush et al., 2001), and tomato (*Lycopersicon esculentum*; Orfila and Knox, 2000) have shown that HGA chains with different patterns of methyl esterification are differentially distributed across the primary cell wall. Unesterified HGA chains (recognized by PAM1) or those with relatively low degrees of methylation (DM; recognized by JIM5) are localized to the middle lamella, the cell corners, and at the interface between the cell wall and the plasma membrane. This distribution is even more restricted in walls stained with LM7, since the epitope it recognizes is found only at the expanded middle lamella of cell corners and/or the outer edges of the wall that line the intercellular space (Willats et al., 2001a). LM7 is thought to recognize HGA with a non block-wise pattern of methylesterification based on its ability to bind only to pectins that have been generated by base de-esterification or by treatment with fungal pectin methylesterases (Willats et al., 2001a). However, recent studies using synthetic methyl hexagalacturonates with varying

patterns of methylesterification suggest that the LM7 epitope may recognize HGA chains with a more sparsely distributed pattern of methylesterification than that recognized by JIM5 (Clausen et al., 2003).

Conversely, more highly methylated HGA chains recognized by JIM7 are distributed evenly throughout the cell walls of all tissues that have been studied (Carpita and Gibeaut, 1993; Willats et al., 2001). JIM7 also uniformly labels the walls of pea testae at different days post anthesis (McCartney and Knox, 2002), and the walls of sugar beet during different stages of anther development (Majewska-Sawka et al., 2004). JIM5 and PAM1 epitopes are restricted to specific cell layers in pea testae (McCartney and Knox, 2002) and JIM5 labeling in anthers from sugar beet shows that the epitope appears only in meiocyte walls after cells have entered meiotic prophase (McCartney and Knox, 2000). These results indicate that different regions of the cell wall may have discrete domains of HGA polymers that differ in their degree and pattern of methylesterification.

Great diversity in pectic epitope distribution is also visualized in cells stained with antibodies against side chains of RG-I (e.g. LM5 and LM6). LM5 and LM6 recognize (1,4)-linked β-D-galactans and [1,5]-linked α-L-arabinans, respectively; however, recent, unpublished results suggest that LM6 may also bind to arabinogalactan proteins (AGPs; http://www.bmb.leeds.ac.uk/staff/jpk/antibodies.htm). In pea cotyledons, LM5 epitopes appears late in seed development, occurring at 25-34 days after anthesis (McCartney et al., 2000). This epitope is also found adjacent to the plasma membrane of parenchyma cells, and is absent from the outer epidermal cell wall. LM6 epitopes are seen throughout the wall in all cell layers, and its appearance is not as highly regulated as that of LM5. Distal root cap, vascular cylinder and vascular cortex cells from carrot exhibit strong LM5 labeling, while cells of the meristem and of

the cortical cells emerging from it stain with LM6 (Willats et al., 1999b). The appearance of the galactan epitope also correlates with root cell elongation as strong LM5 staining is seen in cells of the stele, and the endodermal and cortical cell layers in transition zone of the root (McCartney et al., 2003). The LM5 epitope is absent in the endodermal and cortical cell layers in more mature regions of the root, suggesting that the appearance of the LM5 epitope in these cell layers is a transient event (McCartney et al., 2003). The appearance of the LM5 epitope also seems to occur transiently in pea testae, as LM5 labeling of the macrosclereid layer attenuates with increasing days after anthesis. In contrast, strong LM6 labeling appears only in the crushed parenchyma layer late (30 days after anthesis) in testae development (McCartney and Knox, 2002). LM5 and LM6 epitopes are present in different cell types and at different stages of sugar beet anther development. (Majewska-Sawka et al., 2004). Weak LM5 labeling is detected in walls of the epidermis and endothecium in premeiotic anthers while strong labeling of meiocyte walls appears during meiotic prophase and persists as microspores mature. LM6 labels anther walls during all stages of anther development whereas meiocytes lose LM6 labeling as they mature into microspores. The walls of pit fields from mature green tomato pericarp tissue also show differential staining of LM5 and LM6 (Orfila and Knox, 2000). The LM6 epitope is present throughout the cell wall while the LM5 epitope is absent from walls of pit fields. Results from these studies indicate that subsets of RG-I molecules, and possibly AGPs, possessing distinct side chains exist in specific tissues, at different times, and at different developmental stages within the wall.

LM8 is an antibody that recognizes XGA from pea testae (Le Goff et al., 2001; Willats et al., 2004). The LM8 epitope is detected in only two areas of the pea plant: the crushed parenchyma layer of pea testae that is recognized by LM6, and cells of the root cap. LM8

staining of the crushed parenchyma layer is developmentally regulated. Its appearance in this cell layer mimics that of the LM6 epitope, with greater staining appearing late in pea testae development (~25 days after anthesis). A gradient of LM8 staining occurs in the root cap, with greater staining occurring in cells that are in the process of separating from the root. The localization of the LM8 epitope to these specific tissues seems to be common to angiosperms, as LM8 labeling was detected in the same tissues from lupin (*Lupinus arboreus*), carrot, maize and Arabidopsis (Willats et al., 2004).

The epitope that is recognized by the RG-II-specific antibody CCRC-R1, has not been defined (Williams et al., 1996). Competitive ELISA and immunolabeling studies show that binding to RG-II is only inhibited by excess RG-II, and not by individual RG-II monosaccharides or OGAs. Labeling of sycamore suspension-cultured cells with CCRC-R1 occurs in all areas of the cell wall except the middle lamella. Further characterization of the epitope recognized by CCRC-R1 will be required before definitive conclusions can be made concerning the localization of RG-II in the wall.

The differential staining of pectic epitopes spatially within cell walls and tissues, and during different developmental processes, suggests that specific subsets of pectin molecules may play specific roles in the wall. One of the problems that is associated with the interpretation of immunocytochemistry studies such as the ones listed above is that it is difficult to determine whether the appearance of these epitopes is due to *de novo* biosynthesis of the pectic epitopes or to the unmasking of existing epitopes within the wall (Mohnen, 1999).

Furthermore, the appearance of specific epitopes does not automatically prove a particular function within the wall. For example, transgenic potato plants expressing a cell wall-targeted fungal (1,4)-β-D-*endo*galactanase (Oxenboll Sorensen et al., 2000) or a Golgi-targeted

(1,5)-α-L-*endo*arabinanase (Skjot et al., 2002) were decreased by roughly 70% in tuber cell walls in galactan and arabinan content, respectively. The transgenic plants grew normally and had no apparent phenotypes, suggesting that the loss of these polysaccharides in the tuber had no effect on plant viability.

The effects of transgenic expression of glycanases in these studies may be dependent on the location of enzyme expression and on the type of enzyme that is expressed. For example, cell wall-targeted expression of the fungal (1,5)-α-L-*endo*arabinanase produced transgenic plants with severe phenotypes, such as the production of plants lacking side shoots, flowers, stolons and tubers (Skjot et al., 2002). Furthermore, potato plants expressing a fungal rhamnogalacturonan lyase had a variety of adverse phenotypes including the production of smaller tubers, changes in pectic polysaccharide glycosyl composition and extractability, and altered localization of LM5 and LM6 epitopes in the wall (Oomen et al., 2002). Results such as these suggest that more research into the effects of changes in pectin structure on plant growth and development will be required before accurate models describing pectin function can be designed.

PECTIN FUNCTION

The elucidation of the functions of pectin in the wall has been challenging due to the paucity of published studies where specific well-characterized changes in pectin structure caused changes in pectin function. Based on correlations between the location of pectic epitopes, changes in the expression of pectinolytic enzymes during different developmental stages, and the mechanical properties of pectins *in vitro*, pectic polysaccharides have been implicated in fruit ripening (Rose et al., 1998; Orfila et al., 2001), flower and leaf abscission (Roberts et al., 2002), pollen differentiation (Rhee and Somerville, 1998), root cap cell differentiation (Stephenson and Hawes, 1994; Willats et al., 2004), and the control of cell wall porosity (McCann and Roberts,

1991). Pectin has also been implicated in the elicitation of plant defense responses based on the ability of purified oligogalacturonides (OGAs) from plant cell walls or purified pectins (Spiro et al., 1993) to cause the accumulation of phytoalexins (Nothnagel et al., 1983), and reactive oxygen species (Ridley et al., 2001). Additionally, these OGAs are involved in the regulation of plant growth and development as it has been shown that discretely sized OGAs can change the morphogenetic fate of tobacco (*Nicotiana tabacum* L. cv. Samsun) thin cell-layer explants (Eberhard et al., 1989). Recently, a pectic fraction purified from lily (*Lilium longiflorum* Thumb cv. Nelly White) styles has been shown to be required for pollen tube binding in an *in vitro* adhesion assay, suggesting that pectin is also involved in pollen tube adhesion (Mollet et al., 2000).

Several excellent reviews on the possible involvement of pectic polysaccharides in these processes have been written (Darvill et al., 1992; Carpita and Gibeaut, 1993; Mohnen and Hahn, 1993; Hadfield and Bennett, 1998; Brummell and Harpster, 2001; Ridley et al., 2001; Willats et al., 2001; Roberts et al., 2002). The functions of pectins described in this section represent cases where changes in pectin function occurred due to well-defined changes in cell wall pectin structure.

Boron-induced RG-II dimerization is important for plant growth

Boron is an essential micronutrient in plants and is absolutely required for plant growth (Blevins and Lukaszewski, 1998). The basis for this requirement went largely unknown for almost a century, until the recent discovery that RG-II forms dimers in the presence of boron (Ishii and Matsunaga, 1996; Kobayashi et al., 1996; O'Neill et al., 1996). This discovery has led to the proposal that one of the functions of boron in plants is to cross-link RG-II polymers (O'Neill et al., 2004). Evidence for the importance of boron-induced RG-II dimer (dRG-II)

formation in plants is seen when plants are grown in the absence of boron (Fleischer et al., 1999; Ishii et al., 2001a). Pumpkin (*Cucurbia moschata* Duchesne, cv. Tokyou-Kabocha) seedlings grown in the absence of boron for one week had approximately a 10-fold reduction in the amount of boron in the second, third and fourth leaves compared to normally grown seedlings (Ishii et al., 2001a). This reduction resulted in a corresponding increase in the amount of RG-II monomer (mRG-II) that could be extracted from the cell walls. Boron deficient cell walls were significantly swollen compared to wild type walls, a phenotype that could be reversed by treating boron-deficient plants for 5 h with boric acid. Similarly, suspension-cultured *Chenopodium album* cells grown in the absence of boron have significantly greater wall pore size (Fleischer et al., 1999). The difference in wall pore size between boron-deficient and wild type cells could be corrected within 50 minutes by the addition of boric acid to the culture medium. Glycosyl composition and linkage analysis showed no difference in the structure of RG-II isolated from wild type and boron-deficient tissues (Fleischer et al., 1999; Ishii et al., 2001a) and incubation of mRG-II from deficient or wild type pumpkin seedlings in the presence of lead acetate and boric acid showed that RG-II molecules were equally capable of forming dRG-II (Ishii et al., 2001a).

Further evidence for the requirement of dRG-II formation for plant growth is seen in *mur1* plants of Arabidopsis (O'Neill et al., 2001). MUR1 encodes a GDP-D-mannose-4,6-dehydratase that is required for the synthesis of GDP-L-Fuc*p* (Bonin et al., 1997). Mutant plants exhibiting the *mur1* mutation have 5% of the wild type levels of fucose in their cell walls (Reiter et al., 1993). These plants are dwarfed, have brittle leaves, and have significantly reduced wall mechanical strength (Reiter et al., 1997; Ryden et al., 2003).

Cell wall analysis of *mur1* plants demonstrated that L-Fuc*p* was replaced by L-Gal*p* on the side chains of RG-II (Figure 1.4), causing a concurrent reduction (50%) in the level of 2-*O*-

methyl D-Xyl*p* in side chain A (O'Neill et al., 2001; Reuhs et al., 2004). Further analysis demonstrated that dRG-II accounted for only 50% of the total RG-II in *mur1* plants, while the dimer accounted for 95% of the total RG-II in wild-type plants, suggesting that the exchange of L-Fuc*p* for L-Gal*p* and/or the reduction in 2-*O*-methyl D-Xyl*p* inhibited the ability of RG-II to dimerize in the presence of boron. This hypothesis was confirmed by the fact that *mur1* dRG-II forms less rapidly and is less stable than wild-type dRG-II *in vitro* (O'Neill et al., 2001).

The *mur1* phenotype can be corrected by spraying plants with L-Fuc*p* (Reiter et al., 1993) or with boric acid (O'Neill et al., 2001). Spraying *mur1* plants with L-Fuc*p* restores the wild-type glycosyl composition of RG-II, wild-type levels of fucose in the wall, and wild-type levels of dRG-II that can be extracted from the walls of *mur1* plants (O'Neill et al., 2001). *Mur1* plants sprayed with boric acid are not altered in the glycosyl composition of RG-II; however, these plants grow normally, have wild-type levels of dRG-II that can be isolated from their walls, and have walls with comparable mechanical strength as those of wild type walls (O'Neill et al., 2001; Ryden et al., 2003). These results suggest that a plant's ability to form dRG-II in the presence of boron has a direct effect on plant growth and on the mechanical properties of the cell wall.

Pectins are involved in cell adhesion

The Ca^{2+} cross-linked matrix formed by HGA chains at the middle lamella is thought to be one of the main forces involved in plant cell adhesion (McCann and Roberts, 1991; Willats et al., 2001a). This is based in part by the fact that pectins and individual plant cells can be released from plant material by treatment by with Ca^{2+} chelating agents such as *trans*-(1,2)-diaminocyclohexane-*N*, *N*, *N*', *N*'-tetraacetic acid (CDTA; Thomas et al., 1989; McCann and Roberts, 1991; McCartney and Knox, 2002). However, a substantial amount of pectin remains in the primary wall, even after treatment with strong base (O'Neill et al., 1990; Zablackis et al.,

1995). Furthermore, treatment of pea testae with CDTA results in the separation of some, but not all, cells found within this tissue (McCartney and Knox, 2002), suggesting that there may be other linkages involved in maintaining pectin structures within the wall (Ridley et al., 2001; Jarvis et al., 2003).

A series of mutants with cell adhesion and shoot development defects were generated by T-DNA transformation of *in vitro* cultures of haploid leaf discs of *Nicotiana plumbaginifolia* (Iwai et al., 2001). One of the mutants, *nolac-H18*, was defective in a proposed glycosyltransferase gene, NpGUT1, with high amino acid identity to mammalian glucuronosyltransferases (Iwai et al., 2002). *nolac-H18* mutants had several differences in cell wall glycosyl composition compared to wild-type walls. RG-II isolated from mutant walls lacked the disaccharide [α-L-Gal*p*-(1→2)-β-D-Glc*p*A-(1→] from side chain A (Figure 1.4), suggesting that the mutated gene encoded a β-(1,4)-glucuronosyltransferase. dRG-II accounted for only 50% of the total RG-II that could be isolated from *nolac-H18* walls, compared to 95% in wild-type cells, and *nolac-H18* mRG-II had a severe reduction in its ability to form RG-II dimers in the presence of boron. The changes in wall composition of *nolac-H18* mutants, as well as the cell adhesion and RG-II dimerization defects, could be complemented by transforming mutant cells with wild-type NpGUT1 DNA. These results suggest that the removal of the β-D-Glc*p*A-containing disaccharide from side chain A of RG-II severely reduces the ability of RG-II to dimerize in the presence of boron, and causes defects in cell adhesion.

The arabinan side chains of RG-I are essential for proper stomatal function

Stomata are pores on the surface of plant leaves that allow for the exchange of gases required for photosynthesis. The control of stomatal opening is a tightly regulated process due to the excessive loss of water vapor, or transpiration, which can occur when stomata are open.

Elongated, kidney-shaped cells that lie adjacent to the stomatal pore, called guard cells, regulate the opening and/or closing of stomatal pores (Salisbury and Ross, 1992). Stomatal guard cells regulate the size of the stomatal pore by expanding or contracting in response to changes in internal hydrostatic (or turgor) pressure (Franks et al., 2001), and hence, the cell walls of guard cells must be extremely elastic.

An investigation into the cell wall polysaccharides that may be involved in regulating guard cell function was conducted using epidermal strips from *Commelina communis* (Jones et al., 2003). Epidermal strips were treated with a number of purified *endo*glycanases. Normal guard cell function was then tested using fusicoccin and either abscisic acid (ABA) or external osmoticant (i.e. mannitol) which induced stomatal opening and stomatal closure, respectively.

Treatment of guard cells with a purified (1,5)-α-L-*endo*arabinanase disrupted their ability to open in the presence of fusicoccin. This effect could be blocked by pre-incubating epidermal strips with the arabinan/AGP-binding antibody LM6. A similar effect on stomatal opening was seen (to a lesser extent) when guard cells were treated with a feruloyl esterase. In contrast, treatment of guard cells with both the *endo*polygalacturonase (EPGase) and the pectin methylesterase (PME) caused greater stomatal opening compared to untreated cells, while treatment of the guard cells with either the EPGase or the PME alone had very little effect on stomatal opening.

Guard cells incubated with (1,5)-α-L-*endo*arabinanase or with feruloyl esterase also failed to close in the presence of ABA or mannitol. No effect on stomatal closure was observed in cells treated with both EPGase and PME. However, (1,5)-α-L-*endo*arabinanase or feruloyl esterase-treated guard cells closed normally after they were treated with both EPGase and PME. These results suggest that the disruption of arabinan chains from RG-I disrupt normal guard cell

function and that this effect may be due to the increased association of HGA chains following arabinan digestion.

The exact roles of pectic polysaccharides in the wall are still poorly understood. The study of pectin structure mutants or the directed alteration of pectin structures during physiological events will greatly aid in our understanding of pectin function. These studies, coupled with the discovery of pectin biosynthetic genes, should allow us to acquire a more complete picture of the role of pectin in the wall and its physiological function in the plant.

BIOSYNTHESIS

Pectic polysaccharides are synthesized in the Golgi apparatus

Pectin was hypothesized to be synthesized in the Golgi as early as the 1960's (Northcote and Pickett-Heaps, 1966). Autoradiographical analysis of plant tissues incubated with radiolabeled glucose demonstrated the appearance of radiolabeled D-Gal*p*, L-Ara*f*, and D-Gal*p*A associated with the Golgi fraction from pea (Ray, 1967; Harris and Northcote, 1971), oat (*Arena sativa*) (Ray, 1967) and wheat (*Triticum aestivum*) (Northcote and Pickett-Heaps, 1966). Immunocytochemistry studies using antibodies such as JIM5 (Knox et al., 1990) and JIM7 (Zhang and Staehelin, 1992) confirmed these results and suggested that HGA was synthesized in the cis and medial Golgi stacks, with methyl-esterification and pectin branching occurring in the medial to trans Golgi (Zhang and Staehelin, 1992; Vicre et al., 1998). Pectins are believed to be packaged into vesicles and secreted into the cell wall in a highly esterified form (Zhang and Staehelin, 1992; Carpita and Gibeaut, 1993; Dolan et al., 1997), although this observation may be dependent on the cell and/or tissues that are examined (Lynch and Staehelin, 1992; Dolan et al., 1997).

Recent enzymatic evidence demonstrating the subcellular localization of pectin biosynthetic enzymes (Sterling et al., 2001; Geshi et al., 2004) supports the Golgi apparatus as the proposed site for pectin biosynthesis (Mohnen, 2002). The first enzymatic evidence for the subcellular localization and topology of a pectin biosynthetic glycosyltransferase was conducted using pea epicotyl membranes (Chapter 3). An α-(1,4)-D-galacturonosyltransferase (GalAT) involved in HGA biosynthesis was shown to co-localize with Golgi membrane markers in both linear and discontinuous sucrose gradients. Proteinase K protection experiments confirmed that the catalytic site of the enzyme faced the lumen of the Golgi apparatus. Similar results were obtained for a β-(1,4)-D-galactosyltransferase (GalT) from potato involved in RG-I β-D-galactan biosynthesis (Geshi et al., 2004), and a HGA methyltransferase from tobacco (Goubet and Mohnen, 1999a). Subcellular fractionations of French (*Phaseolus vulgaris*; (Bolwell and Northcote, 1983) and mung (*Vigna radiata* var. *radiata*) (Nunan and Scheller, 2003) bean membranes using discontinuous sucrose density gradient centrifugation indicated the presence of Golgi-resident arabinosyltransferase activity in these systems. The presence of Golgi-localized galactosyltransferase activity thought to be involved in the biosynthesis of RG-I side chains has also been identified in pea (Baydoun et al., 2001) and radish (Kato et al., 2003) seedlings and in flax (*Linum usitatissimum*) suspension cultured cells (Goubet and Morvan 1993). These results demonstrate that pectin biosynthetic transferases are Golgi-localized and that the primary site for pectin biosynthesis is in the Golgi apparatus.

Nucleotide sugars appear to be the activated sugar donors for pectin biosynthetic glycosyltransferase activity (Hassid et al., 1959; Hassid, 1967; Brett and Waldron, 1990; Mohnen, 2002). The biosynthesis of nucleotide sugars is thought to occur mainly in the cytosol via the action of nucleotide-sugar interconverting enzymes (Seifert et al., 2004a), although recent

studies have suggested that nucleotide biosynthesis may also occur in the Golgi (Hayashi et al., 1988; Harper and Bar-Peled, 2002; Burget et al., 2003). Nucleotide sugars made in the cytosol gain access into the lumen of the Golgi via the action of Golgi-localized nucleotide sugar transporters (Munoz et al., 1996; Baldwin et al., 2001; Norambuena et al., 2002; Seifert et al., 2002).

The biosynthesis of pectin is likely to involve the coordinated action of close to 100 proteins, including nucleotide-sugar interconverting enzymes (NIEs), nucleotide sugar transporters (NSTs), and a variety of methyl-, acetyl- and glycosyltransferases (Figure 1.7). Due to the intricate relationship between pectin structure and function, increased efforts have been made to identify pectin biosynthetic genes. This section will detail what is currently known about pectin biosynthesis, with an emphasis on the identification of genes that are known, or hypothesized, to be involved in this process.

Nucleotide-sugar substrates are required for pectin biosynthesis

Early experiments testing the substrate specificities of pectin glycosyltransferases have shown that nucleotide-sugars are the activated sugar substrates for these enzymes (Hassid et al., 1959; Hassid, 1967). At least 12 different nucleotide-sugar substrates are required to produce all of the known pectic structures (O'Neill et al., 2004). The activated sugar forms of most of these nucleotide-sugars are known; however, those of D-Dha*p* and L-Ace*f*A have yet to be discovered (Mohnen, 2002).

The synthesis of nucleotide-sugars in plants occurs via the interconversion of existing nucleotide-sugars by NIEs (Figure 1.8; Reiter and Vanzin, 2001; Seifert, 2004) or via the activation of monosaccharides by sugar kinases and pyrophosphorylases (the salvage pathway; Feingold and Avigad, 1980). NIEs are thought to be responsible for the production of

Figure 1.7. Proposed model of pectin biosynthesis. A representative picture of a plant cell is drawn, showing several Golgi stacks and a close-up of an individual Golgi cisterna. A) Pectin biosynthesis occurs in the Golgi apparatus. B) Nucleotide-sugars are synthesized in the cytosol by nucleotide-sugar interconverting enzymes (NIE). Membrane-associated activity has also been detected for several NIEs (Feingold and Barber, 1990) and several genes encoding NIEs have putative transmembrane domains (Harper and Bar-Peled, 2002; Burget et al., 2003). The subcellular localization and topology of these membrane-bound NIEs is largely unknown (the catalytic site can be cytosolically or lumenally oriented); however, MUR4 has been shown to associate with the Golgi (Burget et al., 2003) and a UDP-D-GlcA decarboxylase has been shown to co-localize with Golgi membranes and to have its catalytic site facing the Golgi lumen (Hayashi et al., 1988). C) Nucleotide-sugars made in the cytosol are transported into the Golgi apparatus by nucleotide-sugar transporters (NSTs). These proteins catalyze the specific import of nucleotide-sugars in an equimolar exchange for NMP (Hirschberg et al., 1998). D) Golgi lumenal pectin glycosyl- (GlyT), acetyl-, and methyltransferases (M/AT), with a predicted type II membrane topology (Gleeson, 1998), catalyze the formation of pectic polysaccharides (Sterling et al., 2001; Geshi et al., 2004). E) UDP released from nucleotide-sugars by the action of glycosyltransferases is hydrolyzed by a Golgi lumenal nucleoside diphosphatase (NDPase) into the corresponding nucleoside monophosphate (Orellana et al., 1997; Neckelmann and Orellana, 1998). F) Synthesized pectic polysaccharides are packaged into Golgi-derived vesicles, sent to the plasma membrane and ultimately fuse with it, releasing their contents into the cell wall.

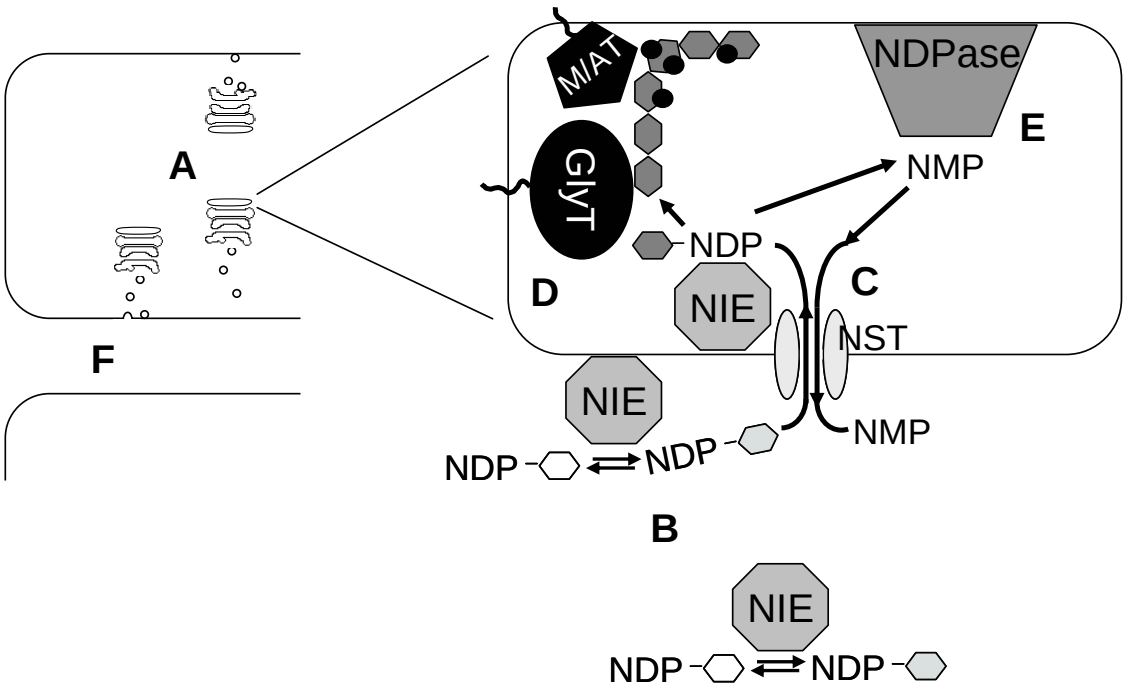
A
F
M/AT
GlyT
NDPase
E
NMP
NDP
D
NIE
C
NST
NIE
NMP
NDP
NDP
B
NIE
NDP
NDP

Figure 1.8. Simplified nucleotide-sugar interconversion pathways in plants. Most of the nucleotide-sugars involved in pectin biosynthesis can be made through the interconversion of UDP-D-Glc*p* or GDP-D-Man*p*. The genes involved in the interconversion of nucleotide sugars are shown adjacent to the reactions they catalyze. The function of the RHM gene has not been demonstrated, although it is thought to be involved in the biosynthesis of UDP-L-Rha*p*. A) Nucleotide-sugars that arise from the conversion of UDP-D-Glc*p*. B) Nucleotide-sugars that arise from the conversion of GDP-D-Man*p*. UGE, UDP-D-Glc*p* 4-epimerase; RHM, NDP-L-Rha*p* biosynthetic gene; NRS/ER, UDP-4-keto-6-deoxy-D-Glc 3',5'-epimerase-4-reductase (NDP-L-Rha*p* synthase/epimerase-reductase); UGD, UDP-D-Glc*p* dehydrogenase; GAE, UDP-D-Glc*p*A 4-epimerase; UXS, UDP-D-Glc*p*A decarboxylase (UDP-D-Xyl*p* synthase); AXS, UDP-D-Api*f*/UDP-D-Xyl*p* synthase; MUR4, UDP-D-Xyl*p* 4-epimerase; GMD, GDP-D-mannose 4,6-dehydratase; GER, GDP-4-keto-6-deoxy-D-Man 3',5'-epimerase-4-reductase; GME, GDP-D-Man*p* 3',5'-epimerase.

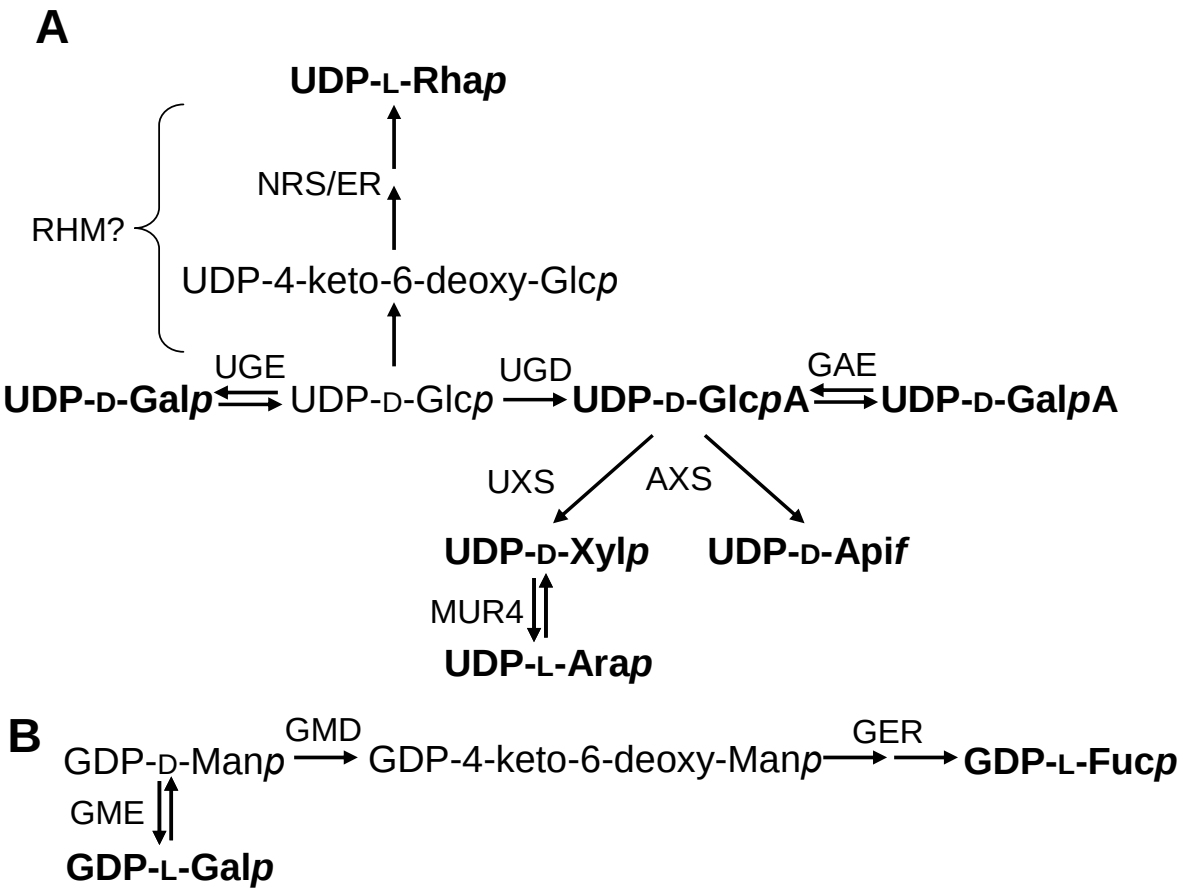
A
UDP-L-Rhap
NRS/ER
RHM?
UDP-4-keto-6-deoxy-Glcp
UGE
UGD
GAE
UDP-D-Galp
UDP-D-Glcp
UDP-D-GlcpA
UDP-D-GalpA
UXS
AXS
UDP-D-Xylp
UDP-D-Apif
MUR4
UDP-L-Arap
B
GMD
GER
GDP-D-Manp
GDP-4-keto-6-deoxy-Manp
GDP-L-Fucp
GME
GDP-L-Galp

the majority of the nucleotide-sugars required for pectin biosynthesis (Mohnen, 1999; Reiter and Vanzin, 2001; Seifert, 2004). Nucleotide-sugar interconversion starts with either UDP-D-Glc*p* or GDP-D-Man*p* produced by the activation of either α-D-Man*p*-1-phosphate or α-D-Glc*p*-1-phosphate into the corresponding NDP-sugar (Figure 1.8). Through the actions of several enzymes, UDP-D- Gal*p*, UDP-L-Rha*p*, UDP-D-Glc*p*A, UDP-D-Gal*p*A, UDP-D-Xyl*p*, UDP-L-Ara*p*, UDP-D-Api*f*, GDP-L-Fuc*p*, and GDP-L-Gal*p* can be synthesized (Hassid et al., 1959; Feingold and Avigad, 1980; Feingold and Barber, 1990).

Plant extracts have been shown to salvage free D-Gal*p*, D-Glc*p*A, D-Gal*p*A, D-Xyl*p*, and L-Ara*f* and L-Fuc*p* released as a result of metabolic processes into the corresponding sugar-1-phosphate by C-1 kinases (Hassid et al., 1959; Feingold and Avigad, 1980). Pyrophosphorylases then convert the sugar-1-phosphates into NDP-sugars in the presence of the appropriate NTP. It is commonly believed that the salvage pathway is used mainly in the recycling of monosaccharides from the cell wall (Feingold and Avigad, 1980; Mohnen, 2002). However, recent studies on the conversion of *myo*-inositol into UDP-D-Glc*p*A (Seitz et al., 2000) suggest that the salvage pathway may play a role in the tissue-specific biosynthesis of some nucleotide-sugars (Figure 1.9, B). In light of these results, certain aspects of the salvage pathway will be considered in this section. For a more detailed summary of the salvage pathways in plants, the reader is directed to several excellent reviews (Hassid et al., 1959; Hassid, 1967; Feingold and Avigad, 1980; Feingold and Barber, 1990).

The synthesis of CMP-D-Kdo*p* (Figure 1.9, A) is unique in that it does not involve the interconversion of existing nucleotide-sugars and instead starts with the condensation of D-Ara*p*-5-phosphate and phosph*enol*pyruvate (PEP) to form D-Kdo*p*-8-phosphate (Doong et al., 1991).

Figure 1.9. Biosynthesis of CMP-D-Kdo*p* and an alternative method for the biosynthesis of UDP-D-Glc*p*A in plants. A) CMP-D-Kdo*p* is synthesized from D-Ara*p*-5-phosphate and phospho*enol*pyruvate by the action of Kdo-8-phosphate synthase (KDSA). The enzyme encoding Kdo-8-phosphate phosphorylase has not been identified in plants. The gene encoding CMP-Kdo synthetase (CKS) has been isolated from maize and its ability to catalyze the conversion of D-Kdo*p* and CTP into CMP-D-Kdo*p* has been confirmed (Royo et al., 2000). B) *myo*-inositol can be converted into D-Glc*p*A by *myo*-inositol oxygenase (MIOX). D-Glc*p*A can then be converted into UDP-D-Glc*p*A by the sequential action of (1) D-glucuronokinase and (2) UDP-GlcA pyrophosphorylase. The activities of these two enzymes have been detected in plant extracts; however, no genes encoding these enzymes have been identified.

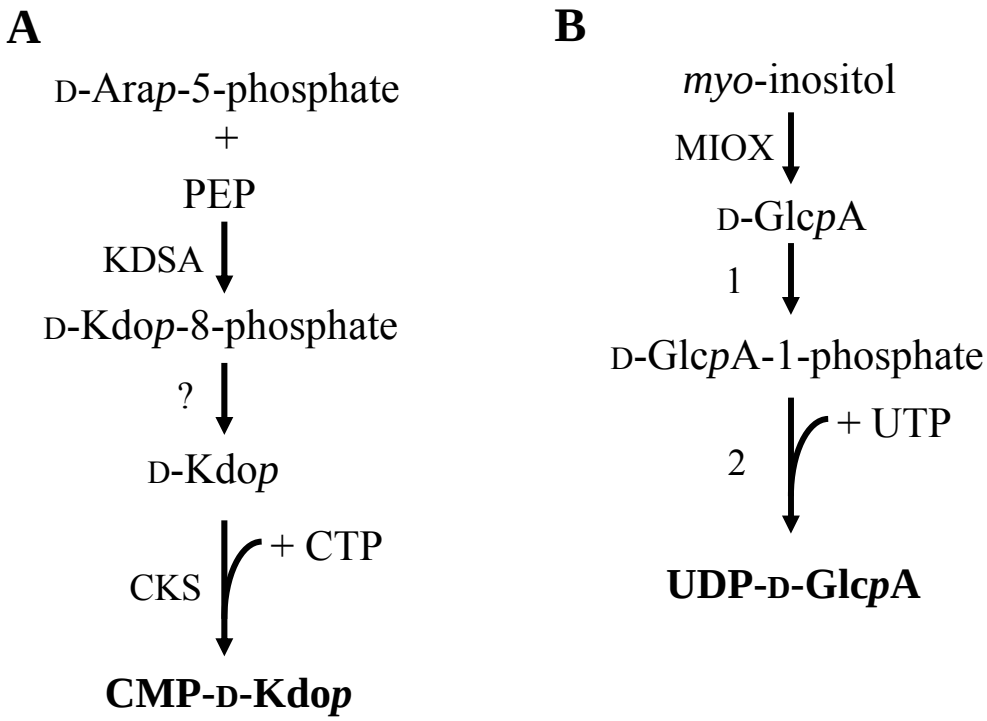

D-Kdo*p*-8-phosphate is then dephosphorylated (Wu and Woodard, 2003) and converted into CMP-D-Kdo*p* in the presence of CTP (Royo et al., 2000).

The recent identification and characterization of a number of NIEs has greatly enhanced our understanding of the synthesis of these substrates. Proof of their activity has been demonstrated in most cases by heterologous expression. Our current understanding of the biosynthesis of each activated sugar substrate will be considered in this section.

*UDP-D-Gal*p*:* UDP-Glc 4-epimerase (EC 5.1.3.2) catalyzes the reversible conversion of UDP-D-Glc*p* to UDP-D-Gal*p*. The reaction involves the transfer of a hydride ion from the C-4 of the sugar moiety to an enzyme-bound NAD^+, creating a 4-keto intermediate. The non-stereospecific return of the hydride ion to the 4-keto intermediate causes the formation of either UDP-D-Glc*p* or UDP-D-Gal*p*.

$$\text{E-NAD}^+ + \text{UDP-D-Glc}p \rightleftharpoons \text{E-NADH} + \text{UDP-4-keto-Glc}p \rightleftharpoons \begin{matrix}\text{E-NAD}^+ + \text{UDP-D-Gal}p \\ \text{E-NAD}^+ + \text{UDP-D-Glc}p\end{matrix} \quad (1)$$

Soluble and membrane-bound UDP-Glc 4-epimerase activity could be detected in several plant species (Feingold and Avigad, 1980) and was purified 1000-fold from wheat germ (Fan and Feingold, 1969). The first gene encoding an active UDP-Glc 4-epimerase (UGE1) was isolated from an Arabidopsis cDNA library by searching for genes that had sequence similarity to cloned UDP-Glc 4-epimerases from rat and bacteria (Table 1.2; Dormann and Benning, 1996). The cDNA encoded a 39 kDa protein that could partially complement a *Saccharomyces cerevisiae* mutant (*gal10*) deficient in its ability to grow on galactose as a sole carbon source. The recombinantly expressed protein purified from *Escherichia coli* was active in the absence of exogenous NAD^+, had a K_m for UDP-D-Glc*p* of 0.11 mM, and a V_{max} of 3.96 mmol min^{-1} mg^{-1}

Table 1.2. Putative and identified UDP-Glc 4-epimerase genes in plants

Gene name	Plant source	Protein accession	Protein size (kDa)[a]	Function confirmed[b]	Apparent K_m for UDP-D-Glc*p* (mM)	V_{max} (mmol min^{-1} mg^{-1})	pH optimum	References
UGE1	Arabidopsis	CAA90941	39	Complementation/ Activity	0.11	3.96	7.0-9.5	(Dormann and Benning, 1996)
UGE2	Arabidopsis	CAB43892	38	Unpublished	ND[c]	ND	ND	(Reiter and Vanzin, 2001)
UGE3	Arabidopsis	AAG51599	39	Unpublished	ND	ND	ND	(Reiter and Vanzin, 2001)
UGE4	Arabidopsis	AAG51709	38	Activity	ND	ND	ND	(Reiter and Vanzin, 2001) (Seifert et al., 2002)
UGE5	Arabidopsis	CAB40064	39	No	ND	ND	ND	(Reiter and Vanzin, 2001)
GALE1	Pea	AAA86532	39	No	ND	ND	ND	(Lake et al., 1998)
GEPI42	Guar seeds	CAA06338	39	Complementation	ND	ND	ND	(Joersbo et al., 1999)
GEPI48	Guar seeds	CAA06339	38	Complementation	ND	ND	ND	(Joersbo et al., 1999)

[a]Molecular weight deduced by the amino acid sequence.

[b]The function of certain genes has been confirmed by activity assays of recombinantly expressed protein (activity) or by complementation of UDP-Glc 4-epimerase mutants (complementation).

[c]ND: not determined.

(Dormann and Benning, 1996). Antisense suppression of UGE1 expression in Arabidopsis caused a 90% reduction in UDP-Glc 4-epimerase activity in stems, yet these plants had no discernable phenotype when compared to wildtype plants (Dormann and Benning, 1998). Transgenic plants overexpressing UGE1 had 3-fold higher levels of UDP-Glc 4-epimerase activity in leaves and grew normally in the presence of toxic levels of galactose (Dormann and Benning, 1998). Putative UDP-Glc 4-epimerases have also been isolated from pea (Lake et al., 1998) and from developing guar (*Cyamopsis tetragonoloba*) seeds (Joersbo et al., 1999). The function of the gene from pea has not been confirmed; however, the two cDNA's from guar seeds were identified by functional complementation of a UDP-Glc 4-epimerase mutant of *E. coli*, suggesting that they encode functional UDP-Glc 4-epimerases (Table 1.2).

Analysis of the Arabidopsis genome revealed the presence of 4 open reading frames (UGE2-5) with 65-89% amino acid sequence identity to UGE1 (Reiter and Vanzin, 2001). UGE isoforms have been shown by β-glucuronidase (GUS) fusions to be differentially expressed in Arabidopsis roots (Seifert et al., 2004a). The gene encoding UGE4 is allelic to the Arabidopsis mutants root-epidermal-bulger 1 (Reiter and Vanzin, 2001; Seifert et al., 2002) and root hair development 1 (Schiefelbein and Somerville, 1990) that are characterized by bulging root epidermal cells. The bulging of these cells is most likely due to altered levels of galactose in epidermal cell wall polymers; evidenced by the differential visualization of wildtype and root hair development 1 (*rdh1*) plants using antibodies that recognize galactose-containing epitopes (Seifert et al., 2002). The *rdh1* phenotype can be corrected by growing plants on galactose (Seifert et al., 2002) or in the presence of ethylene (Seifert et al., 2004a). Ethylene treatment reduces the expression of UGE1 and UGE3 in roots and causes wildtype staining of specific galactose-containing epitopes found on arabinogalactans and xyloglucans. The staining of other

galactose-containing epitopes, such as those recognized by LM5, is even more reduced in ethylene-treated *rdh1* plants, suggesting that the limited UDP-D-Gal*p* pool is preferentially used for the synthesis of arabinogalactans and xyloglucan, instead of the synthesis of the (1,4)-linked β-D-galactan chains found on RG-I. These results led the authors to speculate that specific UGE isoforms are involved in the channeling of the UDP-D-Gal*p* pool into specific polysaccharide synthase complexes that synthesize cell wall polymers (Seifert et al., 2002; Seifert et al., 2004a). Evidence supporting the existence of glycosyltransferase-glycosyltransferase and glycosyltransferase-NST enzyme complexes involved in glycoconjugate production has been obtained using mammalian cell lines (Opat et al., 2000; Bieberich et al., 2002; Sprong et al., 2003); however, substrate channeling may not be the sole explanation for the effect of ethylene treatment on the Arabidopsis *rdh1* mutant.

Differences in cell surface glycosyl residue composition have also been well documented in NST mutants of yeast and mammalian cell lines (Deutscher and Hirschberg, 1986; Hirschberg et al., 1998; Kawakita et al., 1998). Mutation of the NST in these cell lines resulted in the reduction of the nucleotide-sugars accessible to the Golgi-localized glycosyltransferases. This has led some researchers to speculate that the differences in glycosyl residue content and composition at the cell surface of NST mutant lines were due to differences in the affinities of the Golgi-localized glycosyltransferases (K_m) for their nucleotide-sugar substrates (Kawakita et al., 1998). Glycosyltransferases with the lowest K_m for a particular nucleotide-sugar substrate would sequester the available nucleotide-sugar pool for the production of specific carbohydrate epitopes (Kawakita et al., 1998) and cause these epitopes to be detected at the cell surface.

Such a scenario could also be occurring in *rdh1* mutants of Arabidopsis. Mutations in *rdh1* reduce the amount of UDP-D-Gal*p* synthesized in the root, causing cell wall

glycosyltransferases to compete for the available pool of UDP-D-Gal*p*. This competition causes changes to occur in the carbohydrate epitopes detected on the root cell surface (Seifert et al., 2002). The down-regulation of UGE1 and UGE3 by ethylene treatment most likely causes a further reduction in the UDP-D-Gal*p* pool in the root, thereby allowing only glycosyltransferases involved in the synthesis of arabinogalactan or xyloglucan polymers to utilize this pool for the production of galactose-containing cell wall polysaccharides (Seifert et al., 2004a). The cloning, characterization, and mutation of specific cell wall polysaccharide glycosyltransferases, NIEs and NSTs may be required before the question of UDP-D-Gal*p* substrate channeling can be solved.

*UDP-D-Glc*p*A*: The synthesis of UDP-D-Glc*p*A is an integral part of pectin biosynthesis as nucleotide sugars derived from it comprise as much as 40% of the primary wall of plants (Zablackis et al., 1995). The main pathway for the production of UDP-D-Glc*p*A is thought to be through the dehydrogenation of UDP-D-Glc*p* catalyzed by UDP-Glc dehydrogenase (EC 1.1.1.22). The reaction is irreversible, proceeds via a UDP-α-D-gluco-hexodialdose intermediate, and produces 2 moles of NADH per mole of UDP-D-Glc*p*A in the process (Nelsestuen and Kirkwood, 1971).

$$\text{UDP-D-Glc}p \xrightarrow{2\ \text{NAD}^+ \;\rightarrow\; 2\ \text{NADH}} \text{UDP-D-Glc}pA \qquad (2)$$

Soluble UDP-Glc dehydrogenase activity was purified from germinating lily pollen (Davies and Dickinson, 1972), soybean nodules (Stewart and Copeland, 1998), sugarcane (Turner and Botha, 2002), and pea seedlings (Strominger and Mapson, 1957). A protein with UDP-Glc dehydrogenase activity was also purified from elicitor-treated French bean cell cultures (Robertson et al., 1996). This protein had characteristics that differed from the other UDP-Glc

dehydrogenases (Table 1.3). Furthermore, the UDP-Glc dehydrogenase activity from French bean co-purified with alcohol dehydrogenase activity, which led some researchers to speculate that the 40 kDa protein purified from French bean was an alcohol dehydrogenase and not a UDP-Glc dehydrogenase (Tenhaken and Thulke, 1996).

A cDNA with high sequence identity to bovine UDP-Glc dehydrogenase (61%) was identified in soybean (Tenhaken and Thulke, 1996). The cDNA encoded a 52.9 kDa protein that was inactive when expressed recombinantly in *E. coli*. Antibodies raised against the recombinant protein could immunoprecipitate UDP-glucose dehydrogenase activity from soybean extracts in a concentration-dependent manner, suggesting that the gene (UDP-GlcDH; Table 1.4) encoded an active UDP-Glc dehydrogenase. Northern analysis showed that UDP-GlcDH was highly expressed in root tips and lateral roots, with moderate expression in epicotyls and expanding leaves.

Genes with high sequence identity to soybean UDP-GlcDH were also identified in Arabidopsis (Seitz et al., 2000; Reiter and Vanzin, 2001) and poplar (*Populus tremula*; Johannson et al., 2002). The function of these putative UDP-Glc dehydrogenase genes has not been confirmed (Table 1.4); however, the expression pattern of UGD1 from Arabidopsis is similar to that of soybean UDP-GlcDH (Seitz et al., 2000).

UDP-D-Glc*p*A is a competitive inhibitor of UDP-Glc dehydrogenase (Strominger and Mapson, 1957; Davies and Dickinson, 1972; Stewart and Copeland, 1999; Turner and Botha, 2002). All eukaryotic UDP-Glc dehydrogenases are also cooperatively inhibited by UDP-D-Xyl*p* (Feingold and Avigad, 1980). This latter feature of UDP-Glc dehydrogenase may be part of a feedback inhibition mechanism involved in the control of UDP-D-Glc*p*A synthesis and nucleotide sugars that can be derived from it (Feingold and Avigad, 1980).

Table 1.3. Properties of purified UDP-Glc dehydrogenases from plants

Plant source	Fold purification	Protein size (kDa)[a]	Apparent K_m for UDP-D-Glc*p* (mM)	V_{max} (μmol min^{-1} mg^{-1})	pH optimum	References
Lily pollen	12	ND[b]	0.3	ND	8.7	(Davies and Dickinson, 1972)
Soybean	62	47	0.051	ND	8.4	(Stewart and Copeland, 1998)
Sugarcane	197	52	0.019	2.17	8.4	(Turner and Botha, 2002)
Pea	1000	ND	0.07	ND	9	(Strominger and Mapson, 1957)
French bean	341	40	5.5	ND	ND	(Robertson et al., 1996)

[a]Molecular weight estimated by SDS-PAGE.

[b]ND: not determined.

Table 1.4. Putative and identified plant UDP-Glc dehydrogenase genes.

Gene name	Plant source	Protein accession	Protein size (kDa)[a]	Function confirmed[b]	References
UDP-GlcDH	soybean	Q96558	53	Immunoprecipitation	(Tenhaken and Thulke, 1996)
UGD1	Arabidopsis	NP_198748	53	ND[c]	(Seitz et al., 2000; Reiter and Vanzin, 2001)
UGD2	Arabidopsis	NP_189582	53	ND	(Reiter and Vanzin, 2001)
UGD3	Arabidopsis	NP_197053	53	ND	(Reiter and Vanzin, 2001)
UGD4	Arabidopsis	NP_173979	53	ND	(Reiter and Vanzin, 2001)
UGDH	poplar	AAF04455	53	ND	(Johansson et al., 2002)

[a]Molecular weight deduced by the amino acid sequence.

[b]The function of UDP-GlcDH from soybean has been confirmed by immunoprecipitation of UDP-Glc dehydrogenase activity from soybean extracts.

[c]ND: not determined.

UDP-D-Glc*p*A can also be synthesized through the conversion of *myo*-inositol into D-Glc*p*A (Figure 1.9, B). Whole plants or extracts from parsley (*Petroselinum crispum*) leaves and strawberry (*Fragaria ananassa*) fruits can convert radioactive *myo*-inositol into radioactive pectin (Loewus and Kelly, 1963). Roughly 40% of the radioactivity from parsley leaves and strawberry fruits is found in D-Gal*p*A, D-Xyl*p*, L-Ara*f*, and D-Glc*p*A, and this conversion is performed without rearrangement or cleavage of the carbon chain of *myo*-inositol (Loewus and Kelly, 1963).

Myo-inositol is produced in plants via the conversion of D-Glc-6-P or phytic acid by *myo*-inositol-1-P synthetase or phytase, respectively (Loewus and Loewus, 1983). Both enzymes produce *myo*-inositol-1-P which is then converted into *myo*-inositol by inositol monophosphatase (IMP; EC 3.1.3.25). Three genes encoding IMPs have been cloned from tomato and shown to be active by recombinant expression in *E. coli* (Gillaspy et al., 1995).

Myo-inositol oxygenase (MIOX; EC 1.13.99.1) converts *myo*-inositol into D-Glc*p*A (Figure 1.9, B). A gene encoding a *myo*-inositol oxygenase (MIOX4) was recently cloned from Arabidopsis (Lorence et al., 2004). Recombinant MIOX4 expressed in *E. coli* could convert *myo*-inositol into D-Glc*p*A with a specific activity of 2.2 μmol min^{-1} mg^{-1}. MIOX4 is highly expressed in leaf and flower tissue and is part of a 4 member gene family in Arabidopsis (Table 1.5).

D-Glc*p*A applied to plant extracts or produced by MIOX can be converted into UDP-D-Glc*p*A by sequential action of D-glucuronokinase (EC 2.7.1.43) and UDP-GlcA pyrophosphorylase (EC 2.7.7.44). The activity of both enzymes have been detected in mung bean seedlings (Feingold et al., 1958; Neufeld et al., 1961). UDP-GlcA pyrophosphorylase activity has been purified 80-fold from barley (*Hordeum vulgare*) seedlings (Roberts, 1971).

Table 1.5. Putative and cloned MIOX genes from Arabidopsis.

Gene name	Protein accession	Protein size (kDa)[a]	Function confirmed[b]	References
MIOX1	NP_172904	37	Activity	(Lorence et al., 2004)
MIOX2	NP_565459	37	ND[c]	(Lorence et al., 2004)
MIOX4	NP_194356	37	ND	(Lorence et al., 2004)
MIOX5	NP_200475	37	ND	(Lorence et al., 2004)

[a]Molecular weight deduced by amino acid sequence.

[b]The function of MIOX4 has been confirmed by activity assays of the recombinantly expressed protein (activity) in *E. coli*.

[c]ND: not determined.

The protein had an estimated molecular weight of 35 kDa by size exclusion chromatography, had a K_m for UDP-D-Glc*p*A of 0.5 mM, and pH optimum of 8-9. No genes encoding either D-glucuronokinase or UDP-GlcA pyrophosphorylase have been cloned from any plant source.

It has been hypothesized that the conversion of *myo*-inositol into UDP-D-Glc*p*A may be a major pathway involved in the synthesis of this nucleotide-sugar (Roberts, 1971; Loewus and Loewus, 1983). Firstly, UDP-Glc dehydrogenase activity can not be detected in some plant species (Feingold and Avigad, 1980). Secondly, it has been shown that the incubation of Arabidopsis seedlings with [^{3}H]*myo*-inositol causes the incorporation of radioactivity into areas of the plant where UGD1 expression is absent, such as the hypocotyl and the cotyledons (Seitz et al., 2000). The incubation of Arabidopsis seedlings with *myo*-inositol does not change the level of UGD1 expression, suggesting that the synthesis of UDP-D-Glc*p*A may occur through different biochemical pathways in different parts of the plant or during specific developmental stages. Alternatively, the differential locations of these two biochemical pathways may reflect their involvement in different plant processes. For example, UGD1 and UDP-GlcDH are highly expressed in the root, which is the major site of D-Glc*p*A uptake by the plant (Hassid, 1967; Feingold and Avigad, 1980). *Myo*-inositol, on the other hand, is a precursor for the biosynthesis of L-ascorbic acid in leaves, flowers and other above-ground organs (Smirnoff et al., 2001; Agius et al., 2002; Lorence et al., 2004). Plants fed [^{3}H]*myo*-inositol may be converting the surplus *myo*-inositol into UDP-D-Glc*p*A (and ultimately pectin) as a means of controlling the production of L-ascorbic acid in above-ground tissues. Although it is commonly believed that the dehydrogenation of UDP-D-Glc*p* is the main pathway involved in the production of UDP-D-Glc*p*A, further research into the role of the *myo*-inositol pathway needs to be conducted in order to determine its role in pectin biosynthesis.

*UDP-D-Gal*p*A*: UDP-D-Gal*p*A is the source of the most abundant glycosyl residue found in pectic polysaccharides (Mohnen, 2002). It is synthesized by the reversible 4-epimeration of UDP-D-Glc*p*A catalyzed by UDP-GlcA 4-epimerase (EC 5.1.3.6; Neufeld et al., 1958). The catalytic mechanism of UDP-GlcA 4-epimerase is similar to that of UDP-Glc 4 epimerase and proceeds via the oxidation of the C-4 of UDP-D-Glc*p*A by an enzyme bound $NAD(P)^+$ resulting in a 4-keto intermediate (Feingold and Avigad, 1980). Subsequent non-stereospecific reduction of the 4-keto group causes the production of equimolar concentrations of UDP-D-Glc*p*A and UDP-D-Gal*p*A.

$$E\text{-}NAD^+ + UDP\text{-}D\text{-}Glc\textit{p}A \rightleftharpoons E\text{-}NADH + UDP\text{-}4\text{-}keto\text{-}Glc\textit{p}A \rightleftharpoons E\text{-}NAD^+ + UDP\text{-}D\text{-}Gal\textit{p}A \quad (3)$$

UDP-GlcA 4-epimerase activity was first identified in particulate fractions from mung bean, and later detected in membrane fractions from asparagus (*Asparagus officinalis*), radish and spinach (Neufeld et al., 1958; Feingold et al., 1960). Enzyme activity was later found to also be associated with soluble fractions from mung bean (Feingold et al., 1960). Membrane-bound activities were also found in radish roots (Liljebjelke et al., 1995) and Arabidopsis leaves (Molhoj et al., 2004). Soluble UDP-D-Glc*p*A 4-epimerase was partially purified from the blue-green algae *Anabaena flos-aquae* (Gaunt et al., 1974). The partially purified enzyme had a pH optimum of 8.5, a K_m for UDP-D-Glc*p*A of 37 μM, and an approximate molecular weight of 54 kDa. The enzyme was also allosterically inhibited by UDP-D-Xyl*p* (Gaunt et al., 1974).

A gene encoding an active UDP-GlcA 4-epimerase (GAE1) was recently cloned from Arabidopsis and expressed recombinantly in *Pichia pastoris* (Molhoj et al., 2004). GAE1 was identified by screening the Arabidopsis genome for sequences that were similar to a UDP-GlcA 4-epimerase (Cap1J) from *Streptococcus pneumoniae* (Munoz et al., 1999). Recombinant GAE1

reacted with UDP-D-Glc*p*A producing roughly equimolar concentrations of UDP-D-Gal*p*A and UDP-D-Glc*p*A. The enzyme had a pH optimum of 7.6, a K_m for UDP-D-Glc*p*A of 0.19 mM and was inactive on UDP-D-Glc*p* and UDP-D-Xyl*p*. GAE1 activity was significantly inhibited by UDP-D-Xyl*p*, a property that was associated with the partially purified enzyme from *A. flos-aquae*. GAE1 activity was not dependent on the presence of divalent cations, nor on the exogenous addition of $NAD(P)^+$, suggesting that the recombinant enzyme contained a tightly bound nicotinamide derivative. GAE1:β-glucuronidase fusions suggested that GAE1 was expressed in all major tissues of Arabidopsis (Molhoj et al., 2004).

GAE1 is part of a 6 member gene family in Arabidopsis (Table 1.6; Reiter and Vanzin, 2001). All GAE genes are predicted type II membrane proteins and have an N-terminal extension that encodes a putative transmembrane domain (Reiter and Vanzin, 2001; Molhoj et al., 2004). While the absolute topology of any GAE gene has not been determined, recombinant GAE1 activity associates only with the membrane fraction from *P. pastoris*. Soluble UDP-GlcA 4-epimerase activity was not detected in Arabidopsis leaves, contrary to results obtained from mung bean seedlings. At this point, it is not known whether the soluble UDP-GlcA 4-epimerase activity represents a different subset of proteins in these tissues, or whether the soluble enzymes are produced by proteolytic events that occur during tissue preparation. The isolation of UDP-GlcA 4-epimerase genes from different plant species will allow us to determine whether soluble isoforms of these enzymes exist in other plants.

*UDP-D-Xyl*p: UDP-D-Xyl*p* is produced by the irreversible decarboxylation of UDP-D-Glc*p*A that is catalyzed by UDP-GlcA decarboxylase (EC 4.1.1.35). The reaction mechanism for plant UDP-GlcA decarboxylases was investigated (Schutzbach and Feingold, 1970) using the purified enzyme from wheat germ (Ankel and Feingold, 1965). The reaction commences with

Table 1.6. Putative and cloned UDP-GlcA 4-epimerases from Arabidopsis.

Gene name	Protein accession	Protein size (kDa)[a]	Function confirmed[b]	References
GAE1	NP_194773	47	Activity	(Reiter and Vanzin, 2001; Molhoj et al., 2004)
GAE2	NP_171702	48	ND[c]	(Reiter and Vanzin, 2001)
GAE3	NP_191922	48	ND	(Reiter and Vanzin, 2001)
GAE4	NP_182056	49	ND	(Reiter and Vanzin, 2001)
GAE5	NP_192962	48	ND	(Reiter and Vanzin, 2001)
GAE6	NP_189024	51	ND	(Reiter and Vanzin, 2001)

[a]Molecular weight deduced by amino acid sequence.

[b]The function of MIOX4 has been confirmed by activity assays of the recombinantly expressed protein (activity) in *P. pastoris*.

[c]ND: not determined.

the oxidation of C-4 by an enzyme-bound NAD^+ producing a 4-keto intermediate. The irreversible decarboxylation of C-5 on the intermediate occurs with the release of CO_2. The stereospecific reduction of the C-5 and the 4-keto group by a proton from water and by an enzyme-bound NADH, respectively, produces UDP-D-Xyl*p* as the final product.

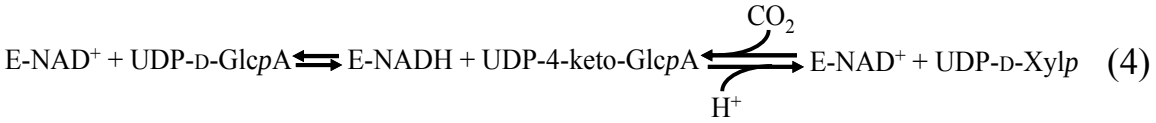

(4)

All plant UDP-GlcA decarboxylases are allosterically inhibited by UDP-D-Xyl*p* and do not require the addition of exogenous NAD^+ for activity (John et al., 1977; Hayashi et al., 1988; Harper and Bar-Peled, 2002). UDP-GlcA decarboxylase activity from wheat germ is also allosterically activated by low concentrations of UDP-D-Glc*p*A (John et al., 1977). The inhibition of NIEs by UDP-D-Xyl*p* has also been demonstrated for UDP-Glc dehydrogenase, and suggests that the synthesis of UDP-D-Xyl*p* may be one of the main regulatory factors controlling the production of many of the nucleotide-sugars involved in pectin biosynthesis (John et al., 1977; Harper and Bar-Peled, 2002).

UDP-GlcA decarboxylase exists in many plant species as both soluble and membrane-bound isoforms (Table 1.7). Activity was first detected in particulate fractions from mung bean, and later detected in membrane fractions from radish, asparagus and spinach (Neufeld et al., 1958; Feingold et al., 1960). Soluble UDP-GlcA decarboxylase was first purified from wheat germ by Ankel and Feingold (1965). The enzyme was later found to exist in wheat germ as two different 210 kDa isoforms that differed in their binding to DEAE-cellulose, kinetic properties, and response to allosteric effectors (John et al., 1977).

Table 1.7. Properties of purified plant UDP-GlcA decarboxylases.

Plant source	Fold purification	Protein size (kDa)	Apparent K_m for UDP-D-Glc*p*A (mM)	pH optimum	References
Wheat germ (soluble)	350	ND[a]	0.3	6.8-7.0	(Ankel and Feingold, 1965)
Wheat germ (soluble isoform 1)	1056	210[b]	0.18	~7	(John et al., 1977)
Wheat germ (soluble isoform 2)	117	210[b]	0.53	~7	(John et al., 1977)
Pea (soluble)	780	41, 42[c] (250)[b]	ND	5-6	(Kobayashi et al., 2002)

[a]ND: not determined.

[b]Molecular weight estimated by size exclusion chromatography.

[c]Molecular weight determined by SDS-PAGE.

Hayashi et al. (1988) demonstrated that membrane-bound UDP-GlcA decarboxylase activity co-localized with the Golgi apparatus following linear and discontinuous sucrose gradient centrifugation. They further demonstrated that decarboxylation of UDP-D-Glc*p*A only occurred within intact Golgi vesicles. These results provided the first evidence that some nucleotide-sugar interconversions occurred within the lumen of the Golgi apparatus.

The first plant gene encoding a UDP-GlcA decarboxylase was identified following the purification of a soluble decarboxylase from pea seedlings (Kobayashi et al., 2002). The purified pea enzyme was comprised of two identical polypeptides that differed slightly in their migration by SDS-PAGE. The pea UDP-GlcA decarboxylase gene (PsUXS1) was cloned from a pea cDNA library using degenerate primers made against internal peptide sequences (Table 1.8). The N-terminus of the deduced amino acid sequence of PsUXS1 was found to be 26 amino acids longer than that of the purified protein, suggesting that UDP-GlcA decarboxylase from pea underwent some form of post-translational modification. PsUXS1 expressed in *E. coli* was able to convert UDP-D-Glc*p*A into UDP-D-Xyl*p* without the addition of exogenous NAD^+. The native, recombinant protein (320 kDa) was significantly larger than the purified pea protein (250 kDa), but suggested that both enzyme forms existed as high molecular weight, oligomeric complexes. Northern analysis showed that PsUXS1 was expressed in pea roots, stems, and leaves.

Five putative UXS genes (UXS1-5) were identified in Arabidopsis by searching for gene homologs to a cloned UDP-GlcA decarboxylase from *Crytococcus neoformans* (Table 1.8; Harper and Bar-Peled, 2002). Sequence analysis suggested that UXS1, 2 and 4 had putative N-terminal transmembrane domains and encoded putative type II membrane proteins. Recombinant expression of N-terminally truncated UXS1 and 2 (lacking the transmembrane

Table 1.8. Putative and cloned plant UDP-GlcA decarboxylases.

Gene name	Plant source	Protein accession	Protein size (kDa)[a]	Function confirmed[b]	References
PsUXS1	pea	BAB40967	39	Activity	(Kobayashi et al., 2002)
UXS1	Arabidopsis	NP_190920	48	Activity	(Harper and Bar-Peled, 2002)
UXS2	Arabidopsis	NP_191842	50	Activity	(Harper and Bar-Peled, 2002)
UXS3	Arabidopsis	NP_200737	39	Activity	(Harper and Bar-Peled, 2002)
UXS4	Arabidopsis	NP_182287	50	ND[c]	(Harper and Bar-Peled, 2002)
UXS5	Arabidopsis	NP_190228	38	ND	(Harper and Bar-Peled, 2002)
SUD3	Arabidopsis	NP_180443	39	ND	(Reiter and Vanzin, 2001)

[a]Molecular weight deduced by amino acid sequence.

[b]The function of UXS genes have been confirmed by activity assays of the recombinantly expressed protein (activity) in *E. coli*.

[c]ND: not determined.

domain) and full length UXS3 demonstrated that all three genes encoded active UDP-GlcA decarboxylases. Recombinant UXS3 was inactive on UDP-D-Glc*p*, UDP-D-Gal*p*, and UDP-D-Gal*p*A, was inhibited by UDP-D-Xyl*p*, and did not require the addition of exogenous NAD^+ for activity. Reverse transcriptase-PCR analysis demonstrated that UXS1, 2 and 3 were expressed in stem, root, flower, and leaf tissues of Arabidopsis.

The UXS genes were also identified in Arabidopsis by searching for sequences that had high similarity to a 4,6-dehydratase from *E. coli* (rmlB; Reiter and Vanzin, 2001). This search identified one additional gene named SUD3 (soluble UDP-GlcA decarboxylase 3) that had high sequence identity to the UXS genes (Seifert, 2004). The function of SUD3, UXS4 and UXS5 has not yet been elucidated.

*UDP-L-Ara*p: UDP-L-Ara*p* is synthesized by the reversible 4-epimerization of UDP-D-Xyl*p* catalyzed by UDP-Xyl 4-epimerase (EC 5.1.3.5) in a reaction mechanism that is thought to be identical to that of UDP-Glc and UDP-GlcA 4-epimerases (Feingold and Avigad, 1980).

$$\text{E-NAD}^+ + \text{UDP-D-Xyl}p \rightleftharpoons \text{E-NADH} + \text{UDP-4-keto-Xyl}p \rightleftharpoons \text{E-NAD}^+ + \text{UDP-L-Ara}p \quad (5)$$

UDP-Xyl 4-epimerase activity was first detected in membrane fractions from mung bean, radish, asparagus, and spinach (Neufeld et al., 1958; Feingold et al., 1960). The partially purified enzyme from wheat germ and could catalyze the conversion of UDP-D-Xyl*p* to UDP-L-Ara*p* without the addition of exogenous NAD^+, had a K_m for UDP-D-Xyl*p* of 1.5 mM, and a pH optimum of 8.0 (Fan and Feingold, 1970).

A mutant in Arabidopsis, *mur4*, was discovered that had a 50% reduction in L-Ara*f* content in leaves (Burget and Reiter, 1999). Wildtype MUR4 expressed in the *mur4* mutant background could complement the L-Ara*f* deficiency and allowed for the recovery of up to 2.4-fold higher levels of L-Ara*f* in some transgenic lines (Burget et al., 2003). Expression of MUR4

in *P. pastoris* demonstrated that the gene encoded a functional UDP-Xyl 4-epimerase. Examination of the MUR4 gene indicated that it contained a putative N-terminal transmembrane domain and encoded a predicted type II membrane protein (Burget et al., 2003). MUR4:green fluorescent protein fusions showed that the Mur4 protein co-localized with Golgi membranes. The topology of MUR4 was not investigated. MUR4 is expressed in roots, leaves, stems, flowers and siliques, and is part of a 4 member gene family in Arabidopsis (Table 1.9; Burget et al., 2003).

While L-Ara*p* is present as a minor component of rhamnogalacturonan II, the majority of the L-arabinose found in pectin is in the form of L-Ara*f* (Feingold and Avigad, 1980; Mohnen, 2002). It is currently unclear as to how L-Ara*f* gets incorporated into plant cell walls. A bacterial enzyme known as UDP-galactopyranose mutase is capable of converting UDP-D-Gal*p* into UDP-D-Gal*f* (Koplin et al., 1997). This enzyme was also shown to be able to convert chemically-synthesized UDP-L-Ara*f* into UDP-L-Ara*p* (Zhang and Liu, 2001). However, the existence of UDP-L-Ara*f* has not been demonstrated in any plant species, making it unlikely that this mechanism exists in plants.

It has been proposed that arabinosyltransferases may catalyze the conversion of UDP-L-Ara*p* into UDP-L-Ara*f* immediately before their incorporation into L-Ara*f*-containing polymers (Mohnen, 2002). It has also been hypothesized that L-Ara*p* ring contraction can occur directly on the synthesized polymers (Feingold and Avigad, 1980). The recent discovery that an arabinosyltransferase from mung bean adds L-Ara*p* to arabinan acceptors (Nunan and Scheller, 2003) may be proof that the latter scenario occurs in plant cell walls. The exact mechanism(s) that accounts for the presence of L-Ara*f* in plant cell walls remains to be proven.

Table 1.9. Putative and cloned UDP-Xyl 4-epimerases[a] and UDP-apiose/UDP-xylose synthases[b] from Arabidopsis.

Gene name	Protein accession	Protein size (kDa)[c]	Function confirmed[d]	References
MUR4/UXE1[a]	NP_174350	46	Activity	(Burget et al., 2003)
UXE2[a]	NP_193779	42	ND[e]	(Burget et al., 2003)
UXE3[a]	NP_850238	26	ND	(Burget et al., 2003)
UXE4[a]	NP_199261	48	ND	(Burget et al., 2003)
AXS1[b]	NP_180353	44	Activity	(Molhoj et al., 2003)
AXS2[b]	NP_563807	44	ND	(Molhoj et al., 2003)

[c]Molecular weight deduced by amino acid sequence.

[d]The function of MUR4/UXE1 has been confirmed by activity assays of the recombinantly expressed protein (activity) in *P. pastoris* or in *E. coli*.

[e]ND: not determined.

*UDP-D-Api*f: A soluble, NAD^+-dependent enzyme known as UDP-D-Api*f*/UDP-D-Xyl*p* synthase (AXS) is capable of catalyzing the decarboxylation and rearrangement of UDP-D-Glc*p*A to produce approximately equimolar concentrations of UDP-D-Api*f* and UDP-D-Xyl*p* (Sandermann et al., 1968; Wellmann and Grisebach, 1971; Baron et al., 1973; Kindel and Watson, 1973; Watson and Orenstein, 1975; Matern and Grisebach, 1977). The initial stages of the reaction are identical to that of UDP-GlcA decarboxylase and proceeds with the formation of a 4-keto intermediate and decarboxylation of C-5 (Gebb et al., 1975). AXS then either catalyzes the reduction of C-4 or the further rearrangement of the intermediate producing UDP-D-Xyl*p* or UDP-D-Api*f*, respectively (Kindel and Watson, 1973; Watson and Orenstein, 1975). The exact mechanism(s) involved in the rearrangement of the intermediate to produce UDP-D-Api*f* is unknown (Molhoj et al., 2003).

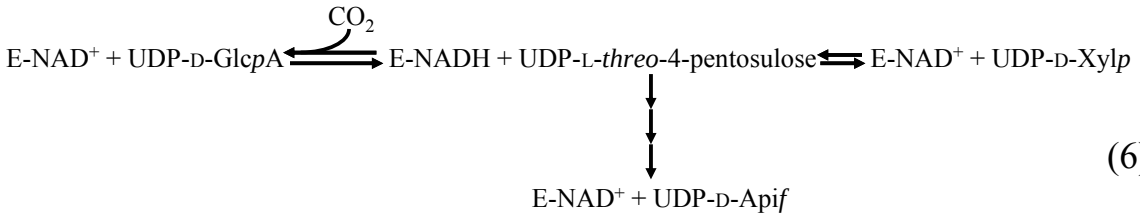

(6)

AXS activity has been partially purified from duckweed and parsley (Wellmann and Grisebach, 1971; Baron et al., 1973; Kindel and Watson, 1973; Matern and Grisebach, 1977). AXS activity from duckweed was purified 26-fold and had a pH optimum of 8.0. The enzyme was purified 1,400-fold from parsley cell suspensions, yielding two proteins of 34 and 44 kDa in size. Both proteins were thought to form homodimers of approximately 65 and 86 kDa, however, only the 86 kDa protein complex was shown to possess AXS activity. The role of the 65 kDa complex was not elucidated, but it was thought to be involved in maintaining the stability of AXS.

AXS genes were cloned from Arabidopsis by searching for genes with sequence similarity to UDP-GlcA decarboxylases (Molhoj et al., 2003). Two genes were identified with 29% amino acid identity to UXS3 (Table 1.9). Recombinant AXS1 in *E. coli* existed as a dimer and was capable of catalyzing the production of UDP-D-Api*f* and UDP-D-Xyl*p* at a ratio of 0.6:1. The K_m and V_{max} of recombinant AXS1 for UDP-D-Glc*p*A was 7 μM and 3.1 nmol min^{-1} mg^{-1}, respectively. The enzyme had a pH optimum of 8.0, was inhibited by UDP-D-Gal*p*A and UDP-D-Xyl*p*, and did not require an exogenous supply of NAD^+ for activity. AXS1::GUS fusions and RT-PCR analysis suggested that AXS1 was expressed in all major tissues of Arabidopsis.

*UDP-L-Rha*p: The preferred nucleotide-sugar donor for the production of rhamnose-containing flavonoids and other plant secondary metabolites is UDP-L-Rha*p* (Barber, 1963; Bar-Peled et al., 1991; Bar-Peled et al., 1993; Jones et al., 2003). Enzyme activities capable of converting UDP-D-Glc*p* into UDP-L-Rha*p* have been detected in mung bean (Barber, 1962), tobacco (Barber, 1963), pummelo (*Citrus maxima*) (Bar-Peled et al., 1991), *Chlorella pyrenoidosa* (Barber and Chang, 1967), and *Silene dioica* (Kamsteeg et al., 1978). Bacteria such as *Streptococcus enterica* and *E. coli* use dTDP-L-Rha*p* as the nucleotide sugar donor for O-antigen biosynthesis (Stevenson et al., 1994; Li and Reeves, 2000; Dong et al., 2003). dTDP-L-Glc*p* has been found in some plant tissues (Delmer and Albersheim, 1970) and can be converted into dTDP-L-Rha*p* by tissue extracts from *C. pyrenoidosa* at a lower rate than UDP-D-Glc*p*. Since both UDP-L-Rha*p* and dTDP-L-Rha*p* can be found in plants, it is not known which of these activated sugar donors are involved in pectin biosynthesis.

The conversion of UDP-D-Glc*p* into UDP-L-Rha*p* (or dTDP-D-Glc*p* into dTDP-L-Rha*p*) requires three separate enzyme activities (Mohnen, 1999). UDP-D-Glc*p* is first converted into UDP-4-keto-6-deoxy-Glc*p* by (a) an NADH-dependent, UDP-Glc 4,6-dehydratase (EC 4.2.1.76)

(Barber, 1963). This reaction has been proposed to start with the transfer of a hydride ion from the C-4 of the sugar moiety to an enzyme-bound NAD^+, creating a 4-keto intermediate. The removal of the hydride ion from C-5 by an enzyme bound Glu residue, followed by the elimination of water and stereospecific return of NADH-bound hydride to C-6, results in the formation of the intermediate UDP-4-keto-6-deoxy-Glc*p* (Allard et al., 2001). This intermediate is then epimerized into UDP-4-keto-L-Rha*p* and finally reduced to UDP-L-Rha*p* by (b) UDP-4-keto-6-deoxy-Glc*p* 3,5-epimerase and (c) an NADPH-dependent, UDP-4-keto-L-Rha*p* reductase, respectively (Watt et al., 2004). The reaction mechanism of the 3,5-epimerase has not been determined, while that of the 4-reductase involves hydride transfer from NADPH to the 4-keto group. In bacteria, these reactions are catalyzed by RmlB, RmlC, and RmlD, respectively (Dong et al., 2003).

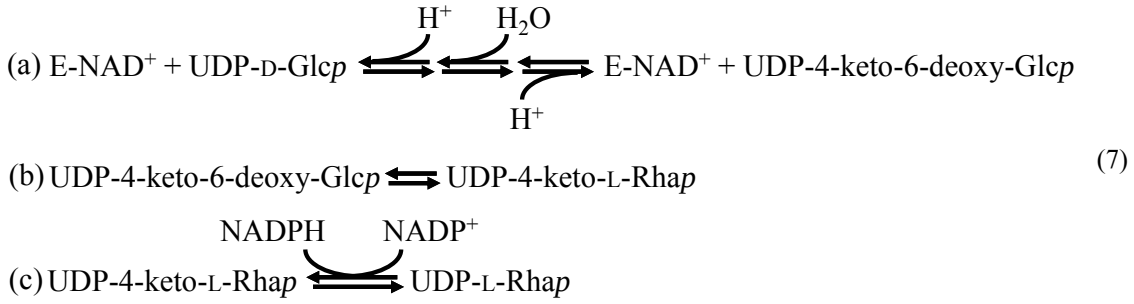

(7)

The first gene encoding a UDP-L-Rha*p* synthase was cloned from Arabidopsis (Watt et al., 2004) by searching for genes with high sequence similarity to dTDP-4-keto-rhamnose reductases from *S. enterica* and *E. coli* (Graninger et al., 1999; Dong et al., 2003). The Arabidopsis gene product had 40% sequence identity to RmlD from *S. enterica* and *E. coli*. The gene expressed in *E. coli* was capable of converting the intermediate dTDP-4-keto-6-deoxy-Glc*p* into dTDP-L-Rha*p*, and was named nucleotide-rhamnose synthase/epimerase-reductase (NRS/ER1) because it possessed both 3,5-epimerase and 4-keto reductase activity (Table 1.10).

The 35 kDa recombinant protein required NADPH for activity, had a pH optimum between 5.5-7.5, and a K_m for dTDP-4-keto-6-deoxy-Glc*p* of 17 μM. Recombinant Nrs/Er1 protein could also convert UDP-4-keto-6-deoxy-Glc*p* into UDP-L-Rha*p*, but the amount of starting substrate was too low to allow for the determination of enzyme kinetics. Genes with high sequence identity to NRS/ER1 have been identified in a number of other plant species, including cotton (*Gossypium arboreum*), wheat, loblolly pine (*Pinus taeda*), soybean, barley, barrel medic (*Medicago truncatula*), maize, rice, and sugar beet. NRS/ER1 is expressed in Arabidopsis leaves, flowers, roots, and stems, and has significant sequence identity to the C-terminal domains of three other genes (RHM1-3) in Arabidopsis (Watt et al., 2004).

These three genes from Arabidopsis were also identified in a database search looking for genes with sequence similarity to a dTDP-Glc*p* 4,6-dehydratase gene (RmlB) from *E. coli* (Reiter and Vanzin, 2001). The genes, named RHM1, RHM2, and RHM3 (Table 1.11) are >84% identical (at the amino acid level) and are thought to consist of two distinct domains. The N-terminal domain has sequence similarity to dTDP-Glc*p* 4,6-dehydratase (RmlB) from *E. coli*, while the C-terminal domain is identical to the 3,5-epimerase/4-keto-reductase of Nrs/Er1 from Arabidopsis and is similar to a 4-keto reductase (RmlD) from *E. coli*. Based on the sequence similarity of Rhm1, Rhm2, and Rhm3 to 4,6-dehydratases, 3,5-epimerases and 4-keto reductases, the authors speculated that the Rhm proteins were capable of catalyzing the direct conversion of UDP-D-Glc*p* into UDP-L-Rha*p* without the need for any additional enzymes (Reiter and Vanzin, 2001; Seifert, 2004).

Recently, mutants in the RHM2 gene were identified by a high-throughput screen of EMS-mutagenized Arabidopsis seeds (Western et al., 2001) and by screening T-DNA mutant lines of Arabidopsis (Usadel et al., 2004). Both mutants were found to be deficient in the

Table 1.10. Putative and cloned UDP-L-Rha*p* synthases from Arabidopsis.

Gene name	Protein accession	Protein size (kDa)[a]	Function confirmed[b]	References
NRS/ER1	NP_564806	34	Activity	(Watt et al., 2004)
RHM1	NP_188097	75	ND[c]	(Watt et al., 2004)
RHM2	NP_564633	75	ND	(Watt et al., 2004)
RHM3	NP_177978	75	ND	(Watt et al., 2004)

[a]Molecular weight deduced by amino acid sequence.

[b]The function of NRS/ER1 has been confirmed by activity assays of the recombinantly expressed protein (activity) in *E. coli*.

[c]ND: not determined.

production of seed mucilage, the pectin-rich polysaccharide coat found surrounding the seed after imbibition (Western et al., 2001; Usadel et al., 2004). *Rhm2* mutants synthesized lower amounts of mucilage than wildtype seeds. Furthermore, composition analysis showed that the extractable mucilage from *rhm2* mutant seeds was significantly reduced in L-Rha*p* and D-Gal*p*A content, a phenotype consistent with the involvement of RHM2 in L-Rha*p* biosynthesis (Usadel et al., 2004; Western et al., 2004). Expression analysis shows that all three RHM genes are expressed in all major tissues of Arabidopsis (Western et al., 2004). At present, the activity of any RHM protein has not been confirmed.

*GDP-L-Fuc*p: GDP-L-Fuc*p* is synthesized from GDP-D-Man*p* in a pathway that is identical to the one used for the production of UDP-L-Rha*p*. GDP-D-Man*p* is converted into GDP-L-Fuc*p* through the sequential actions of a) GDP-Man 4,6-dehydratase (EC 4.2.1.47), b) GDP-4-keto-6-deoxy-Man*p* 3,5-epimerase, and c) GDP-4-keto-L-Fuc*p* reductase. GDP-Man 4,6-dehydratase activity was purified 47-fold from soluble extracts of French bean seedlings (Liao and Barber, 1972). The purified protein had an estimated molecular weight of 120 kDa, a K_m for GDP-D-Man*p* of 28 μM, and a pH optimum between 6.6 and 7.1.

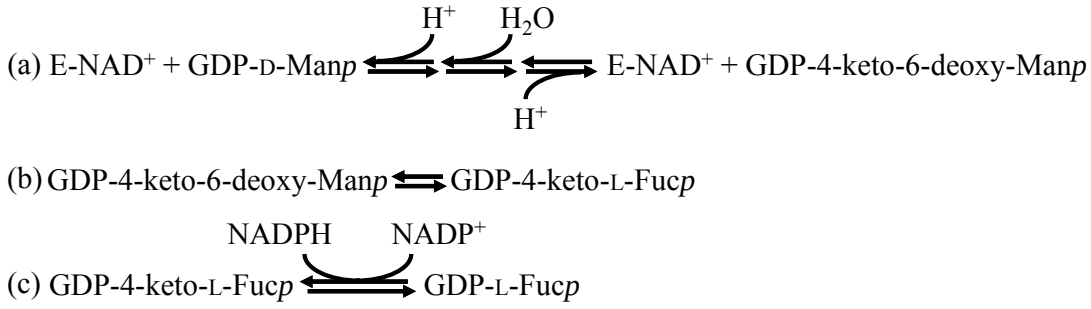

(8)

The first plant gene encoding a GDP-Man 4,6-dehydratase was identified following the isolation of the fucose-deficient mutant of Arabidopsis, *mur1* (Reiter et al., 1993; Zablackis et

al., 1996). Further analysis of soluble leaf extracts from *mur1* plants revealed that they were unable to catalyze the first step of the GDP-L-Fuc*p* biosynthesis pathway (Bonin et al., 1997). A BLAST search of the Arabidopsis EST database revealed two sequences, named GMD1 and GMD2, with high sequence similarity to bacterial GDP-Man 4,6-dehydratases (Table 1.11). The *mur1* mutation was found to co-segregate with GMD2 and PCR analysis confirmed that all *mur1* alleles were a result of point mutations in GMD2 (Bonin et al., 1997). GMD1 (Bonin et al., 2003) or GMD2 (Bonin et al., 1997) expressed in *E. coli* were active and could convert GDP-D-Man*p* into the GDP-4-keto-6-deoxy-Man*p* intermediate.

Expression analysis of GMD1 and GMD2 showed that the two genes were differentially expressed in Arabidopsis (Reiter and Vanzin, 2001). Promoter:GUS fusions showed that GMD2 was expressed in all major tissues of Arabidopsis, while GMD1 expression was restricted primarily to the root meristem, leaf stipules, and pollen grains. These expression patterns are consistent with the *mur1* phenotype and suggest that GMD1 and GMD2 may play different roles in the production of GDP-L-Fuc*p* in Arabidopsis (Bonin et al., 2003).

A single gene encoding a bi-functional GDP-4-keto-6-deoxy D-mannose 3,5-epimerase-4-reductase (GER1, EC 1.1.1.271) was identified by searching the Arabidopsis EST database for homologs to putative bacterial enzymes (Bonin and Reiter, 2000). Recombinantly expressed GER1 was active and could convert the GDP-4-keto-6-deoxy-D-Man*p* intermediate into GDP-L-Fuc*p*. Incubation of GDP-D-Man*p* with recombinant GMD2 and GER1 was also found to cause the production of GDP-L-Fuc*p* (Bonin and Reiter, 2000).

GER1 is expressed in all major tissues of Arabidopsis; however, GER1 antisense lines have wildtype levels of L-fucose in their walls (Bonin and Reiter, 2000). BLAST analysis indicates the presence of an Arabidopsis gene, named GER2, with significant sequence identity

Table 1.11. Putative and cloned GDP-L-Fuc*p*[a] and GDP-L-Gal*p*[b] synthases from Arabidopsis.

Gene name	Protein accession	Protein size (kDa)[c]	Function confirmed[d]	References
GMD1[a]	NP_201429	41	Activity	(Bonin et al., 2003)
GMD2/MUR1[a]	NP_190685	42	Activity	(Bonin et al., 1997)
GER1[a]	NP_177468	36	Activity	(Bonin and Reiter, 2000)
GER2[a]	NP_564040	36	ND[e]	(Bonin and Reiter, 2000)
GME1[b]	NP_198236	43	Activity	(Wolucka et al., 2001)

[c]Molecular weight deduced by amino acid sequence.

[d]The function of these proteins has been confirmed by activity assays of the recombinantly expressed protein (activity) in *E. coli*.

[e]ND: not determined.

to GER1 (Table 1.11). This gene is also highly expressed in Arabidopsis, but its function has not yet been proven.

*GDP-L-Gal*p: L-Gal*p* was originally thought to be a minor component of the cell walls of a limited number of plant species including the hornwort *Anthoceros caucasicus* (Popper et al., 2003) and jojoba (*Simmodsia chinensis*) seeds (Hantus et al., 1997). Recent structural analysis now indicates that L-Gal*p* is a constituent of RG-II (Reuhs et al., 2004).

GDP-L-Gal*p* is the activated nucleotide-sugar form of L-Gal*p*. It is synthesized by the 3,5-epimerization of GDP-D-Man*p* by GDP-Man 3,5-epimerase (EC 5.1.3.18). The reaction is thought to proceed with 4-keto oxidation, ene-diol formation at either C-3 or C-5, followed by inversion of configuration at each site, and finally stereospecific reduction of the 4-keto group (Barber, 1979). It is currently not known which of the reduced nicotinamide-adenine dinucleotides (NAD+ or NADP+) is found at the active site of GDP-Man 3,5-epimerase. Furthermore, the order of epimerization (3' followed by 5' or vice versa) has not been established. The nucleotide-sugar that results from a single epimerization event at C-5, GDP-L-gulopyranose (GDP-L-Gul*p*), has been detected in extracts from *Chlorella pyrenoidosa* (Barber, 1979) and Arabidopsis (Wolucka and Van Montagu, 2003). These results suggest that the epimerization occurs first at the C-5 of GDP-D-Man*p*, followed by epimerization at C-3.

$$\text{E-NAD(P)}^{+} + \text{GDP-D-Man}p \rightleftharpoons \text{GDP-L-Gul}p? \rightleftharpoons \text{E-NAD(P)}^{+} + \text{GDP-L-Gal}p \quad (9)$$

GDP-Man 3,5-epimerase activity has been detected in several plants including soluble extracts from *Chlorella pyrenoidosa* (Barber, 1979; Hebda et al., 1979) and pea (Wheeler et al., 1998). The enzyme was purified 66-fold from Arabidopsis seedlings (Wolucka et al., 2001). The purified protein had a K_m for GDP-L-Man*p* of 4.5 μM and a V_{max} of 0.033 μmol/min/mg.

In-gel digestion of two partially purified protein bands (43 and 46 kDa) resulted in peptides that matched a putative 43 kDa Arabidopsis protein. Further analysis showed that the partially purified 43 and 46 kDa proteins were post-translationally modified isoforms of the same protein (Wolucka et al., 2001). The 43 kDa protein sequence expressed in E. coli was active and could catalyze the conversion of GDP-D-Man*p* into GDP-L-Gul*p* and GDP-L-Gal*p* (Wolucka and Van Montagu, 2003). BLAST searches indicated that the gene (GME1; Table 1.11) is conserved in other plant species including tomato and potato (Wolucka and Van Montagu, 2003).

*CMP-D-Kdo*p: CMP-D-Kdo*p* is synthesized in a series of reactions that starts with the condensation of phosph*oeno*lpyruvate (PEP) and D-Ara*p*-5-phosphate by (a) Kdo-8-phosphate synthase (EC 4.1.2.16) to form D-Kdo*p*-8-phosphate (Kdo-8-P). Kdo-8-P is dephosphorylated by (b) Kdo-8-P phosphatase (EC 3.1.3.45) and the D-Kdo*p* that is released is converted in the presence of CTP into CMP-D-Kdo*p* by (c) CMP-Kdo synthetase (EC 2.7.7.38). The catalytic mechanisms of all three enzymes have not been fully elucidated (Royo et al., 2000a).

(a) D-arabinose-5-phosphate + PEP $\xrightarrow{P_i}$ Kdo-8-phosphate

(b) Kdo-8-phosphate $\xrightarrow{P_i}$ Kdo (10)

(c) Kdo + CTP $\xrightarrow{PP_i}$ CMP-Kdo

Kdo-8-P synthase activity has been detected in tissue extracts from potato, carrot, cucumber (*Cucumis sativus*), broccoli (*Brassica oleracea* var. *italica*), onion (*Allium cepa*), and sweet potato (*Ipomoea batatas*), and spinach (Doong et al., 1991). The first gene encoding a Kdo-8-P synthase was cloned from a pea cDNA library by functional complementation of the temperature sensitive *kdsA*^{ts} mutant of *S. enterica* (Brabetz et al., 2000). The 290 amino acid recombinant protein catalyzed the formation of Kdo-8-P in *in vitro* assays, caused a 7-fold

increase in Kdo-8-P synthase activity in recombinant *kdsA*^{ts} cell extracts, and had a pH optimum of 6.1. Similar results were obtained by the functional complementation of the *kdsA*^{ts} mutant by a tomato gene isolated from a young fruit cDNA library (Delmas et al., 2003). Site-directed mutagenesis of the tomato gene also revealed the presence of essential amino acids known to be required for bacterial Kdo-8-P synthase activity (Delmas et al., 2003).

BLAST analysis of the Arabidopsis genome database detected two genes, named AtKDS1 and AtKDS2, with sequence similarity to a Kdo-8-P synthase from *E. coli* (Matsuura et al., 2003). Heterologous expression of AtKDS1 in *E. coli* showed that the recombinant protein could catalyze the formation of Kdo-8-P. The tomato and Arabidopsis Kdo-8-P synthase genes are expressed in meristematic cells of roots and shoots suggesting that they are active during cell wall formation (Table 1.12).

Genes encoding Kdo-8-P phosphatases have not been isolated from any plant species; however, it has been shown that spinach extracts rapidly convert Kdo-8-P into D-Kdo*p* (Doong et al., 1991). A gene encoding an active Kdo-8-P phosphatase was recently purified and cloned from *E. coli* (Wu and Woodard, 2003). Based on the functional conservation of plant and bacterial Kdo-8-P synthases (Brabetz et al., 2000; Delmas et al., 2003) and CMP-Kdo synthetases (Royo et al., 2000), it is likely that the Kdo-8-P phosphatase from E. coli can be used to identify candidate genes from plants.

A gene encoding an active CMP-Kdo synthetase was isolated from a maize endosperm cDNA library (Table 1.12; Royo et al., 2000). The maize gene, named ZmCKS, expressed in *E. coli* catalyzed the formation of CMP-D-Kdo*p* at a pH optimum of 9.5 and a K_m for CTP of 70 μM. ZmCKS could also functionally complement the *kdsB*^{ts} mutant of *Salmonella typhimurium*.

Table 1.12. Putative and cloned Kdo-8-P synthases[a] and CMP-Kdo synthetases[b] from plants

Gene name	Plant source	Protein accession	Protein size (kDa)[c]	Function confirmed[d]	References
PsKDS[a]	pea	CAA74645	32	Complementation/ Activity	(Brabetz et al., 2000)
LeKDS[a]	tomato	CAC35366	32	Complementation/ Activity	(Delmas et al., 2003)
AtKDS1[a]	Arabidopsis	NP_974176	32	Activity	(Matsuura et al., 2003)
AtKDS2[a]	Arabidopsis	NP_173084	32	ND[e]	(Matsuura et al., 2003)
ZmCKS[b]	maize	CAB89846	33	Complementation/ Activity	(Royo et al., 2000)

[c]Molecular weight deduced by amino acid sequence.

[d]The function of these proteins have been confirmed by functional complementation of temperature-sensitive mutants of S. enterica (complementation) and activity assays of the recombinantly expressed protein (activity).

[e]ND: not determined.

ZmCKS is expressed in all major tissues of maize (Royo et al., 2000). Furthermore, genes with high sequence similarity to ZmCKS have been detected in Arabidopsis, loblolly pine tomato, rice, wheat, and barley (Royo et al., 2000; Royo et al., 2000a). All putative plant CMP-Kdo synthetases differ from bacterial enzymes in that they are predicted to have an N-terminal signal sequence that targets them to the endomembrane system (Royo et al., 2000a). The. subcellular location of ZmCKS or any other putative CMP-Kdo synthetase has yet to be determined.

*XXP-*D*-Dha*p *and XXP-*L*-Ace*f*A*: The enzymes and/or pathways involved in synthesizing D-Dha*p*, L-Ace*f*A, or their activated nucleotide-sugar forms have not been determined. It has been hypothesized that plant 2-keto-3-deoxy-D-*arabino*-heptulosonic acid-7-P (DAH-7-P) synthases may be able to catalyze the condensation of D-threose-4-P and PEP to form D-Dha*p*-7-P (Doong et al., 1992), a precursor of D-Dha*p*. At present, the absolute configuration of the product from this reaction is not known (Doong et al., 1992). Further research on the synthesis of D-Dha*p* and L-Ace*f*A will be required before their biosynthetic pathways can be elucidated.

Nucleotide sugar transporters involved in pectin biosynthesis

The results from the previous section suggest that the nucleotide-sugar biosynthesis occurs mainly in the cytosol. Nucleotide-sugar transporters (NSTs) are multiple-membrane spanning, antiport proteins that transfer nucleotide-sugars into the lumen of the endoplasmic reticulum (ER) or the Golgi in exchange for their corresponding nucleotide-monophosphates (Hirschberg et al., 1998). Many NSTs are specific for only one type of nucleotide-sugar, while others, such as the GDP-D-Man*p* transporter from *Leishmania* (Hong et al., 2000) and the UDP-D-Gal*p* transporter from humans and Drosophila (Segawa et al., 2002) are able to transport more than one type of nucleotide-sugar. The study of NSTs has recently gained prominence with the

discovery that NST mutants are defective in protein glycosylation (Dean et al., 1997; Ma et al., 1997), have altered cell surface decorations (Deutscher and Hirschberg, 1986; Kawakita et al., 1998; Hoeflich et al., 2004), and can result in developmental defects (Berninsone et al., 2001).

Genes encoding NSTs have been identified in yeast (Dean et al., 1997), *Leishmania donovani* (Ma et al., 1997), mammals (Deutscher and Hirschberg, 1986; Hirschberg et al., 1998; Aoki et al., 2003), *Drosophila melanogaster* (Segawa et al., 2002), *Caenorhabditis elegans* (Berninsone et al., 2001; Hoeflich et al., 2004), and *Arabidopsis thaliana* (Baldwin et al., 2001; Norambuena et al., 2002; Bakker et al., 2004; Handford et al., 2004). The transport of GDP-L-Fuc*p* (Wulff et al., 2000), UDP-D-Glc*p* (Munoz et al., 1996), UDP-D-Gal*p* (Norambuena et al., 2002), UDP-D-Glc*p*A, and UDP-D-Xyl*p* (Hayashi et al., 1988) has been shown to occur in pea Golgi vesicles, and plant genes encoding NSTs have recently been identified and cloned. This section will describe what is currently known about NST genes from plants that are involved in pectin biosynthesis.

*UDP-D-Glc*p*/UDP-D-Gal*p *transporter*: A NST capable of transporting both UDP-D-Glc*p* and UDP-D-Gal*p* was cloned from Arabidopsis by searching for genes with high sequence similarity to UDP-D-Gal*p* transporters from humans and yeast (Norambuena et al., 2002). The gene (AtUTr1) could functionally complement a canine MDCK mutant cell line deficient in UDP-D-Gal*p* transport. Expression of AtUTr1 in *S. cerevisiae* yielded an increase in the transport of UDP-D-Glc*p* and UDP-D-Gal*p* in intact Golgi vesicles, but not the transport of any other nucleotide-sugar that was tested. AtUTr1 is thought to be part of a 6 member gene family in Arabidopsis (Table 1.13).

*UDP-D-Gal*p *transporter*: Two genes from an Arabidopsis cDNA library were identified that could functionally complement a Chinese hamster ovary cell line deficient in the transport of

UDP-D-Gal*p* (Table 1.13). The genes (UDP-GalT1 and 2) expressed in *S. cerevisiae*, caused a 10-fold increase in UDP-D-Gal*p* transport in intact Golgi vesicles (Bakker et al., 2004).

GONST transporters: A GDP-D-Man*p* transporter from Arabidopsis was recently cloned and named GONST1 (Baldwin et al., 2001). While the transport of GDP-D-Man*p* is not predicted to be required for pectin biosynthesis, GONST1 is part of a 5 member gene family for which 3 of the members have no known function (Handford et al., 2004). BLAST analysis of GONST5 shows that it has 91% sequence identity to UDP-GalT1, suggesting that it may also be a UDP-D-Gal*p* transporter. Further research on these and other putative NSTs should allow us to determine which of these proteins are involved in pectin biosynthesis.

Pectin glycosyltransferases

Nucleotide-sugars transported into the lumen of the Golgi apparatus become substrates for Golgi-localized glycosyltransferases. At least some of these glycosyltransferases are type II membrane proteins that catalyze the transfer of the sugar moiety of the nucleotide-sugar onto the non-reducing end of oligo- or polysaccharide acceptors (Keegstra and Raikhel, 2001; Perrin et al., 2001). It has been estimated that at least 62 different glycosyltransferase activities would be required to synthesize all of the pectic polysaccharides found in the primary wall based on the current structure of pectin (Table 1.14; Mohnen, 2002). Of these predicted enzyme activities, only three [α-(1,4)-galacturonosyltransferase, α-(1,2)-galacturonosyltransferase and α-(1,4)-rhamnosyltransferase] are involved in the synthesis of the backbone structures of pectin (Table 1.14). These backbone glycosyltransferases may be processive enzymes that catalyze the synthesis of polymeric products (Mohnen, 2002). The other glycosyltransferases are predicted to catalyze the addition of glycosyl residues producing the side branches found in pectic polysaccharides.

Table 1.13. Putative and cloned NST transporter genes from Arabidopsis.

Gene name	Sugar specificity	Protein accession	Protein size (kDa)[b]	Function confirmed[c]	References
AtUTr1	UDP-D-Gal*p*/ UDP-D-Glc*p*	NP_565290	37	Complementation/ Transport	(Norambuena et al., 2002)
AtUTr2	ND[a]	NP_194032	38	ND	(Norambuena et al., 2002)
AtUTr3	ND	NP_563949	37	ND	(Norambuena et al., 2002)
AtUTr4	ND	NP_172720	39	ND	(Norambuena et al., 2002)
AtUTr5	ND	NP_190204	39	ND	(Norambuena et al., 2002)
AtUTr6	ND	NP_850721	45	ND	(Norambuena et al., 2002)
UDP-GalT1	UDP-D-Gal*p*	NP_565158	38	Complementation	(Bakker et al., 2004)
UDP-GalT2	UDP-D-Gal*p*	NP_565138	38	Complementation	(Bakker et al., 2004)
GONST1	GDP-D-Man*p*	NP_849952	37	Complementation	(Baldwin et al., 2001)
GONST2	GDP-D-Man*p*	CAD83086	42	Complementation	(Handford et al., 2004)
GONST3	ND	NP_177760	42	ND	(Handford et al., 2004)
GONST4	ND	NP_197498	37	ND	(Handford et al., 2004)
GONST5	ND	NP_173605	39	ND	(Handford et al., 2004)

[a]ND: not determined.

[b]Molecular weight deduced by amino acid sequence.

[c]The function of these proteins has been confirmed by complementation of a UDP-D-Gal*p* or GDP-D-Man*p* transport mutants (complementation) or transport assays of the expressed protein (activity) in intact Golgi vesicles from *S. cerevisiae*.

Table 1.14. Distinct glycosyltransferase activities hypothesized to be required for pectin biosynthesis[a.b].

Type of glycosyltransferase	Parent polymer	Enzyme acceptor[d]	Activity detected[e]	References for structure
HGA glycosyltransferases[c]				
α-(1,4)-GalAT	HGA	*D-Gal*p*A-(1→4)-α-D-Gal*p*A-(1→	Yes	(O'Neill et al., 1990)
RG-I glycosyltransferases				
α-(1,2)-GalAT	RG-I	L-Rha*p*-(1→4)-α-D-Gal*p*A-(1→	No	(McNeil et al., 1980; Lau et al., 1985; Eda et al., 1986; O'Neill et al., 1990)
α-(1,4)-GalAT	RG-I/HGA	D-Gal*p*A-(1→2)-α-L-Rha*p*-(1→	No	(Nakamura et al., 2002a)
α-(1,4)-RhaT	RG-I	D-Gal*p*A-(1→2)-α-L-Rha*p*-(1→	No	(McNeil et al., 1980; Lau et al., 1985; Eda et al., 1986; O'Neill et al., 1990)
α-(1,4)-RhaT	HGA/RG-I	D-Gal*p*A-(1→4)-α-D-Gal*p*A-(1→	No	(Nakamura et al., 2002a)
β-(1,4)-GalT	RG-I	L-Rha*p*-(1→4)-α-D-Gal*p*A-(1→	Yes	(Lau et al., 1987; O'Neill et al., 1990; Schols et al., 1995a)
β-(1,4)-GalT	RG-I	D-Gal*p*-(1→4)-β-L-Rha*p*-(1→	Yes	(Lau et al., 1987; O'Neill et al., 1990)
β-(1,4)-GalT	RG-I	D-Gal*p*-(1→4)-β-D-Gal*p*-(1→	Yes	(Aspinall et al., 1967; Aspinall, 1980; Lau et al., 1987; O'Neill et al., 1990; Nakamura et al., 2001)
β-(1,6)-GalT	RG-I	D-Gal*p*-(1→4)-β-D-Gal*p*-(1→	No	(Lau et al., 1987; O'Neill et al., 1990; Nakamura et al., 2001)
β-(1,3)-GalT	RG-I	D-Gal*p*-(1→4)-β-L-Rha*p*-(1→	No	(O'Neill et al., 1990; Carpita and Gibeaut, 1993)

β-(1,3)-GalT	RG-I/AGP	D-Gal*p*-(1→3)-β-D-Gal*p*-(1→	No	(O'Neill et al., 1990; Carpita and Gibeaut, 1993)
β-(1,6)-GalT	RG-I/AGP	D-Gal*p*-(1→3)-β-D-Gal*p*-(1→	?	(O'Neill et al., 1990; Carpita and Gibeaut, 1993)
β-(1,3)-GalT	RG-I/AGP	D-Gal*p*-(1→6)-β-D-Gal*p*-(1→3)-β-D-Gal*p*-(1→	No	(O'Neill et al., 1990; Carpita and Gibeaut, 1993)
α-(1,4)-AraT	RG-I	L-Rha*p*-(1→4)-α-D-Gal*p*A-(1→	No	(Lau et al., 1987)
α-(1,5)-AraT	RG-I	L-Ara*f*-(1→4)-α-L-Rha*p*-(1→	No	(Huisman et al., 2001)
α-(1,5)-AraT	RG-I	L-Ara*f*-(1→5)-α-L-Ara*f*-(1→	?	(Lerouge et al., 1993)
α-(1,3)-AraT	RG-I	D-Gal*p*-(1→4)-β-L-Rha*p*-(1→	No	(Lau et al., 1987; O'Neill et al., 1990)
α-(1,2)-AraT	RG-I	L-Ara*f*-(1→3)-β-D-Gal*p*-(1→	No	(Lau et al., 1987; O'Neill et al., 1990)
α-(1,5)-AraT	RG-I	L-Ara*f*-(1→2)-α-L-Ara*f*-(1→	No	(Lau et al., 1987; O'Neill et al., 1990)
α-(1,3)-AraT	RG-I	L-Ara*f*-(1→5)-α-L-Ara*f*-(1→	No	(Carpita and Gibeaut, 1993)
α-(1,2)-AraT	RG-I	L-Ara*f*-(1→5)-α-L-Ara*f*-(1→	No	(Carpita and Gibeaut, 1993)
α-(1,3)-AraT	RG-I	L-Ara*f*-(1→3)-α-L-Ara*f*-(1→	No	(Carpita and Gibeaut, 1993)
α-(1,5)-AraT	RG-I	L-Ara*f*-(1→3)-α-L-Ara*f*-(1→	No	(Carpita and Gibeaut, 1993)
α-(1,3)-AraT	RG-I	D-Gal*p*-(1→4)-β-D-Gal*p*-(1→	No	(Aspinall et al., 1967; Aspinall, 1980; Carpita et al., 2001)
α-(1,5)-AraT	RG-I	L-Ara*f*-(1→3)-β-D-Gal*p*-(1→	No	(Aspinall et al., 1967; Aspinall, 1980)
α-(1,6)-AraT	RG-I	D-Gal*p*-(1→4)-β-D-Gal*p*-(1→	No	(Nakamura et al., 2001)
α-(1,4)-AraT	RG-I	D-Gal*p*-(1→4)-β-D-Gal*p*-(1→	No	(Huisman et al., 2001)
α-(1,4)-AraT	RG-I	D-Gal*p*-(1→6)-β-D-Gal*p*-(1→	No	(Nakamura et al., 2001)
α-(1,5)-AraT	RG-I	L-Ara*f*-(1→6)-β-D-Gal*p*-(1→	No	(Nakamura et al., 2001)
α-(1,3)-AraT	RG-I/AGP	D-Gal*p*-(1→6)-β-D-Gal*p*-(1→	No	(Carpita and Gibeaut, 1993)
α-(1,6)-AraT	RG-I/AGP	D-Gal*p*-(1→6)-β-D-Gal*p*-(1→	No	(Carpita and Gibeaut, 1993)
α-(1,2)-FucT	RG-I	D-Gal*p*-(1→4)-β-D-Gal*p*-(1→	No	(Lau et al., 1987; O'Neill et al., 1990)
β-(1,3)-GlcAT	RG-I	D-Gal*p*A-(1→4)-α-L-Rha*p*-(1→	No	(Renard et al., 1999)

β-(1,4)-GlcAT	RG-I	Gal...	No	(An et al., 1994)
β-(1,6)-GlcAT	RG-I	Gal...	No	(An et al., 1994)
XGA glycosyltransferases				
β-(1,3)-XylT	XGA	D-Gal*p*A-(1→4)-α-D-Gal*p*A-(1→	No	(Schols et al., 1995a; Kikuchi et al., 1996; Yu and Mort, 1996; Nakamura et al., 2002)
β-(1,4)-XylT[f]	XGA	D-Xyl*p*-(1→3)-α-D-Gal*p*A-(1→	No	(Nakamura et al., 2002)
β-(1,2)-XylT[f]	XGA	D-Xyl*p*-(1→3)-α-D-Gal*p*A-(1→	No	(Nakamura et al., 2002)
β-(1,2)-XylT[f]	XGA	D-Xyl*p*-(1→4)-β-D-Xyl*p*-(1→	No	(Nakamura et al., 2002)
AGA glycosyltransferases				
β-(1,2)-ApiT	AGA	D-Gal*p*A-(1→4)-α-D-Gal*p*A-(1→	No	(Cheng and Kindel, 1997; Golovchenko et al., 2002)
β-(1,3)-ApiT	AGA	D-Gal*p*A-(1→4)-α-D-Gal*p*A-(1→	No	(Cheng and Kindel, 1997; Golovchenko et al., 2002)
β-(1,3)-ApiT	AGA	D-Api*f*-(1→2)-β-D-Gal*p*A-(1→	No	(Cheng and Kindel, 1997; Golovchenko et al., 2002)
β-(1,3)-ApiT	AGA	D-Api*f*-(1→3)-β-D-Gal*p*A-(1→	No	(Cheng and Kindel, 1997; Golovchenko et al., 2002)
RG-II glycosyltransferases				
α-(1,2)-GalAT	RG-II-A	L-Rha*p*-(1→3')-β-D-Api*f*-(1→	No	(Thomas et al., 1989; Puvanesarajah et al., 1991; Reuhs et al., 2004)
β-(1,3)-GalAT	RG-II-A	L-Rha*p*-(1→3')-β-D-Api*f*-(1→	No	(Thomas et al., 1989; Puvanesarajah et al., 1991; Reuhs et al., 2004)
β-(1,3')-RhaT	RG-II-A/B	D-Api*f*-(1→2)-β-D-Gal*p*A(1→	No	(Thomas et al., 1989; Puvanesarajah et al., 1991;

				Reuhs et al., 2004)
α-(1,3)-RhaT	RG-II-B	L-Ara*p*-(1→4)-β-D-Gal*p*-(1→	No	(Thomas et al., 1989; Pellerin et al., 1996; Glushka et al., 2003; Reuhs et al., 2004)
α-(1,2)-RhaT	RG-II-B	L-Ara*p*-(1→4)-β-D-Gal*p*-(1→	No	(Pellerin et al., 1996; Reuhs et al., 2004)
α-(1,5)-RhaT	RG-II-C	D-Kdo*p*-(2→3)-α-D-Gal*p*A-(1→	No	(York et al., 1985; Reuhs et al., 2004)
α-(1,2)-L-GalT	RG-II-A	D-Glc*p*A-(1→4)-β-L-Fuc*p*-(1→	No	(York et al., 1985; Thomas et al., 1989; Reuhs et al., 2004)
β-(1,2)-GalT	RG-II-B	L-Ace*f*A-(1→3)-α-L-Rha*p*-(1→	No	(Thomas et al., 1989; Puvanesarajah et al., 1991; Reuhs et al., 2004)
α-(1,4)-Ara*p*T	RG-II-B	D-Gal*p*-(1→2)-β-L-Ace*f*A	No	(Thomas et al., 1989; Puvanesarajah et al., 1991; Reuhs et al., 2004)
β-(1,3)-AraT	RG-II-B	L-Rha*p*-(1→2)-α-L-Ara*p*-(1→	No	(Pellerin et al., 1996; Reuhs et al., 2004)
β-(1,5)-AraT	RG-II-D	D-Dha*p*-(2→3)-β-D-Gal*p*A-(1→	No	(Stevenson et al., 1988; Puvanesarajah et al., 1991; Reuhs et al., 2004)
α-(1,4)-FucT	RG-II-A	L-Rha*p*-(1→3')-β-D-Api*f*-(1→	No	(Thomas et al., 1989; Reuhs et al., 2004)
α-(1,2)-FucT	RG-II-B	D-Gal*p*-(1→2)-β-L-Ace*f*A-(1→	No	(Thomas et al., 1989; Puvanesarajah et al., 1991; Reuhs et al., 2004)
β-(1,2)-ApiT	RG-II-A/B	D-Gal*p*A-(1→4)-α-D-Gal*p*A-(1→	No	(Thomas et al., 1989; Puvanesarajah et al., 1991; Reuhs et al., 2004)
α-(1,3)-XylT	RG-II-A	L-Fuc*p*-(1→4)-α-L-Rha*p*-(1→	No	(Thomas et al., 1989; Reuhs et al., 2004)
β-(1,4)-GlcAT	RG-II-A	L-Fuc*p*-(1→4)-α-L-Rha*p*-(1→	Yes[g]	(Thomas et al., 1989; Iwai et al., 2002; Reuhs et al., 2004)

α-(2,3)-KdoT	RG-II-C	D-Gal*p*A-(1→4)-α-D-Gal*p*A-(1→	No	(York et al., 1985; Reuhs et al., 2004)
β-(2,3)-DhaT	RG-II-D	D-Gal*p*A-(1→4)-α-D-Gal*p*A-(1→	No	(Stevenson et al., 1988; Puvanesarajah et al., 1991; Reuhs et al., 2004)
α-(1,3)-AceT	RG-II-B	L-Rha*p*-(1→3')-β-D-Api*f*-(1→	No	(Thomas et al., 1989; Puvanesarajah et al., 1991; Reuhs et al., 2004)

[a]Adapted from Mohnen (2002).

[b]This list of glycosyltransferase activities is based on the currently accepted structures of HGA, RG-I, XGA, AGA, and RG-II as determined by the listed references.

[c]α-(1,4)-GalAT is only listed once in this table even though GalATs involved in synthesizing the backbone structures of substituted galacturonans (i.e. XGA, AGA and RG-II) may be different from those involved in HGA biosynthesis. All of these enzymes catalyze the same reaction, and therefore α-(1,4)-GalATs synthesizing the backbones of substituted galacturonans are not distinguished from the ones synthesizing HGA in this table.

[d]Glycosyltransferases catalyze the transfer of the indicated glycosyl residue to the non-reducing* (left hand side) terminus of the indicated acceptor substrate.

[e]The activity of some pectin glycosyltransferases has been detected in certain plant species. These enzymes were shown to catalyze the transfer of the indicated glycosyl residue onto specific pectic acceptors forming the indicated linkage.

[f]Analysis of XGA fragments from soybean cotyledons suggest that (1,2)- and (1,4)-linked β-D-Xyl*p* may be attached to the (1,3)-linked β-D-Xyl*p* of XGA.

[g]While the gene encoding RG-II:β-(1,4)-GlcAT (NpGUT1) has been cloned (Iwai et al., 2002), *in vitro* enzyme activity has not been demonstrated.

The most common assay method for the detection of pectin glycosyltransferase activity uses radioactive nucleotide-sugars as a substrate and measures the amount of radiolabel that is transferred to endogenous or exogenous acceptors. Endogenous acceptors are used mainly during the determination of glycosyltransferase activity in microsomal membranes (Mohnen, 1999). These endogenous acceptors are lost when the microsomal fraction is treated with detergent, and hence, the addition of exogenous oligo- or polysaccharide pectic acceptors are required to determine transferase activity in detergent solubilized or permeabilized membranes (Mohnen, 1999). The unincorporated radiolabeled nucleotide-sugar is separated from the radiolabeled product by thin layer chromatography (TLC) (Villemez et al., 1966; Takeuchi and Tsumuraya, 2001) or by organic solvent precipitation (Doong and Mohnen, 1998; Geshi et al., 2000). The amount of radiolabeled product made during the reaction is determined by scintillation counting.

Alternative, non-radioactive assay methods using fluorescently-labeled OGA acceptors have been developed that use high performance liquid chromatography (HPLC) for product isolation and analysis (Ishii, 2002; Ishii et al., 2004). Unfortunately, the uniformly-sized acceptors that are required for these non-radioactive assays are difficult to obtain in large quantities.

The identification of pectin glycosyltransferases is a challenging process as most nucleotide sugar substrates are commercially unavailable, enzyme acceptors have to be generated and purified in sufficient quantities for activity assays, and gene homologs of pectin glycosyltransferases are not present in sequence databases. The activities of most glycosyltransferases thought to be involved in pectin biosynthesis have not been detected in any plant extracts (Table 1.14) and no pectin glycosyltransferase has been purified to homogeneity or

recombinantly expressed (Mohnen, 1999; Mohnen, 2002). Recent studies analyzing mutant plants with altered pectin structures have allowed the identification of putative pectin glycosyltransferase genes (Bouton et al., 2002; Iwai et al., 2002); however, the function of these genes has not been demonstrated through heterologous expression.

Glycosyltransferase activities (EC 2.4.-) involved in pectin biosynthesis have been discussed in great detail in previous reviews (Mohnen, 1999; Ridley et al., 2001; Mohnen, 2002). The following section will summarize published results on the identification and characterization of glycosyltransferases involved in pectin biosynthesis.

Galacturonosyltransferases (GalATs): GalATs catalyze the transfer of D-Gal*p*A from UDP-D-Gal*p*A onto the non-reducing end of a pectin acceptor (Scheller et al., 1999). Plants are expected to contain four distinct GalAT activities based on pectin structure (Table 1.14). Only the activity of α-(1,4)-GalAT has been detected in plant extracts.

α-(1,4)-GalAT (EC 2.4.1.43) activity has been detected in membrane fractions from mung bean (Villemez et al., 1965; Villemez et al., 1966), tomato (Lin et al., 1966), tobacco (Doong et al., 1995; Doong and Mohnen, 1998; Scheller et al., 1999), Arabidopsis (Guillaumie et al., 2003), sycamore (Bolwell et al., 1985), pumpkin (Ishii, 2002), azuki (*Vigna angularis*) bean (Takeuchi and Tsumuraya, 2001), petunia (*Petunia axillaris*) (Akita et al., 2002), and pea (Sterling et al., 2001). All α-(1,4)-GalATs have a strict requirement for Mn^{2+} and are strongly inhibited by divalent cation chelators such as EDTA. While all α-(1,4)-GalATs have similar pH optima, the published kinetic characteristics of these enzymes are variable, and depend on the original plant tissue source and on the method used to test for enzyme activity (Table 1.15).

The type of acceptor used in the GalAT activity assay contributes to some of the observed differences in the kinetic constants of membrane-bound and detergent-solubilized

GalATs (Table 1.15). For example, GalAT activity from tobacco (Doong et al., 1998), pumpkin (Ishii, 2002), and petunia (Akita et al., 2002) are more active on exogenous OGA acceptors that are greater than DP 12. A 20-50% reduction in GalAT activity is observed using DP 10 or 11 acceptors, and little to no activity is observed using OGA acceptors that are DP 9 or smaller. Furthermore, assays using fluorescently-labeled acceptors demonstrate that the affinity of GalAT for different OGA acceptors increases with the increasing length of the acceptor (Akita et al., 2002). These results suggest that OGA acceptors need to be a certain length either to properly occupy the active site of GalAT, or that OGAs of a certain length form the appropriate secondary structure to allow the OGA to be properly oriented in the active site for catalysis to occur.

Exogenously added acid-soluble HGA (~10 kDa) acceptors have also been shown to be better acceptor substrates than the endogenous acceptors found in membrane fractions from azuki bean (Takeuchi and Tsumuraya, 2001). This difference in acceptor substrates resulted in a 6-fold increase in V_{max} when exogenous, acid-soluble acceptors were used versus endogenous acceptors. Similar results were obtained during the incubation of solubilized Arabidopsis membranes with either OGAs or heat-inactivated endogenous acceptors from Arabidopsis (Chapter 2).

Despite these differences in the observed kinetic constants of α-(1,4)-GalATs from different plant sources, membrane-bound and solubilized α-(1,4)-GalATs from different plant sources are consistent in the types of products they produce. Membrane-bound α-(1,4)-GalATs in the presence of endogenous acceptors produce high molecular weight products (Villemez et al., 1966; Takeuchi and Tsumuraya, 2001; Doong et al., 1995; Sterling et al., 2001). For example, the products made from pea Golgi and tobacco were estimated to be >500 kDa and approximately 105 kDa, respectively (Doong et al., 1995; Chapter 3). These radiolabeled

Table 1.15. Properties of α-(1,4)-GalATs from plants[a,b]

Plant Source	Apparent K_m for UDP-GalA (μM)	pH optimum	V_{max} (pmol $mg^{-1}min^{-1}$)	Type of acceptor[f]	References
mung bean	1.7	6.3-7.0	~4700	endogenous	(Villemez et al., 1966)
tomato	ND[e]	ND	ND	endogenous	(Lin et al., 1966)
pea Golgi	ND	ND	ND	exogenous/oligo	(Sterling et al., 2001)
sycamore	770	ND	ND	endogenous	(Bolwell et al., 1985)
tobacco	8.9	7.8	150	endogenous	(Doong et al., 1995)
tobacco (sol)[c]	37	6.3-7.8	290	exogenous/oligo	(Doong and Mohnen, 1998)
azuki bean (per)[d]	140	6.8-7.8	2700	exogenous/poly	(Takeuchi and Tsumuraya, 2001)
pumpkin	700	6.25-7.5	7000	exogenous/fluor	(Ishii, 2002)
petunia (sol)	170	7	480	exogenous/fluor	(Akita et al., 2002)

[a]Adapted from (Mohnen, 2002)

[b]Unless otherwise indicated, all enzymes activities were measured in membrane fractions

[c](sol): detergent-solubilized enzyme

[d](per): detergent-permeabilized enzyme

[e]ND: not determined

[f]The type of acceptor used in each study is divided into endogenous or exogenous acceptors. Exogenous acceptors have been subdivided into OGA (oligo), HGA (poly), or fluorescently-labeled OGA (fluor) acceptors.

products could be almost completely degraded (89% and 91% for tobacco and pea Golgi, respectively) into mono-, di- and triGalA following exhaustive treatment with a purified EPGase (Doong and Mohnen, 1998; Sterling et al., 2001), indicating that the D-[^{14}C]Gal*p*A residues were α-(1,4)-linked to the endogenous acceptors. Neither the size of the endogenous acceptors nor the number of contiguous D-[^{14}C]Gal*p*A residues added onto the non-reducing termini have been determined.

Solubilized or detergent-permeabilized α-(1,4)-GalAT from tobacco (Doong and Mohnen, 1998; Scheller et al., 1999), petunia pollen tubes (Akita et al., 2002), and pea Golgi (Chapter 3) in the presence of exogenous OGA acceptors (DP ≥ 10) add from 1 to 10 D-Gal*p*A residues onto the non-reducing end of the OGA acceptor in a non-processive manner. These products can also be completely degraded into mono-, di- and triGalA following their treatment with a purified EPGase (Doong and Mohnen, 1998; Sterling et al., 2001; Akita et al., 2002) suggesting that the product was (1,4)-α-linked. Similar products were obtained from pumpkin microsomal membranes incubated with fluorescently labeled OGAs (Ishii, 2002). These results indicate that OGAs may not be the correct acceptor for processive α-(1,4)-GalAT activity or that tissue homogenization may disrupt protein complexes required for processive glycosyltransferase activity, or that the enzymes may not be processive *in vivo*. The purification and eventual cloning of an α-(1,4)-GalAT should enable us to determine the catalytic mechanism of the enzyme.

A T-DNA insertion mutant of Arabidopsis, named *qua1*, was recently discovered that had phenotypes expected for a mutation in a α-(1,4)-GalAT gene, including dwarfism, reduced cell adhesion, and a 25% reduction in D-Gal*p*A content in leaves (Bouton et al., 2002). While the enzymatic activity of the QUA1 gene has yet to be demonstrated, recent studies described in this

thesis have shown that QUA1 has high sequence similarity to two putative α-(1,4)-GalAT genes from Arabidopsis (Chapter 4).

Arabinosyltransferases (AraTs): Arabinosyltransferase activity has been detected in microsomal membranes from mung (Odzuck and Kauss, 1972; Nunan and Scheller, 2003) and French bean (Bolwell and Northcote, 1983; Rodgers and Bolwell, 1992) using radiolabeled UDP-L-Ara*p* as a substrate. The products from these reactions have never been unequivocally shown to be a part of any pectic structure (Mohnen, 1999; Mohnen, 2002). Questions remain as to whether any of the detected activities are involved in pectin biosynthesis.

The first report of the addition of L-Ara to a well defined, pectic acceptor was conducted using solubilized AraT activity from mung bean (Nunan and Scheller, 2003). Solubilized AraT activity from mung bean catalyzed the transfer of a single L-Ara residue to a (1,5)-linked α-L-arabinooctaose (Ara8) acceptor. The radiolabeled product synthesized by the enzyme could be completely converted to arabinose by strong acid hydrolysis; however, the radiolabel was found to be resistant to treatment with a purified (1,5)-α-L-*endo*arabinase and (1,2;1,3;1,5)-α-D-arabinofuranosidase, respectively. Mild acid hydrolysis and methylation analysis of the radiolabeled product indicated that the added L-Ara residue was in the pyranose ring form, but linkage analysis of the product could not be determined due to the limited quantities of material that were available. The presence of terminal L-Ara*p* residues on pectic structures other than RG-II has been observed in specific plant species, for example arabinans from pigeon pea (*Cajanus cajan*) cotyledons (Swamy and Salimath, 1991), and arabinogalactans from *Angelica acutiloba* (Kitagawa) roots (Kiyohara et al., 1987), and soybean cotyledons (Huisman et al., 2001). These results suggest that L-Ara*p* may be a common component of the arabinans and/or

arabinogalactans of RG-I, or that other plant enzymes are required to convert the incorporated L-Ara*p* residues into the L-furanose form during pectin arabinan biosynthesis.

(1,5)-linked α-L-arabinosyl oligomers smaller than DP 8 were less efficient acceptors for solubilized AraT activity, as were large arabinans, galactans and RG-I fragments. AraT activity was greatest in young (2 d old) tissue and decreased significantly with the age of the plant. The AraT also had a requirement for Mn^{2+} in the reaction mixture with 3 mM $MnCl_2$ giving the greatest levels of incorporation. The AraT had a pH optimum of 6.5 and K_m for UDP-L-Ara*p* of 0.33 mM.

Recently, a mutant in *Nicotiana plumbaginifolia*, named *nolac-H14*, was discovered that exhibited similar non-organogenic and cell adhesion defects as *nolac-H18* (Iwai et al., 2001). Glycosyl composition and linkage analysis of the pectic and hemicellulosic fractions indicate a significant reduction in L-Ara*f* in *nolac-H14* mutant callus. These results suggest that the gene encoded by *nolac-H14* may be involved in the incorporation of L-Ara*f* in *Nicotiana plumbaginifolia*.

Galactosyltransferases (GalTs): An activity capable of transferring D-[^{14}C]Gal*p* from UDP-D-[^{14}C]Gal*p* to an endogenous acceptor forming a water-soluble, high molecular weight polymer was first detected in microsomal membranes from mung bean seedlings (McNab et al., 1968). Strong acid hydrolysis indicated that the radiolabeled polymer was composed solely of D-[^{14}C]Gal*p* (McNab et al., 1968). The majority of the D-[^{14}C]Gal*p* labeled product (>90%) made by mung bean membranes was shown in a later study to be composed of (1,4)-linked β-D-galactan by treatment of the product with a purified (1,4)-β-D-*exo*galactanase and a (1,4)-β-D-*endo*galactanase, respectively (Brickell and Reid, 1996). The β-(1,4)-GalT from mung bean had

Table 1.16. Properties of GalTs from plants.

Plant Source[a]	Apparent K_m for UDP-D-Gal*p* (μM)	pH optimum	V_{max} (pmol $mg^{-1}min^{-1}$)	Linkage of product	References
mung bean	ND[d]	6.5	ND	(1,4)-β	(Brickell and Reid, 1996)
pea	ND	7-8	ND	(1,4)-β	(Abdel-Massih et al., 2003)
flax	38	7.5-8.5	75	(1,4)-β	(Goubet and Morvan 1993, 1994)
flax (sol)[b]	460	7.5-8.5	180	(1,4)-β	(Peugnet et al., 2001)
potato	ND	6-6.5	ND	(1,4)-β	(Geshi et al., 2000)
potato (sol)	ND	7.5	ND	(1,4)-β	(Geshi et al., 2002)
potato (sol)	ND	5.6	ND	?	(Geshi et al., 2002)
soybean (per)[c]	1200	6.5	6000	(1,4)-β	(Konishi et al., 2004)
mung bean (per)	32	6.5	240	(1,4)-β	(Ishii et al., 2004)
radish (per)	410	5.9-6.3	1000	(1,6)-β[e]	(Kato et al., 2003)

[a]Unless otherwise indicated, all enzymes activities were measured in membrane fractions

[b](sol): detergent-solubilized enzyme

[c](per): detergent-permeabilized enzyme

[d]ND: not determined

[e]Linkage analysis of the product made by permeabilized radish membranes was not done and so the absolution configuration of the transferred D-Gal*p* residue is not known.

a pH optimum of 6.5 and was stimulated by Mg^{2+} (Table 1.16). A similar enzyme activity was identified in pea epicotyl membranes (Abdel-Massih et al., 2003).

Two, pH-dependent, GalT activities were detected in microsomes from flax suspension-cultured cells (Goubet and Morvan 1993). Both activities were capable of synthesizing a polymeric product in the presence of endogenous acceptors composed entirely of D-Gal*p*, but had different pH optima. GalT activities with pH optima of 5-6.5 and 7.5-8.5 produced an alkali-soluble product that was composed mainly of (1,3)- and (1,6)-linked β-D-galactan and a water-soluble product that was composed mainly of (1,4)-linked β-D-galactan, respectively. The GalT activities were solubilized from flax membranes and the activity with the higher pH optimum (pH 8) was shown to catalyze the transfer of D-[^{14}C]Gal*p* onto purified RG-I acceptors (Table 1.16). The radiolabeled products from these reactions were highly resistant to rhamnogalacturonan depolymerases, (i.e. rhamnogalacturonase A and B); however, a significant portion (60%) of the D-[^{14}C]Gal*p* could be removed from the products by treatment with a purified (1,4)-β-D-galactosidase suggesting that the product was (1,4)-β-linked (Peugnet et al., 2001).

Microsomal membranes from potato suspension cultures incubated with UDP-D-[^{14}C]Gal*p* in the presence of endogenous acceptors and Mn^{2+} at pH 6 were able to produce a large molecular weight (>500 kDa) radiolabeled product that released D-[^{14}C]Gal*p* as the sole glycosyl residue upon complete acid hydrolysis (Geshi et al., 2000). The majority of the radioactivity from the product made by dark grown cells (73%) could be released by treatment with a purified (1,4)-β-D-*endo*galactanase. Furthermore, treatment of the large molecular weight product with base followed by rhamnogalacturonase A (RGase A), an *endo*hydrolase that cleaves the [→4)-α-D-GalpA-(1→2)-α-L-Rhap] linkage of RG-I backbone structures (Azadi et al., 1995),

released approximately 50% of the radioactivity as a series of smaller RG-I oligomers (~14 kDa). The combined treatment of the RG-I oligomers with a purified (1,4)-β-D-galactosidase and a (1,4)-β-D-*endo*galactanase released all of the radioactivity from the RG-I oligomers as D-[^{14}C]Gal*p*. These results suggest that membranes from potato suspension-cultured cells catalyze the initiation and elongation of (1,4)-linked β-D-galactan chains found on RG-I (Table 1.14 and 1.16).

Two distinct β-(1,4)-GalT activities could be solubilized from potato suspension cultures that differed in their pH optima and acceptor substrate specificities (Geshi et al., 2002). Both enzyme activities catalyze the addition of D-[^{14}C]Gal*p* from UDP-D-[^{14}C]Gal*p* onto RG-I acceptors that contained short (1,4)-β-D-galactan side chains consisting of a single D-Gal*p* residue. β-(1,4)-GalT activity at pH 5.6 and 7.5 preferred high molecular weight (~1.2 MDa) RG-I acceptors and medium-sized (~21 kDa) acceptors, respectively. Shorter RG-I oligomers, linear galactans, degalactosylated RG-I fragments, or RG-I molecules with high galactose content did not function as viable acceptors for the solubilized activity. The radiolabeled product made using the medium-sized acceptor at pH 7.5 was determined to be (1,4)-β-linked by digestion with a purified (1,4)-β-D-*endo*galactanase (Table 1.16). Product made using the high molecular weight acceptor at pH 5.6 was impervious to this treatment, suggesting that either the β-(1,4)-GalT produced side chains that were resistant to (1,4)-β-D-*endo*galactanase cleavage (meaning that they were shorter than 3 contiguous D-[^{14}C]Gal*p* residues) or that the enzyme catalyzed the formation of a linkage other than (1,4)-linked β-D-Gal*p*.

A β-(1,4)-GalT activity capable of transferring D-[^{14}C]Gal*p* to chemically modified, large molecular weight (60-70 kDa) galactan acceptors from lupin seeds was identified in microsomal membranes from soybean (Konishi et al., 2004). The radiolabeled product could be degraded by

treatment with a purified (1,4)-β-D-*endo*galactanase, indicating that it was (1,4)-β-linked. This β-(1,4)-GalT from soybean membranes could also catalyze the addition of 1 to 5 D-Gal*p* residues onto fluorescently-labeled, (1,4)-linked β-D-galactosyl oligomers with a DP greater than 5. A similar activity (capable of catalyzing the addition of D-Gal*p* residues onto fluorescently-labeled (1,4)-linked β-D-galactosyl oligomers) was detected in microsomal membranes from mung bean (Ishii et al., 2004). Both the activity from soybean and mung bean had a pH optimum of 6.5 and were stimulated by Mn^{2+} (Ishii et al., 2001a; Konishi et al., 2004).

Radish microsomal membranes incubated with a chemically-modified, (1,3)-linked β-D-galactan acceptor from acacia gum in the presence of UDP-D-[^{14}C]Gal*p* produced a radiolabeled product (Kato et al., 2003). Treatment of the radiolabeled product with a purified (1,3)-β-D-*exo*galactanase released a product that migrated the same distance as (1,6)-linked β-D-galactobiose upon TLC analysis (Kato et al., 2003). These results suggested that the enzyme activity that was identified was a β-(1,6)-GalT capable of transferring a single (1,6)-linked β-D-Gal*p* residue onto (1,3)-linked β-D-galactans. Linkage analysis of the synthesized product was not conducted and so the absolute configuration of the added β-D-Gal*p* residue remains to be confirmed.

Apiosyltransferases (ApiT): An activity capable of transferring D-[^{14}C]Api*f* from UDP-D-[^{14}C]Api*f* onto an endogenous acceptor was detected in membrane preparations from duckweed (Pan and Kindel, 1977). The radiolabeled product could be partially degraded by treatment with a fungal pectinase and partial acid hydrolysis released 46% of the radioactivity from the product as D-[^{14}C]Api*f* and D-[^{14}C]apiobiose. ApiT activity could be increased 2-fold with the addition of UDP-D-Gal*p*A to reaction mixtures, suggesting that the ApiT was partially dependent on HGA biosynthesis. The absolute configuration of the radiolabeled product was not determined, nor

was the composition of the endogenous acceptor. The ApiT had a pH optimum of 5.7 and K_m for UDP-D-Api*f* of 4.9 μM.

Glucuronosyltransferases (GlcATs): A gene encoding a β-(1,4)-GlcAT involved in RG-II biosynthesis was cloned by analyzing a T-DNA mutant of *Nicotiana plumbaginifolia* (Iwai et al., 2002). The mutant, *npgut1*, exhibited a number of developmental and cell adhesion defects that were caused by the absence of the [α-L-Gal*p*-(1→2)-β-D-Glc*p*A-(1→] disaccharide from side chain A of RG-II (Figure 1.4). Kinetic data on this enzyme is lacking as NpGUT1 has not been heterologously expressed and β-(1,4)-GlcAT activity has not been detected in any plant tissue. This is the first published report of the cloning of a pectin glycosyltransferase (Table 1.17).

Acetyl- and methyltransferases involved in pectin biosynthesis

The biosynthesis of pectic polysaccharides in the Golgi requires more than the catalytic activities of pectin glycosyltransferases. Pectic structures made in Golgi are modified by a series of acetyl- and methyltransferases that act late in pectin biosynthesis (Table 1.17; Zhang and Staehelin, 1992). The methyl- and acetylation of pectic polymers may be an important process regulating the secretion and assembly of pectins into the primary wall (Zhang and Staehelin, 1992; Carpita and Gibeaut, 1993; Dolan et al., 1997). Furthermore, pectin methyl- and acetylation has also been associated with cell separation events (Willats et al., 2001a), with the resistance of pectic polysaccharides to hydrolytic enzymes (Schols et al., 1990; Schols and Voragen, 1994; Renard and Jarvis, 1999a) and may also be developmentally regulated (Kauss and Hassid, 1967a; Vannier et al., 1992; Liners et al., 1994; Pauly and Scheller, 2000). No genes encoding these enzymes have been cloned, but significant progress has been made in identifying and characterizing pectin methyl- and acetyltransferases from a variety of plant sources.

Table 1.17. Distinct methyl- and acetyltransferase activities hypothesized to be required for pectin biosynthesis[a,b].

Type of transferase	Parent polymer	Enzyme acceptor	Activity detected[c]	References
Methyltransferases				
D-Gal*p*A-6-*O*-MT	HGA[d]	D-Gal*p*A-(1→4)-α-D-Gal*p*A-(1→	Yes	(Kauss and Hassid, 1967a; Mort et al., 1993)
D-Glc*p*A-4-*O*-MT	RG-I	D-Glc*p*A-(1→6)-β-D-Gal*p*-(1→	No	(Kauss and Hassid, 1967; An et al., 1994)
D-Xyl*p*-2-*O*-MT	RG-II	D-Xyl*p*-(1→3)-α-L-Fuc*p*-(1→	No	(Darvill et al., 1978; Pellerin et al., 1996)
L-Fuc*p*-2-*O*-MT	RG-II	L-Fuc*p*-(1→2)-α-D-Gal*p*-(1→	No	(Darvill et al., 1978; Pellerin et al., 1996)
Acetyltransferases				
D-Gal*p*A-3-*O*-AT	HGA	D-Gal*p*A-(1→4)-α-D-Gal*p*A-(1→	Yes	(Komalavilas and Mort, 1989; Ishii, 1997)
D-Gal*p*A-2-*O*/3-*O*-AT	RG-I	D-Gal*p*A-(1→2)-α-L-Rha*p*-(1→	Yes	(Lerouge et al., 1993; Ishii, 1997)
2-*O*-Me-L-Fuc*p*-AT	RG-II	2-*O*-Me-L-Fuc*p*-(1→2)-α-D-Gal*p*-(1→	No	(Whitcombe et al., 1995; Glushka et al., 2003)
L-Ace*f*A-AT	RG-II	L-Ace*f*A-(1→3)-α-L-Rha*p*-(1→	No	(Whitcombe et al., 1995; Glushka et al., 2003)

[a]Adapted from Mohnen (2002).

[b]This list of methyl- and acetyltransferase activities is based on the currently accepted structures of HGA, RG-I, XGA, AGA, and RG-II as determined by the listed references.

[c]The activity of some pectin methyl- and acetyltransferases has been detected in certain plant species.

[d]While the possibility exists that D-Gal*p*A residues on RG-I and RG-II are also methylated, methylation of D-Gal*p*A has only been shown to occur on HGA.

Pectin methyltransferases

HGA methyltransferase (HGA-MT) activity was first discovered in membranes from mung bean seedlings (Kauss and Hassid, 1967a). Membranes incubated with *S*-adenosyl-L-[^{14}C]methionine catalyzed the incorporation of [^{14}C]methyl groups onto endogenous acceptors to form radiolabeled products. Approximately 95% of the radioactivity could be removed from the product as [^{14}C]methanol by treatment of the radiolabeled material with base or a purified pectin methylesterase (PME), suggesting that the [^{14}C]methyl groups were added onto HGA (Table 1.18). Addition of UDP-D-Gal*p*A to the reaction mixture increased the rate of [^{14}C]methyl transfer (Kauss and Swanson, 1969). A similar activity was characterized in membranes from suspension-cultured tobacco cells (Table 1.18) where approximately 59% of the radiolabeled product made by tobacco membranes was shown to be methylated HGA (Goubet et al., 1998). The results suggested that HGA-MT activity in membranes may be dependent upon HGA biosynthesis.

In contrast, a membrane-bound HGA-MT activity from soybean hypocotyls was not stimulated by the addition of UDP-D-Gal*p*A (Ishikawa et al., 2000). The detergent-permeabilized soybean enzyme catalyzed the transfer of [^{14}C]methyl groups onto exogenous pectin acceptors. Similar to HGA-MTs from mung bean and tobacco, treatment of the radiolabeled products with a purified PME or EPGase released the incorporated radiolabel, suggesting that the addition was onto HGA.

HGA-MT from tobacco was solubilized and shown to use endogenous acceptors, HGA or pectins with a degree of esterification (DE) of 30 as an acceptor (Goubet and Mohnen, 1999). The radiolabeled products from endogenous and exogenous acceptors were extracted with boiling water and ammonium oxalate (conditions that solubilize pectins from the cell wall).

Table 1.18. Properties of pectin methyltransferases from plants[a,b]

Plant Source	Apparent molecular weight (kDa)[c]	Apparent K_m for SAM[f] (μM)	pH optimum	V_{max} (pmol $mg^{-1}min^{-1}$)	Type of acceptor[h]	References
mung bean	-	59	6.8	2.7	HGA	(Kauss and Hassid, 1967a; Kauss et al., 1967b; Kauss and Swanson, 1969)
flax	-	10-30	6.8	ND[e]	ND	(Vannier et al., 1992)
flax (sol)[d]	-	0.5	5.5/7.1	ND	ND	(Bruyant-Vannier et al., 1996; Bourlard et al., 1997; Bourlard et al., 1997a)
tobacco	-	38	7.8	49	HGA	(Goubet et al., 1998)
tobacco (sol)	-	18	7.8	7.3	HGA	(Goubet and Mohnen, 1999)
soybean (per)[e]	-	230	6.8	1360	HGA	(Ishikawa et al., 2000)
flax (PMT5)	40	ND[g]	5.0	ND	ND	(Bourlard et al., 2001)
flax (PMT7)	110	ND	6.5	ND	ND	(Bourlard et al., 2001)
flax (PMT18)	18	ND	ND	ND	ND	(Bourlard et al., 2001)

[a]Adapted from (Mohnen, 2002).

[b]Unless otherwise indicated, all enzymes activities were measured in membrane fractions.

[c]The apparent molecular weights of the identified proteins were determined by SDS-PAGE or size exclusion chromatography.

[d](sol): detergent-solubilized enzyme.

[e](per): detergent-permeabilized enzyme.

[f]SAM: *S*-adenosyl-L-methionine.

[g]ND: not determined.

[h]The type of acceptor used in each study.

Treatment of the extracted products with a purified PME and EPGase released approximately 64% and 62.5% of the incorporated [^{14}C]methyl groups, respectively, suggesting that the bulk of the [^{14}C]methylated product was HGA.

Membrane-bound PMT activity was also detected and characterized from flax hypocotyls and suspension-cultured cells (Bruyant-Vannier et al., 1996; Bourlard et al., 1997a). Flax PMT transferred [^{14}C]methyl groups from *S*-adenosyl-L-[^{14}C]methionine onto an endogenous product. The transferred radiolabel could be released as [^{14}C]methanol by treatment with base. Although the endogenous acceptor was not characterized, membrane-bound PMT activity from flax was stimulated by the addition of exogenous pectins with both high (50%) and low (10%) degrees of esterification (Bourlard et al., 1997a).

The flax PMT activity was solubilized using detergent and two PMT isoforms were identified that differed in their pH optima and preference for pectins with low or high DE (Bruyant-Vannier et al., 1996; Bourlard et al., 1997a). Purification of the two flax PMT isoforms (PMT5 and PMT7) identified an 18 kDa protein (PMT18). It has been proposed that the PMT18 encodes the catalytic domain of both isoforms of flax PMT (Bourlard et al., 2001). At present, the identity of the gene encoding the 18 kDa protein is unknown.

A solubilized PMT activity from suspension-cultured flax cells was also stimulated 1.6- and 7-fold by the addition of exogenous RG-I or RG-II acceptors, respectively (Bourlard et al., 1997). The location of [^{14}C]methyl transfer onto the RG-I and RG-II acceptors was not determined. Therefore, it is not known whether the transfer of [^{14}C]methyl groups occurred onto backbone D-Gal*p*A residues or onto the methylated, side chain glycosyl residues found on RG-I and RG-II (Table 1.18).

Pectin acetyltransferases

Membrane-bound pectin acetyltransferase (PAT) activity was recently characterized from suspension-cultured potato cells (Pauly and Scheller, 2000). Potato PAT activity catalyzed the transfer of [^{14}C]acetyl groups from [^{14}C]acetyl-CoA onto endogenous potato acceptors. Approximately 23% of salt/ethanol precipitated, radiolabeled product could be solubilized following its treatment with both EPGase and PME, suggesting that at least 23% of the [^{14}C]acetyl groups transferred were onto HGA. Approximately 33% of the [^{14}C]acetyl groups were transferred onto RG-I acceptors greater than 500 kDa in size as determined by their susceptibility to an RG-I-specific acetylesterase. The RG-I acetyltransferase (RGAT) activity was partially characterized and found to have a pH optimum of 7.0, a K_m for [^{14}C]acetyl-CoA of 35 μM and a V_{max} of 54 pmol min^{-1} mg^{-1}. The radiolabeled product generated by potato RGAT could also be digested into smaller oligomers using rhamnogalacturonan lyase (RGase B) providing further evidence supporting the existence of a RGAT activity in these membranes. Acetyltransferases that transfer acetyl groups to the 2-O-Me-L-Fuc*p* or L-Ace*f*A residues on side chain B of RG-II (Figure 1.4) have yet to be identified.

CONCLUSIONS AND RELEVANCE

It has been demonstrated that mutations in pectin biosynthetic genes create alterations in pectin structure that can have severe deleterious effects on pectin function in the wall. While a number of pectin biosynthetic genes, especially those involved in nucleotide-sugar biosynthesis, have been discovered in plants, almost no genes encoding pectin methyl-, acetyl- and glycosyltransferases have been identified to date. Furthermore, pectin transferase activities have not been extensively characterized and information is lacking as to the location and mode of action of pectin biosynthesis in plants.

At the commencement of this research, the subcellular localization of pectic glycosyltransferases was not known. The elucidation of the subcellular location of a pectin galacturonosyltransferase, α-(1,4)-GalAT, from pea epicotyl membranes confirmed more indirect evidence suggesting that pectin biosynthesis occurred in the Golgi apparatus. Furthermore, it presented the first evidence of the topology of a pectin glycosyltransferase and allowed for the development of the currently accepted model for pectin biosynthesis in plants.

A new radioactive GalAT activity assay was developed that alleviates some of the time and expense required to assay multiple samples for GalAT activity. Furthermore, this assay was shown to be useful for the detection of GalAT activity using either endogenous or exogenous acceptors and may be an effective tool for the detection of other pectin glycosyltransferase activities.

Using this newly developed assay and a novel solubilization procedure, α-(1,4)-GalAT activity was purified 17-fold from Arabidopsis membranes, the highest recorded purity of any α-(1,4)-GalAT characterized to date. This allowed for the identification of two putative α-(1,4)-GalAT genes (JS36 and JS33) from Arabidopsis. N-terminally truncated versions of these genes were cloned into a vector designed for recombinant protein secretion, and were heterologously expressed in human embryonic kidney (HEK) 293 cells. Media from cells transfected with the JS36 gene construct was able to catalyze the transfer of D-[^{14}C]Gal*p*A from UDP-D-[^{14}C]Gal*p*A onto exogenous OGA acceptors in one transient experiment. These results suggest that JS36 encodes an α-(1,4)-GalAT. However, subsequent transient and stable expression of JS33 or JS36 in HEK293 cells did not confirm these initial results.

Both JS33 and JS36 are part of a 25 member gene family in Arabidopsis. Mutants in two members of this gene family, *qua1* and *parvus*, give phenotypes that are expected for the

mutation of pectin glycosyltransferases. The characterization of mutant plants in putative GALAT family members and their expression in heterologous systems may be required to determine the role of the putative GALAT family in pectin biosynthesis.

CHAPTER 2

THE CATALYTIC SITE OF THE PECTIN BIOSYNTHETIC ENZYME α-(1,4)-GALACTURONOSYLTRANSFERASE (GALAT) IS LOCATED IN THE LUMEN OF THE GOLGI[1]

[1] Jason Sterling, Heather F. Quigley, Ariel Orellana and Debra Mohnen 2001. *Plant Physiol*. 127: 360-371. Reprinted here with permission of publisher

ABSTRACT

α-(1,4)-galacturonosyltransferase (GalAT) is an enzyme required for the biosynthesis of the plant cell wall pectic polysaccharide homogalacturonan (HGA). GalAT activity in homogenates from pea (*Pisum sativum* L. var. Alaska) stem internodes co-localized in linear and discontinuous sucrose gradients with latent UDPase activity, an enzyme marker specific for Golgi membranes. GalAT activity was separated from antimycin A-insensitive NADH:cytochrome *c* reductase and cytochrome *c* oxidase activities, enzyme markers for the endoplasmic reticulum and the mitochondria, respectively. GalAT and latent UDPase activities were separated from the majority (80%) of callose synthase activity, a marker for the plasma membrane, suggesting that little or no GalAT is present in the plasma membrane. GalAT activities in proteinase K-treated and untreated Golgi vesicles were similar, whereas no GalAT activity was detected after treating Golgi vesicles with proteinase K in the presence of Triton X-100. These results demonstrate that the catalytic site of GalAT resides within the lumen of the Golgi. The products generated by Golgi-localized GalAT were converted by *endo*polygalacturonase treatment to mono- and digalacturonic acid, thereby showing that GalAT synthesizes (1,4)-linked α-D-galacturonan. Our data provide the first enzymatic evidence that a glycosyltransferase involved in HGA synthesis is present in the Golgi apparatus. Together with prior results of *in vivo* labeling and immunocytochemical studies, these results show that pectin biosynthesis occurs in the Golgi. A model for the biosynthesis of the pectic polysaccharide HGA is proposed.

INTRODUCTION

Pectins are a family of polysaccharides present in all plant primary walls (O'Neill et al., 1990). Homogalacturonan (HGA) accounts for approximately 60% of the total pectin in plants (O'Neill et al., 1990; Mohnen et al., 1996). HGA is a linear polymer composed of (1,4) linked α-D-galactosyluronic acid residues (D-Gal*p*A) that are often methylesterified at the C-6 carboxyl group (Mort et al., 1993) and may also be *O*-acetylated at *O*-2 and *O*-3 (Ishii, 1997). The D-Gal*p*A residues may, in some plants, be substituted at *O*-3 with a β-linked xylosyl residue (Schols et al., 1995; Yu and Mort, 1996).

An enzyme that catalyzes the transfer of D-Gal*p*A from UDP-D-Gal*p*A onto endogenous HGA was first identified in particulate suspensions from *Phaseolus aureus* and was named polygalacturonate 4-α-galacturonosyltransferase [EC 2.4.1.43] (Villemez et al., 1965; Villemez et al., 1966). A similar enzyme was characterized in microsomal membranes from suspension-cultured tobacco (*Nicotiana tabacum* L. cv. Samsun) cells (Doong et al., 1995) and solubilized from tobacco membranes (Doong and Mohnen, 1998). The solubilized enzyme was shown to catalyze the addition of an D-Gal*p*A residue onto *O*-4 of the non-reducing end (Scheller et al., 1999) of exogenous oligomeric HGA acceptors (Doong and Mohnen, 1998) and thus was named homogalacturonan 4-α-galacturonosyltransferase (HGA-GalAT).

No direct evidence has yet been reported for the subcellular localization of the glycosyltransferases responsible for pectin biosynthesis. However, the results of *in vivo* labeling and immunocytochemical analyses have suggested that pectin is synthesized in the Golgi apparatus (Northcote and Pickett-Heaps, 1966; Harris and Northcote, 1971; Staehelin and Moore, 1995). Immunocytochemical studies using antibodies that recognize the pectic polysaccharides homogalacturonan and rhamnogalacturonan I, suggest that these pectic

polysaccharides are synthesized within different compartments of the Golgi (Zhang and Staehelin, 1992) and are transported from the Golgi in vesicles that migrate to, and fuse with, the plasma membrane. The polysaccharides are then released into the extracellular space and incorporated into the wall (Northcote and Pickett-Heaps, 1966).

We now provide evidence that an α-(1,4)-galacturonosyltransferase (GalAT) from pea (*Pisum sativum* L. var. Alaska) epicotyls, with properties similar to the previously described HGA-GalAT from tobacco, is located in the Golgi apparatus and that the catalytic site of this enzyme is in the Golgi lumen. The third internodes of etiolated pea epicotyls were used for this study since the different subcellular membranes from this tissue can be separated using Suc density gradients, making such tissue useful for topological and localization studies of enzymes involved in cell wall polysaccharide biosynthesis (Brummell et al., 1990; Orellana et al., 1997; Wulff et al., 2000). Our data provide strong evidence that HGA is synthesized in the Golgi apparatus and a model for the biosynthesis of this pectic polysaccharide is proposed.

MATERIALS AND METHODS

Chemicals

Uridine diphosphate-α-D-[^{14}C]glucuronic acid (UDP-D-[^{14}C]Glc*p*A, 293.6 mCi mmol^{-1}) and uridine diphosphate-α-D-[^{14}C]glucose (UDP-D-[^{14}C]Glc*p*, 286.2 mCi mmol^{-1}) were purchased from DuPont-New England Nuclear (Boston, MA). Uridine diphosphate-α-D-[^{14}C]galacturonic acid (UDP-D-[^{14}C]Gal*p*A) was prepared by the epimerization of UDP-D-[^{14}C]Glc*p*A as described previously (Liljebjelke et al., 1995). OGAs with a DP of 14 and a mixture of OGAs of DP 7 to 23 were prepared according to Doong et al. (1995). Proteinase K was purchased from Boehringer Mannheim (Indianapolis, IN). Homogeneous EPGase (748 units ml^{-1}, 1 unit releases 1 μmole D-Gal*p*A per min) from *Fusarium moniliforme* was a gift from

Carl Bergmann (Complex Carbohydrate Research Center, Athens, GA). All other reagents were purchased from Sigma (St. Louis, MO).

Plant materials

Pea (*Pisum sativum* L. var. Alaska) seeds were purchased from the Green Seed Company (Athens, GA). Seedlings were grown in moist vermiculite for 7 to 8 d at 25°C in the dark.

Linear sucrose gradient fractionation of pea homogenates

Third internodes (from the cotyledon, 1 cm in length, 5 g total weight) from 7 to 8 d old etiolated peas (*Pisum sativum* L. var Alaska) were excised and homogenized in 50 mM HEPES [4-(2-hydroxyethyl)-1-piperazineethanesulfonic acid]/KOH, pH 7.0, containing 0.4 M sucrose, 1 mM $MgCl_2$, 10 mM KCl, 1 mM EDTA, and 1 mM dithiothreitol using a razor blade and a mortar and pestle. The homogenate was filtered through two layers of Miracloth (Calbiochem, San Diego, CA) and the filtrate centrifuged for 10 min at 1,000*g*. The 1,000*g* supernatant (5 mL) was overlaid onto 24 mL of a 20% to 50% sucrose (Suc; w/w) gradient (Munoz et al., 1996) in 50 mM HEPES/KOH, pH 7.0 containing 0.1 mM $MgCl_2$, 1 mM EDTA and 1 mM dithiothreitol and centrifuged for 3.5 h at 100,000*g*. Fractions (0.5 mL) were collected and analyzed for enzyme marker activity. All manipulations were done at 4°C. Suc concentrations were determined using an Abbe refractometer (model 3L, Milton Roy Company, Rochester, NY) and the densities were calculated using an ambient temperature of 20°C.

Isolation of Golgi membranes

Enriched Golgi membranes were isolated using discontinuous Suc gradients according to a previously described method (Munoz et al., 1996). All manipulations were done on ice or at 4°C. The third internodes (1 cm, 40-70 g total mass) of 7 to 8 d old etiolated pea stem epicotyls were excised and homogenized in 1 volume of buffer A (0.1 M KH_2PO, pH 6.65 containing 5

mM $MgCl_2$, 1 mM dithioerythritol, and 16% [w/w] Suc) using a razor blade and a mortar and pestle. The homogenate was filtered through two layers of Miracloth and centrifuged for 2 min at 1,000*g*. The supernatant was layered onto 38% (w/w) Suc in buffer A (8 ml) and centrifuged for 90 min at 100,000*g*. The upper phase was removed without disturbing the interface layer and replaced with 33% (w/w) Suc (15 ml) and 8% (w/w) Suc (5 ml) in buffer A. The gradient was centrifuged for a further 100 min at 100,000*g*. The pellet was resuspended in 10 mM Tris, pH 7.5 containing 0.25 M Suc (ST buffer) and stored at −80°C. The membranes that equilibrated at each of the interfaces were collected, diluted with an equal volume of water, and centrifuged for 50 min at 100,000*g*. These pellets were resuspended in ST buffer and stored at ¯80°C. In some experiments (Table 2.2), membranes from the 33% and 38% Suc phases were also collected and stored as described above. Otherwise, the 33% and 38% Suc phases with no prior membrane collection were used for enzyme analysis (Table 2.1).

Enzyme assays

Cyt *c* oxidase activity was measured as described (Briskin et al., 1987) with some modifications. Cyt *c* oxidase was assayed spectrophotometrically at 550 nm using a Shimadzu scanning spectrophotometer (model UV-2101; Columbus, MD). A portion (35 µl) of each gradient fraction was added to 30 mM K_2HPO_4, pH 7.4 (735 µl) containing 1 mM EDTA, 1 mM $NaHCO_3$, 0.00045% Triton X-100, and 50 µM Cyt *c* (reduced with sodium dithionite). The total activity of Cyt *c* oxidase was calculated for each fraction using the initial linear rate of Cyt *c* oxidation (decrease in A_{550}) and the extinction coefficient of Cyt *c* (18.5 mM^{-1} cm^{-1}).

Antimycin A-resistant NADH:Cyt *c* reductase was measured according to a previously described method with some modifications (Vannier et al., 1992). A portion (0.1 ml) of each gradient fraction was combined with 50 mM KH_2PO_4, pH 7.5 (0.9 ml) containing 50 µM Cyt *c*,

0.3 mM NADH, 5 mM KCN and 1 μM antimycin A. The linear increase in A_{550} was taken as the rate of Cyt *c* reduction and was used to calculate the total activity in each fraction.

Latent UDPase activity was measured as described (Briskin et al., 1987) with some modifications. A reaction mixture (15 μl) containing 6 mM UDP, 6 mM $MgSO_4$, and 60 mM Tris/Mes [2-(*N*-morpholino)-ethanesulfonic acid], pH 6.5, with or without 0.1% (v/v) Triton X-100, was added to 15 μl of gradient fraction in a microtiter plate (Nunc, Suwanee, GA) and kept for 15 min at 25°C. The reaction was stopped by the addition of Ames reagent (270 μl) and processed as described (Ames, 1966). The A_{690} of the sample was measured using a Tikertek Multiscan ELISA plate reader (model MCC/340 MKII; Flow Laboratories, McLean, VA) and was converted to the amount of P_i released from UDP (UDPase activity) using a standard curve of KH_2PO_4. Latent UDPase activity was considered to be present in those fractions in which an increase in A_{690} was observed when fractions were incubated in the presence 0.1% (v/v) Triton X-100. The latent UDPase activity reported in Tables 2.1 and 2.2 and in Figure 2.1 was calculated by subtracting the amount of P_i released from UDP by enzyme in the absence of Triton X-100 from the amount of P_i released from UDP by enzyme in the presence of Triton X-100.

Callose synthase activity was measured according to a previously described method by (Dhugga and Ray, 1994) with some modifications. Gradient fractions (10 μl of one-tenth diluted sample) were incubated for 5 min in 10 mM MOPS [3-(*N*-morpholino)-propanesulfonic acid], pH 7.0 containing 1 mM UDP-D-Glc*p*, 10 mM cellobiose, 2 mM $CaCl_2$, 0.3 mM spermine, 0.02% (v/v) Triton X-100, and 0.32 μM UDP-D-[^{14}C]Glc*p*. The reaction was stopped by the addition of 70% (v/v) ethanol (2 ml) and the insoluble products were collected by filtration through a GF/A glass-microfiber disc (Whatman, Maidstone, UK). The discs were washed with

70% ethanol (15 ml), dried, and the amount of radioactivity on the discs measured by scintillation counting.

GalAT activity was measured as described by Doong et al. (1995) with some modifications. Samples (10 μL) were incubated for 2 min in 50 mM HEPES, pH 7.8, containing 100 μg of OGAs (DP of 7-23), 1.1 μM UDP-D-[^{14}C]Gal*p*A (specific activity 293.6 mCi mmol^{-1}), 0.25 mM $MnCl_2$, 25 mM KCl and 0.1% (v/v) Triton X-100 in a total volume of 30 μl (unless otherwise stated). The reaction was stopped by the addition of 700 μl chloroform:methanol (3:2, v/v) and centrifuged to collect the precipitable products. The product was washed twice with 500 μl of 65% (v/v) ethanol and the amount of radioactivity quantified by scintillation counting.

All enzyme assays were conducted at room temperature with the exception of the GalAT assay which was conducted at 30°C. Protein concentrations were determined by protein assay (BioRad, Hercules, CA) using bovine serum albumin as a standard. Uronic acids were analyzed colorimetrically using the meta-hydroxybiphenyl assay (Blumenkrantz and Asboe-Hansen, 1973).

Product characterization

The products generated by GalAT in pea Golgi vesicles were analyzed according to Doong et al. (1995). The products were formed using either detergent-permeabilized Golgi in the presence of OGAs of DP 14 as exogenous acceptor or using intact Golgi without exogenous acceptor.

Four separate GalAT reactions containing 12 μl of Golgi vesicles (approximately 43 μg of protein) and 5 μM UDP-D-[^{14}C]Gal*p*A in 50 mM HEPES, pH 7.8, 0.25 mM $MnCl_2$, and 25 mM KCl were incubated with or without 0.1% (v/v) Triton X-100 and 15 μg of OGA 14 mer for 35 min at 30°C in a total volume of 60 μl. The products were recovered, washed as described

above, resuspended in 0.5 ml of 50 mM NaOAc, pH 6.0 containing 5 mM EDTA, and pooled (total volume 2 ml). Individual pools were analyzed as follows by either HPAEC or SEC. For example, a 500 μl aliquot was analyzed directly by HPAEC. A second aliquot of 500 μl was treated for 8 h at 30°C with a homogeneous EPGase (2 units) and the products generated were analyzed by HPAEC. A third aliquot of the pooled products (1 ml) was adjusted to pH 12 by the addition of 1 N NaOH and kept at 4°C for 8 h. The solution was adjusted to pH 5.0 with 1 N HCl and a portion (500 μl) was analyzed by HPAEC. The remaining base-treated product (500 μl) was treated with EPGase for 8 h and analyzed by HPAEC.

Alkaline phosphatase treatment of D*-Gal*p*A-1-P*

Aqueous extracts from a GalAT reaction were prepared by incubating 12 μl of Golgi vesicles (approximately 43 μg of protein) for 60 min at 30°C in 50 mM HEPES, pH 7.8, containing 2.5 μM UDP-D-[^{14}C]Gal*p*A, and 15 μg of OGAs of DP 12, 0.25 mM $MnCl_2$, 25 mM KCl, 0.1% (v/v) Triton X-100 in a total volume of 60 μl. The reaction was terminated by the addition of chloroform:methanol (5:1 [v/v], 300 μl) and 240 μl 50 mM NaOAc, pH 6.0 containing 5 mM EDTA was added. The mixture was centrifuged at 13,000*g* for 2 min. The aqueous upper phase was mixed with 300 μl of chloroform:methanol (5:1 [v/v]), centrifuged and removed. The organic phase from the first centrifugation was mixed with 50 mM NaOAc, pH 6.0 (300 μl) containing 5 mM EDTA, centrifuged, and the aqueous phase was combined with the previously obtained aqueous phase. An aliquot (80 μl) of the combined aqueous phases was adjusted to pH 8.5 with Tris (10 mM). Water or 10 units of alkaline phosphatase was added, and the mixture kept for 60 min at 37°C. The reaction was stopped by heating at 85°C for 10 min. The resulting mixture was filtered (0.2 μm) and chromatographed by HPAEC. Fractions (1 ml)

were collected and the amount of radioactivity in each fraction was quantified by liquid scintillation counting.

Size-exclusion chromatography of the [^{14}C]-labeled product generated using intact and permeabilized Golgi

The products made by GalAT in intact Golgi without exogenous acceptor, and the products formed by detergent-permeabilized (0.1% [v/v] Triton X-100) Golgi in the presence of exogenous OGA 14 mer (15 μg) were separated using a Superose12 HR10/30 SEC column (Pharmacia, Uppsala, Sweden). The column was eluted with 50 mM sodium acetate containing 5 mM EDTA at 0.35 ml min^{-1}. Fractions (0.5 ml) were collected and the radioactivity in a portion (400 μl) of each fraction was determined by scintillation counting. The SEC elution profiles of dextran molecular mass standards, D-Gal*p*A, triGalA, and OGAs of a DP of 7, 12, 15 and 16 were detected using a pulsed electrochemical detector (Dionex, Sunnyvale, CA) with post-column addition of 400 mM NaOH at a flow rate of 0.2 ml min^{-1} (see below).

HPAEC of the [^{14}C]-labeled product made using intact and permeabilized Golgi

D-[^{14}C]Gal*p*A-labeled product generated by GalAT in pea Golgi vesicles, and D-Gal*p*A and oligogalacturonide standards, were filtered (0.2 μm nylon microfilterfuge tubes, Rainin Instrument Co., Inc., Woburn, MA) and chromatographed on a CarboPac PA100 column (4 X 250 mm) fitted with a CarboPac PA100 guard column (3 X 25 mm) using a Dionex DX 500 LC, (Dionex, Sunnyvale, CA). Samples were eluted from the column at 1 ml min^{-1} with a gradient formed from ultra-pure deionized water (eluant A) and 1 M sodium acetate containing 5 mM EDTA (eluant B) as follows: 0% (v/v) B at 0-2 min, 40% (v/v) B at 17 min, 80% (v/v) B at 49 min, 100% (v/v) B at 50-52 min, 0% (v/v) B at 57 min (modified from Doong et al., 1995). The non-radiolabeled standards were detected by pulsed electrochemical detection after post-column

addition of 400 mM NaOH at 0.5 ml min^{-1}. The pulse sequence for the electrochemical detector was 0.05 V at 0 s, 0.05 V at 0.2 s (begin integration), 0.05 V at 0.4 s (end integration), 0.75 V at 0.41 to 0.6 s, and −0.15 V at 0.61 to 1.0 s. Fractions (0.75 ml) were collected, an aliquot (500 μl) of each fraction was combined with 10 volumes of scintillation cocktail (Scintiverse, Fisher Scientific, Norcross, GA), and the amount of radioactivity was measured using a scintillation counter. Quenching by salt and/or base was found to be negligible.

Proteinase K digestion

Proteinase K treatment of Golgi vesicles was conducted according to Orellana et al. (1997). In brief, Golgi vesicles (100 μg protein) were incubated for 30 min at 30°C in 10 mM Tris, pH 7.5 containing 0.25 M Suc and 1 mM $MgCl_2$ (100 μl total volume) in the presence and absence of 0.1% (v/v) Triton X-100 and 4 μg Proteinase K. Proteolysis was stopped by the addition of 1 mM phenylmethylsulfonylfluoride and 10 μl of each treatment was brought to a final concentration of 0.1% (v/v) Triton X-100 and assayed for GalAT activity in the presence of exogenous OGA acceptors.

RESULTS

Subcellular localization of GalAT activity in pea membranes

Subcellular membrane fractions obtained by linear sucrose (Suc) gradient centrifugation of homogenates from etiolated pea third internodes were analyzed for GalAT activity and for organelle-specific enzyme activity (Figure 2.1). GalAT activity was detected almost exclusively in fractions 26 through 30 (1.17-1.14 g ml^{-1}; Figure 2.1, A). The presence of GalAT activity in such a limited number of fractions suggests that it is associated with an organelle of a distinct density. Enzyme marker assays for the ER and for the mitochondria (antimycin A-insensitive

Figure 2.1. Location of GalAT activity and enzyme markers in pea membranes fractionated by linear Suc density gradient centrifugation. A) GalAT activity (▼) and sucrose density (▽). The data were obtained from a single analysis of each fraction. Similar results were obtained in three separate gradients. B) Cytochrome (Cyt) *c* oxidase (■) and Antimycin A resistant NADH Cyt *c* reductase (◇), enzyme markers for mitochondria and endoplasmic reticulum (ER), respectively. Activities are expressed as the percentage of the highest total activity (191.2 nmol Cyt *c* reduced min^{-1} and 397.6 nmol Cyt *c* oxidized min^{-1} for Cyt *c* reductase and Cyt *c* oxidase, respectively) obtained in the peak fraction. The data were obtained from a single analysis of each fraction. Similar results were obtained in two independent gradients. C) Latent UDPase activity, a Golgi marker, is detected as the increase in A_{690} obtained in fractions permeabilized with 0.1% (v/v) Triton X-100 compared to the absorbance obtained in fractions in the absence of detergent. The position of greatest latent activity is depicted with a double-headed arrow (Golgi). Data are the average of duplicate samples from each fraction. Similar results were obtained in three separate gradients.

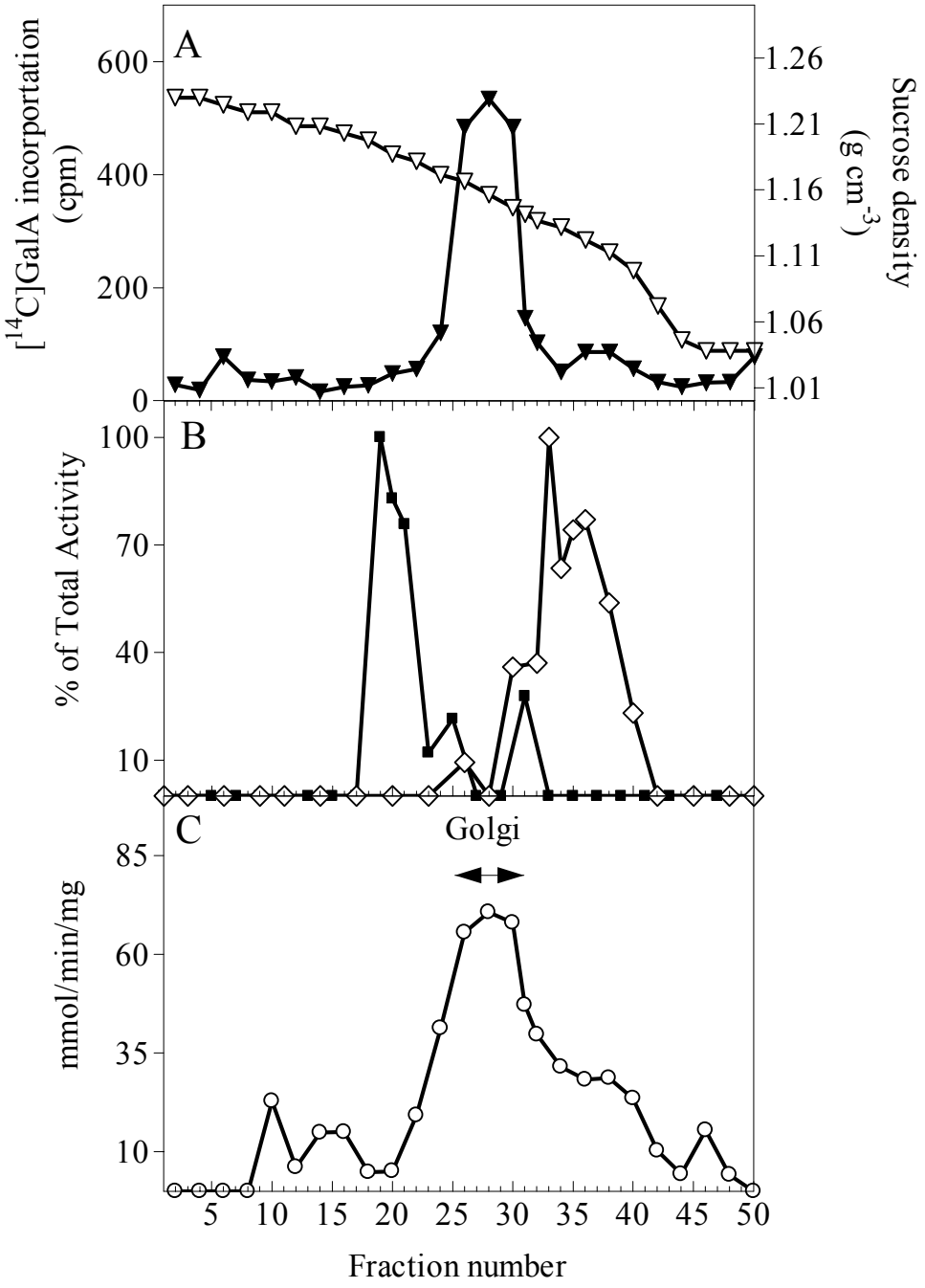
A
B
C
[14C]GalA incorporation (cpm)
Sucrose density (g cm-3)
% of Total Activity
mmol/min/mg
Golgi
Fraction number
600
400
200
0
1.26
1.21
1.16
1.11
1.06
1.01
100
70
40
10
85
60
35
10
5
10
15
20
25
30
35
40
45
50

NADH:Cyt *c* reductase and Cyt *c* oxidase, respectively) showed that the ER (fractions 30-40, 1.14-1.10 g ml^{-1}) and mitochondria (fractions 19-22, 1.20-1.18 g ml^{-1}) were present in a different subset of fractions (Figure 2.1, B) than those that contained the greatest amount of GalAT activity.

Latent UDPase activity is a well-characterized Golgi-specific enzyme marker (Orellana et al., 1997) that is detected following the permeabilization of membranes with detergent. The greatest amount of latent UDPase activity was present in fractions 24 through 32 of a density of 1.17 to 1.14 g cm^{-3} (Figure 2.1, C). These fractions coincide with the fractions that contain the greatest amount of GalAT activity, suggesting that GalAT is a Golgi-localized enzyme.

To confirm that GalAT is present in a Golgi-enriched fraction, pea homogenates were separated using discontinuous Suc gradient centrifugation. Each fraction (Figure 2.2) was analyzed for GalAT activity and for membrane marker activities (Table 2.1). Latent UDPase activity was highest in the membranes that banded at the 8-33% (w/w) Suc interface suggesting that these membranes were Golgi-enriched (Tanford and Reynolds, 1976). The Golgi-enriched fraction also contained approximately 90% of the total GalAT activity (Table 2.1). Some (21% of total) ER-specific enzyme marker activity was also detected in the Golgi-enriched fraction. However, the ER-enriched fraction (33-38% [w/w] Suc interface) contained no GalAT activity (Table 2.1). These results, when taken together with the results shown in Figure 2.1, strongly suggest that the GalAT from pea membranes is a Golgi-localized enzyme.

The biosynthesis of cellulose and callose has been shown to occur at the plasma membrane (Frederikson and Larsson, 1989; Delmer, 1999), and the possibility could not be discounted that GalAT may also be localized to the plasma membrane. Thus, experiments were conducted, using discontinuous Suc gradient centrifugation, to separate Golgi membranes from

Figure 2.2. Illustration of the gradient fractions collected following discontinuous Suc gradient centrifugation. The collected gradient fractions were analyzed for enzyme marker activity and for the presence of GalAT activity (see Table 2.1). The membranes that banded at the 8% to 33% (w/w) Suc interface were defined as the Golgi vesicle-enriched fraction and the membranes that banded at the 33% to 38% (w/w) Suc interface were defined as the ER-enriched fraction.

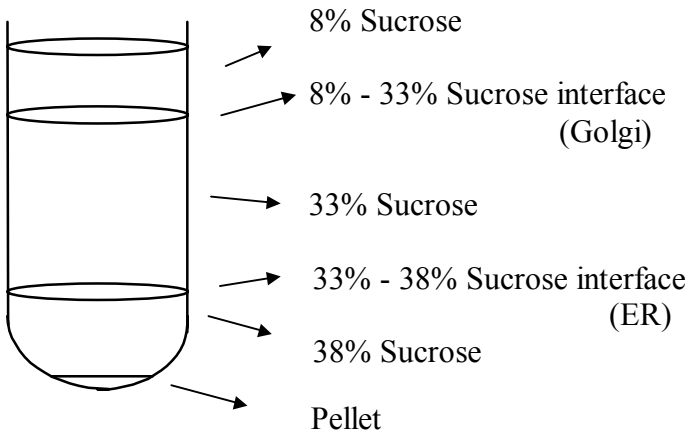

Table 2.1. Distribution of enzyme activities within pea homogenates fractionated by discontinuous Suc gradient centrifugation. Discontinuous Suc gradients were made and enzyme assays conducted as described in the "Materials and Methods". Total enzyme activity in each gradient fraction is shown. The data are the average of two replicates ± SE from one gradient. Similar results were obtained in two independent gradients.

Gradient fraction	Latent UDPase (μmol PO_4 released min^{-1})	Cyt c oxidase (μmol Cyt c oxidized min^{-1} ± SE)	NADH:Cyt c reductase (μmol Cyt c reduced min^{-1} ± SE)	GalAT[a] (pmol D-Gal*p*A incorporated min^{-1} ± SE)
GV[b]	33.9	0	3.38 ± 0.12	1.46 ± 0.08
33%	ND[c]	0	0	0
ER[d]	11.3	2.19 ± 0.15	6.21 ±0.60	0
38%	ND[c]	4.07 ± 0.20	3.98 ±0.26	0
Pellet	5.87	2.17 ± 0.47	2.74 ± 0.16	0.12 ±0.08

[a]Assayed using 1.1 μM UDP-D-[^{14}C]Gal*p*A.

[b]The interface between the 8% and the 33% (w/w) Suc layers enriched in Golgi membranes.

[c]ND, not determined due to the presence of phosphate in the buffer.

[d]The interface between the 33% and the 38% (w/w) Suc layers enriched in ER membranes.

plasma membranes. The gradient fractions were assayed for GalAT activity, for latent UDPase and for callose synthase activity, a known marker for plasma membrane vesicles in plants (Morre et al., 1987; Dhugga and Ray, 1994). Callose synthase activity was present in all of the discontinuous sucrose gradient fractions assayed. These results indicate that the Golgi-enriched membranes obtained using discontinuous Suc gradients also contained some plasma membranes. Thus, the possibility cannot be ruled out that GalAT is localized to a subset of plasma membrane vesicles that co-localize with Golgi membranes. Nevertheless, because approximately 80% of the callose synthase activity is located in fractions that are distinct from those that contain the majority of the GalAT and latent UDPase activities (Table 2.2), these results most strongly support the conclusion that GalAT is Golgi localized and is not a component of the plasma membrane.

Characterization of the products made by GalAT in enriched Golgi membranes from pea.

The subcellular fractionation of GalAT activity with the Golgi-enriched fraction from pea suggested that a pectin biosynthetic enzyme was localized in the Golgi. To test whether HGA is formed by the GalAT in pea Golgi, the [^{14}C]-labeled products generated by incubating UDP-D-[^{14}C]Gal*p*A with intact pea Golgi were analyzed by size exclusion chromatography (SEC) and by high performance anion exchange chromatography (HPAEC). The products were analyzed both before and after treatment with base (to remove methyl and other esters), with *endo*polygalacturonase (EPGase; to fragment HGA), and with base plus EPGase. Fractions were collected, analyzed by scintillation counting, and the elution times of the radioactive products compared to the elution times of D-Gal*p*A, oligogalacturonides (OGAs), and dextran molecular mass standards.

Table 2.2. Distribution of latent UDPase, callose synthase and GalAT activities in membranes collected by discontinuous density gradient centrifugation. Total enzyme activity in each gradient fraction is shown. The data are the average of duplicate samples ± standard error from one gradient. Similar results were obtained in two separate gradients.

Gradient fraction	Latent UDPase (μmol PO_4 released min^{-1})	Callose synthase (nmol Glc incorporated min^{-1} ± SE)	GalAT[a] (pmol D-Gal*p*A incorporated min^{-1} ± SE)
GV	145.5	463.9 ± 70.8	1453.3 ± 150.9
33%	49.6	585.5 ± 98.2	0
ER	31.6	465.6 ± 43.3	200.5 ± 48.2
38%	15.7	768.2 ± 52.0	0
Pellet	11.6	404.0 ±70.8	0

[a]Assayed with 0.92 μM UDP-D-[^{14}C]Gal*p*A and 100 μM UDP-D-Gal*p*A.

The SEC elution profiles of untreated and the EPGase-treated products from intact pea Golgi are shown in Figure 2.3. The untreated product gave a peak (20% of the total radioactivity) with a retention time earlier than the 500 kDa dextran standard, and a peak (42% of the total radioactivity) that co-eluted with D-Gal*p*A. Some radioactivity eluted between these two peaks and most likely corresponded to variously sized HGA. EPGase treatment of the intact product resulted in the conversion of the high-molecular mass material into products that have the same retention time as mono- and diGalA (Figure 2.3). These results suggest that most of the D-[^{14}C]Gal*p*A-labeled product made using intact Golgi membranes is α-(1,4)-linked HGA.

The untreated and EPGase-treated products, and the products that were formed upon base and base plus EPGase treatment, were analyzed by HPEAC (Figure 2.4, A-D). The untreated product contained a peak (27% of total radioactivity) that had a retention time similar to D-Gal*p*A, as well as a series of smaller peaks (32% of total radioactivity) that eluted at retention times comparable with medium-sized OGAs (DPs of 12, and 15-20; Figure 2.4, A). Base treatment of the untreated product did not alter the retention time of the radioactive peaks, suggesting that the products formed by intact pea Golgi were not extensively methoxylated or otherwise esterified (Figure 2.4, C). EPGase treatment of the untreated (Figure 2.4, B) or base-treated (Figure 2.4, D) products resulted in the appearance of diGalA, an increase in the amount of D-Gal*p*A and the disappearance of the mid-sized OGAs, thereby confirming that the oligomeric peaks in the untreated and the base-treated products were HGA.

The amount of radiolabeled mono- and diGalA recovered after EPGase digestion and HPAEC was not equal to the amount of radioactivity detected as the series of small peaks in the untreated product (compare Figure 2.4, A with B). Furthermore, the absence of a peak corresponding to the high molecular mass product (see Figure 2.3) in either Figure 2.4, A or C

Figure 2.3. SEC of products made by the GalAT in intact pea Golgi membranes. The untreated (▼) and EPGase-treated (□) products recovered following incubation of intact Golgi membranes with 4.7 μM UDP-D-[^{14}C]Gal*p*A in the absence of exogenous acceptor were separated by SEC. The amount of radioactivity in each fraction was determined by scintillation counting. The cpm of each fraction minus the background is shown. Base (0.1 N NaOH) was included in the eluant solutions to enable electrochemical detection of D-Gal*p*A and dextran molecular mass standards by pulsed electrochemical detection.

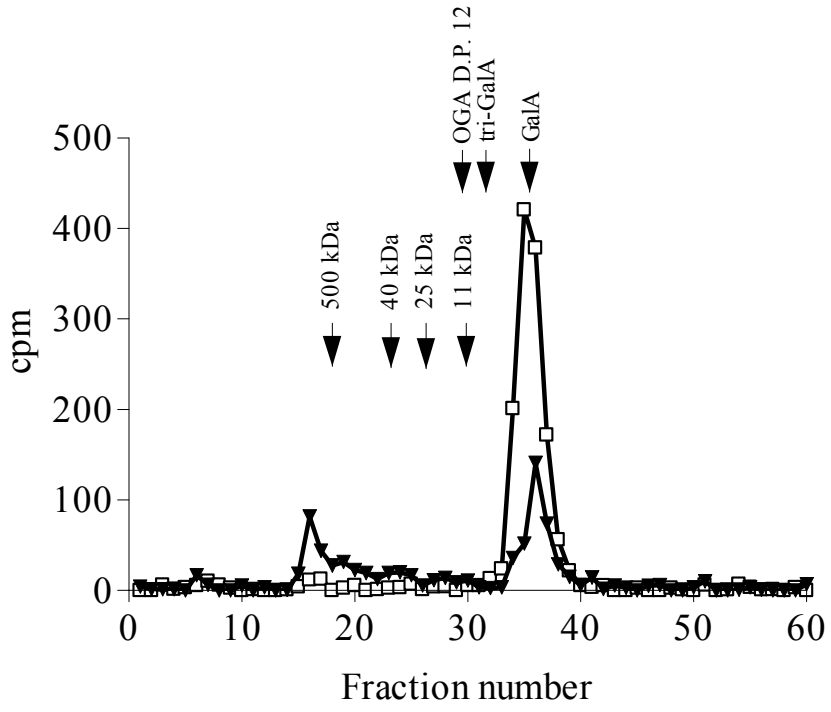

Figure 2.4. HPAEC of the product made by the GalAT in intact pea Golgi membranes. The A) untreated, B) EPGase-treated, C) base-treated, and D) base plus EPGase-treated products were analyzed by HPAEC. The amount of radioactivity present in each fraction was determined by scintillation counting. The cpm of each fraction minus the background is shown. Base (0.1 N NaOH) was included in the eluant solutions to enable electrochemical detection of the size standards D-Gal*p*A, diGalA, triGalA, UDP-D-Gal*p*A and OGAs of a degree of polymerization (DP) of 14 by pulsed electrochemical detection. A smaller amount (20% less) of the base + EPGase-treated products were injected into the column than the amount injected of the other products and therefore the cpm in panel D) have been adjusted to correct for this difference.

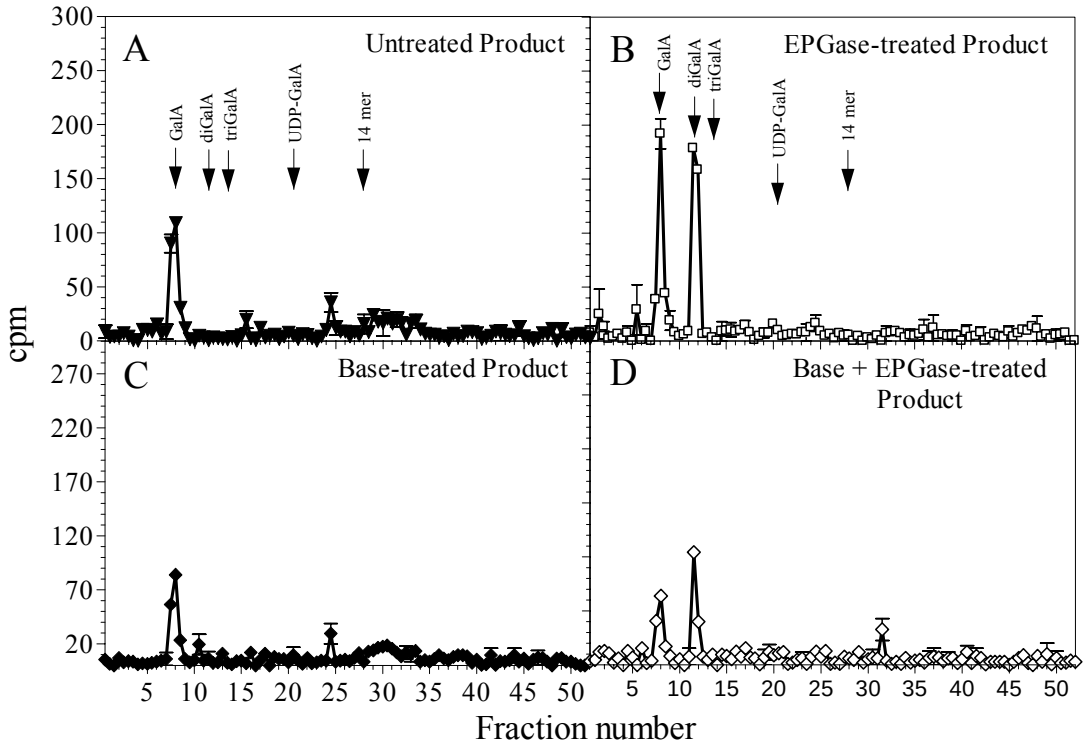

suggests either that the high molecular mass material was unable to elute as a defined peak on the anion exchange column or that the material was unable to pass through the 0.2 μm filters used prior to HPAEC analysis (see "Materials and Methods"). Analysis of the 0.2 μm filters revealed that approximately 47% and 26% (for untreated and base treated products, respectively) of the total label incorporated into product remained on the filter following filtration.

In a preliminary study, we found that the amount of radiolabeled product formed by membrane-bound GalAT from pea increased with the addition of exogenous OGA acceptors in the presence of 0.1% (v/v) Triton X-100 (data not shown). Therefore, the product formed by Golgi membranes in the presence of 0.1% (v/v) Triton X-100 and an OGA acceptor (DP 14) was analyzed to confirm that pea GalAT produced HGA under these conditions.

Several differences were observed between the products made by intact and detergent-permeabilized Golgi membranes. For example, approximately 47% of untreated product made by intact Golgi bound to the HPLC prefilter, whereas only 12% of the untreated product from Triton X-100-permeabilized Golgi bound to the filter. Comparable amounts of radioactive product (83% for intact Golgi and 98% for permeabilized Golgi) passed through the filter after base and EPGase treatment. These results suggested that the products formed using detergent permeabilized Golgi and exogenous oligomeric HGA acceptors were smaller and/or had different characteristics than the products made by intact Golgi vesicles.

The [^{14}C]-labeled products formed using 0.1% Triton X-100-permeabilized pea Golgi in the presence of an OGA acceptor (DP 14) were analyzed by SEC and HPAEC (Figures 2.5 and 2.6) before and after, base treatment, EPGase treatment, and base plus EPGase treatment. SEC of the untreated product (Figure 2.5) gave two peaks that eluted with the same retention time as an authentic OGA of DP 15 (15 mer, 32% of total) and D-Gal*p*A (22% of total), respectively.

Figure 2.5. SEC of products produced by the GalAT in detergent-permeabilized Golgi in the presence of exogenous acceptor. Untreated (▼) and EPGase-treated (□) products made by Triton X-100-permeabilized Golgi vesicles incubated with 5 μM UDP-D-[^{14}C]Gal*p*A and OGA of DP 14 as acceptor were analyzed by SEC. The collected fractions were analyzed by scintillation counting. The cpm in each fraction minus background is plotted. D-Gal*p*A, OGAs of DP 7 (7 mer) and 15 (15 mer), and dextran molecular mass standards were detected by pulsed electrochemical detection.

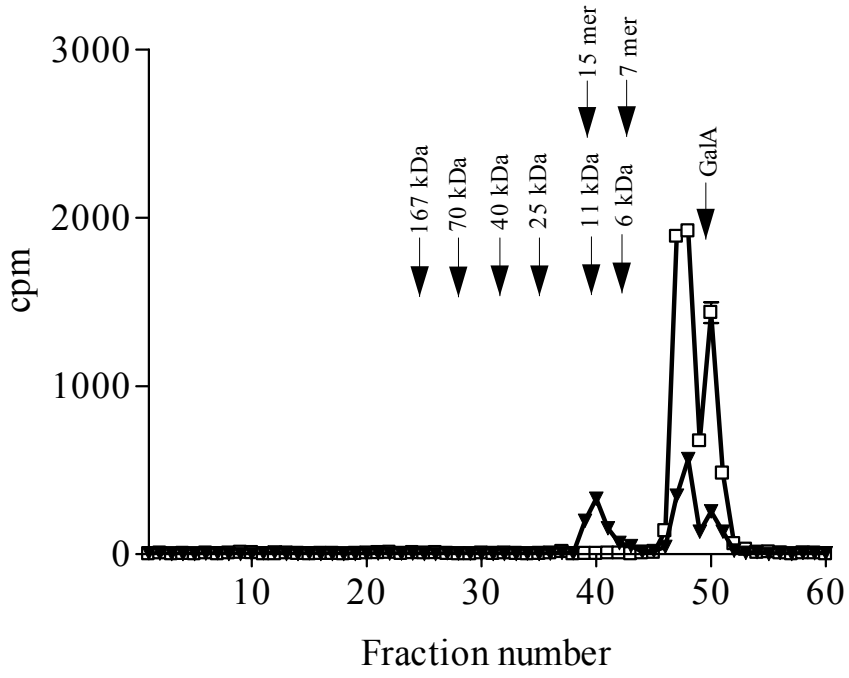

Figure 2.6. HPAEC of products produced by the GalAT in detergent-permeabilized Golgi in the presence of exogenous acceptor. HPAEC analysis of the A) untreated, B) EPGase-treated, C) base-treated, and D) base plus EPGase-treated products. The collected fractions were analyzed by scintillation counting and the cpm in each fraction minus background is plotted. D-Gal*p*A, diGalA, triGalA, tetraGalA and OGA of DP 14 were detected by pulsed electrochemical detection. The untreated product was diluted 1:1 with 10 mM EDTA before it was spin-filtered and separated by HPAEC and therefore the cpm in panel A) have been adjusted to correct for this dilution.

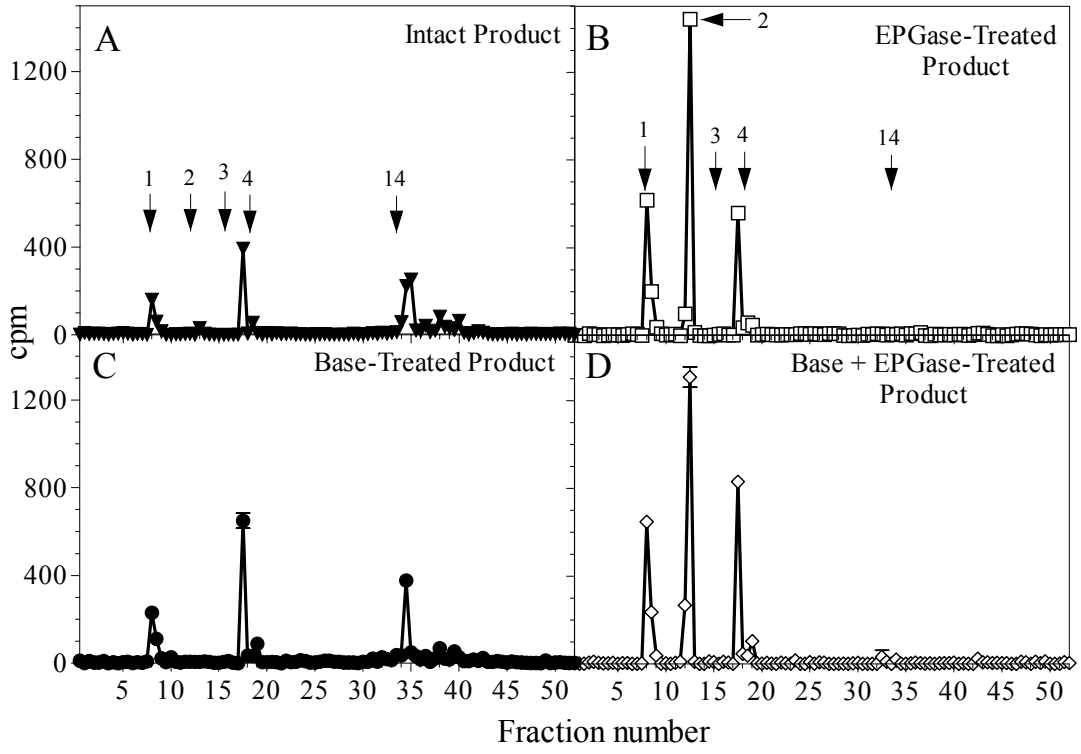

The peak that eluted before D-Gal*p*A was shown (see below) to be D-Gal*p*A-1-phosphate (D-Gal*p*A-1-P; 44% of total; Figure 2.5). The radioactive 15 mer peak was completely converted by EPGase treatment into peaks that had the same retention time as D-Gal*p*A and diGalA (Figure 2.5). No large molecular mass peak was detected in the untreated product formed by Triton X-100-treated pea Golgi, suggesting that in the presence of exogenous acceptor the GalAT in Triton X-permeabilized membranes does not synthesize a large molecular mass product. Similar results have been obtained with a GalAT solubilized from tobacco membranes (Doong and Mohnen, 1998).

HPEAC analysis of the products made by Triton X-100-treated pea Golgi in the presence of an OGA acceptor is consistent with the results obtained by SEC. The untreated product (Figure 2.6, A) eluted as three predominant peaks of radioactivity that co-eluted with D-Gal*p*A, D-Gal*p*A-1-P (elutes slightly earlier than tetraGalA, see below) and the OGA 15 mer, respectively. A small amount of larger-sized material was also present.

Two methods were used to establish that the radiolabeled peak that eluted between triGalA and tetraGalA was D-Gal*p*A-1-P. Authentic D-Gal*p*A-1-P was chromatographed by HPAEC, fractions collected, and the uronic acid content of each fraction determined colorimetrically. The retention time of the radiolabeled peak and D-Gal*p*A-1-P were the same (data not shown). To confirm that the identity of the radiolabeled D-Gal*p*A-1-P, radiolabeled product generated by permeabilized Golgi in the presence of OGA of DP 12 was recovered by extraction of the product with chloroform:methanol and a portion of the aqueous phase was treated with alkaline phosphatase. The untreated (Figure 2.7, A) and phosphatase-treated products (Figure 2.7, B) were separated by HPAEC. As anticipated, the putative D-Gal*p*A-1-P peak disappeared after treatment with phosphatase and the amount of D-Gal*p*A increased.

Figure 2.7. Alkaline phosphatase treatment of an aqueous extract of the radiolabeled products produced in pea Golgi. Permeabilized Golgi vesicles were incubated for 60 min at 30°C with an exogenous OGA acceptor of DP 12 and 2.5 μM UDP-D-[^{14}C]Gal*p*A. The reaction was stopped by the addition of chloroform:methanol (5:1 [v/v]) and the aqueous phase was extracted, washed, and treated for 60 min at 37°C with A) water (■), or with B) 10 units of alkaline phosphatase (□). The reaction was terminated by incubation at 85°C for 10 min, filtered and analyzed by HPAEC. Fractions were collected and analyzed by scintillation counting. The cpm in each fraction minus background is shown.

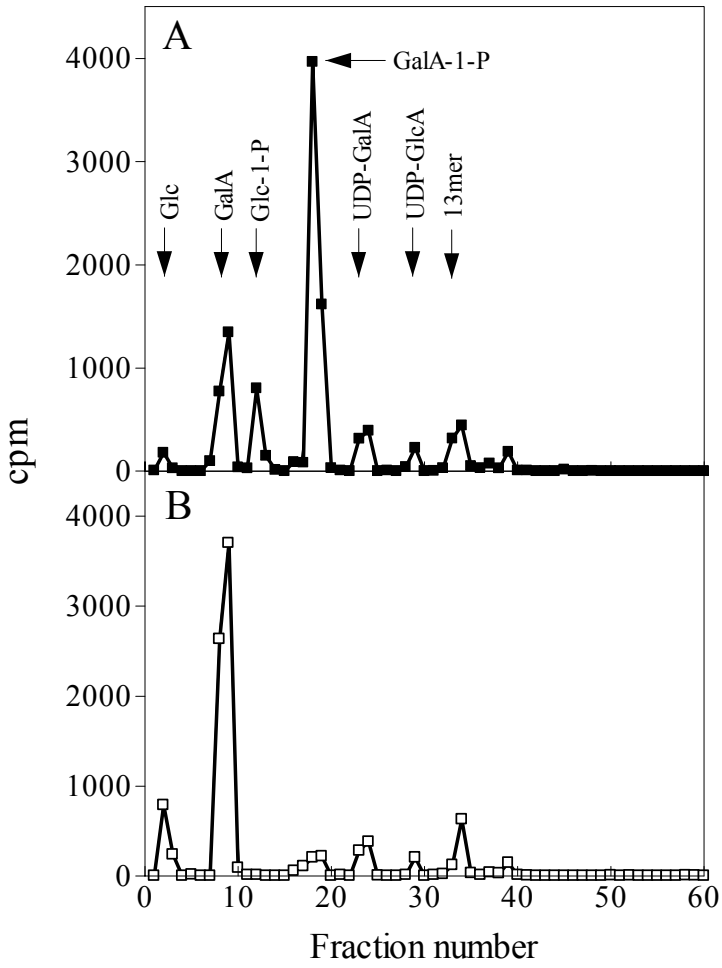

Phosphatase treatment did not change the retention time of OGA (DP 13) or D-Gal*p*A. These results establish that the radioactive product that elutes by HPEAC between triGalA and tetraGalA is phosphorylated D-Gal*p*A.

Base treatment of the intact product made by detergent-permeabilized Golgi did not shift the retention time of the peaks (Figure 2.6, C), suggesting that the products were not methoxylated or otherwise esterified. Treatment of the untreated or base-treated products with an EPGase resulted in the disappearance of the OGA 15 mer and larger peaks, the appearance of diGalA, and an increase in the amount of D-Gal*p*A (Figure 2.6, C and D). These results show that most of the D-[^{14}C]Gal*p*A-labeled product made in Triton X-100-permeabilized Golgi membranes in the presence of exogenous OGA 14 mer is OGA of DP 15.

The GalAT in permeabilized Golgi vesicles and the GalAT solubilized from tobacco synthesize similar products. Therefore, it was possible that 0.1% (v/v) Triton X-100 was solubilizing the enzyme from Golgi membranes rather than permeabilizing the membranes. To test this, Golgi vesicles were treated with 0.1% (v/v) Triton X-100, centrifuged at 100,000*g* for 1 h, and the GalAT activity in the supernatant and in the pellet was determined (data not shown). All of the activity was present in the pellet, suggesting that 0.1% (v/v) Triton X-100 alone was not sufficient to solubilize GalAT activity from Golgi membranes and that the changes in product formation upon Triton X-100 treatment were due either to the permeabilization of the Golgi membranes or to the effect of the detergent on the GalAT itself. Nevertheless, the characteristics of the products formed by GalAT from pea (Figures 2.3-2.6) are consistent with the characteristics of the membrane-bound (Doong et al., 1995) and solubilized forms of GalAT from tobacco (Doong and Mohnen, 1998).

Topography of GalAT in pea Golgi.

Pectin biosynthesis is believed to occur in the lumen of the Golgi endomembrane system (Northcote and Pickett-Heaps, 1966; Zhang and Staehelin, 1992) and it is likely that the glycosyltransferases, or at least their catalytic sites, face the lumen of the Golgi. To test this hypothesis, isolated Golgi membranes were treated with proteinase K (a protease that cannot pass through intact membranes) in the presence and in the absence of 0.1% (v/v) Triton X-100 and then assayed for GalAT activity. GalAT activity was similar in intact Golgi vesicles, Triton X-100-treated vesicles, and Proteinase K-treated vesicles (Figure 2.8). However, GalAT activity in Golgi membranes treated with both Triton X-100 and proteinase K was reduced to levels comparable with that of boiled Golgi vesicles. These results demonstrate that the intact Golgi membranes protect the catalytic site of GalAT from proteinase K digestion and strongly suggest that the catalytic domain of GalAT is located within the lumen of the Golgi.

DISCUSSION

The results presented here provide the first direct enzymatic evidence that GalAT is located in the Golgi apparatus. GalAT activity localizes exclusively to fractions that contain the majority of the latent UDPase activity, a well characterized Golgi-specific enzyme marker. A combination of detergent and proteinase K treatments show that pea GalAT is a membrane-bound protein whose catalytic site faces the lumen of the Golgi apparatus. The catalytic site of tobacco HGA methyltransferase has also been localized to the lumen of the Golgi apparatus (Goubet and Mohnen, 1999a). Taken together, our results show that pectin biosynthetic enzymes are present in the Golgi and confirm that pectin biosynthesis occurs in the Golgi endomembrane system (Northcote and Pickett-Heaps, 1966; Harris and Northcote, 1971; Zhang and Staehelin, 1992).

Figure 2.8. Proteinase K treatment of pea Golgi membranes. Golgi vesicles (100 μg protein) were incubated for 30 min at 30°C in the presence or absence of 0.1% (v/v) Triton X-100 and/or 4 μg Proteinase K under the following conditions: BGV, Golgi vesicles boiled for five minutes prior to incubation; GV, intact Golgi vesicles; +TX, Golgi vesicles incubated in the presence of 0.1% (v/v) Triton X-100; +PK, intact Golgi vesicles incubated with 4 μg Proteinase K; +TX and PK, Golgi vesicles incubated with both 0.1% (v/v) Triton X-100 and 4 μg Proteinase K. An aliquot (10 μl) of the Golgi vesicle mixture from each treatment was brought to a final concentration of 0.1% (v/v) Triton X-100 and assayed for GalAT activity (see "Materials and Methods"). The amount of radioactivity recovered in each of the products is shown. Data are the average of triplicates from one experiment. Similar results were obtained in three separate experiments.

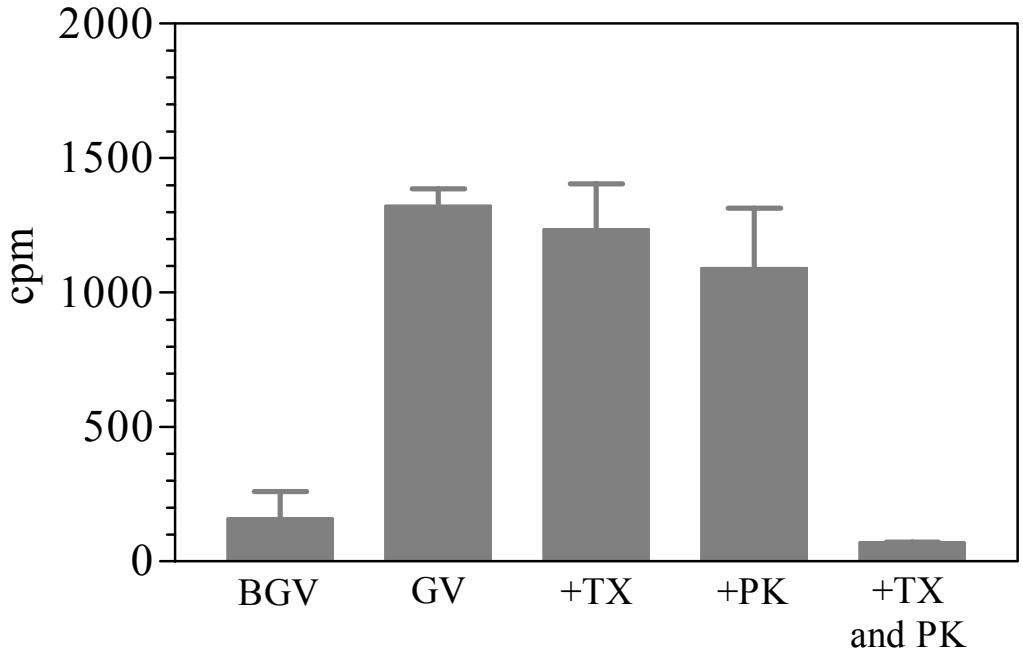

A model summarizing our current understanding (Doong et al., 1995; Liljebjelke et al., 1995; Doong and Mohnen, 1998) of the biosynthesis of HGA is shown in Figure 2.9. UDP-D-Gal*p*A, the substrate for GalAT, is believed to be formed on the cytosolic side of the Golgi by the epimerization of UDP-D-Glc*p*A catalyzed by a UDP-D-glucuronate-4-epimerase (EC 5.1.3.6) (Feingold et al., 1960; Feingold and Avigad, 1980; Mohnen, 1999) that is associated with Golgi membranes (K. Adams and D. Mohnen, unpublished results). UDP-D-Gal*p*A is thought to be transported into the lumen of the Golgi apparatus by a proposed membrane-bound UDP-D-Gal*p*A:UMP antiport transport protein. Similar NSTs involved in protein glycosylation have been identified, purified and cloned from several mammalian and yeast sources (Hirschberg et al., 1998). GalAT, a Golgi-resident protein with its catalytic site in the lumen of the Golgi, binds UDP-D-Gal*p*A and catalyzes the transfer of D-Gal*p*A onto a growing HGA chain and the production of UDP. The UDP is hydrolyzed in the lumen into inorganic phosphate and UMP by a Golgi-resident, membrane-bound nucleoside diphosphatase (NDP/UDPase; Orellana et al., 1997). UMP is exported out of the Golgi in exchange for UDP-D-Gal*p*A by the proposed UDP-D-Gal*p*A:UMP antiport transporter.

The products synthesized by the GalAT from pea are comparable with the products synthesized by the GalAT from tobacco (Doong et al., 1995; Doong and Mohnen, 1998). The GalAT in detergent-permeabilized pea Golgi membranes produces a product that is predominantly only one GalA residue longer than the exogenous acceptor. This result is similar to that obtained with the solubilized GalAT from tobacco, where the product generated is also only one residue longer than the exogenous acceptor (Doong and Mohnen, 1998). In contrast, the GalAT in intact pea Golgi and in tobacco membranes both use endogenous acceptors to generate high molecular mass products, with the product in pea (> 500 kDa) being larger than

Figure 2.9. A model for HGA biosynthesis *in planta*. 1) UDP-D-Gal*p*A is formed by the epimerization of UDP-D-glucuronic acid on the cytosolic side of the Golgi. 2) UDP-D-Gal*p*A is transported by a proposed UDP-D-Gal*p*A:UMP antiporter into the lumen of the Golgi apparatus. 3) D-Gal*p*A is transferred from UDP-D-Gal*p*A onto a growing HGA chain by a GalAT that has its catalytic site facing the lumen of the Golgi. The UDP released is hydrolyzed to UMP and inorganic phosphate by a Golgi-localized UDPase. The UMP is then exported by a UDP-D-Gal*p*A:UMP antiporter in exchange for UDP-D-Gal*p*A.

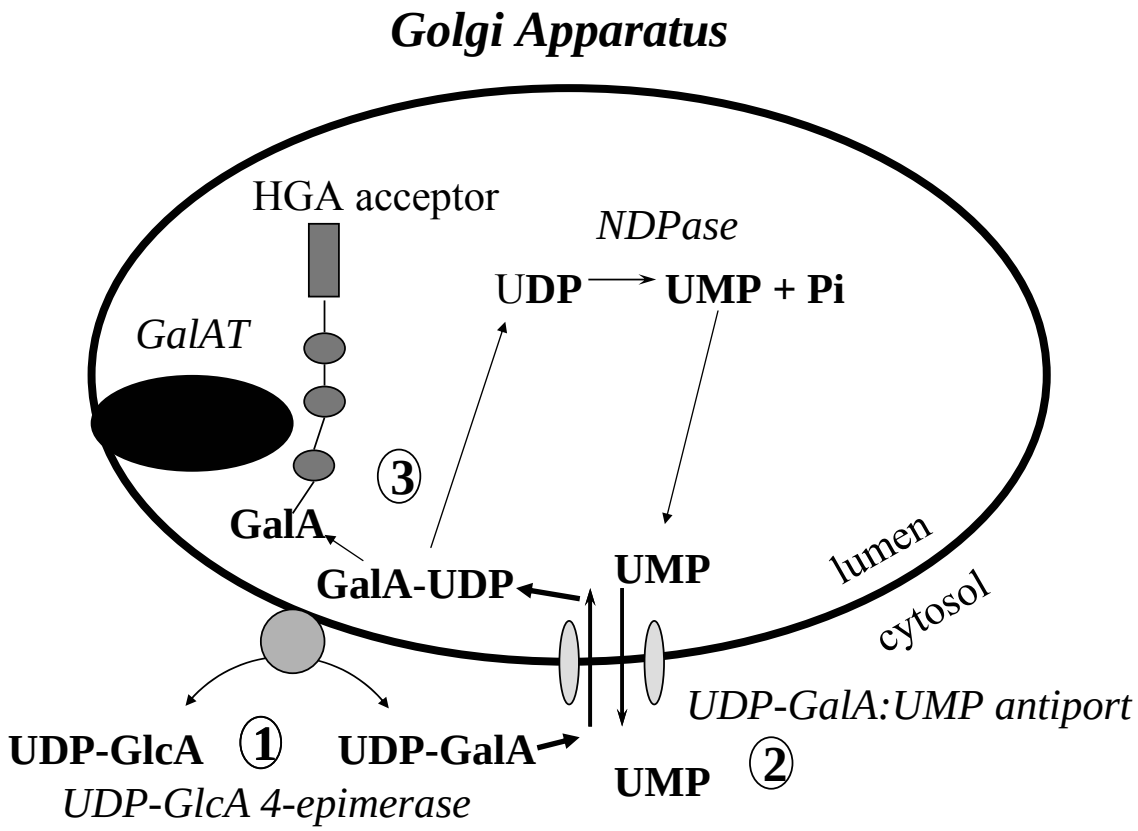

that produced in tobacco (approximately 105 kDa; Doong et al., 1995). The number of GalA residues added onto the endogenous acceptor(s) in the pea and tobacco membranes *in vitro* has not yet been determined.

There are a number of possible reasons why the pea detergent-permeabilized and the tobacco solubilized GalATs add only a single D-Gal*p*A to the end of the exogenous acceptors. For example, treating pea Golgi vesicles with detergent and exogenous OGA acceptors may cause the GalAT to preferentially use the exogenous OGAs as acceptors, whereas the GalAT in intact Golgi uses an endogenous acceptor. The exogenous OGA (e.g. DP 14) acceptor may not be the optimal substrate for the GalAT, whereas the endogenous product found in intact Golgi membranes presumably contains the necessary structural information for the enzyme to synthesize a polymeric product. Such acceptor-mediated control of enzyme processivity has been demonstrated for a mammalian α-2,8-polysialic acid synthase (Kojima et al., 1996), where the placement of an (1,6)-linked α-fucose residue in the acceptor was shown to be necessary for polysialylation. It is also possible that treating Golgi membranes with Triton X-100 disrupts an enzyme complex (protein-protein or other interaction) or removes an element that is required for polymer synthase activity. Protein-protein complexes involved in glycan biosynthesis have been demonstrated for glycogenin, a self-glucosylating protein that initiates glycogen biosynthesis (Lin et al., 1999).

The presence of D-Gal*p*A among the products formed by both intact and detergent-permeabilized pea Golgi membranes, and the presence of D-Gal*p*A-1-P in the products formed by detergent-permeabilized pea Golgi membranes, are a major difference between the reaction products formed by pea and tobacco membranes (Doong and Mohnen, 1998). The presence of D-Gal*p*A and D-Gal*p*A1-P most likely results from the hydrolysis of UDP-D-[^{14}C]Gal*p*A by a

phosphodiesterase (Feingold et al., 1958) and a phosphatase (Neufeld et al., 1961). Such hydrolases have been reported to be released during the homogenization and isolation of membranes from some plant tissues (Villemez et al., 1966; Rodgers and Bolwell, 1992; Brickell and Reid, 1996) and it is likely that such enzymes were released during the preparation of the pea Golgi.

Several enzymes including latent UDPase (Orellana et al., 1997) and mammalian glycosyltransferases (Paulson and Colley, 1989) such as the polysialyltransferases that function in the polysialylation of neural cell adhesion molecules and other *N*-linked glycoproteins (Tsuji, 1996) have their catalytic sites located in the lumen of the Golgi. Most Golgi-localized glycosyltransferases are type II integral membrane proteins with a single N-terminal membrane-spanning region and a lumenal C-terminal catalytic domain (Paulson and Colley, 1989; Tsuji, 1996). On the other hand, plasma membrane-localized polymer synthases such as hyaluronan synthase (Weigel et al., 1997) and the putative cellulose synthase (Delmer, 1999) are predicted to have multiple transmembrane-spanning regions at the amino and carboxy termini and a large central domain containing the catalytic site. The purification of the GalAT, the determination of its amino acid sequence, and the identification of its gene will be required to elucidate the structure of GalAT and will allow the comparison of GalAT structure with that of known glycosyltransferases and polymer synthases.

CHAPTER 3

DEVELOPMENT OF A FILTER ASSAY FOR MEASURING HOMOGALACTURONAN:α-(1,4)-GALACTURONOSYLTRANSFERASE ACTIVITY[2]

[2] Jason D. Sterling, Jason A. Lemons, Ivy F. Forkner, and Debra Mohnen. To be submitted to *Anal. Biochem.*

ABSTRACT

α-(1,4)-galacturonosyltransferases (GalATs) are enzymes that catalyze the addition of (1,4)-linked α-D-galacturonsyl residues onto the non-reducing end of homogalacturonan chains. The nucleotide-sugar donor for the reaction is uridine diphospho-D-galacturonic acid (UDP-D-Gal*p*A). Many GalAT activity assays are based on the incorporation of D-[^{14}C]Gal*p*A from UDP-D-[^{14}C]Gal*p*A onto exogenously added homogalacturonan acceptors. Reactions based on this method can be time consuming as multiple centrifugations and labor intensive washes with organic solvents are required to remove the unincorporated UDP-D-[^{14}C]Gal*p*A from the [^{14}C]-labeled products. An alternative GalAT filter assay was developed based on the ability of homogalacturonan to bind to cetylpyridinium chloride (CPC). GalAT assay reaction products made using radish (*Raphanus sativus*) microsomal membranes or solubilized proteins from tobacco (*Nicotiana tabacum* L. cv. Samsun) and *Arabidopsis thaliana* (cv. Columbia) were spotted onto Whatman 3MM paper impregnated with 2.5% (w/v) CPC. Unincorporated UDP-D-[^{14}C]Gal*p*A could be selectively removed from the filters by washing with 150-250 mM NaCl. The versatility of this assay is demonstrated by testing multiple chromatographic fractions obtained during the partial purification of tobacco GalAT on the cation exchange resin SP Sepharose, and by detecting the GalAT-catalyzed incorporation of D-[^{14}C]Gal*p*A onto endogenous acceptors from Arabidopsis membranes.

INTRODUCTION

Pectins are classified as a group of acidic plant cell wall polysaccharides that contain (1,4)-linked α-D-galacturonic acid (D-Gal*p*A) as part of their backbone structure (O'Neill et al., 1990; Ridley et al., 2001). Collectively, pectins comprise roughly 30% of the primary cell walls of eudicots and non-graminaceous monocots and 10% of the walls of *Poaceae* (O'Neill et al., 1990; Carpita and Gibeaut, 1993). It has been estimated that as many as 62 different glycosyltransferases are required to synthesize all of the pectic polysaccharides found in plant primary cell walls (Chapter 1), but to date, only a few glycosyltransferases believed to be involved in pectin biosynthesis have been identified (Bouton et al., 2002; Iwai et al., 2002).

Much of the difficulty that researchers have encountered in being able to clone pectin biosynthetic glycosyltransferases is due to the lack of gene homologs in the database. Once putative pectin glycosyltransferase genes have been identified, the lack of commercially available nucleotide-sugar substrates, oligo/polysaccharide acceptors, and/or reproducible methods for assaying glycosyltransferase activities make it difficult to definitively prove the functions of the cloned genes.

The glycosyltransferases responsible for the incorporation of D-Gal*p*A into pectin are known as galacturonosyltransferases (Ridley et al., 2001). Hassid and colleagues first detected galacturonosyltransferase (GalAT) activity in the 1960's in mung bean seedlings (Villemez et al., 1965; Villemez et al., 1966) by incubating microsomes with radioactive uridine diphospho-[^{14}C]galacturonic acid (UDP-D-[^{14}C]Gal*p*A). The [^{14}C]-labeled products generated from the reaction were separated from the unincorporated UDP-D-[^{14}C]Gal*p*A by thin layer chromatography (TLC; Villemez et al., 1966). Alternatively, the radiolabeled products could be precipitated using trichloroacetic acid, washed extensively with water and precipitated with

organic solvents to remove the unincorporated nucleotide-sugar prior to analysis (Villemez et al., 1965). The amount of D-[^{14}C]Gal*p*A incorporated into TLC-purified or precipitated products was estimated by scintillation counting (Villemez et al., 1965; Villemez et al., 1966).

A number of researchers have used modifications of these initial methods to detect GalAT activity in extracts from different plant species, including tobacco (Doong et al., 1995; Doong and Mohnen, 1998; Scheller et al., 1999) and Arabidopsis (Guillaumie et al., 2003) suspension cultured cells, sycamore cambial cells (Bolwell et al., 1985), pumpkin (Ishii, 2002), and azuki bean (Takeuchi and Tsumuraya, 2001) seedlings, petunia pollen tubes (Akita et al., 2002), and pea Golgi (Sterling et al., 2001). Methods that employ UDP-D-[^{14}C]Gal*p*A as a substrate (Doong et al., 1995; Doong and Mohnen, 1998; Sterling et al., 2001; Takeuchi and Tsumuraya, 2001) still require extensive washing of the precipitated products in order to remove the unincorporated radiolabeled substrate. Other methods employ fluorescently-labeled acceptors (Akita et al., 2002; Ishii, 2002), which eliminates the need for radioactively labeled substrates, but adds the additional time and expense of producing uniformly labeled oligogalacturonides acceptors. All of these methods are both quantitative and reliable; however, they are too time consuming and labor intensive to be useful as a simple method to detect enzyme activity in numerous plant extracts (i.e. mutant screens), in multiple media or cell extract samples from recombinant tissue cultures, or to assay several column fractions during the purification of native or recombinant GalAT.

In this paper, we report the development of a facile and rapid filter assay for measuring GalAT activity *in vitro*. The assay is based on a method by Brandan and Hirschberg (1988) that is used to detect *N*-heparan-sulfate sulfotransferase activity from rat liver. We show that the filter assay gives results similar to those obtained using the well established GalAT precipitation

assay (Doong et al., 1995; Doong and Mohnen, 1998), that it can be used to detect GalAT activity in microsomes and solubilized membrane proteins from different plant sources, and that it is an effective method for the detection of GalAT activity in column fractions during enzyme purification.

MATERIALS AND METHODS

Chemicals

Uridine diphospho-D-[^{14}C]glucuronic acid (UDP-D-[^{14}C]Glc*p*A; 272.54 mCi/mM) was purchased from DuPont New England Nuclear (Boston, MA). Uridine diphospho-D-[^{14}C]galacturonic acid (UDP-D-[^{14}C]Gal*p*A) was prepared by the 4-epimerization of UDP-D-[^{14}C]Glc*p*A using an extract from radish roots as described (Liljebjelke et al., 1995) or was synthesized using modifications of previously developed methods (Basu et al., 2000). Briefly, 50 μCi of uridine diphospho-D-[^{14}C]galactose (UDP-D-[^{14}C]Gal*p*) was purified over a CarboPac PA-1 column (Dionex; Sunnyvale, CA) using a 0.05-1 M linear gradient of ammonium formate, pH 6.6, at a flow rate of 1 mL/min. Purified UDP-D-[^{14}C]Gal*p* was lyophilized and resuspended in 0.5 mL of 25 mM NaH_2PO_4, pH 7.0, containing 250 units of galactose oxidase and 13,000 units of catalase. The reaction was incubated in the dark at room temperature for 24 h, at which point another 250 units of galactose oxidase and 13,000 units of catalase were added. The reaction was incubated for another 24 h in the dark and terminated by the addition of 600 μl of 5:1 (v/v), chloroform:methanol. The resultant mixture containing UDP-D-[^{14}C]Gal*p*A was extracted and purified as described previously (Liljebjelke et al., 1995)..

Oligogalacturonides (OGAs) of degrees of polymerization (DP) from 7-23 were prepared as described (Spiro et al., 1993). Chloroform, methanol, and glycerol were purchased from J.T.

Baker (Phillipsburg, NJ). Scintiverse was purchased from Fisher-Scientific (Springfield, NJ). All other reagents were purchased from Sigma (St. Louis, MO).

Plant material

Radishes (*Raphanus sativus*) were obtained from a local grocer. The roots were cut in fourths and stored at –80°C. Tobacco (*Nicotiana tabacum* L. cv. Samsun) cell suspension cultures, originally isolated from pith callus tissue, were grown and harvested by filtration as described (Doong and Mohnen, 1998). Suspension-cultured *Arabidopsis thaliana* (cv. Columbia) cells derived from leaf calli were grown in the dark for 10 days in Gamborg's B-5 basal medium containing 58.4 mM sucrose, 9 mM 2,4-dichlorophenoxyacetic acid, and 0.23 mM kinetin. Cells were harvested by filtration, washed extensively with deionized water and stored at –80°C until use.

Preparation of GalAT

Radish roots (50 g) were homogenized in a blender for 3 x 30s at high speed in 100 mL extraction buffer (50 mM HEPES [4-(2-hydroxyethyl)-1-piperazineethanesulfonic acid], pH 7.3, 50% [v/v] gylcerol, 25 mM KCl, 0.25 mM $MnCl_2$, and 0.1% [v/v] 2-mercaptoethanol) at 4°C. The suspension was filtered through two layers of Miracloth (Calbiochem, La Jolla, CA) and the filtrate was centrifuged at 4°C for 60 minutes at 40,000*g*. The supernatant was discarded and the pellet was homogenized in 1 mL of storage buffer (50 mM HEPES, pH 6.8, 0.25 mM $MnCl_2$, 25 mM KCl, 25% [v/v] glycerol) using a glass, hand-held homogenizer (Kontes Glass Co., Vineland, NJ). This suspension was used as a source of membrane-bound GalAT.

Solubilized tobacco GalAT was obtained as described (Doong and Mohnen, 1998) with some modifications. Briefly, tobacco cells (20 g) were homogenized in 100 mL extraction buffer for 6 x 30 seconds at 4°C using a polytron (Kinematica, Switzerland). The resulting suspension

was filtered through two layers of Miracloth and the filtrate was centrifuged for 60 minutes at 40,000*g* at 4°C. The supernatant was discarded and the pellet was homogenized in 2.5 mL of solubilization buffer (100 mM NaOAc, 200 mM NaCl, 2 mM EDTA, and 0.04% [v/v] Triton X-100) using a glass, hand-held homogenizer. The resulting suspension was centrifuged for 60 minutes at 100,000*g* at 4°C. The supernatant was used as a source of solubilized tobacco GalAT.

Arabidopsis cells (700 g) were homogenized in 1.2 L of extraction buffer at 4°C using a Parr bomb. The homogenate was filtered through two layers of nylon mesh and the filtrate was centrifuged at 28,000*g* for 5 h at 4°C. The supernatant was decanted and the top layer of the microsomal pellet was resuspended in 9 mL of storage buffer. The resuspended membranes could be stored for several months at –80°C before use. Arabidopsis membranes used as a source of endogenous acceptors were heat-inactivated by incubating an aliquot at 95°C for 10 min.

Solubilized GalAT was isolated from resuspended Arabidopsis membranes by adding Triton X-100, NaCl, NaOAc, and EDTA to a final concentration of 4% (v/v), 0.2 M, 0.1 M, and 2 mM, respectively. The mixture was centrifuged at 150,000*g* for 1.5 h at 4°C and the supernatant containing proteins that were soluble in 4% (v/v) Triton X-100 was removed and diluted with 4 volumes of 50 mM HEPES, pH 7.3, 0.25 mM $MnCl_2$, 2 mM EDTA, 25% (v/v) glycerol, and 0.25% (v/v) Triton X-100. The diluted fraction, subsequently called solubilized enzyme, was filtered through a 0.2 μm nylon filter and either used immediately or stored at −80°C until use.

Precipitation assay

The precipitation assay was performed as described (Doong et al., 1995) with some modifications. An aliquot (10 μl) of membrane-bound or solubilized GalAT was incubated with

50 mM HEPES, pH 7.8, 0.2 M sucrose, 0.05% (w/v) bovine serum albumin, 100 μM UDP-D-Gal*p*A, 70 μg of OGAs, 1.1 μM UDP-D-[^{14}C]Gal*p*A, and with either 0.25 mM (membrane-bound GalAT) or 1 mM (solubilized GalAT) $MnCl_2$ in a total volume of 30 μl at 30°C for 30 min. The reactions were terminated by the addition of 700 μL chloroform:methanol (3:2, v/v) and centrifuged at 13,200*g* for five minutes. The pellet was resuspended in 65% (v/v) ethanol by sonication for 15 min, centrifuged at 13,200*g* and the supernatant was removed. The 65% (v/v) ethanol washing step was repeated and the final washed pellet was dissolved in 200 μL 10 mM EDTA. The amount of D-[^{14}C]Gal*p*A incorporated into precipitated product was estimated by scintillation counting.

SP Sepharose chromatography

An aliquot of solubilized tobacco GalAT (6 mL) was loaded onto a 5 mL SP sepharose column (Amersham) equilibrated with binding buffer (50 mM Hepes, pH 7.3, 1% [v/v] TX-100, 25% [v/v] glycerol, 2 mM EDTA and 0.25 mM $MnCl_2$). Unbound proteins (flow through) were collected in 1 mL aliquots. The column was washed with 5 column volumes of binding buffer and bound proteins were eluted from the column using a step gradient of NaCl in binding buffer (5 mL; 100-600 mM, increasing in 100 mM increments). Column fractions (1 mL) were tested for GalAT activity using the filter assay as described. All procedures were conducted at 4°C.

Original GalAT filter assay

The filter assay was developed based on the method of Brandan and Hirschberg (1988) that was used to assay N-heparan sulfate sulfotransferase activity. Whatman (Maidstone, England) 3MM paper was cut into 2x2 cm squares and soaked for 15 min in 2.5% (w/v) cetylpyridinium chloride (CPC). The filters were dried at 65°C overnight prior to use. Reaction mixtures prepared as described above were terminated by the addition of 5 μL 1 M NaOH and

the entire mixture from each individual reaction was spotted onto a CPC-coated filter. The filters were allowed to air dry for 5 min and washed as described in the "Results". Washed filters were dried for 2 h and the amount of radioactivity bound to each filter was estimated by scintillation counting.

Optimized GalAT filter assay

The filter assay was modified to improve reproducibility and to lower background levels of unincorporated UDP-D-[^{14}C]Gal*p*A on the filters. Following the incubation of 3MM squares in 2.5 % CPC, the filters were washed 3 times for 5 min with 1L of deionized H_2O to remove residual CPC prior to drying. Once the reaction mixtures had been spotted on the filters, the filters were washed twice with 150 mM NaCl at a ratio of 1:100 (filter/ml of NaCl). Washed filters were dried at room temperature for at least 1 h and the amount of radioactivity bound to each filter was estimated by scintillation counting.

RESULTS

Comparison of the sensitivity of the GalAT filter assay to the GalAT precipitation assay

The development of an effective filter assay to detect GalAT activity required that the unreacted UDP-D-[^{14}C]Gal*p*A substrate be separated from the radiolabeled products formed during the GalAT reaction, and that the assay be as, or more, sensitive than previously established methods. The anionic nature of OGAs acceptors and of the substrate, UDP-D-[^{14}C]Gal*p*A, promotes their binding to the positively-charged, CPC-treated filter squares. UDP-D-Gal*p*A, however, has a lower total negative charge than the OGA acceptors and the products formed from the GalAT reaction (Doong and Mohnen, 1998). It was thus predicted that washing the filters with salt solutions would remove the unreacted substrate from the retained polyanionic OGA products.

To test this hypothesis, GalAT activity was assayed using microsomal membranes and solubilized membrane proteins from tobacco and radish. Reactions containing 10 µl of solubilized or membrane-bound GalAT were incubated for 30 min at 30°C in a buffer containing 100 µM UDP-D-Gal*p*A, 70 µg of OGAs and 1.1 µM UDP-D-[^{14}C]Gal*p*A in the presence of 1 mM (solubilized GalAT) or 0.25 mM (membrane-bound GalAT) $MnCl_2$. The reaction products were either spotted onto CPC-treated filters, or precipitated as described previously (Doong et al., 1995). The CPC filters were washed with 50-250 mM NaCl and the amount of radioactivity remaining on each filter was quantified (Figure 3.1).

Washing with 50 or 100 mM NaCl was not sufficient to yield reproducible estimations of radioactivity remaining on each filter using either solubilized (Figure 3.1, A) or membrane-bound (Figure 3.1, B) GalAT, suggesting that non-specifically bound UDP-D-[^{14}C]Gal*p*A had not been effectively removed from filters using these salt concentrations. Washing with higher concentrations of NaCl significantly reduced the amount of radioactivity left on the filters, with 150-250 mM NaCl giving the lowest background (T_0) values and the most reproducible estimates of radioactive incorporation when compared to the values acquired with the precipitation assay. These results demonstrate that the GalAT filter assay can be used to determine GalAT activity in membranes and solubilized proteins from different plant and tissue sources.

Efficacy of the filter assay for use in the purification of GalAT

In order to be an effective assay for GalAT purification studies, it must be shown that the filter assay can be reliably used to detect GalAT activity in different column fractions. Previous results using the precipitation assay showed that GalAT activity elutes from the cation exchange

Figure 3.1. Comparison of the filter assay and the precipitation assay for measuring GalAT activity. A) Tobacco solubilized proteins (50 μg) or B) microsomal membranes from radish (250 μg) were incubated in a reaction buffer containing 1.1 μM UDP-D-[^{14}C]Gal*p*A, 100 μM UDP-D-Gal*p*A and 70 μg of OGAs in the presence of $MnCl_2$ for 0 (white bars) or 30 (grey bars) min at 30°C. The reaction products were either spotted onto filters and washed with 50-250 mM NaCl or precipitated (ppt) as described in the "Materials and Methods". Duplicate reactions with ± standard error are shown. Similar results were obtained in two independent experiments.

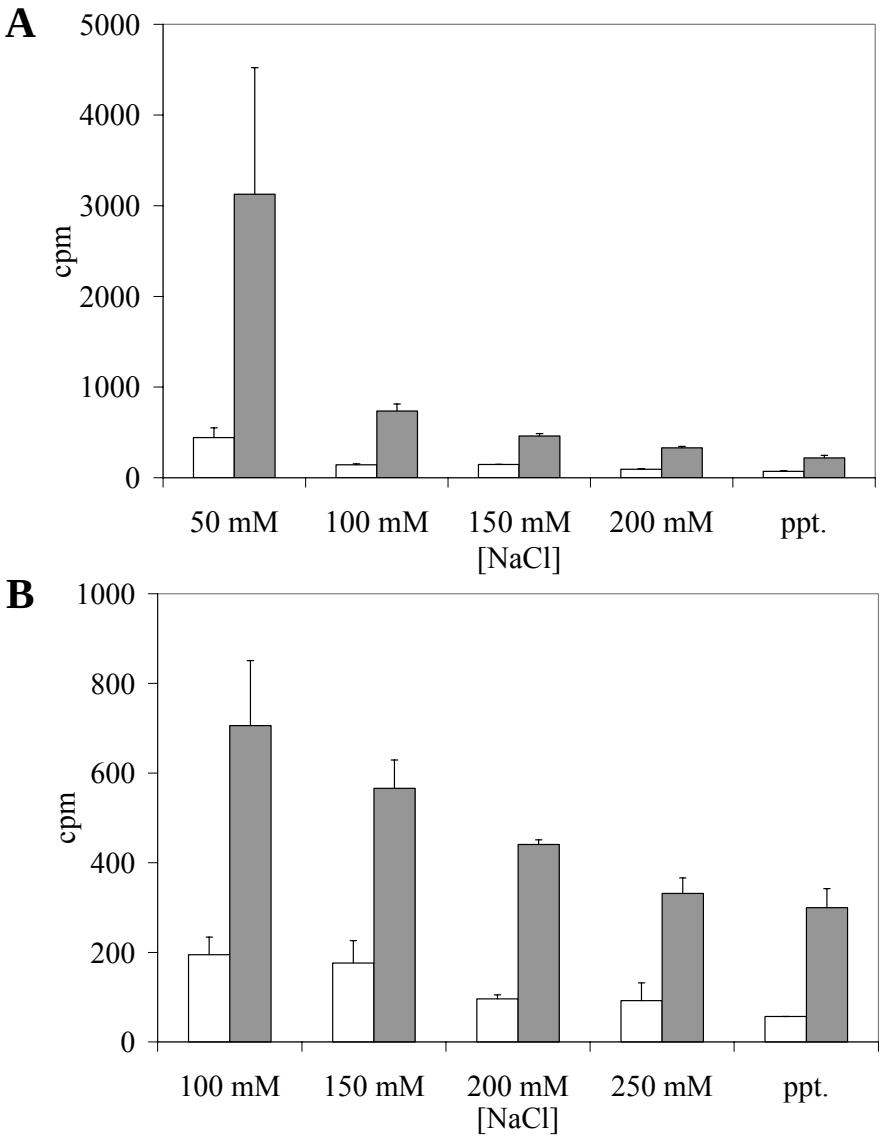

resin SP Sepharose upon the addition of 300-400 mM NaCl (data not shown). A solubilized enzyme preparation from tobacco was partially purified by SP Sepharose chromatography and the GalAT filter assay was used to detect GalAT activity in the collected fractions (Figure 3.2). As expected, the bulk of the GalAT activity from solubilized tobacco proteins eluted from the SP Sepharose column with the addition of 300 mM NaCl (fractions 20-22), with a smaller peak of activity eluting with 400 mM NaCl in later fractions (fractions 24-28). These results demonstrate that the filter assay is as effective as the precipitation assay for measuring *in vitro* GalAT activity in fractions obtained by column chromatography.

Measurement of GalAT activity using endogenous acceptors

GalAT activity in the preceding experiments was measured using either solubilized membrane proteins plus added exogenous homogalacturonan acceptors (OGAs) of DP 7-23 (Figure 3.1, A) or membrane preparations containing endogenous acceptors (Figure 3.1, B). To determine if the filter assay was also effective for measuring solubilized GalAT activity in the presence of endogenous acceptors, heat-inactivated Arabidopsis membranes were incubated with solubilized GalAT from Arabidopsis, and the amount of D-[^{14}C]Gal*p*A incorporated onto endogenous acceptors was determined using the optimized filter assay (Figure 3.3). As was previously shown for solubilized tobacco GalAT (Doong and Mohnen, 1998), solubilized GalAT from Arabidopsis was able to produce low amounts of radiolabeled product in the absence of exogenous acceptor (Figure 3.3, Sol). However, the addition of OGA acceptors leads to a 2.8-fold increase in the amount of product that formed (Figure 3.3, OGA). The fact that boiled Arabidopsis membranes also increased the amount of product formed compared to solubilized Arabidopsis GalAT alone showed that heat-inactivated Arabidopsis membranes contained

Figure 3.2. Effectiveness of the filter assay to detect GalAT activity in fractions obtained by column chromatography. A preparation (6 mL) of solubilized GalAT from tobacco was passed through an SP sepharose column (5 mL) using a 100-600 mM NaCl gradient. An aliquot (10 µl) of each fraction was incubated in a reaction containing 1.1 µM UDP-D-[^{14}C]Gal*p*A, 100 µM UDP-D-Gal*p*A and 70 µg of OGAs in the presence of 0.25 mM $MnCl_2$ for 30 min at 30°C and the amount of radiolabeled product made by each fraction was determined using the filter assay. The cpm recovered minus background cpm from duplicate reactions ± standard error is plotted.

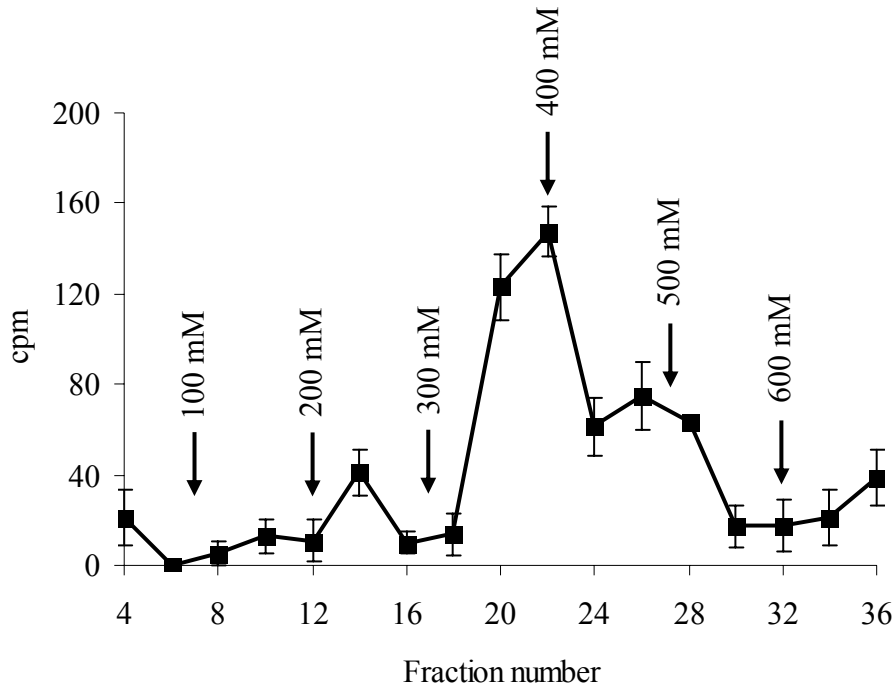

Figure 3.3. Detection of GalAT activity using alternative acceptors. Solubilized GalAT from Arabidopsis (50 μg) was incubated in reaction buffer containing 2.6 μM UDP-D-[^{14}C]Gal*p*A with either water (Sol), 70 μg of OGAs (OGA), or 10 μl (250 μg of protein) of heat-inactivated Arabidopsis membranes (BM) for 0 (white bars) or 90 (grey bars) min. Reactions containing only heat-inactivated membranes were used as a negative control (Con). Reaction mixtures were spotted onto filters and washed using the optimized filter assay. Data are the average ± standard error of duplicate samples. Similar results were obtained in three separate experiments.

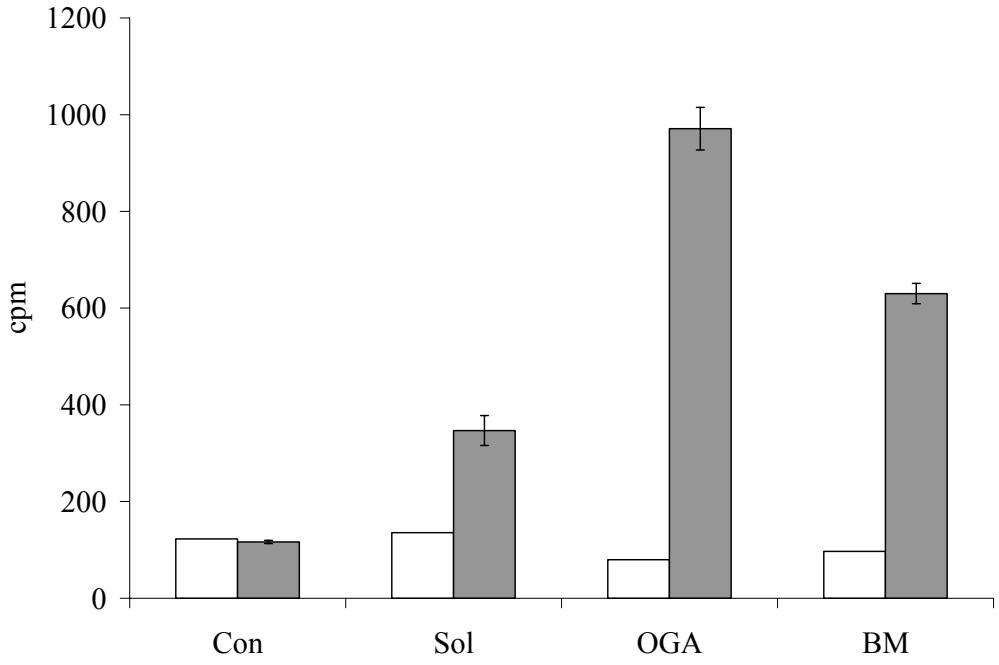

acceptors for GalAT. These results demonstrate that the filter assay can be used to detect the incorporation of D-[^{14}C]Gal*p*A onto exogenously supplied endogenous acceptors.

DISCUSSION

The precipitation assay developed by Doong and co-workers (1995) is a commonly used method for the detection of GalAT activity in plant tissue extracts. One of the main problems with this assay is the amount of time required to separate the unincorporated UDP-D-[^{14}C]Gal*p*A from the radiolabeled products made by GalAT. A rapid and reproducible filter assay was developed that is based on the ability of GalAT reaction products to bind to positively-charged, CPC-coated filters. CPC has previously been used to aid in the salt-facilitated precipitation of radioactive GalAT products (Villemez et al., 1965) and our results show that this association is strong enough to allow for the selective removal of unincorporated UDP-D-[^{14}C]Gal*p*A.

The original *N*-heparan-sulfate sulfotransferase assay used water and 25 mM sodium sulfate to remove unincorporated radiolabeled [^{35}S]-3'-phosphoadenylyl sulfate from filters (Brandan and Hirschberg, 1988). In our hands, unincorporated UDP-D-[^{14}C]Gal*p*A was not separated from the radiolabeled products by washing the filters with water (data not shown) or dilute (50-100 mM) salt solutions. Instead, it was found that washing solutions containing 150-250 mM NaCl were required to remove the unincorporated UDP-D-[^{14}C]Gal*p*A from the filters and to obtain the reproducible binding of the radioactive products to filters in levels that were comparable to the GalAT precipitation assay.

Our results show that the filter assay gives reliable and reproducible estimates of GalAT activity. The GalAT filter assay has been shown to be effective for the determination of GalAT activity in multiple plant species including radish membranes, and solubilized proteins from tobacco and Arabidopsis. The rapidity with which many GalAT reactions can be assayed greatly

enhances our ability to determine GalAT activity in fractions obtained during column chromatography and is an effective tool to aid in the purification of GalAT activity from plant tissues.

The versatility of the GalAT filter assay is exemplified by our ability to test the activity of GalAT using endogenous acceptors. This will allow the development of assays to test for the activity of glycosyltransferases that specifically add neutral and/or acidic sugars onto endogenous or well-defined acidic pectic structures. Products synthesized using such assays can potentially be further analyzed by selective removal with high salt solutions or directly on the filter by treatment of the radioactive products with purified *exo*- or *endo*glycanases. Future experiments will be centered on establishing whether specific pectic polysaccharides, such as RG-I oligosaccharides, can be bound to the filters and used to test for the activity of pectic glycosyltransferases such as RG-I arabinosyl- (Nunan and Scheller, 2003) or galactosyltransferases (Geshi et al., 2002).

CHAPTER 4

IDENTIFICATION AND HETEROLOGOUS EXPRESSION OF TWO PROPOSED GALACTURONOSYLTRANSFERASES FROM *ARABIDOPSIS THALIANA*.[3]

[3] Jason D. Sterling, Kumar Kolli, Ron Orlando, and Debra Mohnen. To be submitted to *Plant Cell.*

ABSTRACT

α-(1,4)-galacturonosyltransferases (GalATs) are enzymes that catalyze the incorporation of α-D-galacturonic acid into pectic polysaccharides. In an attempt to identify putative GalAT genes from *Arabidopsis thaliana*, we partially purified detergent-solubilized GalAT activity from Arabidopsis membranes using a combination of SP-Sepharose, Reactive Yellow 3 (RY3) and UDP-agarose chromatography. Analysis of the partially purified fractions by liquid chromatography-tandem mass spectrometry (LC-MS/MS) led to the identification of two proteins, named JS33 and JS36, which contained sequence motifs found in other glycosyltransferases (Henrissat et al., 2001). JS33 and JS36 transcripts were detected in root, stem, flower, and leaf tissues from Arabidopsis. N-terminally truncated and epitope-tagged versions of JS33 and JS36 were cloned into an expression vector designed for recombinant protein secretion and heterologously expressed in human embryonic kidney (HEK) 293 cells. Transient expression of the JS36 gene construct resulted in low levels of GalAT activity in HEK293 cell media in preliminary transient transfection experiments providing further evidence that JS36 was a putative GalAT gene. HEK cell lines stably transformed with the JS33 and JS36 gene constructs were shown to produce mRNA transcripts and recombinant proteins of the sizes expected for JS33 and JS36. However, recombinant proteins from the stably transformed lines were only detected in cell lysates and did not possess any detectable GalAT activity. Selected regions of JS33, JS36 and JS36L (a protein with high sequence identity to JS36) were used to generate multiple antigenic peptides (MAPs) for the production of polyclonal antibodies. Preliminary results showed that pools of antibodies generated against the three proteins were not able to precipitate significant amounts of GalAT activity from solubilized Arabidopsis proteins. A BLAST search of the Arabidopsis genome identified 23 additional coding regions with

significant sequence identity to JS36 and JS33. These results suggest that these genes comprise a novel gene family in Arabidopsis. More experimentation needs to be conducted in order to determine the roles that JS36 and JS33 play in pectin biosynthesis.

INTRODUCTION

Pectins are a family of plant cell wall polysaccharides that contain (1,4)-linked α-D-galactopyranosyluronic acid (D-Gal*p*A) as part of their backbone structure. Pectins are involved in the regulation of a number of plant processes, including plant growth (O'Neill et al., 2001; Willats et al., 2001), development (Willats et al., 1999b; McCartney et al., 2003) and the initiation of plant defense responses (Mohnen and Hahn, 1993; Ridley et al., 2001). Disruption of pectin structure by the mutation of pectin biosynthetic enzymes, the treatment of cells with glycosyl hydrolases, or the expression of glycosyl hydrolases in transgenic plants cause a wide variety of pleiotropic effects, including dwarfism (O'Neill et al., 2001; Bouton et al., 2002), altered seed coats (Usadel et al., 2004; Western et al., 2004), reduced wall tensile properties (Ryden et al., 2003), impaired guard cell function (Jones et al., 2003), and altered cell adhesion and wall glycosyl residue composition (Bouton et al., 2002; Iwai et al., 2002). While the enzyme activity encoded by some pectin biosynthetic genes has been well characterized (e.g. MUR1), the activity of other genes, especially those encoding putative pectin glycosyltransferases (e.g. QUA1), has not been determined.

α-(1,4)-Galacturonosyltransferases (GalATs) are glycosyltransferases that catalyze the incorporation of D-Gal*p*A into the backbone structures of pectin (Villemez et al., 1965; Doong et al., 1995). D-Gal*p*A is a major component of the backbone of all three types of pectin found in plant primary walls, comprising roughly 70% of total cell wall pectin (Mohnen et al., 1996). It has been estimated that between 5 and 7 distinct GalATs may be required to synthesize all of the backbone structures and side branches found in primary cell wall pectins (Chapter 1; Mohnen 2002). However, genes encoding enzymatically active GalATs have yet to be identified.

In an attempt to identify putative GalAT genes, we partially purified GalAT activity from *Arabidopsis thaliana* and identified two genes, named JS33 and JS36, which contained amino acid motifs found in other glycosyltransferases. We heterologously expressed N-terminally truncated forms of these proteins in HEK293 cells and showed that low levels of GalAT activity could be detected in media from cells transfected with JS36 in preliminary experiments. Analysis of the Arabidopsis genome indicate the presence of 23 additional genes with significant sequence identity to JS33 and JS36, suggesting that these genes are part of a larger gene family in Arabidopsis.

MATERIALS AND METHODS

Chemicals and kits

Uridine diphosphate-α-D-[^{14}C]galactose (UDP-D-[^{14}C]Gal*p*, 11.0 GBq/mmol), PD-10 columns, and SP-, protein A- and protein G-Sepharose were purchased from Amersham Biosciences (Piscataway, NJ). A mixture of OGAs with a degree of polymerization (DP) of 7 to 23 was prepared according to Doong et al. (1995). UDP-agarose was purchased from Calbiochem (La Jolla, CA). Nickel-nitrilotriacetic acid agarose (Ni-NTA) resin, plasmid maxiprep and gel extraction kits were purchased from Qiagen (Valencia, CA). EZNA plasmid miniprep kits were purchased from Omega Bio-tek (Doraville, GA). All restriction enzymes were purchased from New England Biolabs (Beverly, MA). Highly purified, monoclonal anti-hemagluttinin (anti-HA) antibodies were purchased from Covance (Berkeley, CA). Anti-HA conjugated to horseradish peroxidase was purchased from Roche (Indianapolis, CA). 3,3',5,5'-Tetramethylbenzidine (TMB) substrate kits were purchased from Vector Labs (Burlingame, CA). Polyvinylidene difluoride (PVDF) membranes were purchased from Schleicher and Schuell Biosciences (Keene, NH). Protein concentrations were determined using the Bradford assay

(Bio-Rad, Hercules, CA). Reactive Yellow 3 resin and all other chemicals were purchased from Sigma.

Plant material

Cell-suspension cultures of *Arabidopsis thaliana* (cv. Columbia) derived from leaf calli were grown in the dark for 7-10 days in Gamborg's B-5 basal medium containing 58.4 mM sucrose, 9 μM 2,4-dichlorophenoxyacetic acid, and 0.23 μM kinetin as described (Guillaumie et al., 2003). Cells were collected by filtration, washed extensively with water, and stored at -80°C until use.

Mammalian cell culture

Human embryonic kidney (HEK) 293 cells (Edge Biosystems; Gaithersburg, MD) were a gift of Dr. Kelley Moremen (The University of Georgia, Athens). HEK cells were grown in 150 cm^2 culture dishes (Corning, Corning, NY) in bicarbonate-buffered, Dulbeco's modified Eagle's medium (Sigma), pH 7.4, with high glucose (4.5 g/L) supplemented with 10% (v/v) fetal bovine serum (Sigma), 0.6 g/L L-glutamine, 100 μg/mL streptomycin sulfate, and 100 units/mL penicillin. Cells were maintained at 37°C in a humidified incubator (Thermo Electron Corp., Newington, NH) containing 5% CO_2 and passaged when the cells were 80% confluent.

Preparation of GalAT from Arabidopsis

Solubilized GalAT from Arabidopsis suspension cultured cells was prepared as described in Guillaumie et al. (2003). Dark-grown Arabidopsis cells (700 g) were homogenized in 1.2 L of homogenization buffer (50 mM 4-[2-hydroxyethyl]-1-piperazineethanesulfonic acid; HEPES, pH 7.3, 0.25 mM $MnCl_2$, 25 mM KCl, 50% (v/v) glycerol and 0.1% 2-mercaptoethanol) at 4°C using a Parr bomb. The homogenate was filtered through two layers of nylon mesh and the filtrate was centrifuged at 28,000*g* for 5 h at 4°C. The supernatant was decanted and the top layer

of the microsomal pellet was resuspended in 9 mL of cold 50 mM HEPES, pH 6.8, 0.25 mM $MnCl_2$, 25 mM KCl, and 25% (v/v) glycerol. To the resuspended pellet, Triton X-100, NaCl, NaOAc, and EDTA were added to final concentrations of 4% (v/v), 0.2 M, 0.1 M, and 2 mM, respectively, and the mixture was centrifuged at 150,000*g* for 1.5 h at 4°C. The supernatant containing proteins that were soluble in 4% (v/v) Triton X-100 was removed and diluted with 4 volumes of cold 50 mM HEPES, pH 7.3, 0.25 mM $MnCl_2$, 2 mM EDTA, 25% (v/v) glycerol, and 0.25% (v/v) Triton X-100. The diluted fraction, subsequently called solubilized GalAT, was filtered through a 0.2 μm nylon filter (Fisher Scientific) and either used immediately or stored at -80°C until use.

SP-Sepharose chromatography

Solubilized GalAT (125 mL) was loaded twice over a 50 mL column of SP-sepharose (5 x 2.5 cm) equilibrated with buffer A (50 mM HEPES, pH 7.3, 0.25 mM $MnCl_2$, 1% Triton X-100, 2 mM EDTA, and 25% [v/v] glycerol). The column was washed with 3 volumes of buffer B (50 mM HEPES, pH 7.3, 0.25 mM $MnCl_2$, 25% [v/v] glycerol, 2.5% [w/v] 3-[(3-cholamidopropyl)dimethylammonio]propanesulfonic acid, CHAPS) and bound proteins were eluted using a step gradient of NaCl in buffer B as follows: 50 mL of 100 mM, 50 mL of 200 mM, 35 mL of 300 mM, 70 mL of 400 mM. Proteins eluting with 300 and 400 mM NaCl were pooled and desalted in buffer B over PD-10 columns according to the manufacturer's instructions. Briefly, 2.5 mL of sample was loaded per column. Proteins were eluted from the column with the addition of 3.5 mL of buffer B. All operations were carried out at 4°C.

Reactive Yellow 3 chromatography

The pooled and desalted fraction from the SP-sepharose column was loaded onto a 15 mL column (2 x 5 cm) of Reactive Yellow 3 (RY3) equilibrated with buffer B. Bound proteins were

eluted with the sequential addition of one column volume of buffer B containing 1) 10 μM UDP, 2) 10 μM UDP and 2 μM OGAs, 3) 10 μM UDP, 2 μM OGAs and 100 mM NaCl, and 4) 10 μM UDP, 2 μM OGAs and 200 mM NaCl. The proteins that eluted with 100 and 200 mM NaCl were pooled and desalted in buffer B using PD-10 columns.

UDP-agarose chromatography

The pooled RY3 fractions were loaded onto a 7 mL (2.1 x 2 cm) UDP-agarose column that had been equilibrated with buffer B. The most purified fraction from UDP-agarose chromatography shown in Table 4.2, Experiment 1 was obtained using the following elution scheme: bound proteins were eluted with one column volume of buffer B containing 0.01 mg/mL OGAs and 1) 50 mM UDP, 2) 25 mM $MnCl_2$, 3) 25 mM $MnCl_2$ and 0.5 M NaCl, 4) 25 mM EDTA, and 5) 25 mM EDTA and 0.5 M NaCl. The fraction eluted with 25 mM $MnCl_2$ and 0.5 M NaCl was determined to be the most pure following GalAT activity assays and the determination of protein concentration in each of the eluted fractions.

The fraction analyzed by liquid chromatography, tandem mass spectrometry (LC-MS/MS) was obtained by UDP-agarose chromatography in a second experiment (Table 4.2, Experiment 2) using the following elution scheme: bound proteins from the UDP-agarose column were first eluted with one column volume each of 0.01, 0.05, 0.1, 0.5, 1, 5, 10, 15 and 20 mM UDP in buffer B. The column was washed with 1 volume of 1 M NaCl in buffer B and all of the eluted fractions from this step were collected, desalted, and tested for GalAT activity. The fraction that eluted with 1 M NaCl was reapplied to the column and bound proteins were eluted with one column volume of buffer B containing 0.01 mg/mL OGAs and 1) 50 mM UDP, 2) 25 mM $MnCl_2$, 3) 25 mM $MnCl_2$ and 0.5 M NaCl, 4) 25 mM EDTA, and 5) 25 mM EDTA and 0.5 M NaCl. The fraction that eluted with 25 mM $MnCl_2$ and 0.5 M NaCl was further analyzed by

trypsin digestion and LC-MS/MS. OGAs were added to the elution buffers to inhibit the activity of a contaminating *exo*PGase that co-purified with GalAT activity.

Trypsin digestion and analysis of Arabidopsis peptides

The most purified fraction from UDP-agarose chromatography was incubated with 940 units of sequencing grade, modified trypsin (Promega; Madison, WI) for 12 h at 37°C. Peptides were dialyzed overnight in water using Spectro/Por CE 1,000 molecular weight cutoff dialysis membranes (Spectrum Laboratories, Rancho Dominguez, CA), lyophilized and analyzed by LC MS/MS.

Liquid chromatography- tandem mass spectrometry and identification of Arabidopsis proteins

Peptides were introduced into a Q-TOF2 (Waters Micromass, Milford, MA) tandem mass spectrometer using a Waters CapLC delivery system. The mobile phases used for gradient elution consisted of 0.1% formic acid in water (A) or acetonitrile (B). The gradient conditions were 10% B to 70% B over 60 min at a flow rate of 1 μL/min. The Q-TOF2 was operated in a data-dependant scan mode. The survey MS spectra were acquired from 450-1700 mass units. The switch criteria for MS to MS/MS mode were ion count and charge state, with the Q-TOF set to ignore singly charged ions and to acquire MS/MS data for up to 3 co-eluting peptides. The collision energy was varied automatically depending on the peptide mass and charge state. Acquired spectra were used to probe the Arabidopsis genome to identify candidate GalAT genes using the Mascot search engine (www.matrixscience.com) using a peptide and MS/MS tolerance of ±2 and ±1, respectively.

RT-PCR and cloning of JS33 and JS36

Total RNA from flowers, rosette leaves or stems obtained from 3- or 6-week-old Arabidopsis ecotype Columbia plants as well as total RNA from roots of 4-week old Arabidopsis

plants grown in liquid media were gifts of Dr. Maor Bar-Peled (The University of Georgia, Athens; Harper and Bar-Peled, 2002). First cDNA strand synthesis was conducted according to the manufacturer's instructions using 1 mM oligo(dT) primer, 200 units of Superscript II reverse transcriptase (Invitrogen) and 8 μg total RNA. Products from these reactions were treated with 2 units of RNase H (Invitrogen) and used as a template for PCR using gene specific primers. PCR reactions were conducted using high fidelity Platinum Taq polymerase (Invitrogen, Carlsbad, CA) according to manufacturer's instructions. Typical PCR reactions involved 1 cycle at 95°C for 2 min followed by 30 cycles at 95°C for 30 s, 52°C for 30s, and 70°C for 2.5 min, and a final extension at 70°C for 5 min. The PCR products were analyzed on 1% Tris-acetate EDTA (TAE) agarose gels and DNA bands of the appropriate size were excised and purified using QIAquick gel extraction kit (Qiagen; Valencia, CA). Control PCR reactions included actin primers ACT119S and ACT284A (McKinney et al., 1995) as a positive control (a gift from Dr. Richard Meagher, the University of Georgia, Athens).

A full-length cDNA encoding JS33 (accession no. AY091448) in vector pUNI51 was obtained from the Arabidopsis Information Resource Center (ABRC). An N-terminally truncated version of JS33 (JS33Δ1-43) lacking the putative transmembrane domain was generated using the sense primer FJS33Ntru (5'-ttatta<u>cccgggg</u>aattccacaatggctttcactctcctggattt-3') and the antisense primer RpUNI51 (5'-ggcggctatgatctc<u>ggcggccgc</u>tagaattg-3'). The primers contained restriction sites for SmaI and NotI, respectively (underscored in the primers sequences).

A version of JS36 (accession no. NM_115977) lacking its putative N-terminal transmembrane domain (JS36Δ1-41) was generated from total flower RNA using RT-PCR and the gene specific sense primer FJS36Ntru (5'-ttatta<u>cccgggg</u>aattccgaggagtgtatatcgattcctcaaatg-3')

and antisense primer RJS36 (5'-gcggccgcattttattcatgaaggttgcaacgacg-3'). The primers contained restriction sites for SmaI and Not I, respectively (underscored in the primer sequences).

Transcript analysis of JS33 and JS36 in Arabidopsis tissues was conducted using the previously described RT-PCR protocol and the primers FJS33Ntru and RJS33 (5'-aagcattggccgtgtagctacttac-3'), and FJS36Ntru and RJS36 for JS33 and JS36, respectively.

Expression of JS33 and JS36 in HEK293 cells

The purified PCR products for truncated JS33 and JS36 were first cloned into pCR2.1-TOPO (Invitrogen). Positive clones were selected based on their resistance to kanamycin and SmaI/NotI fragments were subcloned into the mammalian expression vector pEAK10 (Edge Biosystems) along with an N-terminal HindIII/SmaI fragment containing a *Trypanosoma cruzi* mannosidase (TCMss) signal sequence (MRLLTALFAYFIVALILAFSVSAKARR), a poly-histidine (HHHHHHHHHH) tag, and two copies of the hemagluttinin (HA) epitope (YPYDVPDYA) that was a gift from Dr. Kelley Moremen (Vandersall-Nairn et al., 1998). Correctly constructed pEAK10 vectors containing both the N-terminal fragment and the appropriate JS gene (Figure 4.1, B) were confirmed by DNA sequencing.

Transient transfection and stable transformation of HEK293 cells (Jordan et al., 1996) was conducted using 25-30 μg of DNA for transient experiments, 6 μg of DNA for the production of clonal lines, and 25-30 μg of DNA for the creation of stable, mixed-population lines. Transformed cells were selected on media containing puromycin (1 μg/mL) and positive transformants were selected by PCR amplification of genomic DNA and/or RT-PCR of total RNA using the gene specific primers FJS33Ntru and RJS33, and FJS36Ntru, RJS36 and. 36IP (5'-tgattctgcagtccttggtaaatacag-3') for JS33 and JS36, respectively. Cells transformed with empty pEAK10 vector or expressing a recombinant, histidine-tagged, rat α-(2,6)-sialyltransferase

(Wlasichuk et al., 1993), a gift of Dr. Kelley Moremen (unpublished results), were used as negative controls. Control RT-PCR reactions that were conducted to test transcript levels in HEK293 cells included the use of primers (FP 5'-caatgacccttcattgacc-3', RP 5'-gtcttctgggtggcagtgat-3') specific to positions 123 and 584, respectively, of human glyceraldehyde 3'-phosphate dehydrogenase (accession no. BC023632) that were gifts from Dr. Michael Pierce (the University of Georgia, Athens, GA).

Ni^{2+}-affinity column chromatography

Media from an HEK293 cell line expressing a recombinant α-(2,6)-sialyltransferase (containing an N-terminal polyhistidine tag) was desalted over a PD-10 column equilibrated with buffer C (50 mM KH_2PO_4, pH 7.5, 300 mM NaCl, 40 mM imidazole). The desalted media (30 mL) was poured over a 200 µL column of Ni-NTA agarose equilibrated with buffer C. The column was washed with 10 volumes of buffer C. Proteins bound to the Ni-NTA resin were denatured in 0.2 volumes of SDS-PAGE sample buffer (Laemmli, 1970) and separated by SDS-PAGE.

Immunoprecipitation of recombinant JS33 and JS36 using anti-HA antibodies

Protein A-Sepharose, equilibrated in ice-cold phosphate-buffered-saline (PBS pH ; 137 mM NaCl, 2.7 mM KCl, 4.3 mM Na_2HPO_4, and 1.4 mM KH_2PO_4, pH 7.3), was incubated with 1 µg of purified monoclonal anti-HA antibodies (Covance, Princeton, NJ) at a ratio of 30:1 (v/v) for 2 h unless otherwise specified. The resulting protein A-Sepharose:anti-HA conjugate was washed 3 times with 10 volumes of cold PBS, brought to a 50% slurry with PBS (media) or cell lysis buffer (cell lysates) and kept at 4°C until use.

Media (3.4 mL) from JS33 and JS36 expressing lines was harvested, brought to 10% (v/v) glycerol, and incubated with 60 µl of protein A-Sepharose:anti-HA conjugate in the

presence of 310 μL of PBS and 80 mg bovine serum albumin (BSA) for 1 h. Proteins bound to the protein A-Sepharose:anti-HA conjugate were washed 4 times with 10 volumes of 0.1% (w/v) TX-100, 50 mM Tris/Cl, pH 7.4, and 300 mM NaCl followed by 2 washes with 10 volumes of PBS and used immediately for GalAT activity assays (10 μL) or SDS-PAGE (10 μL).

Cell lysates from HEK lines were prepared by incubating one 150 cm^2 dish of cells with 1 mL of cold cell lysis buffer (50 mM HEPES, pH 7.3, 1% [v/v] TX-100, 150 mM NaCl , 2 mM EDTA, and 1 tablet of Complete Protease Inhibitor Cocktail, EDTA free; Roche, catalog no. 1-873-580) for 30 min. Cell debris was pelleted by centrifugation and the clear supernatant was incubated with 40 μL (Western blots) or 160 μL (GalAT activity assays) of protein A-Sepharose:anti-HA conjugate for 1 h. Immunoprecipitates were either washed 5 times with 10 volumes of buffer A (activity assays) or 3 times with 10 volumes of buffer A followed by 2 washes of 10 volumes of PBS (Western blot). All manipulations were done at 4°C.

SDS-PAGE and immunoblotting

SDS-PAGE was carried out according to a previously described method (Laemmli, 1970). Samples (10-20 μL) were separated on 7.5 or 10% SDS-PAGE gels. Separated proteins were either visualized by silver staining (Heukeshoven and Dernick, 1985), Coomassie staining (Bio-Safe Coomassie G250 stain, Bio-Rad), or transferred to PVDF membranes for 2 h at 200 mA in 25 mM Tris, 192 mM glycine, and 20% methanol. Membranes were blocked for 1 h in 3% BSA in Tris-buffered-saline (TBS; 100 mM Tris/Cl, pH 7.5, 0.9% [w/v] NaCl) and incubated with a 1:1000 dilution of anti-HA-peroxidase antibody in blocking buffer for 1 h. Membranes were washed 4 times in TTBS (0.1% [v/v] Tween 20 in TBS) and developed using the 3,3',5,5'-tetramethylbenzidine (TMB) substrate kit (Vector Labs, Burlingame, CA) according to manufacturer's instructions.

Synthesis of uridine diphosho-D-[^{14}C]galacturonic acid

Uridine diphosho-D-[^{14}C]galacturonic acid (UDP-D-[^{14}C]Gal*p*A) was synthesized based on previously developed methods (Liljebjelke et al., 1995; Basu et al., 2000) with some modifications. Briefly, 50 μCi of uridine diphospho-D-[^{14}C]galactose (UDP-D-[^{14}C]Gal*p*) was purified over a CarboPac PA-1 column (Dionex; Sunnyvale, CA) using a 0.05-1 M linear gradient of ammonium formate, pH 6.6, at a flow rate of 1 mL/min. Purified UDP-D-[^{14}C]Gal*p* was lyophilized and resuspended in 0.5 mL of 25 mM NaH_2PO_4, pH 7.0, containing 250 units of galactose oxidase and 13,000 units of catalase. The reaction was incubated in the dark at room temperature for 24 h, at which point another 250 units of galactose oxidase and 13,000 units of catalase were added. The reaction was incubated for another 24 h in the dark and terminated with 600 μl of 5:1 (v/v), chloroform:methanol. The resultant mixture containing UDP-D-[^{14}C]Gal*p*A was extracted and purified as described previously (Liljebjelke et al., 1995). The typical yield of UDP-D-[^{14}C]Gal*p*A from the starting UDP-D-[^{14}C]Gal*p* was between 60 to 70%.

GalAT activity assay

The GalAT activity assay was a modification of Doong et al. (1995). Assay conditions used to test solubilized or membrane-bound GalAT activity, or fractions from chromatography columns were conducted in GalAT reaction buffer (50 mM HEPES, pH 7.8, 0.2 M sucrose, 0.05% (w/v) bovine serum albumin, and 25 mM KCl) containing 80 μg of OGAs (DP of 7-23), 1.1 μM UDP-D-[^{14}C]Gal*p*A (specific activity 298 mCi mmol^{-1}), 0.25 mM $MnCl_2$ and 140 μM UDP-D-Gal*p*A in a total volume of 30 μl for 15 min at 30°C (unless otherwise specified). Reaction mixtures were terminated with 5 μL of 0.4 M NaOH.

Media and/or immunoprecipitated media (10 μL) from HEK cell lines were incubated in GalAT reaction buffer containing 80 μg of OGAs (DP of 7-23), 2 μM UDP-D-[^{14}C]Gal*p*A

(specific activity 298 mCi $mmol^{-1}$), 0.25 mM $MnCl_2$ and 100 μM UDP-D-Gal*p*A in a total volume of 30 μl for 45 min (media) or 60 min (immunoprecipitated media). Reaction mixtures were terminated with 5 μL of 0.4 M NaOH.

Cell lysates (20 μL) and/or immunoprecipitated cell lysates (40 μL) from HEK cell lines were incubated in GalAT reaction buffer containing 50 μg of OGAs (DP of 7-23), 2 μM UDP-D-[^{14}C]Gal*p*A, 0.25 mM $MnCl_2$ and 125 μg of heat-inactivated Arabidopsis membranes (as an alternative source of acceptors) in a total volume of 70 μl at 30°C for 30 min (cell lysates) or 90 min (immunoprecipitated cell lysates). Reaction mixtures were terminated with 10 μl of 0.4 M NaOH.

Terminated reaction mixtures were spotted onto cetylpyridinium chloride-coated Whatman (Maidstone, England) 3MM paper (4 cm^2). The filters were allowed to dry for 5 min and washed 3 times for 10 min each in 150 mM NaCl at a ratio of 1 filter/100 mL solution. The amount of radioactivity bound to each filter was estimated by scintillation counting. Statistical analysis of GalAT reaction data was performed using a two-sample, one-tailed Student's *t* test (Zar, 1999) with an *a priori* α of 0.05 (95% confidence).

Production of polyclonal antibodies

Three distinct regions of JS33, JS36 and JS36L (At5g47780), an Arabidopsis protein with significant sequence identity to JS36, were selected and used for the production of soluble, tetrameric, multiple antigenic peptides (MAPs). Peptides sequences (20-25 amino acids) were selected by analysis using hydropathy plots (Kyte and Doolittle, 1982), analyzing beta-turn character (Chou and Fasman, 1978), sequence alignments, and use of GenTHREADER (http://bioinf.cs.ucl.ac.uk/psipred/). Stretches in the amino acid sequence of JS genes that had low hydrophobicity, high beta-turn character (determined using ProtScale;

http://au.expasy.org/cgi-bin/protscale.pl), and were predicted to be loop regions in the protein by sequence alignments (ClustalX, version 1.83) and by GenTHREADER, were chosen as candidate peptides for MAP construction. MAPs were constructed at the Molecular Genetics Instrument Facility (The University of Georgia). Rabbits (New Zealand White, two for each antigen), were immunized (0.5 mL of 0.3 mg mL^{-1} antigen), maintained and bled by the Polyclonal Antibody Facility (The University of Georgia).

Immunoprecipitation of Arabidopsis solubilized GalAT using polyclonal antibodies

Pre-immune serum or polyclonal antibodies (1 µL of pooled serum) from rabbits inoculated with JS33, JS36 and/or JS36L MAP antigens were incubated with 40 µL of protein A-Sepharose (equilibrated in ice-cold PBS) for 2 h at 4°C. Polyclonal antibody:protein A conjugates were washed 6 times with buffer A, and 40 µL of conjugate was incubated with 0.5 mL of solubilized Arabidopsis GalAT overnight at 4°C. Immunoprecipitates were washed 5 times in buffer A and tested for GalAT activity as described above using 2 µM UDP-D-[^{14}C]Gal*p*A and 80 µg of OGAs in a total volume of 70 µL for 30 min at 30°C.

Sequence alignment of JS family genes and phylogenetic analysis

Arabidopsis genes with high sequence identity to JS36 were aligned using ClustalX, version 1.83 (Jeanmougin et al., 1998). Phylogenetic analysis of the Arabidopsis GalAT gene family, along with EST (GenBank, http://www.ncbi.nlm.nih.gov/dbEST) or tentative consensus (TC, http://www.tigr.org/tdb/tgi) sequences from soybean (*Glycine max*, Gm), barrel medic (*Medicago truncatula*, Mt), rice (*Oryza sativa*, Os), tobacco (*Nicotiana tobacum*, Nt) and chickpea (*Cicer arietinum*, Ca) was conducted using PAUP software, version 3.1 (Swofford, 1998).

RESULTS

Solubilization and partial purification of Arabidopsis GalAT

A reproducible method for the solubilization of roughly 20% of the GalAT activity from tobacco membranes was previously established (Doong and Mohnen, 1998). The low yield of total activity from the starting material was a major drawback in this solubilization method. Therefore, an improved solubilization method was developed that allowed the recovery of up to 85% of the starting GalAT activity from tobacco membranes.

The original low-speed centrifugation pellet (4,000*g*, 15 min) generated during the isolation of tobacco membranes (Doong and Mohnen, 1998) contained ~50% of the total activity present in tobacco cell homogenates (data not shown). It was hypothesized that the elimination of this step would greatly improve the yield of GalAT from these cells. Centrifugation of tobacco homogenates at high speed (28,000*g*, 2 h) created a layered pellet. Resuspension and solubilization of the top layer of this pellet with 4% (v/v) Triton X-100 resulted in the solubilization of up to 85% of the total activity present in the top layer of the high speed pellet (Table 4.1). Little or no activity was present in the other layers of the pellet. If the top layer was mixed with the other layers prior to solubilization, the amount of solubilized GalAT activity that could be recovered decreased dramatically (Table 4.1), suggesting that the other layers of the pellet contained a potent inhibitor of GalAT activity and/or a protease capable of digesting tobacco GalAT. This finding was supported by the fact that GalAT activity solubilized using the new method was more stable than that obtained by previous solubilization methods, being stable for up to one year at -80°C, with a 30% loss in activity occurring after one week at 4°C (data not shown).

Table 4.1. A new procedure for the production of solubilized GalAT from tobacco.

	Specific activity (pmol min^{-1} mg^{-1})	Total activity (μmol min^{-1})	Yield (%)
Mixed layers			
Whole pellet[a]	98.2	3.65	100
Solubilized activity[b]	42.0	0.687	18.8
Insoluble pellet[b]	109	1.45	40.0
Separated layers[a]			
Combined layers	ND[d]	14.2	100
Top layer	123	11.1	78.2
Bottom layers	28.9	3.10	21.8
Solubilized activity from top layer[c]	163	12.3	84.5
Insoluble pellet from top layer	40.7	1.71	12.0

[a]GalAT activity was assayed for 10 min.

[b]GalAT activity was assayed for 30 min (within the linear range of the enzyme).

[c]Stimulation of activity is consistently seen following the separation of solubilized GalAT from the insoluble pellet.

[d]ND = not determined.

Tobacco suspension-cultured cells were an ideal starting material for the purification of GalAT due to the apparent lack of plant phosphatases and phosphodiesterases (Saugy et al., 1988; Rodgers and Bolwell, 1992; Doong and Mohnen, 1998). The use of tobacco cells did present a problem, however, for the subsequent cloning of the purified GalAT, as publicly available sequence data was lacking for this experimental system. This made *Arabidopsis thaliana* an ideal system for the identification of putative GalAT genes and we switched to Arabidopsis suspension-cultured cells as a tissue source for the partial purification of GalAT.

GalAT activity was solubilized from suspension cultured Arabidopsis cells using the newly established solubilization protocol from tobacco (Guillaumie et al., 2003). Starting with 700 g of Arabidopsis cells, solubilized Arabidopsis GalAT was purified 17-fold with an overall yield of ~3% (Table 4.2, Experiment 1). The first step in the purification protocol involved the binding of GalAT activity to the cation exchange column SP-sepharose. Roughly 70% of the protein found in the solubilized fraction from Arabidopsis did not bind this column (data not shown). GalAT activity could be eluted from the column with the addition of 300-400 mM NaCl, resulting in an 8-fold purification and a yield of 24%. The yield from this column could be improved to 65% with a slight decrease in protein purity (4.7-fold) if a higher amount of total protein was initially loaded (Table 4.2, Experiment 2).

Initial experiments using the reactive dye resin Reactive Yellow 3 (RY3) suggested that this column could purify GalAT activity an additional 3-fold (data not shown). This extra purification was later determined to be dependent on the initial purity of the GalAT-containing fraction that was obtained following SP-Sepharose chromatography. More purified fractions (>6-fold) from SP-sepharose were negatively affected by this resin as evidenced by the reduction in GalAT purity and yield (Table 4.2, Experiment 1). Bound GalAT activity could be eluted

Table 4.2. Partial purification of Arabidopsis GalAT[a]

Experiment 1:

Step	Total protein (mg)	Specific activity (pmol min^{-1} mg^{-1})	Purification (-fold)	Total activity (μmol min^{-1})	Yield (%)
1. Sol	794	304[b]	1	241	100
2. SP	23.6	2450[b]	8.06	57.7	24
3. RY3	13.7	1720[c]	5.66	23.6	9.8
4. UDP-agarose (2)	1.29	5120[c]	16.8	6.59	2.7

Experiment 2:

Sample	Total protein (mg)	Specific activity (pmol min^{-1} mg^{-1})	Purification (-fold)	Total activity (μmol min^{-1})	Yield (%)
1. Sol	2,200	26.0	1	57.2[e]	100
2. SP	314	121	4.7	37.5[e]	65.6
3. RY3	ND[d]	ND	ND	17.5[f]	30.6
4. UDP-agarose (1)	ND	ND	ND	7.09[f]	12.4
5. UDP-agarose (2)	ND	ND	ND	1.35[f]	2.4

[a]GalAT activity in Experiments 1 and 2 was measured using different amounts of cold UDP-D-Gal*p*A and are therefore not directly comparable.

[b]GalAT activity was measured for 15 min using 1 mM UDP-D-Gal*p*A.

[c]GalAT activity was assayed for 30 min using 1 mM UDP-D-Gal*p*A

[d]ND = Not determined.

[e]GalAT activity was assayed for 15 min using 100 μM UDP-D-Gal*p*A.

[f]GalAT activity was assayed for 1 h using 100 μM UDP-D-Gal*p*A.

from the column with 100-200 mM NaCl in the presence of 10 μM UDP and 2 μM OGAs. UDP and OGAs were included in the elution buffer to aid in the selective removal of GalAT activity that had bound to the column due to an affinity-type interaction between the enzyme active site and the column matrix.

The fraction from RY3 was applied to an UDP-agarose column and an elution scheme was developed based on the purification of whey galactosyltransferase (Barker et al., 1972). Whey galactosyltransferase was found to bind maximally to UDP-Sepharose in the presence of 25 mM $MnCl_2$. This binding occurred even when the column was washed with high (0.5-1 M) concentrations of NaCl (Barker et al., 1972).

Arabidopsis GalAT activity bound to UDP-agarose in the presence of low concentrations of $MnCl_2$ (0.25 mM). Following a washing step containing 50 mM UDP to remove any contaminating proteins, the column was equilibrated with a buffer containing 25 mM $MnCl_2$, washed with NaCl, and finally eluted with a buffer containing 25 mM EDTA. Approximately 30% of the total activity was eluted with 25 mM $MnCl_2$/0.5 M NaCl and GalAT activity present in this fraction was purified an additional 3-fold compared to the most purified fraction from Reactive Yellow 3 (Table 4.2, Experiment 1).

The relative purity of the fractions eluted from the UDP-agarose column was compared to solubilized Arabidopsis proteins and to the eluted fractions from the SP-sepharose and RY3 columns (Figure 4.1). SDS-PAGE analysis showed that while the most purified fraction eluted from the UDP-agarose column (Lane 6) was enriched in specific protein bands compared to fractions from the earlier columns, it also contained a number of abundant protein bands that were found in fractions that did not contain activity (compare Lane 6 to Lanes 4 and 7). Unique bands suggestive of possible GalATs were not visible at this stage of purification suggesting that

Figure 4.1. SDS-PAGE analysis of partially purified GalAT. Partially purified fractions from Experiment 1 (Table 4.1) were separated on 10% SDS-PAGE gels and proteins were visualized by silver staining. Equal amounts of protein (3.7 μg) from each of the indicated column fractions were loaded. *Lane 1*, solubilized Arabidopsis GalAT; *Lane 2*, proteins eluted from the SP-sepharose column using 400 mM NaCl; *Lane 3*, proteins eluted from the Reactive Yellow 3 column using 100-200 mM NaCl in the presence of 10 μM UDP and 2 μM OGAs; *Lanes 4-7*, eluted fractions from the UDP-agarose column (*Lane 4*, 50 mM UDP; *Lane 5*, 25 mM $MnCl_2$; *Lane 6*, 25 mM $MnCl_2$ and 0.5 M NaCl; *Lane 7*, 25 mM EDTA). The percent yield of GalAT activity present in each fraction compared to solubilized GalAT is shown underneath the figure. The positions of the molecular weight markers (M) in kDa are shown on the left.

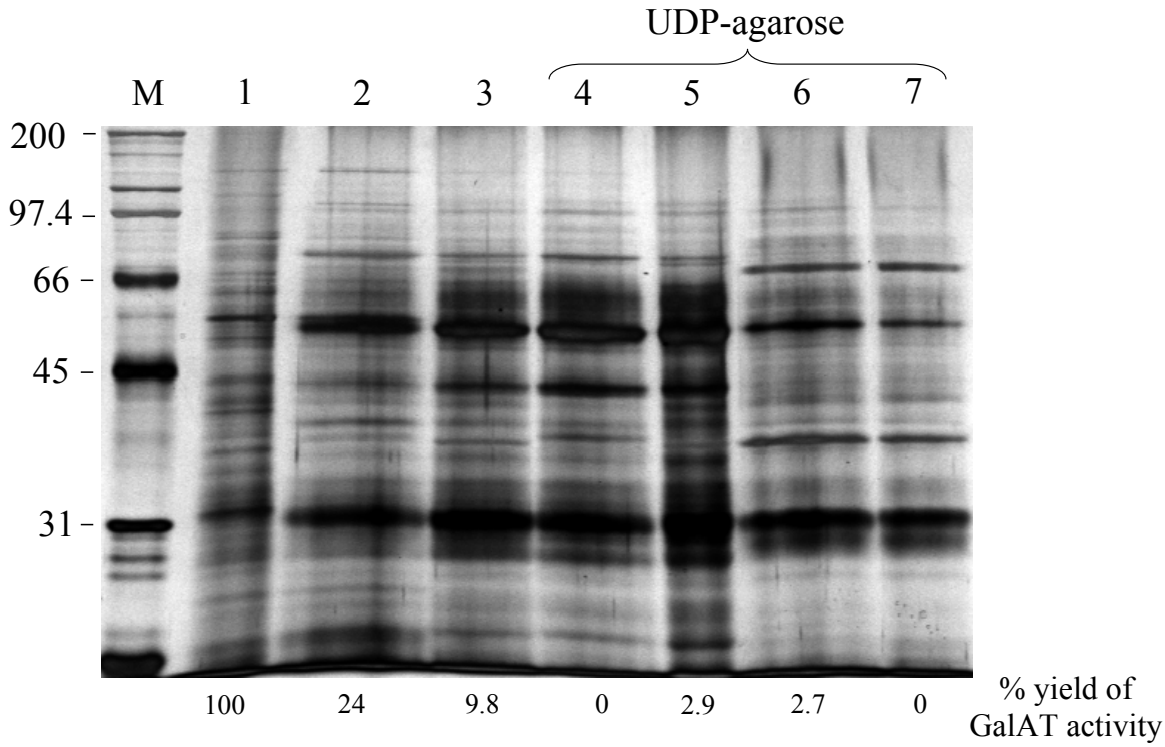

further levels of purification would be required before distinct protein bands corresponding to putative GalAT proteins could be detected.

An additional purification experiment (Table 4.2, Experiment 2) was conducted in order to obtain sufficient amounts of protein for tryptic digestion and LC MS/MS analysis of the proteins contained in the most purified fraction from the UDP-agarose column. This experiment differed from the first experiment in the amount of starting protein used (2,200 mg versus 800 mg), and in the inclusion of an additional purification step using UDP-agarose (Table 4.2). The partially purified fraction from RY3 was bound to UDP agarose and some contaminating proteins were eluted with a step gradient of UDP (data not shown). GalAT activity was eluted from the column with 1 M NaCl, desalted, and reapplied to the column (Table 4.2, Experiment 2, UDP-agarose [1]). The second UDP-agarose chromatography step was conducted using the elution scheme presented in Experiment 1, resulting in a fraction (eluted with 25 mM $MnCl_2$ in the presence of 0.5 M NaCl) that contained 2.4% of the activity found in the solubilized GalAT fraction (Figure 4.2).

Identification of GalAT candidate genes from Arabidopsis

A fraction from the second purification experiment (Figure 4.2, Lane 5) was treated with sequencing-grade trypsin and subjected to LC MS/MS analysis. Sequenced peptides were used to screen the Arabidopsis genome database for putative GalAT genes. A total of 20 distinct proteins were identified in this fraction (Table 4.3). The proposed functions of many of the identified proteins were assigned during the electronic annotation of the Arabidopsis genome, yet none of these functions have been confirmed by biochemical characterization. Two proteins, named JS33 and JS36 (At2g38650 and At3g61130, respectively; Figure 4.3, A) were predicted to be glycosyltransferases and were analyzed further.

Figure 4.2. SDS-PAGE analysis of fractions from the UDP-agarose column. Fractions (20 µL) from the second UDP-agarose chromatography step (Table 4.2, Experiment 2) were separated on a 10% SDS-PAGE gel and visualized by silver staining. *Lane 1*, eluted fraction from the first UDP-agarose chromatography step; *Lane 2-6*, eluted fractions from the second UDP-agarose chromatography step (*Lane 2*, flow-through; *Lane 3*, 50 mM UDP; *Lane 4*, 25 mM $MnCl_2$; *Lane 5*, 25 mM $MnCl_2$ and 0.5 M NaCl; *Lane 6*, 25 mM EDTA). The percent yield of GalAT activity present in each fraction compared to solubilized GalAT is shown underneath the figure. The positions of the molecular weight markers (M) in kDa are shown on the left. * indicates the fraction used for the identification of candidate GalAT proteins.

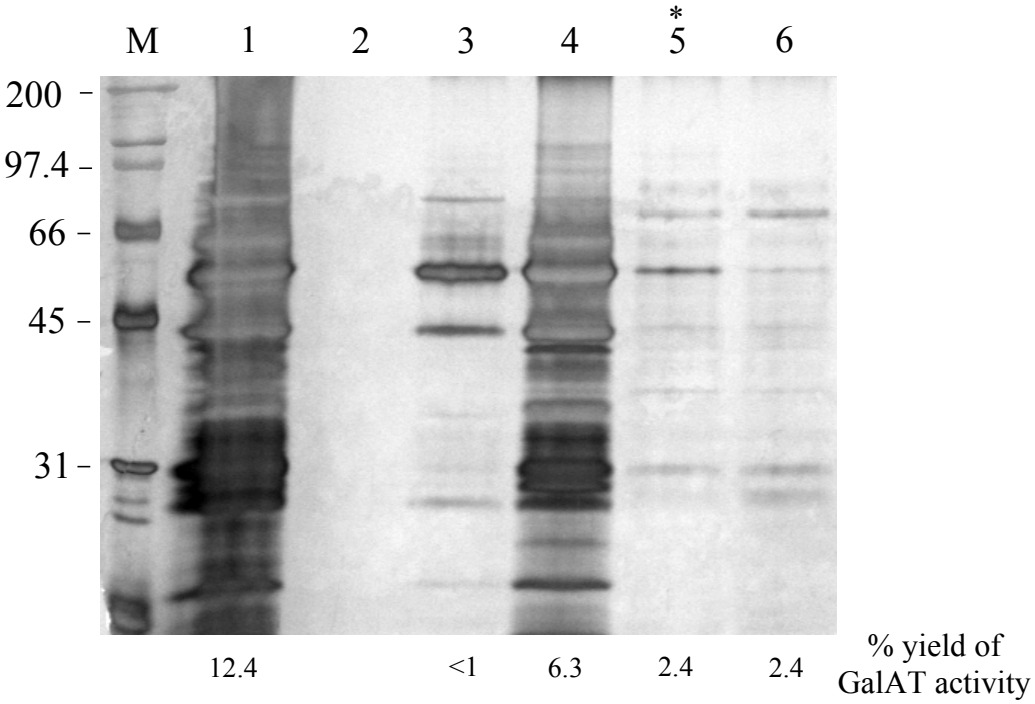

Table 4.3. List of identified proteins from the partially purified UDP-agarose fraction.

Protein ID (accession no.)	Predicted molecular weight (kDa)	Proposed function[a]	Mowse score[b]
BAB01930	65.9	β-fructofuranosidase	282
AAD05539	102	α-xylosidase precursor	236
AAL15216	42.0	putative methionyl-tRNA synthetase	168
BAB40450	76..6	long-chain acyl-CoA synthetase	112
AAD29817	61.7	synaptotagmin A	100
JS33/NP_565893	69.7	putative glycosyltransferase	110
BAB02117	48.5	unknown	81
BAB10278	35.7	unknown	77
JS36/NP_191672	77.4	putative glycosyltransferase	73
AAM66061	52.3	chloroplast nucleiod DNA binding protein	58
BAA20519	63.3	L-ascorbate oxidase	73
CAB78227	97.4	putative phospholipase D	71
CAB51209	13.7	ribosomal protein S20	53
AAK43965	15.4	putative HMG protein	48
AAM65244	36.1	hypothetical protein	48
AAN41337	37.2	quinone reductase-like protein	46
AAG10103	32.8	fibrillarin 1	42
BAB09414	75.9	putative ATP-binding protein	41
AAO42878	46.7	unknown	41
AAN46839	59.1	unknown	40

[a]The proposed functions were previously inferred by electronic annotation.

[b]Mowse scores below 60 are not significant based on an *a priori* α of 0.05.

Figure 4.3. Alignment of the amino acids sequences of JS33 and JS36. (A) The amino acid sequences of JS33 and JS36 were aligned using ClustalX (version 1.83). The peptides obtained by tryptic digestion of proteins found in the most purified fraction from UDP-agarose chromatography are underlined. The site of N-terminal truncation is indicated by the arrows. The conserved DxD motif found in both sequences is boxed. (B) Schematic representation of the gene constructs used in the expression of the JS genes in HEK293 cells. The locations of the N-terminal *Trypanosoma cruzi* mannosidase signal sequence (TCMss), the poly-histidine tag (10xHis-tag) and 2 copies of the hemagluttinin epitope tag (HA-epitope tag) are indicated.

A

```
JS33  --MKGGGGGGG---GGGGCKRRWKVLVIGVLVLVILSMLVPLAFLLGLHN---------G  46
JS36  MALKRGLSGVNRIRGSGGGSRSVLVLLIFFCVFAPLCFFVGRGVYIDSSNDYSIVSVKQN  60

JS33  FHSPGFVTVQPASSFESFTRINATKHTQRDVSERVDEVLQKINPVLPKK-SDINVGSRDV  105
JS36  LDWRERLAMQSVRSLFSKEILDVIATSTADLGPLSLDSFKKNNLSASWRGTGVDPSFRHS  120

JS33  NATSGTDSKKRGLPVSPTVVANPSPANKTKSEASYTG----------------------142
JS36  ENPATPDVKSNNLNEKRDSISKDSIHQKVETPTKIHRRQLREKRREMRANELVQHNDDTI180

JS33  VQRKIVSGDETWRTCEVKYGSYCLWREENKEPMKDAKVKQMKDQLFVARAYYPSIAKMPS  202
JS36  LKLENAAIERSKSVDSAVLGKYSIWRRENENDNSDSNIRLMRDQVIMARVYS-GIAKLKN  239

JS33  QSKLTRDMKQNIQEFERILSESSQDADLPPQVDKKLQKMEAVIAKAKSFPVDCNNVDKKL  262
JS36  KNDLLQELQARLKDSQRVLGEATSDADLPRSAHEKLRAMGQVLAKAKMQLYDCKLVTGKL  299

JS33  RQILDLTEDEASFHMKQSVFLYQLAVQTMPKSLHCLSMRLIVEHFKS--DSLEDPISEKF  320
JS36  RAMLQTADEQVRSLKKQSTFLAQLAAKTIPNPIHCLSMRLIDYYLLSPEKRKFPRSENL  359

JS33  SDPSLLHFVIISDNILASSVVINSTVVHARDSKNFVFHVLTDEQNYFAMKQWFIRNPCKQ  380
JS36  ENPNLYHYALFSDNVLAASVVVNSTIMNAKDPSKHVFHLVTDKLNFGAMNMWFLLNPPGK  419

JS33  STVQVLNIEKLELDDS---------DMKLSLSAEFRVSFPSGDLLASQQNRTHYLSLFSQ  431
JS36  ATIHVENVDEFKWLNSSYCPVLRQLESAAMREYYFKADHPTSGSSNLKYRNPKYLSMLNH  479

JS33  SHYLLPKLFDKLEKVVILDDDVVVQRDLSPLWDLDMEGKVNGAVKSCTVRLGQLRSLK--  489
JS36  LRFYLPEVYPKLNKILFLDDDIIVQKDLTPLWEVNLNGKVNGAVETCGESFHRFDKYLNF  539

JS33  -----RGNFDTNACLWMSGLNVVDLARWRALGVSETYQKYYKEMSSGDESSEAIALQASL  544
JS36  SNPHIAFNFNPNACGWAYGMNMFDLKEWKKRDITGIYHK-WQNMNENRTLWKLGTLPPGL  598

JS33  LTFQDQVYALDDKWALSGLGYDYYINAQAIKNAAILHYNGNMKPWLELGIPNYKNYWRRH  604
JS36  ITFYGLTHPLNKAWHVLGLGYNPSIDKKDIENAAVVHYNGNMKPWLELAMSKYRPYWTKY  658

JS33  LSREDRFLSDCNVNP  619
JS36  IKFDHPYLRRCNLHE  673
```

B

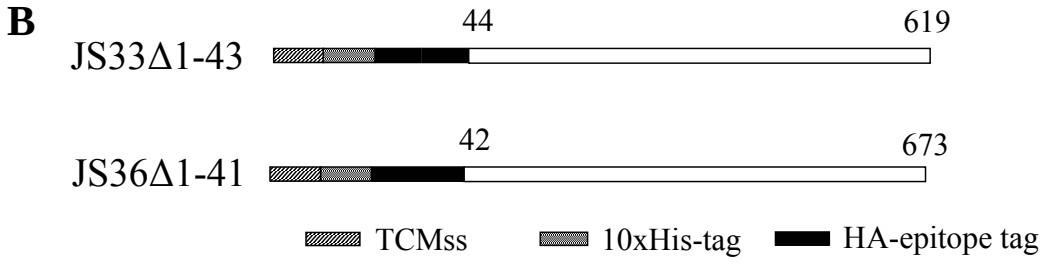

JS33 and JS36 encode predicted type II membrane proteins (TMpred, http://www.ch.embnet.org/software/TMPRED_form.html) whose C-terminal catalytic domains possess sequence identity to a consensus sequence found in family 8 glycosyltransferases (http://afmb.cnrs-mrs.fr/CAZY; Henrissat et al., 2001). Members of family 8 (which include galactinol synthase and lipopolysaccharide galactosyltransferase) are retaining glycosyltransferases able to transfer the glycosyl residue from NDP-α-sugars onto α-linked products (Saxena et al., 1995). The predicted catalytic domains of JS33 and JS36 also contain putative DxD motifs (Figure 4.3, A); a conserved motif found in many well-characterized glycosyltransferase families (Wiggins and Munro, 1998) and are involved in the coordination of divalent cations required for glycosyltransferase activity (Breton and Imberty, 1999; Chen et al., 2001).

Previous studies on a GalAT from pea (*Pisum sativum*) showed that GalAT activity was localized to Golgi vesicles with its catalytic domain facing the lumen (Sterling et al., 2001). This topology is characteristic of type II membrane proteins, which is the predicted topology of JS33 and JS36. Furthermore, preliminary RT-PCR analysis of the expression of JS33 and JS36 transcripts in Arabidopsis tissues showed that JS33 and JS36 were found in all Arabidopsis tissues that were analyzed (Figure 4.4). These findings suggested that JS33 and JS36 were candidates for GalATs genes and we decided to clone their respective cDNAs and express them in a heterologous system in order to prove their function.

N-terminally truncated JS36 exhibits GalAT-like characteristics when transiently expressed in HEK293 cells

cDNA constructs containing N-terminally truncated versions of JS33 (JS33Δ1-43) or JS36 (JS36Δ1-41) were generated (Figure 4.3, A, B). The cDNAs were placed downstream of a

Figure 4.4. Expression analysis of JS33 and JS36 in Arabidopsis. Total RNA isolated from flowers (F), roots (R), stems (S), and rosette leaves (L) was used as a template for the RT-PCR of JS33- and JS36-specific transcripts and separated on 1% agarose gels. The sizes of the amplified transcripts were 1758 bp and 1926 bp for JS33 and JS36, respectively. Primers directed against actin generating a 495 bp fragment (McKinney et al., 1995) were used as a positive control. The positions of molecular weight markers (M) in kb are shown on the left of each figure.

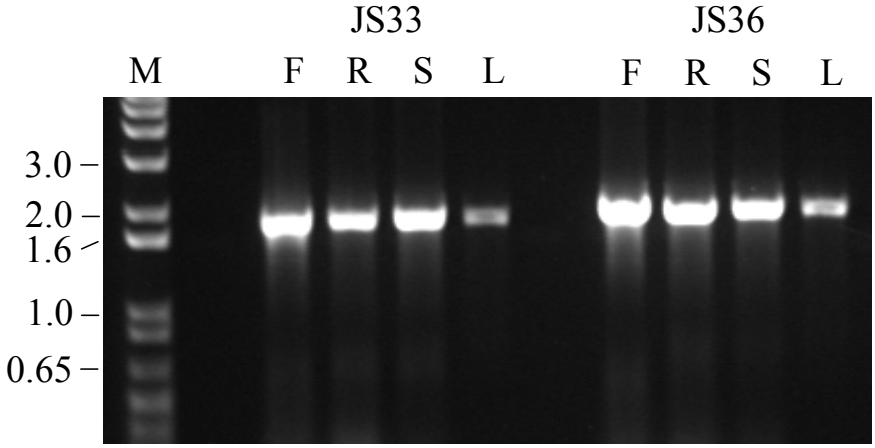

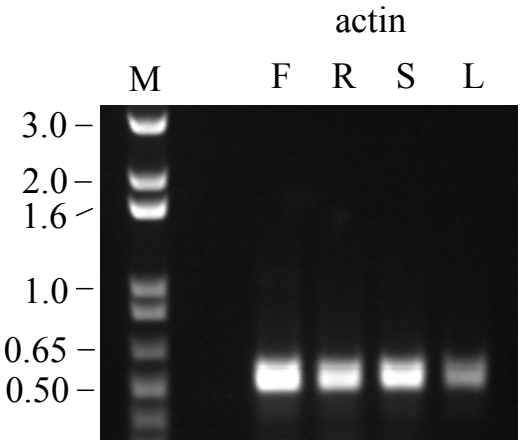

signal sequence from *Trypanosoma cruzi* mannosidase, a poly-histidine tag, and two copies of the hemagluttinin epitope (Figure 4.3, B) in the mammalian expression vector pEAK10. These constructs were used to transiently transfect HEK293 cells that were 50% confluent (4 d old). Media harvested from these cells 48 h post-transfection were tested for GalAT activity (Figure 4.5, A) and the data was analyzed for its significance compared to controls using a two sample, one-tailed Student's *t* test and an *a priori* α of 0.05 (95% confidence).

Media from cells transfected with the JS36Δ1-41 construct were not able to promote the significant incorporation of D-[^{14}C]Gal*p*A from UDP-D-[^{14}C]Gal*p*A into a radiolabeled product compared to cells transfected with empty vector (n = 2, t_{JS36} = 1.589 [$P \approx 0.1$]). In contrast, media from JS36Δ1-41-transfected cells that had been immunoprecipitated using anti-hemagluttinin (anti-HA) antibodies and protein A-Sepharose gave 3 times greater incorporation of radiolabel than that of the empty vector controls (n =2, t_{JS36} = 10.284 [$P \approx 0.005$]). Neither media (t_{JS33} = 0.057 [$P > 0.25$]) nor immunoprecipitates (t_{JS33} = 0.180 [$P > 0.25$]) of cells transfected with the JS33Δ1-43 construct produced incorporation levels that were significantly different from cells transfected with empty vector. These results suggested that JS36 encoded an enzyme capable of catalyzing the transfer of D-[^{14}C]Gal*p*A onto a product and based on these results we proposed that JS36 encoded a putative GalAT.

Analysis of a second set of HEK293 cells transiently transfected with the same cDNA constructs; however, did not result in GalAT activity in immunoprecipitated media (data not shown). The second transient transfection experiment was conducted in a manner similar, but not identical, to that of the first transfection experiment. Both experiments used HEK293 cells that were 50% confluent and media and cell lysates were harvested 48 h post-transfection. However, different buffers were used to prepare the media and cell lysates in the second transient

Figure 4.5. GalAT activity in transiently transfected HEK cells. A) GalAT activity in media from HEK cells transfected with the JS33Δ1-43 (JS33) or JS36Δ1-41 (JS36) cDNA constructs or with empty vector (pEAK) as a control. B) GalAT activity in media immunoprecipitated with 2 μg of anti-HA antibodies conjugated to 60 μL of protein A-Sepharose. The pooled, desalted fraction from SP sepharose (SP; A) or solubilized Arabidopsis GalAT (Sol; B, inset) were used as positive controls. The average of all the time zero reactions (T_o) for each experiment are shown. Reactions were conducted for 45 (A) or 60 (B) min. Data are the average ± standard error of duplicate samples.

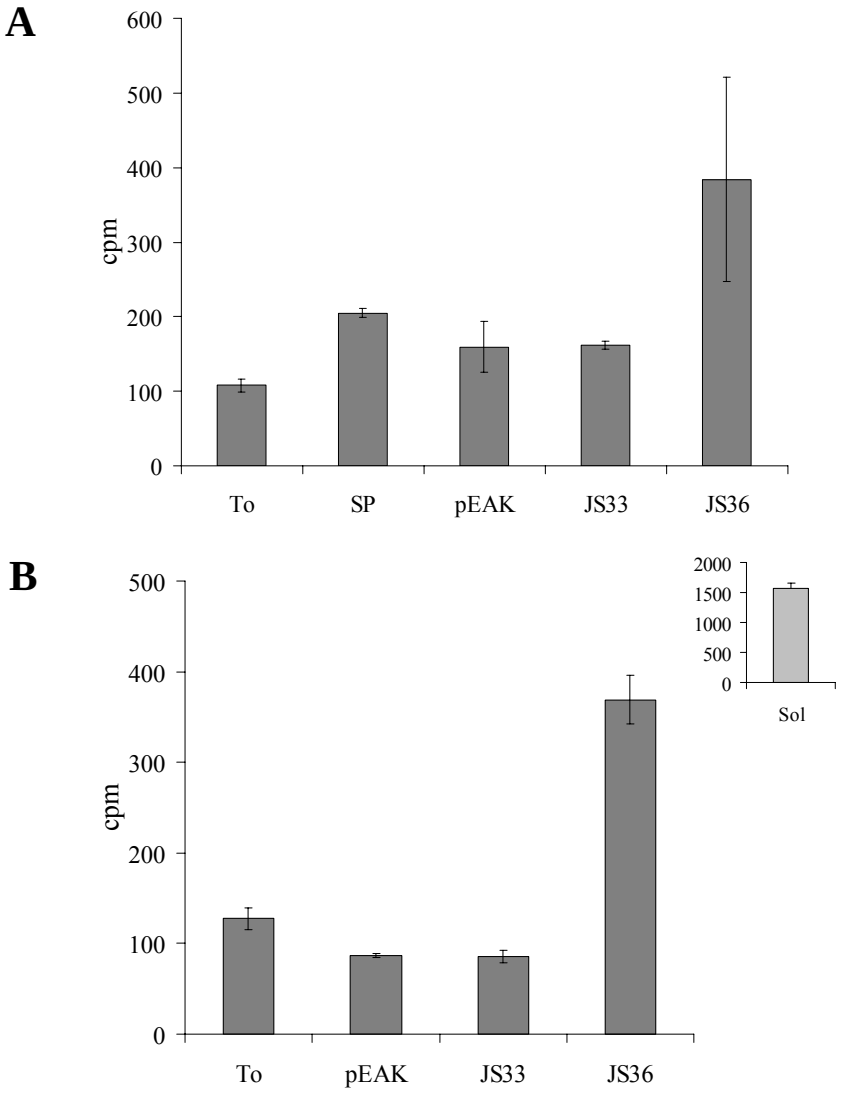

experiment. Protease inhibitors were added to the harvested media and different washing buffers were used for the immunoprecipitation of recombinant proteins from media and cell lysates. The washing buffer used in the second experiment contained 50 mM HEPES, pH 7.3, 0.25 mM $MnCl_2$, 1% Triton X-100, 2 mM EDTA, and 25% [v/v] glycerol compared to 0.1% [w/v] TX-100, 50 mM Tris/Cl, pH 7.4, and 300 mM NaCl used in the first experiment. Both treatments were shown to be compatible with solubilized Arabidopsis GalAT activity. At this point, it is unclear whether the lack of GalAT activity in the second transient transfection experiment was due to the use of different buffers or due to other, as yet unknown, factors.

Western blot analysis of media and cell lysates from the second transient transfection experiment indicated the presence of recombinant JS33 and JS36 proteins in the media of transfected cells, and recombinant JS33 protein in cell lysates (Figure 4.6). The estimated molecular weights of JS33 (86 kDa) and JS36 (88 kDa) were much higher than those calculated from their amino acid sequences (73.2 kDa and 80.7 kDa for JS33 and JS36, respectively), suggesting that both proteins were post-translationally modified.

The immunoblot results suggested that the cells lines were transfected with the JS cDNA constructs and that they were capable of secreting the recombinant proteins into the media as expected. The level of recombinant protein present in the media from cells transfected with JS36 was significantly lower than that of cells transfected with JS33. The reason for this disparity in recombinant protein levels is unknown. In order to further study JS36 and JS33, and to increase the level of recombinant JS36 protein made by HEK cell lines, we decided to create stable lines expressing JS36 and JS33.

Figure 4.6. Western blot analysis of media and cell lysates from transiently transfected HEK293 cells. JS33Δ1-43 (33) or JS36Δ1-41 (36) cDNA constructs were used to transfect HEK293 cells that were 50% confluent (4 d old). A) Media or B) cell lysates were obtained 48 h post-transfection, immunoprecipitated with 1 µg of anti-HA antibodies conjugated to 40 µL of protein A-sepharose and separated on a 7.5% SDS-PAGE gel. The separated proteins were mmunoblotted and probed with a monoclonal anti-HA antibody. Cells transfected with recombinant, histidine-tagged α-2,6-sialyltransferase (ST) lacking the HA epitope were used as a negative control. The positions of molecular weight markers (M) in kDa are shown on the left. The expected sized of the recombinant proteins were 73.2 kDa (JS33), 80.7 kDa (JS36) and 38 kDa (ST).

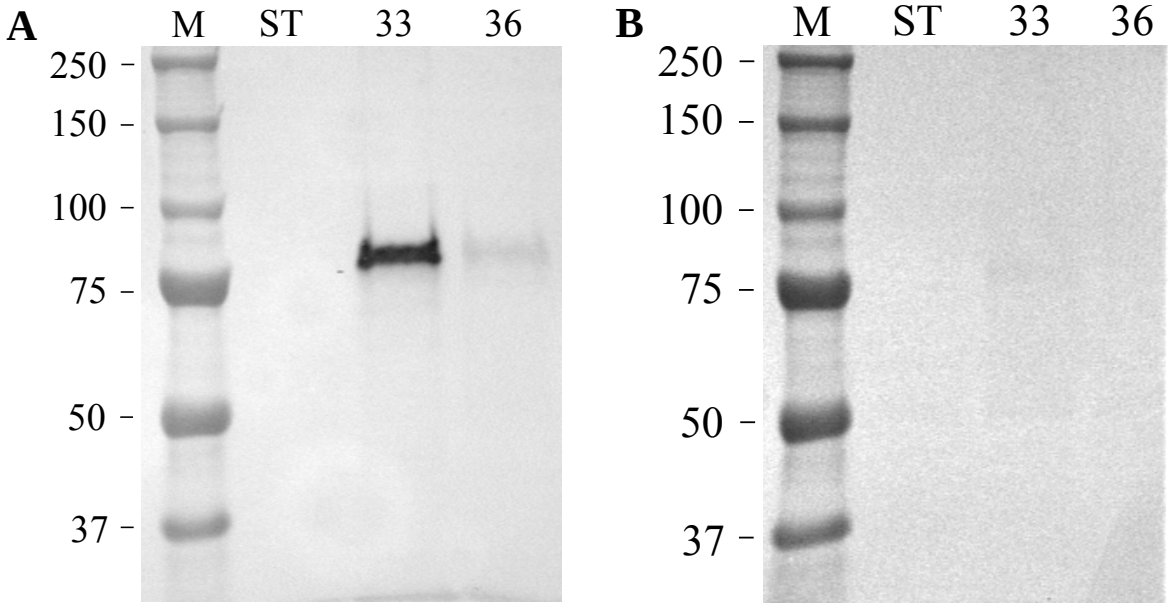

Stable expression of JS36 and JS33 in HEK293 cells

HEK293 cells were stably transformed with the JS cDNA constructs and positive transformants were screened by PCR and immunoblot analysis. Transformation of HEK cell lines with 6 μg of the JS33Δ1-43 cDNA construct generated a clonal line named 33c6 (Figure 4.7, A). Transformation of 33c6 was confirmed by genomic PCR analysis using JS33 specific primers (Figure 4.7, A). Use of the JS36Δ1-41 construct for the generation of stable lines failed to produce cell lines that expressed detectable amounts of recombinant JS36 in media or cell lysates (data not shown). Therefore, the ability of the two JS cDNA constructs to produce stable cell lines that expressed detectable levels of recombinant protein was evaluated by transforming HEK cells with varying amounts of the two JS cDNA constructs and a vector containing a recombinant α-(2,6)-sialyltransferase (α-[2,6]-ST) as a control. After transformation, the lines were maintained as mixed-populations and media or cell lysates from the mixed population lines were analyzed for the presence of recombinant protein by immunoblotting with a monoclonal anti-HA antibody (JS33 and JS36) or by Ni^{2+}-column purification of the recombinant protein followed by SDS-PAGE analysis (α-[2,6]-ST; Table 4.4).

Transforming HEK cells with 5 or 10 μg of JS or α-(2,6)-ST DNA failed to produce mixed-population cell lines that made detectable amounts of recombinant protein. Mixed population lines that expressed recombinant α-(2,6)-ST or JS33 were produced by transforming cells with 22.5 μg of DNA (Table 4.4). A higher amount of the JS36Δ1-41 cDNA construct (25-30 μg of DNA) was required to produce mixed-population lines expressing recombinant JS36 protein (Table 4.4). These results suggested that JS36 was expressed to a lower extent or with less efficiency than the JS33 or α-(2,6)-ST constructs.

Figure 4.7. Stable transformation of HEK cells with the JS33 and JS36 cDNA constructs. PCR analysis of genomic DNA from a clonal line expressing A) JS33 (33c6) and B) JS36 mixed-population lines (36mp1, 2, 3 and 6) was conducted using the gene specific primers described in the Materials and Methods. The expected sizes of the amplified products were 1758 kb for JS33, and 1926 kb (*lane* 1) and 1451 kb (*lane* 2) for JS36. Plasmid DNA containing JS33 (33pl) or JS36 (36pl) were used as a positive controls. The positions of molecular weight markers (M) in kb are shown on the left of each figure.

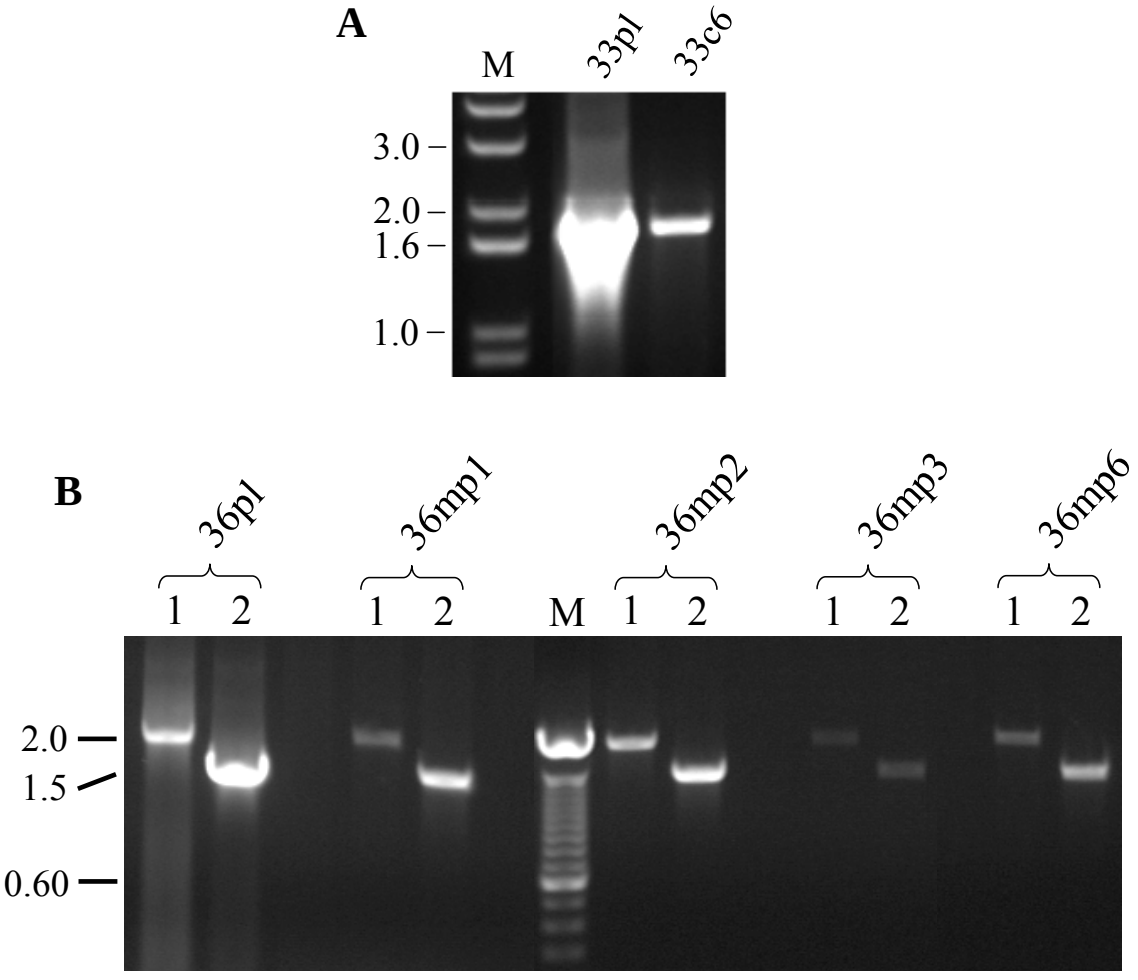

Table 4.4. Correlation between the amount DNA used and the presence of detectable levels of recombinant protein made by cells transformed with α-(2,6)-ST, JS33 and JS36 cDNA constructs.

Amount of DNA (μg)	Gene construct[a]		
	α-(2,6)-ST[b]	JS33[b]	JS36[c]
5	-	-	-
10	-	-	-
15	-	-	-
22.5	+	+	-
25	ND[d]	ND	+
30	ND	ND	+

[a]Media or cell lysates were harvested when the cells were ~80% confluent (6 d after the addition of puromycin) for each mixed population line.

[b]Media from transformed cell lines were tested.

[c]Cell lysates from transformed cell lines were tested.

[d]ND = not determined.

The presence of JS36 in mixed-population lines generated with 25 or 30 μg of the JS36Δ1-41 cDNA construct was determined by PCR analysis of genomic DNA using JS36-specific primers. Four mixed-population lines (36mp1-3, 6) were selected based on the presence of PCR products (1.4 kb and 1.9 kb) of the expected size (Figure 4.7, B). The production of mRNA transcripts in these mixed-population lines was confirmed by RT-PCR analysis using JS36-specific primers (Figure 4.8). RT-PCR products of the expected sizes were generated in all four of the JS36 mixed-population lines that were analyzed, suggesting that these lines all produced mRNA transcripts encoding JS36. PCR reactions performed in the absence of reverse transcriptase gave no product, which excluded the possibility of genomic DNA contamination (Figure 4.8, *lane* 5). These results confirmed that we had successfully transformed HEK293 cells with gene constructs containing truncated versions of JS33 and JS36.

Stable lines expressing recombinant JS36 and JS33 proteins are detected in cell lysates

In contrast to the results obtained from the transient transfection experiments, recombinant JS36 and JS33 proteins were not detected in media from stably transformed lines (data not shown). High levels of recombinant protein were instead detected in cell lysates (Figure 4.9). The estimated molecular weight of recombinant JS33 protein from the 33c6 cell line (Figure 4.9, A) was similar to that detected in media from transiently transfected cells. Recombinant JS36 protein from all 4 mixed-population lines migrated as a doublet, with predicted molecular weights of 87 and 89 kDa, respectively (Figure 4.9, B). The predicted molecular weights of both recombinant JS36 and JS33 were higher than that deduced by the amino acid sequence, suggesting that both proteins were post-translationally modified in stable and/or mixed population lines.

Figure 4.8. RT-PCR analysis of JS36 mixed-population lines. JS36 mixed-population lines (36mp1, 2, 3, and 6) were analyzed by RT-PCR using JS36-specific primers. JS36 plasmid DNA (36pl) was used as a positive control. *Lane 1*, JS36 primers which generate a 1926 bp fragment; *lane 2*, JS36 primers which generate a 1451 bp fragment; *lane 3*, blank; *lane 4*, positive control reactions using primers against glyceraldehyde 3-phosphate dehydrogenase (GAPDH) which generate a 461 bp fragment; *lane 5*, control reaction without reverse transcriptase using primers from lane 1. The positions of molecular weight markers (M) in kb are shown on the left of the figure.

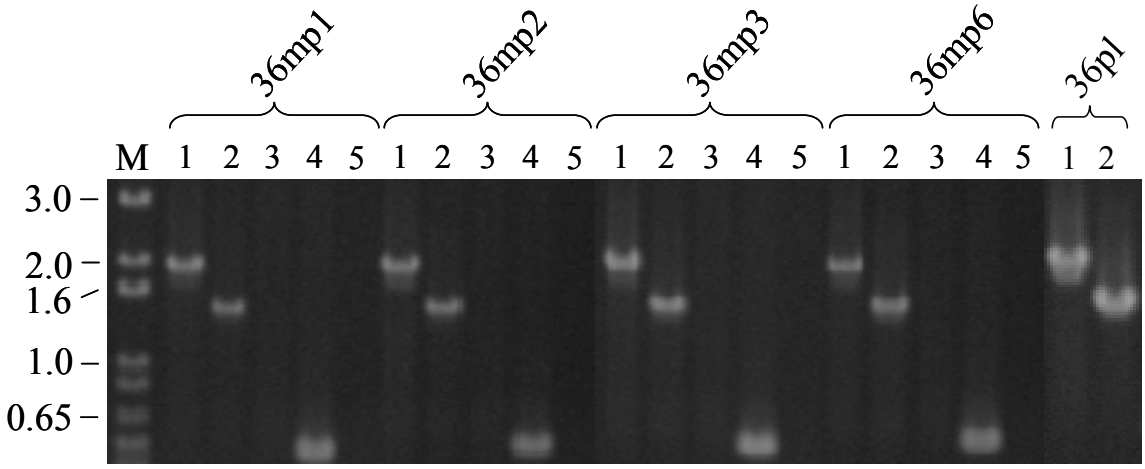

Figure 4.9. Expression of recombinant JS proteins. Cell cultures expressing recombinant forms of JS33 and JS36 were incubated with or without lactacystin (2 μM) for 12 h. Cell lysates were harvested when the cells were ~80% confluent (6 d after the addition of puromycin) and the recombinant proteins were immunoprecipitated with anti-HA monoclonal antibodies conjugated to protein A-Sepharose at a ratio of 1:40 (v/v). Immunoprecipitates (10 μL) were separated on a 7.5% SDS-PAGE gel and immunoblotted. A) The stable line expressing JS33 (33c6) or B) mixed population lines expressing JS36 (36mp1-6), were probed with anti-HA-peroxidase. A clonal line expressing α-(2,6)-sialyltransferase lacking the HA epitope tag (α-[2,6]-ST) was used as a negative control. The positions of molecular weight markers (M) in kDa are shown on the left.

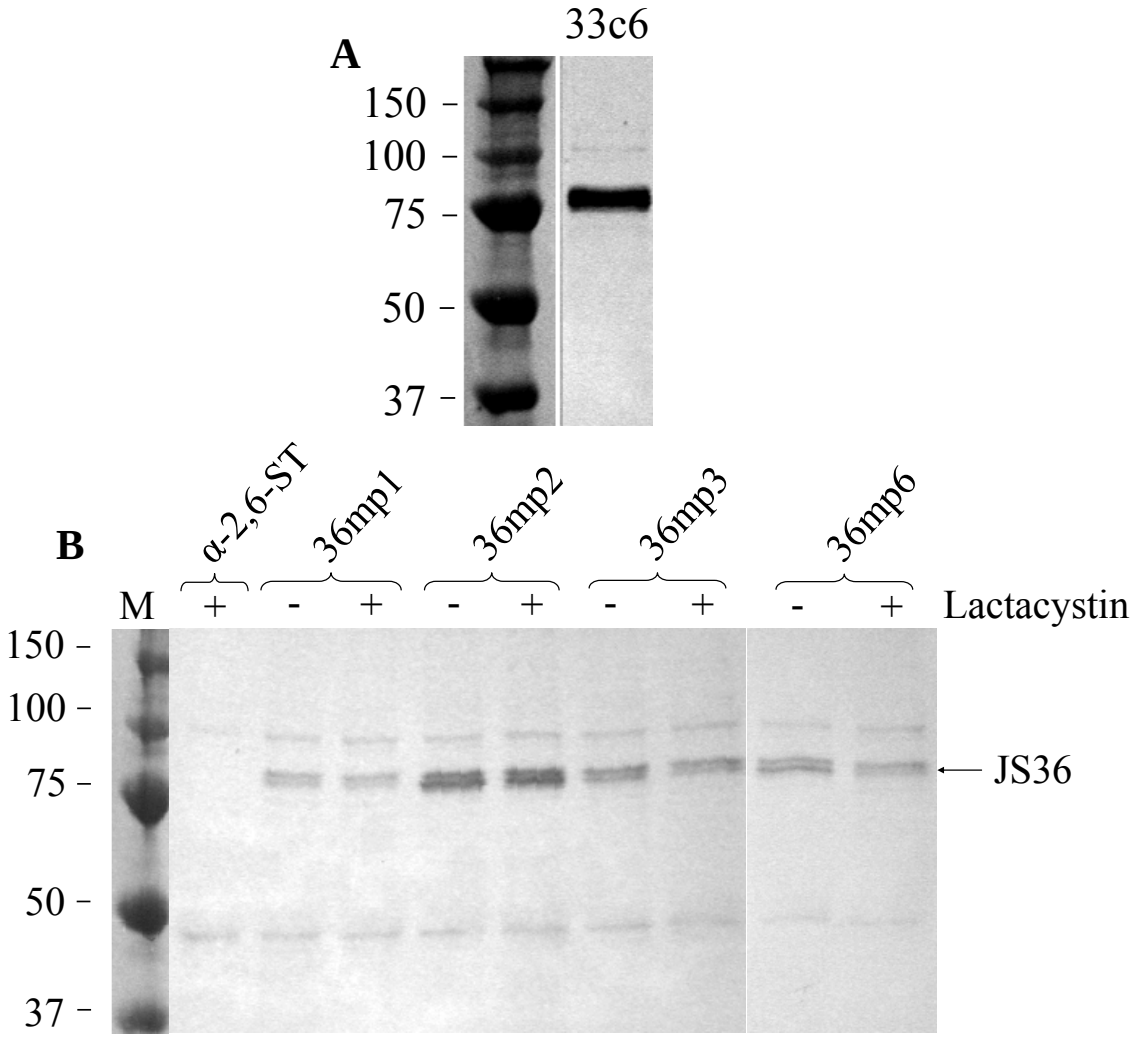

The fusion of the signal sequence from *T. cruzi* mannosidase with JS genes lacking their predicted N-terminal transmembrane domain should have caused the recombinant JS proteins from the stable lines to be secreted into the media. Therefore, the presence of recombinant JS proteins in cell lysates indicated anomalous protein targeting in these stably transformed cell lines. A growth curve conducted on 33c6 and 36mp2 showed that the level of recombinant protein in cell lysates increased with increasing cell density (Figure 4.10). No recombinant protein could be detected in media from either line at any stage of growth (data not shown), indicating that the anomalous protein targeting was not affected by the age of the cells. The anomalous protein targeting in JS36 mixed-population lines also did not seem to be due to proteasome-driven degradation, since cells expressing recombinant JS36 protein grown in the presence of 2 μM lactacystin, a potent proteasome inhibitor from *Streptomyces lactacystinaeus*, had no effect on the amount of JS36 protein made, or on its migration on SDS-PAGE gels (Figure 4.9, B). These results suggested that the stable lines that were generated were incapable of secreting recombinant JS protein.

GalAT activity could not be detected in cell lysates from stably transformed lines

Cell lysates and immunoprecipitated cell lysates were prepared from stable lines expressing recombinant JS33 and JS36 proteins and tested for GalAT activity (Figure 4.11, A and B). Neither cell lysates (Figure 4.11, A) nor their immunoprecipitates (Figure 4.11, B) catalyzed the transfer of D-[^{14}C]Gal*p*A from UDP-D-[^{14}C]Gal*p*A onto a radiolabeled product. The results from these experiments suggested that recombinant JS proteins from cell lysates of stable lines did not express GalAT activity.

Figure 4.10. Growth curve of stable lines expressing recombinant JS33 or JS36. Stable cell lines expressing recombinant A) JS33 (33c6) or B) JS36 (36mp2) were subcultured and allowed to adhere to tissue culture dishes for 24 h. Following the addition of 1 μg/mL puromycin, cells were harvested using 1 mL of cell lysis buffer on the specified days, counted, and cell lysates were immunoprecipitated with 1 μg of anti-HA antibodies conjugated to 40 μL of protein A-Sepharose. Immunoprecipitates (10 μL) were separated on 7.5% SDS-PAGE gels, and immunoblotted. Blots were probed with a 1:1000 dilution of anti-HA-peroxidase. The confluency of the cell lines at day 6 were approximately 70% and 95% for 33c6 and 36mp2 respectively. The positions of molecular weight markers (M) in kDa are shown on the left.

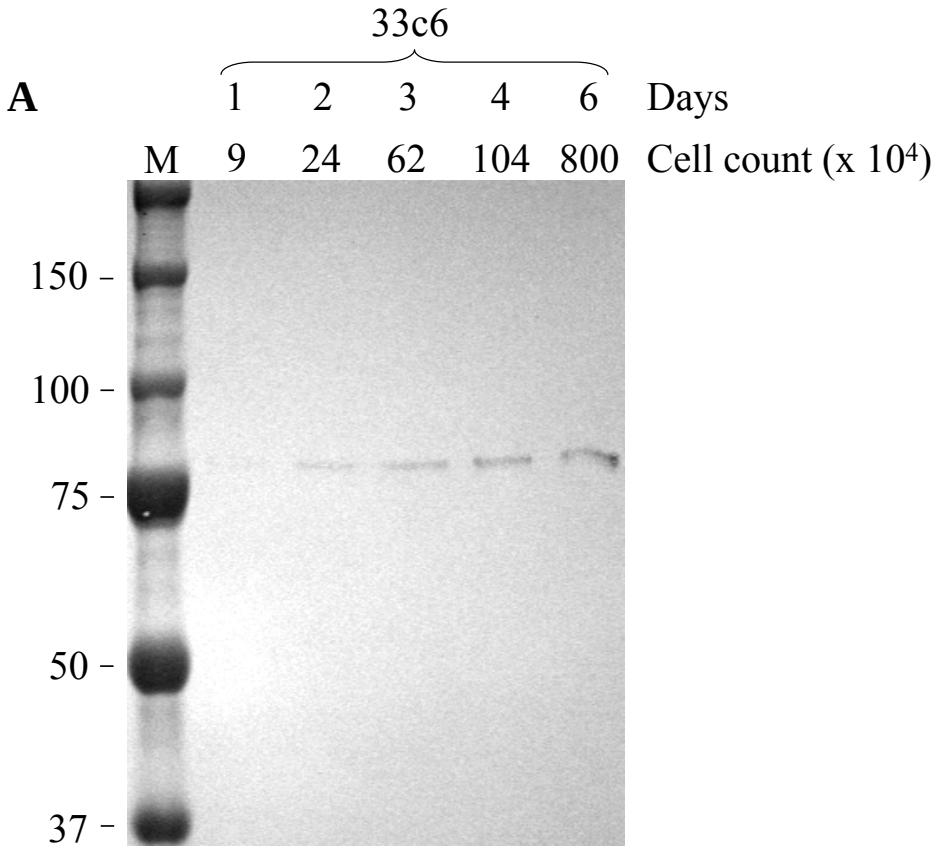

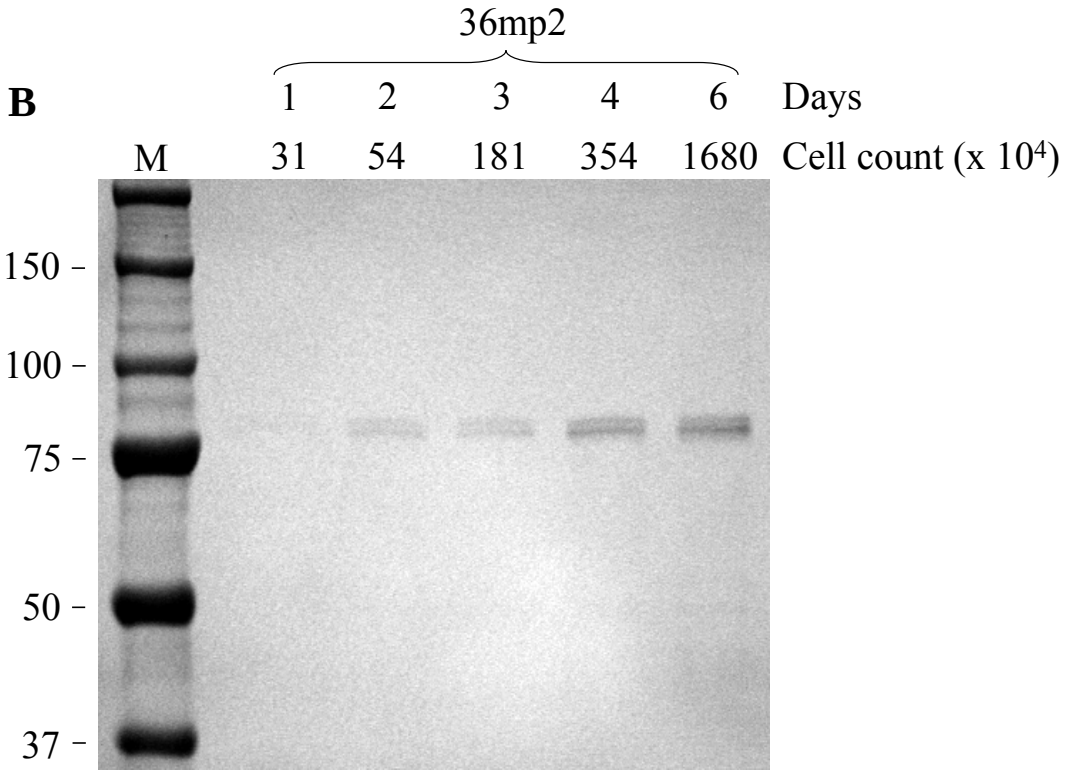
B
36mp2
1 2 3 4 6 Days
M 31 54 181 354 1680 Cell count (x 10^4)
150
100
75
50
37

Figure 4.11. GalAT activity in cell lysates from stable lines expressing recombinant JS33 and JS36 proteins. A) Cell lysates (20 µL) and B) immunoprecipitated cell lysates (40 µL) from JS stable lines were harvested 6 d after the addition of puromycin (~80% confluent) and tested for GalAT activity. Arabidopsis solubilized GalAT (Sol; 50 µg of protein) was used as positive control for the GalAT assay (inset) and the average of all the time zero reactions (bkgr) for each experiment are shown on each graph. Assays were conducted for 30 min A) or 90 min B). The data are the average ± standard error of duplicate samples.

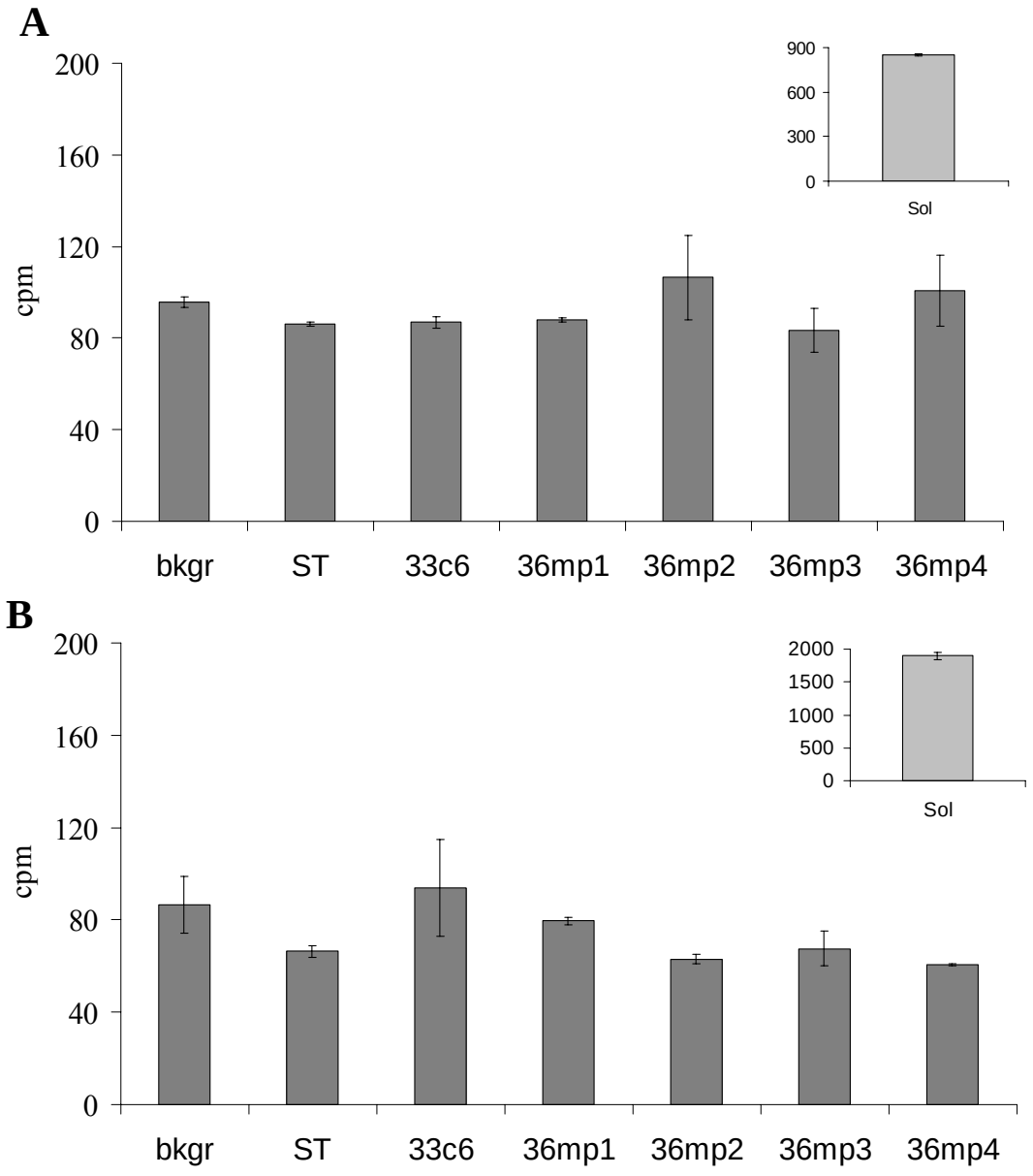

Construction and use of multiple antigenic peptide antibodies for the immunoprecipitation of GalAT activity

As an additional means of proving the function of JS36 and JS33, selected regions of JS36, JS33 and JS36L (At5g47780), an Arabidopsis protein with significant sequence identity to JS36, were chosen for the production of multiple antigenic peptides (MAPs, Table 4.5). Each MAP was used as an antigen for the immunization of two rabbits. Serum from each rabbit was found to contain polyclonal antibodies that could specifically bind to the original MAP antigen (data not shown). An initial experiment was conducted to determine whether any of the polyclonal antibodies that were generated could immunoprecipitate GalAT activity from solubilized Arabidopsis proteins. Polyclonal antibodies directed against JS36, JS33, and JS36L were pooled and conjugated with protein A-Sepharose. The conjugates were then incubated with an aliquot of solubilized proteins from Arabidopsis and the immunoprecipitated material was washed and tested for GalAT activity using pooled preimmune serum as a negative control (Figure 4.12).

The results from this experiment showed that none of the pooled antibodies were able to immunoprecipitate significant amounts of GalAT activity (*a priori* α of 0.05) from solubilized Arabidopsis proteins compared to their preimmune controls (Figure 4.12). The activity using the pooled JS33 antibodies gave the greatest difference compared to the preimmune sera, but the calculated t value (n =2, t_{JS33} = 2.483 [$P > 0.05$]) indicated that the activity was not significantly different with 95% confidence. Our inability to obtain significant levels of immunoprecipitable activity using pooled antibodies could be due to protein A-Sepharose, as its addition to solubilized Arabidopsis proteins inhibited GalAT activity by approximately 40% (Figure 4.12). Recent experiments demonstrated that some of the polyclonal antibodies generated against JS33

Table 4.5. Amino acid sequences of JS36, JS33 and JS36L used for the construction of multiple antigenic peptides (MAPs).

Peptide	Amino acid position	Sequence
JS36		
Pim006	341-365	IDYYLLSPEKRKFPRSENLENPNLY
Pim007	448-472	AMREYYFKADHPTSGSSNLKYRNPK
Pim008	132-154	NLNEKRDSISKDSIHQKVETPTK
JS33		
Pim003	515-540	LGVSETYQKYYKEMSSGDESSEAIL
Pim004	302-326	LTVEHFKSDSLEDPISEKFSDPSLL
Pim005	82-103	DEVLQKINPVLPKKSDINVGSR
JS36L		
Pim009	128-150	LTQQTSEKVDEQPEPNAFGAKKD
Pim010	93-116	ATDDDTHSHTDISIKQVTHDAASD
Pim011	288-306	ALNSSEQQFPNQEKLEDTQ

Figure 4.12. Immunoprecipitation of GalAT activity from solubilized Arabidopsis proteins using pooled polyclonal antibodies against JS proteins or preimmune rabbit serum. Polyclonal antibodies directed against JS33 (33 com), JS36 (36 com), or JS36L (36L com) were pooled and 1 µL of the pooled serum was conjugated to 40 µL of protein A-Sepharose. Conjugates were incubated with 0.5 mL of solubilized proteins from Arabidopsis and the immunoprecipitated material was assayed for GalAT activity for 30 min at 30°C using 2 µM UDP-D-[^{14}C]Gal*p*A and 80 µg of OGAs in a total volume of 70 µl. Pooled preimmune serum from rabbits immunized with JS33 (33 PI), JS36 (36 PI) or JS36L (36L PI) MAPs were used as a negative control. Solubilized Arabidopsis proteins (10 µL) in the presence (Sol + prot A) or absence (Sol) of 40 µL of protein A-Sepharose was used as a positive control for the GalAT assay.

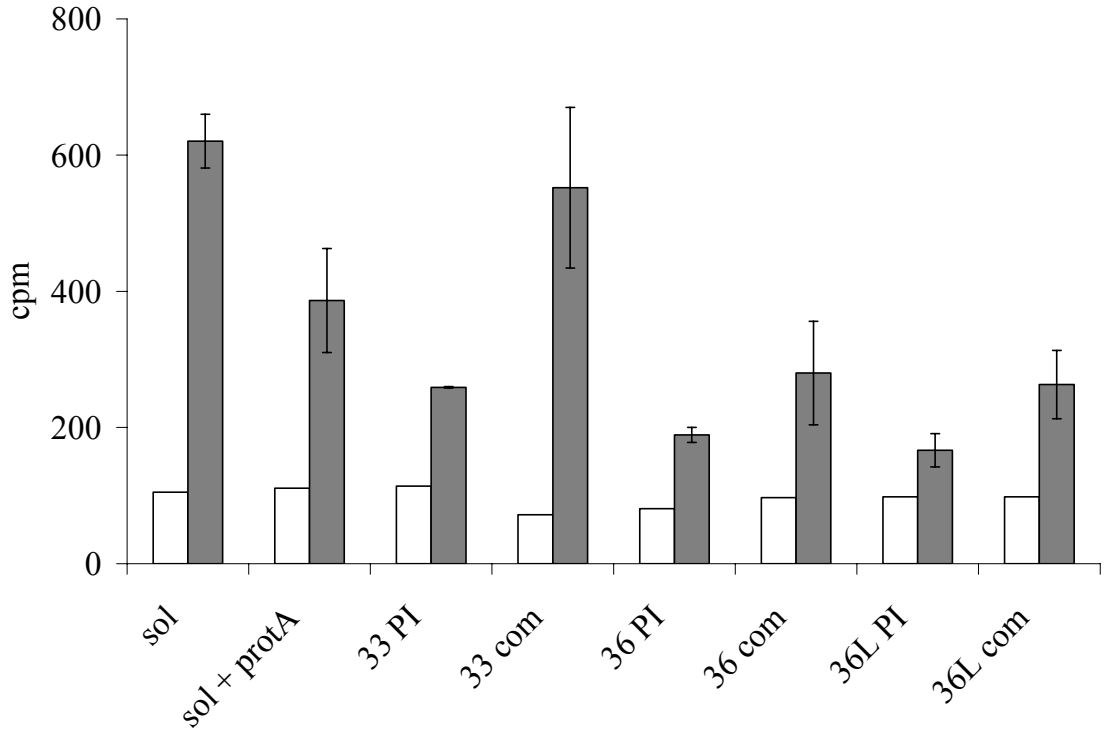

or JS36 recognized the recombinant forms of these proteins made in cell lysates from 33c6 and 36mp2 cell lines (M. Atmodjo and D. Mohnen, unpublished results). New experiments are currently being conducted using these specific antibodies which should enable us to immunoprecipitate proteins from Arabidopsis extracts and determine whether they encode active GalATs.

JS36 and JS33 are part of a putative multi-gene family in Arabidopsis

BLAST analysis of the Arabidopsis genome identified JS33 and an additional 13 GenBank sequences with between 36-68% sequence identity and 56-84% sequence similarity to JS36 (Table 4.6). Further analysis revealed an additional 10 sequences with significant, but reduced, sequence identity to JS36 (23-29% identity and 42-53% similarity). Similar to JS36 and JS33, all of these putative proteins belong to CAZy glycosyltransferase family 8 (Henrissat et al., 2001).

Sequence alignment of all 25 amino acid sequences revealed the presence of highly conserved domains, some of which were found in other glycosyltransferase families (Wiggins and Munro, 1998), and include the putative DXD motif detected in JS33 and JS36 (Figure 4.13). Based on the similarity of these sequences to JS36 and on the results obtained with the activity of recombinant JS36 in transiently transfected HEK cells, we propose that all 25 genes are putative GalATs and are part of a proposed 25-member GALAT (pGALAT) superfamily in Arabidopsis (Table 4.6).

The 25 genes have been subdivided into 15 pGALAT and 10 pGALAT-like (pGALATL) genes according to their sequence identity to JS36 (Table 4.6). Concurrent with this division, many of the encoded proteins are predicted to contain a hypervariable N-terminal extension that contains a putative transmembrane domain (http://www.ch.embnet.org/software/

Table 4.6. The putative GALAT superfamily in Arabidopsis.

GalAT gene[a]	Accession no.[b]	Predicted molecular weight	Amino acid identity/similarity[c]	Signal anchor (SA) versus signal peptide (SP)[d]
JS36/pGALAT1/LGT1	At3g61130	77.3	100/100	SA
pGALAT2	At4g38270	77.8	68/84	SP
JS36L/pGALAT3/LGT3	At5g47780	71.1	66/83	SP
pGALAT4/LGT2	At2g46480	62.1	65/78	none
pGALAT5/QUA1	At3g25140	64.4	58/77	SA
pGALAT6	At3g02350	64.2	57/76	SA
pGALAT7	At1g18580	61.9	51/71	SA
pGALAT8/LGT4	At2g20810	61.8	50/72	SA
pGALAT9/LGT9	At1g06780	67.5	46/64	SA
pGALAT10/LGT5	At2g30575	69.9	45/67	SP
pGALAT11	At3g01040	61.1	43/62	SA
pGALAT12	At5g15470	65.3	43/62	SA
pGALAT13/LGT6	At5g54690	60.9	40/61	SA
pGALAT14	At3g58790	60.6	37/56	SA
JS33/pGALAT15/LGT7	At2g38650	69.7	36/59	SA
pGALATL1/LGT10	At4g02130	39.0	29/52	SP
pGALATL2	At3g06260	40.3	29/51	SP
pGALATL3	At3g62660	41.1	29/51	SP
pGALATL4/PARVUS	At1g19300	39.0	29/49	SP
pGALATL5	At3g28340	41.2	28/53	SP
pGALATL6	At3g50760	32.5	27/52	SP
pGALATL7/LGT8	At1g70090	44.3	27/48	SP
pGALATL8	At1g02720	41.2	25/44	SP
pGALATL9	At1g13250	39.9	23/43	SP
pGALATL10/LGT9	At1g24170	44.0	23/42	SP

[a]The name given to each member of the putative GalAT family includes its designation within the LGT family (Tavares et al., 2000) or the names of any characterized Arabidopsis genes.

[b]From the Arabidopsis Information Resource database or NCBI

[c]Sequence homology is compared to 397 amino acids of pGalAT1/JS36 starting at amino acid position 277.

[d]The presence of either a putative transmembrane domain (SA; signal anchor) or a signal peptide (SP) sequence at the N-terminus of each gene was determined using SignalP version 3.0 (http://www.cbs.dtu.dk/services/SignalP) and confirmed using TMpred (http://www.ch.embnet.org/software/TMPRED_form.html).

Figure 4.13. Amino acid sequence alignment of the putative GALAT superfamily. ClustalX alignment of the amino acid sequences of all 25 proteins in the Arabidopsis pGALAT superfamily. Identical amino acids are designated by an asterisk. Similar amino acids are designated by a colon. The relative position of the hypervariable, N-terminal extension found on all GalAT genes is indicated by the arrow. The position of the putative DXD motif is boxed. Key: light blue = Ala, Leu, Ile, Val, Phe, Trp, Met, or Cys; blue = His or Tyr; green = Ser, Thr, Asn, or Gln; purple = Asp or Glu; light orange= Gly; orange = Lys or Arg; yellow = Pro.

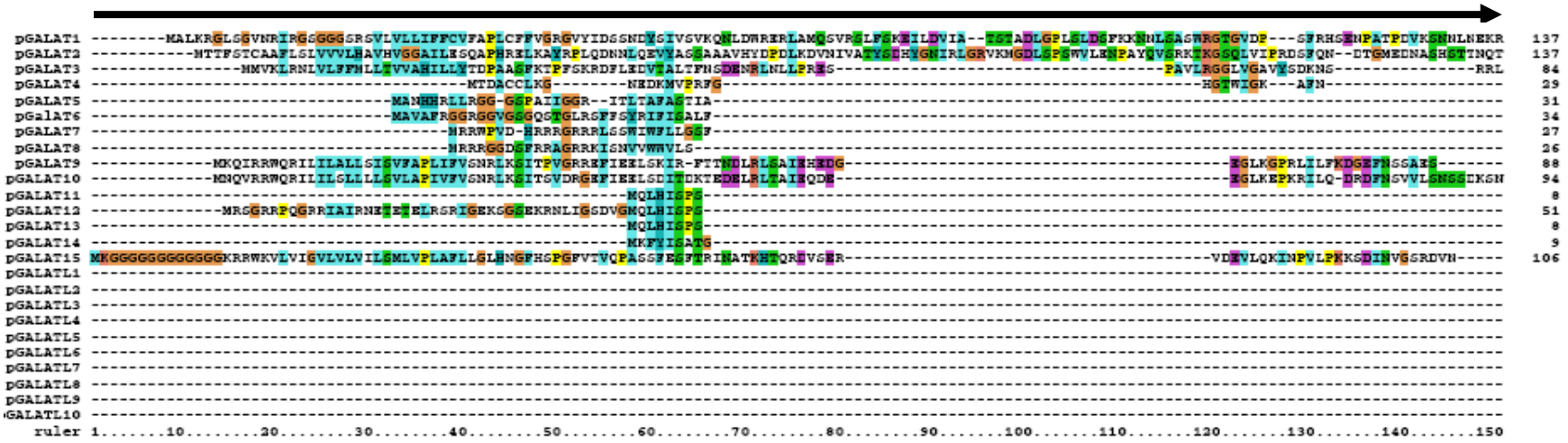

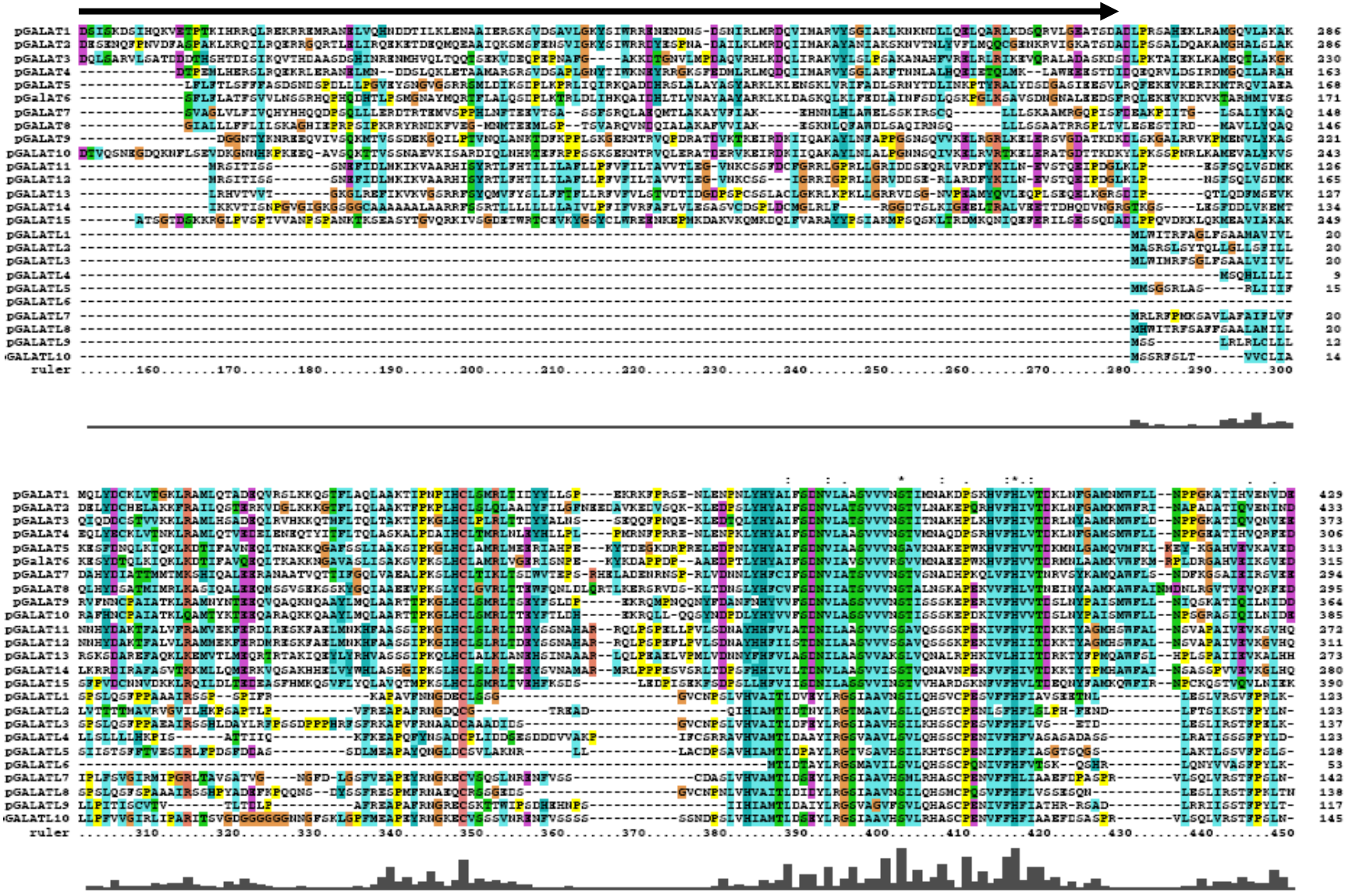
pGALAT1
pGALAT2
pGALAT3
pGALAT4
pGALAT5
pGaLaT6
pGALAT7
pGALAT8
pGALAT9
pGALAT10
pGALAT11
pGALAT12
pGALAT13
pGALAT14
pGALAT15
pGALATL1
pGALATL2
pGALATL3
pGALATL4
pGALATL5
pGALATL6
pGALATL7
pGALATL8
pGALATL9
pGALATL10
ruler

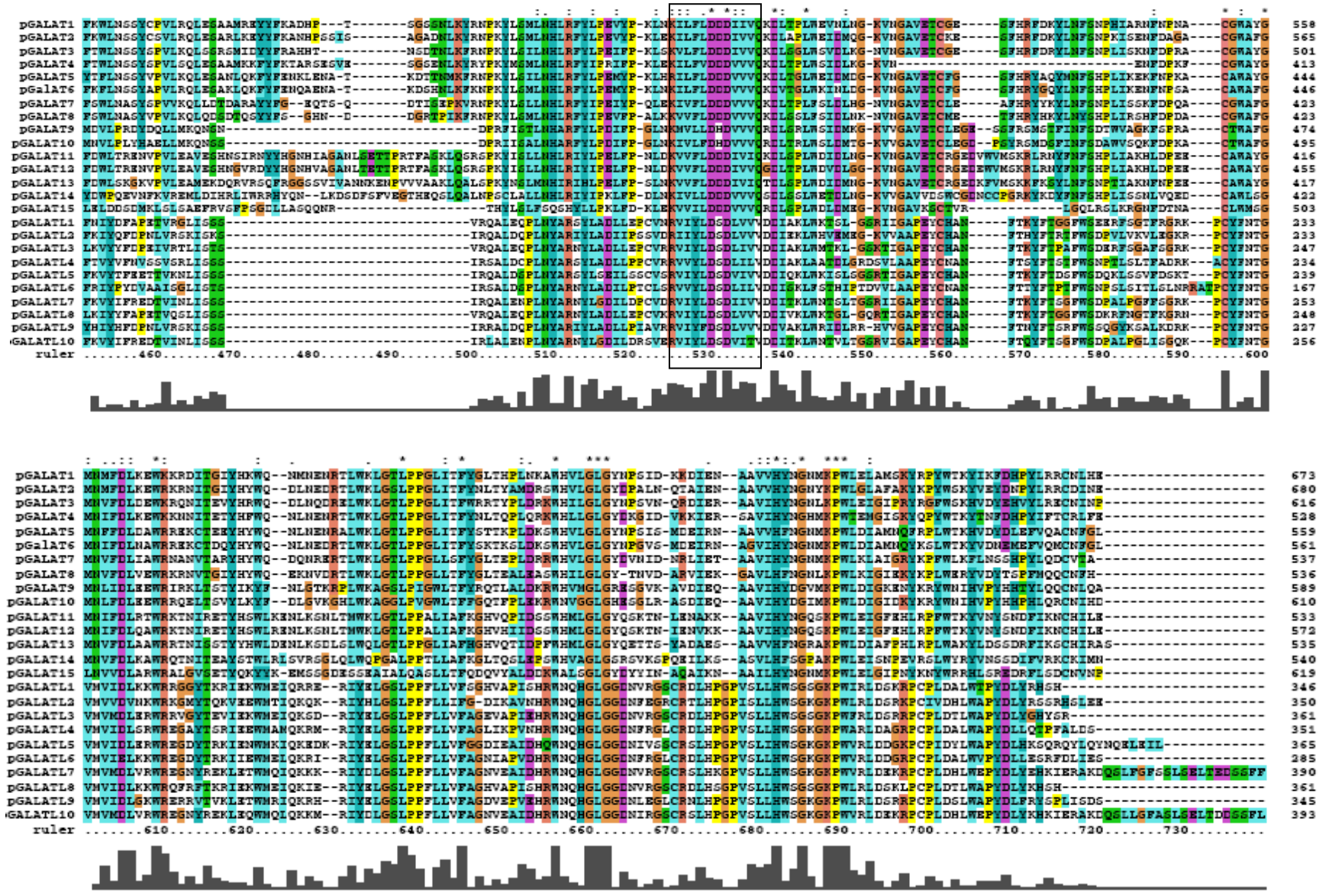
pGALAT1
pGALAT2
pGALAT3
pGALAT4
pGALAT5
pGalAt6
pGALAT7
pGALAT8
pGALAT9
pGALAT10
pGALAT11
pGALAT12
pGALAT13
pGALAT14
pGALAT15
pGALATL1
pGALATL2
pGALATL3
pGALATL4
pGALATL5
pGALATL6
pGALATL7
pGALATL8
pGALATL9
pGALATL10
ruler

TMPRED_form.html; Figure 4.13) and are predicted type II membrane proteins (Paulson and Colley, 1989; Keegstra and Raikhel, 2001). Conversely, pGalAT2, 3, 10 and all pGalATL amino acid sequences lack this N-terminal extension and instead contain a putative signal peptide (http://www.cbs.dtu.dk/services/SignalP; Figure 4.13). The only protein that was not predicted to contain either an N-terminal transmembrane domain or a signal peptide was pGalAT4. At present, the subcellular location and topology of the 25 pGALAT superfamily proteins has not been elucidated and so the exact roles of the putative membrane-bound and soluble pGalAT isoforms remain to be determined.

pGALAT1 (JS36) and 9 other members of the pGALAT superfamily (including pGALAT3, 4, 8-10, 13, 15 and pGALATL1, 7, 10) were initially classified as putative glycosyltransferases (Table 4.6) during the annotation of the Arabidopsis genome (Tavares et al., 2000). This group of genes was called the LGT (like-glycosyl-transferase) family based on their similarity to the LGTC gene from *Neisseria gonorhoeae*, a galactosyltransferase involved in lipopolysaccharide biosynthesis (Gotschlich, 1994). Tavares et al. (2000) were able to identify several conserved domains between members of the LGT family and the amino acid sequence of LGTC, but did not speculate on the function of the LGT gene family in Arabidopsis.

pGALAT5 was previously identified as a T-DNA-insertion mutant of Arabidopsis named *qua1* (Bouton et al., 2002). *Qua1* mutant plants are dwarfed, have reduced cell adhesion and have 25% less D-Gal*p*A in their leaves. Reduced cell adhesion and D-Gal*p*A content are phenotypes that would be expected for the mutation of a gene encoding a GalAT. Although Bouton et al. (2002) were unable to provide enzymatic evidence proving the function of pGALAT5/QUA1, the mutant phenotype provides further validity for our classification of the 25 Arabidopsis sequences into a putative GALAT super-family.

Recently, a mutant of a pGALATL subfamily member was isolated by transposon mutatagenesis. *Parvus* (*pgalatl4*) was isolated as a semi-sterile mutant that exhibited a dwarf phenotype and altered monosaccharide composition when grown under conditions of low humidity (Lao et al., 2003). *pGalatl4/parvus* mutant plants had more α-L-arabinose and less β-D-xylose in their cell walls, and linkage analysis showed an increase in 2-linked rhamnose and 3,4-linked galactose compared to wild-type plants. Furthermore, *galatl4/parvus* plants showed a difference in the developmental regulation of cell wall polysaccharide biosynthesis as older leaves had a significant increase in the amount of 5-linked arabinose while younger leaves were significantly reduced in the amount of 4-linked xylose.

Arabinose, galactose and rhamnose are components of the pectic polysaccharide RG-I. Changes in the relative composition and linkage of these monosaccharides could be caused by the plant's attempt to cope with the mutation, an effect similar to that which occurs in plants with the *mur1* mutation (Zablackis et al., 1996; Reuhs et al., 2004). It is currently unknown whether these changes in the *galatl4/parvus* mutant are caused by an alteration in D-Gal*p*A content as the amount of D-Gal*p*A in *galatl4/parvus* mutant plants was not measured.

Phylogenetic analysis of the putative GALAT superfamily

Phylogenetic analysis of all 25 pGALAT superfamily members and selected amino acid sequences from soybean (*Glycine max*), barrel medic (*Medicago truncatula*), rice (*Oryza sativa*), tobacco (*Nicotiana tobacum*), and chickpea (*Cicer arietinum*), show that they cluster into 5 distinct groups with highly significant bootstrap values (Figure 4.14). Groups A and B contain 4 and 2 members, respectively, of the pGALAT subfamily. Group E contains pGALAT5/QUA1 and one other pGALAT subfamily member. The rest of the pGALAT subfamily, including

Figure 4.14. Phylogenetic analysis of the putative GALAT superfamily and its close homologs. The amino acid sequences of all members of the pGALAT superfamily, along with EST (GenBank accession no.) or tentative consensus (TC) sequences from *Glycine max* (Gm), *Medicago truncatula* (Mt), *Oryza sativa* (Os), *Nicotiana tobacum* (Nt), and *Cicer arietinum* (Ca), lacking their putative N-terminal transmembrane domains, were aligned using ClustalX (version 1.83). Weighted parsimony analysis of this alignment was conducted using PAUP software (version 3.1). Bootstrap (100x) values are given in parentheses.

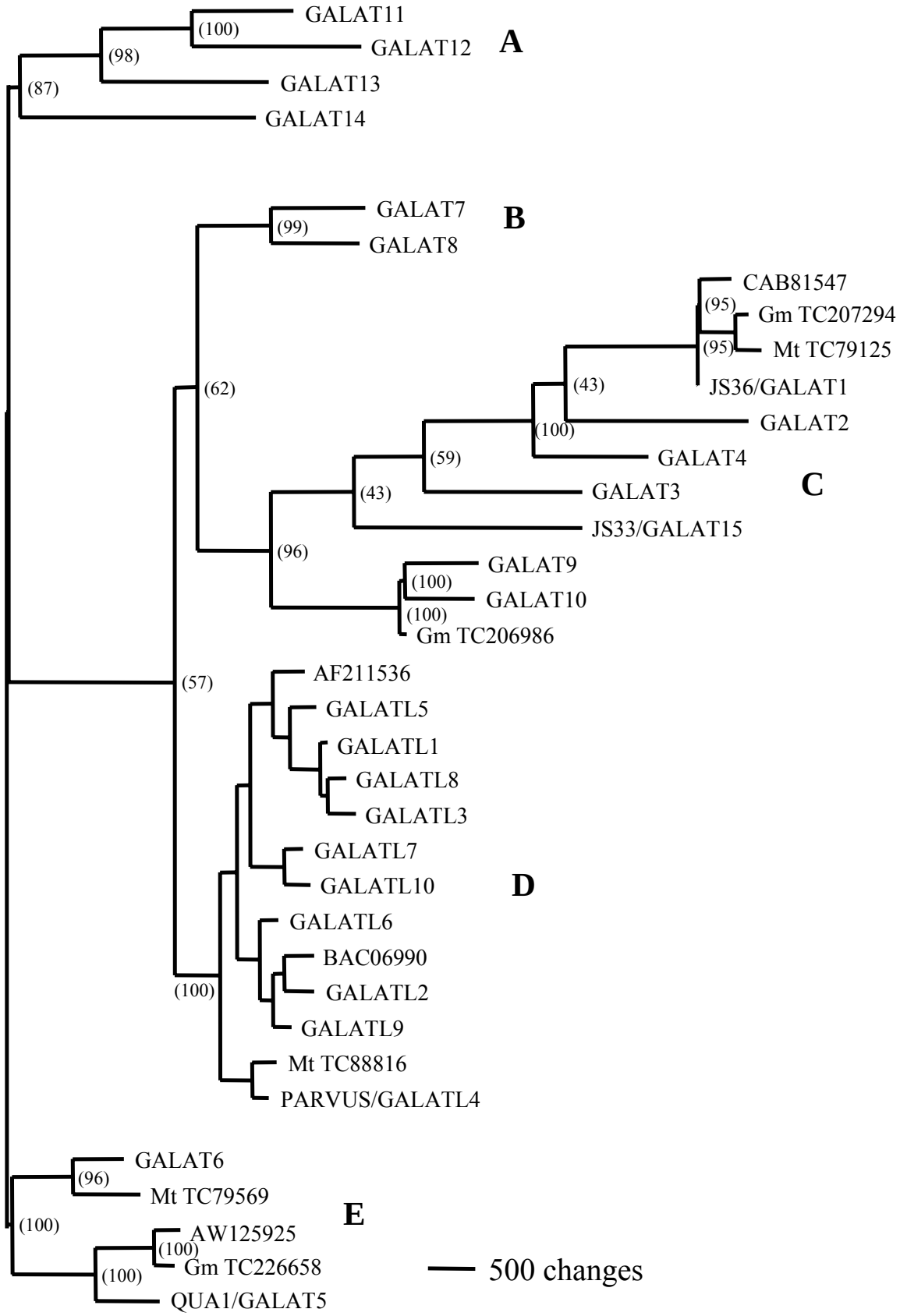
GALAT11
(100)
GALAT12
A
(98)
GALAT13
(87)
GALAT14
GALAT7
B
(99)
GALAT8
CAB81547
(95)
Gm TC207294
(95)
Mt TC79125
JS36/GALAT1
(43)
(62)
GALAT2
(100)
GALAT4
(59)
C
GALAT3
(43)
JS33/GALAT15
(96)
GALAT9
(100)
GALAT10
(100)
Gm TC206986
AF211536
(57)
GALATL5
GALATL1
GALATL8
GALATL3
GALATL7
GALATL10
D
GALATL6
BAC06990
(100)
GALATL2
GALATL9
Mt TC88816
PARVUS/GALATL4
GALAT6
(96)
Mt TC79569
(100)
E
AW125925
(100)
Gm TC226658
(100)
QUA1/GALAT5
500 changes

pGALAT1/JS36 and JS33 (pGALAT15), are clustered into Group C. All members of the pGALATL subfamily, including pGALATL4/PARVUS, are clustered into Group D.

The clustering of specific pGALAT superfamily genes into specific groups suggests that certain members of the pGALAT superfamily may perform distinct functions within Arabidopsis. Based on this assumption, pGALAT1/JS36 and JS33 (pGALAT15) may perform similar functions in Arabidopsis and these functions are may be distinct from those performed by pGALAT5/Qua1. The clustering of the entire pGALATL subfamily into Group D also suggests that it has a distinct role in Arabidopsis. A survey of the Arabidopsis massively parallel signature sequencing (MPSS) database does not provide evidence indicating the differential expression of any specific group of putative GALAT genes in Arabidopsis. Instead, MPSS database analysis suggests that most members of the pGALAT superfamily are expressed in many of the major tissues of Arabidopsis (Table 4.7), with only pGALAT4 and pGALATL8 not detected in any tissue. pGALAT2, pGALAT14, pGALATL5 and pGALATL6 were detected in all tissues except immature inflorescence or flower buds. pGALAT13 and pGALATL4 were not detected in callus tissue, and pGALATL2 was only detected in siliques. Results from Yamada et al. (2003) using whole genome arrays of cold treated seedlings, suspension-cultured cells, flower, and root tissues from Arabidopsis confirmed the expression of most pGALAT superfamily members. Their results also supported the absence of any transcripts corresponding to pGALAT4. In contrast to the MPSS database, Yamada et al. (2003) detected transcripts corresponding to pGALATL8, but were unable to detect the presence of transcripts corresponding to pGALAT10. This disparity between the MPSS database and the results obtained by Yamada and colleagues could be due to differences in the way the two groups prepared their tissue samples. Nevertheless, these results suggest that the majority of the

Table 4.7. Expression analysis of the GALAT superfamily based the Arabidopsis MPSS database (http://mpss.dbi.udel.edu) and Yamada et al. (2003).

GalAT gene	Accession no.	Callus[a]	Inflorescence and early stage floral buds[a]	Leaves[a]	Roots[a]	Siliques[a]	(Yamada et al., 2003)
JS36/GALAT1	At3g61130	+	+	+	+	+	+
GALAT2	At4g38270	+	-	+	+	+	+
GALAT3	At5g47780	+	+	+	+	+	+
GALAT4	At2g46480	-	-	-	-	-	-
GALAT5	At3g25140	+	+	+	+	+	+
GALAT6	At3g02350	+	+	+	+	+	+
GALAT7	At1g18580	+	+	+	+	+	+
GALAT8	At2g20810	+	+	+	+	+	+
GALAT9	At1g06780	+	+	+	+	+	+
GALAT10	At2g30575	+	+	+	+	+	-
GALAT11	At3g01040	+	+	+	+	+	+
GALAT12	At5g15470	+	+	+	+	+	+
GALAT13	At5g54690	-	+	+	+	+	+
GALAT14	At3g58790	+	-	+	+	+	+
JS33/GALAT15	At2g38650	+	+	+	+	+	+
GALATL1	At4g02130	+	+	+	+	+	+
GALATL2	At3g06260	-	-	-	-	+	+
GALATL3	At3g62660	+	+	+	+	+	+
GALATL4	At1g19300	-	+	+	+	+	+
GALATL5	At3g28340	+	-	+	+	+	+
GALATL6	At3g50760	+	-	+	+	+	+
GALATL7	At1g70090	+	+	+	+	+	+
GALATL8	At1g02720	-	-	-	-	-	+

GALATL9	At1g13250	+	+	+	+	+	+
GALATL10	At1g24170	+	+	+	+	+	+

[a]Presence or absence of MPSS signatures for specific pGALAT genes according to the Arabidopsis MPSS database.

[b]Presence or absence of transcripts determined by whole genome array (Yamada et al., 2003).

putative GALAT superfamily is widely expressed in Arabidopsis and therefore little information on the possible roles of the distinct groups in the GALAT superfamily can be gleaned using this database analysis. Mutation analysis and/or the characterization of members of the putative GALAT superfamily will be required before the significance of these groupings can be fully understood.

A BLAST search of the NCBI (http://www.ncbi.nlm.nih.gov/entrez/query.fcgi) and TIGR (http://www.tigr.org) databases indicates the presence of several protein sequences from other plant species with significant identity to pGalAT1/JS36 (Figure 4.14). Phylogenetic analysis of selected sequences demonstrates that the proteins with the most similarity to pGalAT1/JS36 are not from Arabidopsis, but are instead from soybean (TC207294), barrel medic (TC79125), and chickpea (CAB81547). A recent search of the rice genome also revealed a protein (BAD46265) with high sequence identity to pGalAT1/JS36. Other gene sequences (i.e. BAC06990 from rice) cluster into specific groups within the phylogenetic tree. These results strongly suggest that pGALAT1 and other members of the putative GALAT superfamily, are highly conserved across several plant species.

A similar phylogenetic tree was constructed by the group that discovered the *galatl4/parvus* mutant (Lao et al., 2003). Using conserved domains from pGALATL4/Parvus and other CAZy family 8 glycosyltransferases from Arabidopsis, they identified all but two members of the putative GALAT superfamily. Their tree clustered the pGALAT and pGALATL subfamily sequences into two distinct branches. The similarity in the groupings of the pGALAT and pGALATL genes by these two independent analyses strengthens the argument that they represent two distinct subfamilies in Arabidopsis.

DISCUSSION

D-Gal*p*A is the most abundant monosaccharide found in pectic polysaccharides. It has been estimated that between 5-7 distinct GalATs are required for the incorporation of D-Gal*p*A into all of the known pectic structures of the primary cell wall (Mohnen, 2002). While GalAT activity can be detected in tissue extracts from several different plant species (Villemez et al., 1965; Lin et al., 1966; Doong et al., 1995; Sterling et al., 2001; Akita et al., 2002; Ishii, 2002), previous attempts to identify GalAT genes from any plant source have not been successful.

Through the development of new solubilization conditions, we were able to solubilize approximately 80% of the starting activity from Arabidopsis membranes. Instrumental in this process was the elimination of the low-speed centrifugation step in the preparation of solubilized proteins. The direct high-speed centrifugation of tobacco cell homogenates created a multi-layered pellet in which approximately 80% of the total GalAT activity was found in the top-most layer. The formation of this unique GalAT-containing layer was not found to be dependent on the original plant source, as similar pellets could be created using suspension-cultured Arabidopsis cells or radish roots (data not shown). Mixing of the three layers caused a significant reduction in the amount of GalAT activity that could be solubilized, suggesting that the other layers contained a potent inhibitor of GalAT. Our results showed that this layer was enriched in subcellular membranes that contained GalAT activity and therefore could also be an excellent starting material for the study of other pectin glycosyltransferases.

GalAT activity was purified a total of 17-fold through the combined use of SP-Sepharose, RY3 and UDP-agarose chromatography columns. The purification achieved could be an underestimation of the true purity of GalAT activity in the final fraction, as it was determined that several of the enriched GalAT fractions contained a contaminating polygalacturonase

activity that degraded the radioactive product as it was being synthesized (data not shown). Similar polygalacturonase activities have been detected in GalAT-containing membrane fractions from pumpkin (Ishii, 2002) and from solubilized GalAT from petunia pollen tubes (Akita et al., 2002). This degradative activity greatly decreased the amount of D-[^{14}C]Gal*p*A incorporated into product, reducing both the specific and total activity. Attempts to remove this contaminating activity by chromatography were unsuccessful, because the activity bound to all chromatography resins that were negatively charged. The inclusion of low concentrations of OGAs and UDP in the elution buffers used during RY3 and UDP-agarose chromatography was found to aid in the selective removal of GalAT activity from the column, as well as inhibit some of the polygalacturonase activity that had bound to these resins (data not shown).

A critical step in the purification of Arabidopsis GalAT was the use of the affinity resin UDP-agarose. Previous elution schemes using this resin that were based solely on changes in ionic strength were found to be ineffective for the purification of GalAT activity (data not shown). By employing an elution scheme similar to one developed by Barker et al. (1972), we were able to remove a substantial amount of contaminating proteins from the UDP-agarose column and obtained a fraction that was significantly enriched in GalAT activity.

Proteolytic digestion and analysis of the resulting peptides contained within the most purified chromatography fraction from the UDP-agarose column identified two protein sequences, named JS33 and JS36, which contained conserved domains found in other glycosyltransferases. Preliminary analysis of the two protein sequences indicated that they encoded putative type II membrane proteins, were part of a family of retaining glycosyltransferases (CAZy family 8), and were expressed ubiquitously in Arabidopsis. All of these characteristics were properties expected for GalAT genes (Scheller et al., 1999; Sterling et

al., 2001). We successfully cloned and heterologously expressed N-terminally truncated and HA epitope-tagged forms of JS33 and JS36 in mammalian HEK293 cells. The HA epitope tagged proteins also contained the signal sequence from *T. cruzi* mannosidase for secretion of the recombinant proteins into the media surrounding transfected (or transformed) HEK293 cells (Vandersall-Nairn et al., 1998).

Two separate experiments were performed in which media from transiently transfected HEK293 cells was harvested and analyzed for GalAT activity. In the first experiment, immunoprecipitation of media from cells transfected with the JS36 cDNA construct using anti-HA antibodies conjugated to protein A-Sepharose yielded GalAT activity. It was concluded that JS36 encoded a putative GalAT. A second transient transfection experiment did not yield GalAT activity, despite the presence of low levels of recombinant JS36 protein in the media.

There are several reasons why GalAT activity might not have been detected in the later transient expression experiment. One reason may be the low level of recombinant protein expressed in the transiently expressing cells. Our data show that more JS36 cDNA is required to transform HEK293 cells than JS33 or α-(2,6)-ST. Therefore, higher than recommended amounts of DNA (Jordan et al., 1996) may be required to obtain high levels of JS36 expression in HEK cells. It is possible that in the second transient experiment, the transfection efficiency was lower than the previous experiment, resulting in lower levels of recombinant protein and no detectable GalAT activity. The use of higher amounts of cDNA may allow us to detect GalAT activity in cells transfected with the JS36 constructs in future experiments.

Another possible explanation for the difficulty in detecting GalAT activity in the transiently transfected cell lines expressing JS36 is the lack of essential cofactors and/or other proteins that are required for optimal GalAT activity. It is well known that many

glycosyltransferases require additional proteins and/or cofactors for optimal activity and without these proteins exhibit diminished abilities to catalyze their reactions. This phenomenon has been demonstrated for the expression of ganglioside α-(2,8)-sialyltransferase II (STII) and β-(1,4)-*N*-acetylgalactosaminyltransferase I (GalNAcTI) in mouse F-11A neuroblastoma cells (Bieberich et al., 2002). Bieberich et al. (2002) were able to show that transfecting F-11A cells with STII greatly enhanced the endogenous GalNAcTI activity in this cell line and vice versa. Furthermore, they were able to show that STII and GalNAcTI formed protein complexes in the Golgi, suggesting that Golgi glycosyltransferases involved in the production of common glycoconjugates self-associate *in vivo* to form an activated complex that is more active than the individual glycosyltransferases (Bieberich et al., 2002). Pectin biosynthesis is also thought to involve the coordinated action of several glycosyltransferases (Mohnen, 2002) and so it is possible that the co-expression of other pectin biosynthetic enzymes will be required to obtain high levels of GalAT activity in HEK cell lines.

Stably transformed cell lines expressing recombinant JS33 or JS36 proteins also did not possess any GalAT activity. Unlike the transiently transfected lines, media taken from the stable lines expressing JS33 and JS36 did not contain any detectable levels of recombinant protein. Instead, the recombinant proteins were found in cell lysates. The addition of 2 μM lactacystin to stable cell lines expressing JS36 did not change the amount of recombinant protein made in cell lysates or its migration on SDS-PAGE gels. These results suggest that the anomalous JS36 protein targeting is not due to proteasome-directed degradation of the recombinant protein, but is due to some unknown event that occurs during or following protein expression.

The differential location of recombinant proteins in stable versus transient lines could be caused by the retardation of these proteins in the secretory pathway. The retardation of

recombinantly expressed, Golgi-localized glycosyltransferases has been shown to occur during the expression of a secreted form of GlcNAcTI in CHO cells (Opat et al., 2000). The authors speculated that it was caused by the formation of high molecular weight protein complexes within the Golgi apparatus. They also suggested that this property occurred only with glycosyltransferases that were localized to the *medial* Golgi cisternae (Opat et al., 2000).

The specific subcellular localization of JS33 and JS36 protein in the stable HEK cell lines has not been determined. It has been hypothesized that the bulk of the GalAT activity found in plant cells is localized to the *cis* or *medial* Golgi cisternae (Staehelin and Moore, 1995; Vicre et al., 1998). If JS33 and JS36 are GalATs that function in these early cisternae, then it is possible that the recombinant forms of these proteins also create large molecular weight complexes that are retained within the HEK cells.

The intracellular retention and/or production of inactive, recombinant protein could also be caused by the abnormal *N*-glycosylation of recombinant JS33 and JS36. This phenomenon has previously been demonstrated during the recombinant expression of rat α-(2,6)-sialyltransferase in COS-1 cells (Chen and Colley, 2000). α-(2,6)-ST is a Golgi-localized protein that is proteolytically processed in a downstream Golgi compartment into a smaller, secreted isoform in mammalian cells (Chen et al., 2003b). α-(2,6)-ST was shown to be glycosylated at two sites, Asn146 and Asn158. Site-directed mutagenesis showed that while both the glycosylated and non-glycosylated forms of α-(2,6)-ST were correctly targeted to the Golgi, only wildtype and the *Asn146* mutant were proteolytically processed and properly secreted from the COS-1 cells. Furthermore, only these isoforms were active in *in vitro* activity assays. The authors hypothesized that the *Asn158* and *Asn146/Asn158* mutants of α-(2,6)-ST formed protein aggregates upon cell lysis that inactivated the recombinant proteins. They also hypothesized that

the absence of the *N*-linked oligosaccharide at Asn158 caused the recombinant proteins to be restricted to earlier Golgi compartments.

The difference between the calculated and observed molecular weights of recombinant JS33 and JS36 (13 and 6-8 kDa, respectively) suggests that both proteins may be glycosylated in HEK cells. The differential glycosylation of JS36 is also suggested by the appearance of two recombinant isoforms of the protein in stably transformed lines. Both JS33 and JS36 each possess 5 putative *N*-glycosylation sites; however, the nature and pattern of *N*-glycosylation was not explored in this study. Differences in the *N*-glycosylation pattern of recombinant versus native, Arabidopsis isoforms of JS33 and JS36 may be a contributing factor to the localization and activity of the recombinant proteins made by HEK293 cells.

The putative GALAT superfamily constitutes a novel gene family in Arabidopsis. While several members of this family have previously been described (Tavares et al., 2000; Bouton et al., 2002; Lao et al., 2003), this is the first report that combines all 25 coding sequences from Arabidopsis into one superfamily. Alignment of all the sequences within the pGALAT superfamily indicates regions of high sequence conservation between superfamily members. These regions include the Pfam domain PF01501 that is unique to CAZy family 8 glycosyltransferases (http://www.sanger.ac.uk/cgi-bin/Pfam/getacc?PF01501) and a putative DXD motif that is conserved among several glycosyltransferase families (Wiggins and Munro, 1998).

The putative GALAT superfamily can be divided into two subfamilies according to their sequence identity to pGalAT1/JS36. This subdivision is further justified by the clustering of all pGALATL genes into one branch of our phylogenetic tree. All members of the pGalATL subfamily and specific GalAT subfamily proteins (2, 3, and 10) are predicted to contain signal

peptides at their N-terminus, suggesting that they enter the secretory pathway and are either retained within a subcellular compartment or secreted into the cell wall. The former location is the most probable site of action for these genes as pectin biosynthesis occurs in the Golgi apparatus (Zhang and Staehelin, 1992; Sterling et al., 2001) and no glycosyltransferases have been detected in the extracellular matrix (Bacic et al., 1988; Brett and Waldron, 1990).

All other pGalAT subfamily proteins (except pGalAT4 and those mentioned above) have an N-terminal extension containing a putative transmembrane domain and are predicted type II membrane proteins. This topology has been associated with several Golgi-localized plant (Edwards et al., 1999; Keegstra and Raikhel, 2001; Faik et al., 2002; Iwai et al., 2002) and mammalian (Paulson and Colley, 1989; Munro, 1995; Chen et al., 2003b) glycosyltransferases and provides evidence supporting the subcellular location of specific pGalAT proteins in Arabidopsis.

The presence of putative soluble isoforms of pGalAT superfamily proteins in Arabidopsis is unexpected. GalAT activity has not been detected in soluble fractions from any plant source (Villemez et al., 1966; Doong et al., 1995; Takeuchi and Tsumuraya, 2001; Ishii, 2002). This suggests that these soluble proteins are either inactivated during tissue homogenation or isolated as highly associated protein complexes with their membrane-bound counterparts during solubilization.

While the exact roles of the apparent soluble versus membrane-bound proteins are not known, analysis of two putative GALAT superfamily mutants, *pgalat5/qua1* and *pgalatl4/parvus*, shows that they result in somewhat similar phenotypes in Arabidopsis (Bouton et al., 2002; Lao et al., 2003). Both mutant plants are dwarfed and are altered in the relative composition of sugars that are normally associated with pectic polysaccharides. The

pgalat5/qua1 mutant also exhibits a cell adhesion defect that is not seen in the *pgalatl4/parvus* mutant, and the *pgalatl4/parvus* mutant is more sensitive to growth under conditions of low humidity. These results suggest that pGALAT5/QUA1 and pGALATL4/PARVUS may have similar, yet distinct, functions in Arabidopsis and also supports the separation of these genes to different branches of the phylogenetic tree.

Analysis of the expression patterns of all the members of the putative GALAT superfamily indicates that the majority of these genes are expressed in multiple tissues of Arabidopsis. This result suggests that pGALAT genes are important components of all Arabidopsis tissues; however, it provides no insight into the potential functions of pGALAT genes such as pGALAT15/JS33 and pGALAT1/JS36. Of all the genes in the putative GALAT superfamily, pGALAT4 is the only gene that does not contain a putative signal sequence or a transmembrane domain at its N-terminus. Transcript analysis also suggests that this gene is not expressed in any of the Arabidopsis tissues analyzed, indicating that it may be a pseudogene (Tavares et al., 2000).

The generation of stable lines expressing recombinant forms of JS33 and JS36 represents a step forward in the study of the proposed GalATs. Experiments aimed at determining enzyme specificity, discovering associating factors and/or proteins, and developing new methods for expression of JS33 and JS36 can now be carried out. The development of polyclonal antibodies against specific GalAT genes will allow us to determine the subcellular location of these genes in Arabidopsis and will greatly aid in determining the function of these genes. The importance of the putative GALAT superfamily is made evident by the identification of close homologs of specific pGALAT family members in other plant species. Through the use of stable lines expressing pGALAT genes, the analysis of pGALAT mutant plants and the development of tools

such as polyclonal antibodies to specific pGalAT proteins, the specific roles of the putative GALAT superfamily in pectin biosynthesis can be determined.

CONCLUSIONS

This research has significantly increased our understanding of pectin biosynthesis. The localization of α-(1,4)-GalAT activity to the lumen of the Golgi apparatus in pea confirmed previous, more indirect evidence suggesting the Golgi as the main site of pectic biosynthesis. Proteinase K protection experiments indicated that the catalytic site of pea α-(1,4)-GalAT faced the Golgi lumen. Golgi-localized α-(1,4)-GalAT activity also synthesized radiolabeled products that were comparable to those generated by the tobacco enzyme. These results suggest that pea α-(1,4)-GalAT is a Golgi-localized enzyme that synthesizes HGA in the lumen of the Golgi apparatus. This is the first report of the subcellular location of a pectin glycosyltransferase in any plant system.

One of the major problems with identifying pectin glycosyltransferases is the difficulty associated with developing the appropriate assays for catalytic activity. Not only are these assays important for detecting glycosyltransferase activity in plant extracts, but they are also required for testing recombinantly expressed proteins for activity. Earlier methods used to detect α-(1,4)-GalAT activity in microsomal membranes and/or solubilized protein fractions have proven to be too expensive and time consuming to be useful for purification studies. The development of a quick and simple assay for α-(1,4)-GalAT greatly facilitated the development of new universal solubilization methods and aided in the partial purification of Arabidopsis α-(1,4)-GalAT. The further development of this assay will allow its use to detect the activity of other pectin glycosyltransferases.

The identification of the putative GalATs, JS36 and JS33, from partially purified protein fractions from Arabidopsis represents a step forward towards the identification of pectin

biosynthetic glycosyltransferases. While the activity of JS36 and JS33 could not be unequivocally demonstrated, analysis of several Arabidopsis mutants (K. Hosmer and D. Mohnen, unpublished results) indicates that the disruption of several putative GALAT superfamily genes causes alterations in glycosyl residues associated with pectic polysaccharides. These results support the involvement of the putative GALAT superfamily in pectin biosynthesis. The development of tools, such as MAP polyclonal antibodies, should enable the elucidation of the specific roles that putative GALAT superfamily genes play in pectin biosynthesis.

REFERENCES

Abdel-Massih R, Baydoun E, Brett C (2003) In vitro biosynthesis of (1,4)-α-galactan attached to a pectin-xyloglucan complex in pea. Planta **216:** 502-511

Agius F, Gonzalez-Lamothe R, Caballero J, Munoz-Blanco J, Botella M, Valpuesta V (2002) Engineering increased vitamin C levels in plants by overexpression of a D-galacturonic acid reductase. Nat. Biotechnol. **21:** 177-181

Akita K, Ishimizu T, Tsukamoto T, Ando T, Hase S (2002) Successive glycosyltransfer activity and enzymatic characterization of pectic polygalacturonate 4-α-galacturonosyltransferase solubilized from pollen tubes of *Petunia axillaris* using pyridylaminated oligogalacturonates as substrates. Plant Physiol. **130:** 374-379

Albersheim P, Darvill A, O'Neill M, Schols H, Voragen A (1996) An hypothesis: The same six polysaccharides are components of the primary cell walls of all higher plants. *In* J Visser, AGJ Voragen, eds, Pectins and Pectinases. Elsevier Science, Amsterdam, pp 47-55

Allard S, Giraud M, Whitfield C, Graninger M, Messner P, Naismith J (2001) The crystal structure of dTDP-D-glucose 4,6-dehydratase (RmlB) from *Salmonella enterica* serovar *typhimurium*, the second enzyme in the dTDP--rhamnose pathway. J. Mol. Biol. **307:** 283-295

Ames B (1966) Assay of inorganic phosphate, total phosphate and phosphatases. Methods Enzymol. **8:** 115-118

An J, O'Neill M, Albersheim P, Darvill A (1994) Isolation and structural characterization of β-D-glucosyluronic acid and 4-O-methyl-β-D-glucosyluronic acid-containing oligosaccharides from the cell-wall pectic polysaccharide, rhamnogalacturonan I. Carbohydr. Res. **252:** 235-243

An J, Zhang L, O'Neill M, Albersheim P, Darvill A (1994a) Isolation and structural characterization of *endo*-rhamnogalacturonase-generated fragments of the backbone of rhamnogalacturonan I. Carbohydr. Res. **264:** 83-96

Ankel H, Feingold D (1965) Biosynthesis of uridine disphosphate D-xylose I. Uridine diphosphate glucuronate carboxyl-lyase of wheat germ. Biochemistry **4:** 2468-2475

Aoki K, Ishida N, Kawakita M (2003) Substrate recognition by nucleotide sugar transporters: Further characterization of substrate recognition regions by analyses of UDP-galactose/CMP-sialic acid transporter chimerase and biochemical analysis of the substrate specificity of parental and chimeric transporters. J. Biol. Chem. **278:** 22887-22893

Aspinall G (1980) Chemistry of cell wall polysaccharides. *In* J Preiss, ed, The biochemistry of plants, Vol 3. Academic Press, New York, pp 473-500

Aspinall G, Begbie R, Hamilton A, Whyte J (1967) Polysaccharides of soybeans. Part III. Extraction and fractionation of polysaccharides from cotyledon meal. J. Chem. Soc.**:** 1065-1070

Azadi P, O'Neill M, Bergmann C, Darvill A, Albersheim P (1995) The backbone of the pectic polysaccharide rhamnogalacturonan I is cleaved by an *endo*hydrolase and an *endo*lyase. Glycobiology **5:** 783-789

Bacic T, Harris P, Stone B (1988) Structure and function of plant cell walls. *In* J Preiss, ed, The Biochemistry of Plants, Vol 14. Academic Press Inc., New York, pp 297-371

Bakker H, Routier F, Oelmann S, Jordi W, Lommen A, Gerardy-Schahn R, Bosch D (2004) Molecular cloning of two Arabidopsis UDP-galactose transporters by complementation of a deficient chinese hamster ovary cell line. Glycobiology **Epub ahead of print**

Baldwin T, Handford M, Yuseff M, Orellana A, Dupree P (2001) Identification and characterization of GONST1, a Golgi-localized GDP-mannose transporter in *Arabidopsis*. Plant Cell **13:** 2283-2295

Barber G (1962) The enzymatic synthesis of uridine diphosphate L-rhamnose. Biochem. Biophys. Res. Commun. **8:** 204-208

Barber G (1963) The formation of uridine diphosphate L-rhamnose by enzymes of the tobacco leaf. Arch. Biochem. Biophys. **103:** 276-282

Barber G (1979) Observations on the mechanism of the reversible epimerization of GDP-D-mannose to GDP-L-galactose by an enzyme from *Chlorella pyrenoidosa*. J. Biol. Chem. **254:** 7600-7603

Barber G, Chang M (1967) Synthesis of uridine diphosphate L-rhamnose by enzymes of *Chlorella pyrenoidosa*. Arch. Biochem. Biophys. **118:** 659-663

Barker R, Olsen K, Shaper J, Hill R (1972) Agarose derivatives of uridine diphosphate and N-acetylglucosamine for the purification of a galactosyltransferase. J. Biol. Chem. **247:** 7135-7147

Baron D, Streitberger U, Grisebach H (1973) Improved method for purification of UDP-apiose/UDP-xylose synthase from cell cultures of parsley. Biochim. Biophys. Acta. **293:** 526-533

Bar-Peled M, Fluhr R, Gressel J (1993) Juvenile-specific localization and accumulation of a rhamnosyltransferase and its bitter flavonoid in foliage, flowers, and young citrus fruits. Plant Physiol. **103:** 1377-1384

Bar-Peled M, Lewinsohn E, Fluhr R, Gressel J (1991) UDP-rhamnose:flavanone-7-O-glucoside-2"-O-rhamnosyltransferase. Purification and characterization of an enzyme catalyzing the production of bitter compounds in citrus. J. Biol. Chem. **266:** 20953-20959

Basu S, Dotson G, Raetz C (2000) A facile enzymatic synthesis of uridine diphospho-[^{14}C]galacturonic acid. Anal. Biochem. **280:** 173-177

Baydoun E, Abdel-Massih R, Dani D, Rizk S, Brett C (2001) Galactosyl- and fucosyltransferases in etiolated pea epicotyls: Product identification and sub-cellular localisation. J. Plant Physiol. **158:** 145-150

Berninsone P, Hwang H, Zemtseva I, Horvitz H, Hirschberg C (2001) SQV-7, a protein involved in *Caenorhabditis elegans* epithelial invagination and early embryogenesis, transports UDP-glucuronic acid, UDP-N- acetylgalactosamine, and UDP-galactose. Proc. Natl. Acad. Sci. **98:** 3738-3743

Bieberich E, MacKinnon S, Silva J, Li D, Tencomnao T, Irwin L, Kapitonov D, Yu R (2002) Regulation of ganglioside biosynthesis by enzyme complex formation of glycosyltransferases. Biochemistry **41:** 11479-11487

Blevins D, Lukaszewski K (1998) Boron in plant structure and function. Ann. Rev. Plant Physiol. Plant Mol. Biol. **49:** 481-500

Blumenkrantz N, Asboe-Hansen G (1973) New method for quantitative determination of uronic acids. Anal. Biochem. **54:** 484-489

Bolwell G, Dalessandro G, Northcote D (1985) Decrease of polygalacturonic acid synthase during xylem differentiation in sycamore. Phytochemistry **24:** 699-702

Bolwell G, Northcote D (1983) Arabinan synthase and xylan synthase activities in *Phaseolus vulgaris*: Subcellular localization and possible mechanism of action. Biochem. J. **210:** 497-507

Bonin C, Freshour G, Hahn M, Vanzin G, Reiter W (2003) The GMD1 and GMD2 genes of *Arabidopsis* encode isoforms of GDP-D-mannose 4,6-dehydratase with cell type-specific expression patterns. Plant Physiol. **132:** 883-892

Bonin C, Potter I, Vanzin G, Reiter W (1997) The MUR1 gene of *Arabidopsis thaliana* encodes an isoform of GDP-D-mannose-4,6-dehydratase, catalyzing the first step in the de novo synthesis of GDP-L-fucose. Proc. Natl. Acad. Sci. **94:** 2085-2090

Bonin C, Reiter W (2000) A bifunctional epimerase-reductase acts downstream of the MUR1 gene product and completes the *de novo* synthesis of GDP-L-fucose in *Arabidopsis*. Plant J. **21:** 445-454

Bourlard T, Bruyant-Vannier M, Schaumann A, Bruyant P, Morvan C (2001) Purification of several pectin methyltransferases from cell suspension cultures of flax (*Linum usitatissimum* L.). C. R. Acad. Sci. III **324:** 335-343

Bourlard T, Pellerin P, Morvan C (1997) Rhamnogalacturonans I and II are pectic substrates for flax-cell methyltransferases. Plant Physiol. Biochem. **35:** 623-629

Bourlard T, Schaumann-Gaudinet A, Bruyant-Vannier M, Morvan C (1997a) Various pectin methyltransferases activities with affinity for low and highly methylated pectins. Plant Cell Physiol. **38:** 259-267

Bouton S, Leboeuf E, Mouille G, Leydecker M, Talbotec J, Granier F, Lahaye M, Hofte H, Truong H (2002) QUASIMODO1 encodes a putative membrane-bound glycosyltransferase required for normal pectin synthesis and cell adhesion in *Arabidopsis*. Plant Cell **14:** 2577-2590

Bouveng H (1965) Polysaccharides in pollen. Acta. Chim. Scand. **19:** 953-963

Brabetz W, Wolter F, Brade H (2000) A cDNA encoding 3-deoxy-D-*manno*-oct-2-ulosonate-8-phosphate synthase of *Pisum sativum* L. (pea) functionally complements a *kdsA* mutant of the Gram-negative bacterium *Salmonella enterica*. Planta **212:** 136-143

Braccini I, Grasso R, Perez S (1999) Conformational and configurational features of acidic polysaccharides and their interactions with calcium ions: A molecular modeling investigation. Carbohydr. Res. **317:** 119-130

Braccini I, Perez S (2001) Molecular basis of Ca^{2+}-induced gelation in alginates and pectins: The egg-box model revisited. Biomacromolecules **2:** 1089-1096

Brandan E, Hirschberg C (1988) Purification of rat liver N-heparan-sulfate sulfotransferase. J. Biol. Chem. **263:** 2417-2422

Breton C, Imberty A (1999) Structure/function studies of glycosyltransferases. Curr. Opin. Struct. Biol. **9:** 563-571

Brett C, Waldron K (1990) Cell-wall formation. *In* The Physiology and Biochemistry of Plant Cell Walls. Unwin Hyman Ltd., London, pp 58-88

Brickell L, Reid J (1996) Biosynthesis *in vitro* of pectic (1,4)-β-D-galactan. *In* J Visser, AGJ Voragen, eds, Pectins and Pectinases. Elsevier Science, Amsterdam, pp 127-134

Briskin D, Leonard R, Hodges T (1987) Isolation of the plasma membrane: Membrane markers and general principals. Methods Enzymol. **148:** 542-558

Brown J, Fry S (1993) Novel O-D-galacturonoyl esters in the pectic polysaccharides of suspension-cultured plant cells. Plant Physiol. **103:** 993-999

Brummell D, Camirand A, Maclachlan G (1990) Differential distribution of xyloglucan glycosyltransferases in pea Golgi dictyosomes and secretory vesicles. J. Cell Sci. **96:** 705-710

Brummell D, Harpster M (2001) Cell wall metabolism in fruit softening and quality and its manipulation in transgenic plants. Plant Mol. Biol. **47:** 311-339

Bruyant-Vannier M, Gaudinet-Schaumann A, Bourlard T, Morvan C (1996) Solubilization and partial characterization of pectin methyltransferase from flax cells. Plant Physiol. Biochem. **34:** 489-499

Burget E, Reiter W (1999) The *mur4* mutant of *Arabidopsis* is partially defective in the *de novo* synthesis of uridine diphospho L-arabinose. Plant Physiol. **121:** 383-390

Burget E, Verma R, Molhoj M, Reiter W (2003) The biosynthesis of L-arabinose in plants: Molecular cloning and characterization of a Golgi-localized UDP-D-xylose 4-epimerase encoded by the MUR4 gene of *Arabidopsis*. Plant Cell **15:** 523-531

Bush M, Marry M, Huxham M, Jarvis M, McCann M (2001) Developmental regulation of pectic epitopes during potato tuberisation. Planta **213:** 869-880

Cardoso S, Silva A, Coimbra M (2002) Structural characterisation of the olive pomace pectic polysaccharide arabinan side chains. Carbohydr.Res. **337:** 917-924

Carpita N, Gibeaut D (1993) Structural models of primary cell walls in flowering plants: consistency of molecular structure with the physical properties of the walls during growth. Plant J. **3:** 1-30

Carpita N, Tierney M, Campbell M (2001) Molecular biology of the plant cell wall: searching for the genes that define structure, architecture and dynamics. Plant Mol. Biol. **47:** 1-5

Chen C, Colley K (2000) Minimal structural and glycosylation requirements for ST6Gal I activity and trafficking. Glycobiology **10:** 531-583

Chen T, Chen C, Bergeron N, Close B, Bohrer T, Vertel B, Colley K (2003b) The two rat α-(2,6)-sialyltransferase (ST6Gal I) isoforms: Evaluation of catalytic activity and intra-Golgi localization. Glycobiology **13:** 109-117

Chen W, Unligil U, Rini J, Stanley P (2001) Independent Lec1A CHO glycosylation mutants arise from point mutations in N-acetylglucosaminyltransferase I that reduce affinity for both substrates. Molecular consequences based on the crystal structure of GlcNAc-TI. Biochemistry **40:** 8765-8772

Cheng L, Kindel P (1997) Detection and homogeneity of cell wall pectic polysaccharides of *Lemna minor*. Carbohydr. Res. **301:** 205-212

Chou P, Fasman G (1978) Prediction of the secondary structure of proteins from their amino acid sequence. Adv. Enzymol. Relat. Areas Mol. Biol. **47:** 45-148

Clausen M, Willats W, Knox J (2003) Synthetic methyl hexagalacturonate hapten inhibitors of anti-homogalacturonan monoclonal antibodies LM7, JIM5 and JIM7. Carbohydr. Res. **338:** 1797-1800

Darvill A, Augur C, Bergmann C, Carlson R, Cheong J, Eberhard S, Hahn M, Lo V, Marfa V, Meyer B, Mohnen D, O'Neill M, Spiro M, Halbeek H, York W, Albersheim P (1992) Oligosaccharins: Oligosaccharides that regulate growth, development and defence responses in plants. Glycobiology **2:** 181-198

Darvill A, McNeil M, Albersheim P (1978) Structure of plant cell walls VIII. A new pectic polysaccharide. Plant Physiol. **62:** 418-422

Davies M, Dickinson D (1972) Properties of uridine diphosphoglucose dehydrogenase from pollen of *Lilium longiflorum*. Arch. Biochem. Biophys. **152:** 53-61

Dean N, Zhang Y, Poster J (1997) The VRG4 gene is required for GDP-mannose transport into the lumen of the Golgi in the yeast, *Saccharomyces cerevisiae*. J. Biol. Chem. **272:** 31908-31914

Delmas F, Petit J, Joubes J, Seveno M, Paccalet T, Hernould M, Lerouge P, Mouras A, Chevalier C (2003) The gene expression and enzyme activity of plant 3-deoxy-D-*manno*-2-octulosonic acid-8-phosphate synthase are preferentially associated with cell division in a cell cycle-dependent manner. Plant Physiol. **133:** 348-360

Delmer D (1999) Cellulose biosynthesis: Exciting times for a difficult field of study. Ann. Rev. Plant Physiol. Plant Mol. Biol. **50:** 245-276

Delmer D, Albersheim P (1970) The biosynthesis of sucrose and nucleoside diphosphate glucose in *Phaseolus aureus*. Plant Physiol. **45:** 782-786

Deutscher S, Hirschberg C (1986) Mechanism of galactosylation in the Golgi apparatus. A Chinese hamster ovary cell mutant deficient in translocation of UDP-galactose across Golgi vesicle membranes. J. Biol. Chem. **261:** 96-100

Dhugga K, Ray P (1994) Purification of (1,3)-β-D-glucan synthase activity from pea tissue. Two polypeptides of 55 kDa and 70 kDa copurify with enzyme activity. Eur. J. Biochem. **220:** 943-953

Dolan L, Linstead P, Roberts K (1997) Developmental regulation of pectic polysaccharides in the root meristem of Arabidopsis. J. Exp. Bot. **48:** 713-720

Dong C, Beis K, Giraud M, Blankenfeldt W, Allard S, Major L, Kerr I, Whitfield C, Naismith J (2003) A structural perspective on the enzymes that convert dTDP-D-glucose into dTDP-L-rhamnose. Biochem. Soc. Trans. **31:** 532-536

Doong R, Ahmad S, Jensen R (1991) Higher plants express 3-deoxy-D-*manno*-octulosonate 8-phosphate synthase. Plant Cell Environ. **14:** 113-120

Doong R, Gander J, Ganson R, Jensen R (1992) The cytosolic isoenzyme of 3-deoxy-D-*arabino*-heptulosonate synthase in *Spinacia oleracea* and other higher plants: Extreme substrate ambiguity and other properties. Physiol. Plant. **84:** 351-360

Doong R, Liljebjelke K, Fralish G, Kumar A, Mohnen D (1995) Cell-free synthesis of pectin: Identification and partial characterization of polygalacturonate 4-α-galacturonosyltransferase and its products from membrane preparations of tobacco cell-suspension cultures. Plant Physiol. **109:** 141-152

Doong R, Mohnen D (1998) Solubilization and characterization of a galacturonosyltransferase that synthesizes the pectic polysaccharide homogalacturonan. Plant J. **13:** 363-374

Dormann P, Benning C (1996) Functional expression of uridine 5'-diphospho-glucose 4-epimerase (EC 5.1.3.2) from *Arabidopsis thaliana* in *Saccharomyces cerevisiae* and *Escherichia coli*. Arch. Biochem. Biophys. **327:** 27-34

Dormann P, Benning C (1998) The role of UDP-glucose epimerase in carbohydrate metabolism of *Arabidopsis*. Plant J. **13:** 641-652

Eberhard S, Doubrava N, Marfa V, Mohnen D, Southwick A, Darvill A, Albersheim P (1989) Pectic cell wall fragments regulate tobacco thin-cell-layer explant morphogenesis. Plant Cell **1:** 747-755

Eda S, Miyabe K, Akiyama K, Ohnishi A, Kato K (1986) A pectic polysaccharide from cell walls of tobacco (*Nicotiana tabacum*) mesophyll. Carbohydr. Res. **158:** 205-216

Edwards M, Dickson C, Chengappa S, Sidebottom C, Gidley M, Reid J (1999) Molecular characterisation of a membrane-bound galactosyltransferase of plant cell wall matrix polysaccharide biosynthesis. Plant J. **19:** 691-697

Faik A, Price N, Raikhel N, Keegstra K (2002) An *Arabidopsis* gene encoding an α-xylosyltransferase involved in xyloglucan biosynthesis. Proc. Natl. Acad. Sci. **99:** 7797-7802

Fan D, Feingold D (1969) Nucleoside diphosphate-sugar 4-epimerases I. Uridine diphosphate glucose 4-epimerase of wheat germ. Plant Physiol. **44:** 599-604

Fan D, Feingold D (1970) Nucleoside diphosphate-sugar 4-epimerases II. Uridine diphosphate arabinose 4-epimerase of wheat germ. Plant Physiol. **46:** 592-595

Feingold D, Avigad G (1980) Sugar nucleotide transformations in plants. *In* J Preiss, ed, The Biochemistry of Plants, Vol 3. Academic Press, New York, pp 101-170

Feingold D, Barber G (1990) Nucleotide sugars. *In* PM Dey, ed, Methods in Plant Biochemistry, Vol 2. Academic Press Ltd., London, pp 40-78

Feingold D, Neufeld E, Hassid W (1958) Enzymatic synthesis of uridine diphosphate glucuronic acid and uridine diphosphate galacturonic acid with extracts from *Phaseolus aureus* seedlings. Arch. Biochem. Biophys. **78:** 401-406

Feingold D, Neufeld E, Hassid W (1960) The 4-epimerization and decarboxylation of uridine diphosphate D-glucuronic acid by extracts from *Phaseolus aureus* seedlings. J. Biol. Chem. **235:** 910-913

Fleischer A, O'Neill M, Ehwald R (1999) The pore size of non-graminaceous plant cell walls is rapidly decreased by borate ester cross-linking of the pectic polysaccharide rhamnogalacturonan II. Plant Physiol. **121:** 829-838

Franks P, Buckley T, Shope J, Mott K (2001) Guard cell volume and pressure measured concurrently by confocal microscopy and the cell pressure probe. Plant Physiol. **125:** 1577-1584

Frederikson K, Larsson C (1989) Activation of (1,3)-β-glucan synthase by Ca^{2+}, spermine, and cellobiose: Localization of activator sites using inside out plasma membrane vesicles. Physiol. Plantarum **77:** 196-201

Fry S (1982) Phenolic components of the primary cell wall. Biochem. J. **203:** 493-504

Fukuda H (1996) Xylogenesis: Initiation, progession, and cell death. Ann. Rev. Plant Physiol. Plant Mol. Biol. **47:** 299-325

Gaunt M, Maitra U, Ankel H (1974) Uridine diphosphate galacturonate 4-epimerase from the blue-green alga *Anabaena flos-aquae*. J. Biol. Chem. **249:** 2366-2372

Gebb C, Baron D, Grisebach H (1975) Spectroscopic evidence for the formation of a 4-keto intermediate in the UDP-apiose/UDP-xylose synthase reaction. Eur. J. Biochem. **54:** 493-498

Geshi N, Jorgensen B, Scheller H, Ulvskov P (2000) *In vitro* biosynthesis of (1,4)-β-galactan attached to rhamnogalacturonan I. Planta **210:** 622-629

Geshi N, Jorgensen B, Ulvskov P (2004) Subcellular localization and topology of β-(1,4)-galactosyltransferase that elongates β-(1,4)-galactan side chains in rhamnogalacturonan I in potato. Planta **218:** 862-868

Geshi N, Pauly M, Ulvskov P (2002) Solubilization of galactosyltransferase that synthesizes (1,4)-β-galactan side chains in pectic rhamnogalacturonan I. Physiol. Plant. **114:** 540-548

Gillaspy G, Keddie J, Oda K, Gruissem W (1995) Plant inositol monophosphatase is a lithium-sensitive enzyme encoded by a multigene family. Plant Cell **7:** 2175-2185

Gleeson P (1998) Targeting of proteins to the Golgi apparatus. Histochem. Cell Biol. **109:** 517-532

Glushka J, Terrell M, York W, O'Neill M, Gucwa A, Darvill A, Albersheim P, Prestegard J (2003) Primary structure of the 2-O-methyl-α-L-fucose-containing side chain of the pectic polysaccharide, rhamnogalacturonan II. Carbohydr. Res. **338:** 341-352

Golovchenko VV, Ovodova RG, Shashkov AS, Ovodov YS (2002) Structural studies of the pectic polysaccharide from duckweed *Lemna minor* L. Phytochemistry **60:** 89-97

Gotschlich E (1994) Genetic locus for the biosynthesis of the variable portion of *Neisseria gonorrhoeae* lipooligosaccharide. J. Exp. Med. **180:** 2181-2190

Goubet F, Council L, Mohnen D (1998) Identification and partial characterization of the pectin methyltransferase "homogalacturonan-methyltransferase" from membranes of tobacco cell suspensions. Plant Physiol. **116:** 337-347

Goubet F, Mohnen D (1999) Solubilization and partial characterization of homogalacturonan-methyltransferase from microsomal membranes of suspension-cultured tobacco cells. Plant Physiol. **121:** 281-290

Goubet F, Mohnen D (1999a) Subcellular localization and topology of homogalacturonan methyltransferase in suspension-cultured *Nicotiana tabacum* cells. Planta **209:** 112-117

Goubet F, Morriswood B, Dupree P (2003) Analysis of methylated and unmethylated polygalacturonic acid structure by polysaccharide analysis using carbohydrate gel electrophoresis. Anal. Biochem. **321:** 174-182

Goubet F, Morvan C (1993) Evidence for several galactan synthases in flax (*Linum usitassimum* L.) suspension-cultured cells. Plant Cell Physiol. **34:** 1297-1303

Goubet F, Morvan C (1994) Synthesis of cell wall galactans from flax (*Linum usitatissimum* L.) suspension-cultured cells. Plant Cell Physiol. **35:** 719-727

Graninger M, Nidetzky B, Heinrichs D, Whitfield C, Messner P (1999) Characterization of dTDP-4-dehydrorhamnose 3,5-epimerase and dTDP-4-dehydrorhamnose reductase, required for dTDP-L-rhamnose biosynthesis in *Salmonella enterica* serovar Typhimurium LT2. J. Biol. Chem. **274:** 25069-25077

Guillaumie F, Sterling J, Jensen K, Thomas O, Mohnen D (2003) Solid-supported enzymatic synthesis of pectic oligogalacturonides and their analysis by MALDI-TOF mass spectrometry. Carbohydr. Res. **338:** 1951-1960

Hadfield K, Bennett A (1998) Polygalacturonases: Many genes in search of a function. Plant Physiol. **117:** 337-343

Handford M, Sicilia F, Brandizzi F, Chung J, Dupree P (2004) *Arabidopsis thaliana* expresses multiple Golgi-localized nucleotide-sugar transporters related to GONST1. Mol. Genet. Genomics **272:** 397-410

Hantus S, Pauly M, Darvill A, Albersheim P, York W (1997) Structural characterization of novel -galactose-containing oligosaccharide subunits of jojoba seed xyloglucans. Carbohydr. Res. **304:** 11-20

Harper A, Bar-Peled M (2002) Biosynthesis of UDP-xylose. Cloning and characterization of a novel *Arabidopsis* gene family, UXS, encoding soluble and putative membrane-bound UDP-glucuronic acid decarboxylase isoforms. Plant Physiol. **130:** 2188-2198

Harris P, Northcote D (1971) Polysaccharide formation in plant Golgi bodies. Biochim. Biophys. Acta. **237:** 56-64

Hassid W (1967) Transformation of sugars in plants. Ann. Rev. Plant Physiol. **18:** 253-280

Hassid W, Neufeld E, Feingold D (1959) Sugar nucleotides in the interconversion of carbohydrates in higher plants. Proc. Natl. Acad. Sci. **45:** 905-915

Hayashi T, Koyama T, Matsuda K (1988) Formation of UDP-xylose and xyloglucan in soybean Golgi membranes. Plant Physiol. **87:** 341-345

Hebda P, Behrman E, Barber G (1979) The guanosine 5'-diphosphate D-mannose:guanosine 5'-diphosphate L-galactose epimerase of *Chlorella pyrenoidosa*. Arch. Biochem. Biophys. **194:** 496-502

Henrissat B, Coutinho P, Davies G (2001) A census of carbohydrate-active enzymes in the genome of *Arabidopsis thaliana*. Plant Mol. Biol. **47:** 55-72

Heukeshoven J, Dernick R (1985) Simplified method for silver staining of proteins in polyacrylamide gels and the mechanism of silver staining. Electrophoresis **6:** 103-112

Hirschberg C, Robbins P, Abeijon C (1998) Transporters of nucleotide sugars, ATP, and nucleotide sulfate in the endoplasmic reticulum and Golgi apparatus. Annu. Rev. Biochem. **67:** 49-69

Hoeflich J, Berninsone P, Goebel C, Gravato-Nobre M, Libby B, Darby C, Politz S, Hodgkin J, Hirschberg C, Baumeister R (2004) Loss of srf-3 encoded nucleotide sugar transporter activity in *Caenorhabditis elegans* alters surface antigenicity and prevents bacterial adherence. J. Biol. Chem.**:** M402429200

Hong K, Ma D, Beverley S, Turco S (2000) The *Leishmania* GDP-mannose transporter is an autonomous, multi-specific, hexameric complex of LPG2 subunits. Biochemistry **39:** 2013-2022

Huisman M, Brull L, Thomas-Oates J, Haverkamp J, Schols H, Voragen A (2001) The occurrence of internal (1,5)-linked arabinofuranose and arabinopyranose residues in arabinogalactan side chains from soybean pectic substances. Carbohydr. Res. **330:** 103-114

Ishii T (1994) Feruloyl oligosaccharides from cell walls of suspension cultured spinach (*Spinacia oleracea*) cells and sugar beet (*Beta vulgaris*) pulp. Plant Cell Physiol. **35:** 701-704

Ishii T (1997) O-Acetylated oligosaccharides from pectins of potato tuber cell walls. Plant Physiol. **113:** 1265-1272

Ishii T (1997a) Structure and functions of feruloylated polysaccharides. Plant Sci. **127:** 111-127

Ishii T (2002) A sensitive and rapid bioassay of homogalacturonan synthase using 2-aminobenzamide-labeled oligogalacturonides. Plant Cell Physiol. **43:** 1386-1389

Ishii T, Matsunaga T (1996) Isolation and characterization of a boron-rhamnogalacturonan-II complex from cell walls of sugar beet pulp. Carbohydr. Res. **284:** 1-9

Ishii T, Matsunaga T (2001) Pectic polysaccharide rhamnogalacturonan II is covalently linked to homogalacturonan. Phytochemistry **57:** 969-974

Ishii T, Matsunaga T, Hayashi N (2001a) Formation of rhamnogalacturonan II-borate dimer in pectin determines cell wall thickness of pumpkin tissue. Plant Physiol. **126:** 1698-1705

Ishii T, Matsunaga T, Pellerin P, O'Neill M, Darvill A, Albersheim P (1999) The plant cell wall polysaccharide rhamnogalacturonan II self-assembles into a covalently cross-linked dimer. J. Biol. Chem. **274:** 13098-13104

Ishii T, Ohnishi-Kameyama M, Ono H (2004) Identification of elongating β-(1,4)-galactosyltransferase activity in mung bean (*Vigna radiata*) hypocotyls using 2-aminobenzaminated (1,4)-linked β-D-galactooligosaccharides as acceptor substrates. Planta **219:** 310-318

Ishikawa M, Kuroyama H, Takeuchi Y, Tsumuraya Y (2000) Characterization of pectin methyltransferase from soybean hypocotyls. Planta **210:** 782-791

Iwai H, Ishii T, Satoh S (2001) Absence of arabinan in the side chains of the pectic polysaccharides strongly associated with cell walls of *Nicotiana plumbaginifolia* non-organogenic callus with loosely attached constituent cells. Planta **213:** 907-915

Iwai H, Masaoka N, Ishii T, Satoh S (2002) A pectin glucuronyltransferase gene is essential for intercellular attachment in the plant meristem. Proc. Natl. Acad. Sci. **99:** 16319-16324

Jackson C, Dreaden T, Beal T, Eid M, Gao M, Kumar M, Mohnen D (2004) Pectin induces apoptosis in human prostrate cancer cells. in preparation

Jarvis M (1984) Structure and properties of pectin gels in plant cell walls. Plant Cell Environ. **7:** 153-164

Jarvis M, Briggs S, Knox J (2003) Intercellular adhesion and cell separation in plants. Plant Cell Environ. **26:** 977-989

Jeanmougin F, Thompson J, Gouy M, Higgins D, Gibson T (1998) Multiple sequence alignment with Clustal X. Trends Biochem. Sci. **23:** 403-405

Joersbo M, Pedersen S, Nielsen J, Marcussen J, Brunstedt J (1999) Isolation and expression of two cDNA clones encoding UDP-galactose epimerase expressed in developing seeds of the endospermous legume guar. Plant Sci. **142:** 147-154

Johansson H, Sterky F, Amini B, Lundeberg J, Kleczkowski L (2002) Molecular cloning and characterization of a cDNA encoding poplar UDP-glucose dehydrogenase, a key gene of hemicellulose/pectin formation. Biochim. Biophys. Acta. **1576:** 53-58

John K, Schutzbach J, Ankel H (1977) Separation and allosteric properties of two forms of UDP-glucuronate carboxy-lyase. J. Biol. Chem. **252:** 8013-8017

Jones L, Milne J, Ashford D, McQueen-Mason S (2003) Cell wall arabinan is essential for guard cell function. Proc. Natl. Acad. Sci. **100:** 11783-11788

Jones L, Seymour G, Knox J (1997) Localization of pectic galactan in tomato cell walls using a monoclonal antibody specific to (1,4)-β-D-galactan. Plant Physiol. **113:** 1405–1412

Jones P, Messner B, Nakajima J, Schaffner A, Saito K (2003) UGT73C6 and UGT78D1, glycosyltransferases involved in flavonol glycoside biosynthesis in *Arabidopsis thaliana*. J. Biol. Chem. **278:** 43910-43918

Jordan M, Schallhorn A, Wurm F (1996) Transfecting mammalian cells: optimization of critical parameters affecting calcium-phosphate precipitate formation. Nucl. Acids. Res. **24:** 596-601

Kamsteeg J, Van Brederode J, Van Nigtevecht G (1978) The formation of UDP-L-rhamnose from UDP-D-glucose by an enzyme preparation of red campion (*Silene dioica* (L) *clairv*) leaves. FEBS Lett. **91:** 281-284

Kato H, Takeuchi Y, Tsumuraya Y, Hashimoto Y, Nakano H, Kovac P (2003) In vitro biosynthesis of galactans by membrane-bound galactosyltransferase from radish (*Raphanus sativus* L.) seedlings. Planta **217:** 271-282

Kauss H, Hassid W (1967) Biosynthesis of the 4-O-methyl-D-glucuronic acid unit of hemicellulose B by transmethylation from S-adenosyl-L-methionine. J. Biol. Chem. **242:** 1680-1684

Kauss H, Hassid W (1967a) Enzymic introduction of the methyl ester groups of pectin. J. Biol. Chem. **242:** 3449-3453

Kauss H, Swanson A (1969) Cooperation of enzymes responsible for polymerization and methylation in pectin biosynthesis. Z. Naturforsch. **24:** 28-33

Kauss H, Swanson A, Hassid W (1967b) Biosynthesis of the methyl ester groups of pectin by transmethylation from *S*-adenosyl-L-methionine. Biochem. Biophys. Res. Commun. **26:** 234-240

Kawakita M, Ishida N, Miura N, Sun-Wada G, Yoshioka S (1998) Nucleotide sugar transporters: elucidation of their molecular identity and its implication for future studies. J. Biochem. **123:** 777-785

Keegstra K, Raikhel N (2001) Plant glycosyltransferases. Curr. Opin. Plant Biol. **4:** 219-224

Keegstra K, Talmadge K, Bauer W, Albersheim P (1973) The structure of plant cell walls III: A model of the walls of suspension-cultured sycamore cells based on the interconnections of the macromolecular components. Plant Physiol. **51:** 188-196

Kikuchi A, Edashige Y, Ishii T, Satoh S (1996) A xylogalacturonan whose level is dependent on the size of cell clusters is present in the pectin from cultured carrot cells. Planta **200:** 369-372

Kindel P, Watson R (1973) Synthesis, characterization and properties of uridine 5'-α-D-apio-D-furanosylpyrophosphate. Biochem. J. **133:** 227-241

Kiyohara H, Yamada H, Otsuka Y (1987) Unit structure of the anti-complementary arabinogalactan from *Angelica acutiloba* Kitagawa,. Carbohydr. Res. **167:** 221-237

Knox P, Linstead P, King J, Cooper C, Roberts K (1990) Pectin esterification is spatially regulated both within cell walls and between developing tissues of root apices. Planta **181:** 512-521

Kobayashi M, Matoh T, Azuma J (1996) Two chains of rhamnogalacturonan II are cross-linked by borate-diol ester bonds in higher plant cell walls. Plant Physiol. **110:** 1017-1020

Kobayashi M, Nakagawa H, Suda I, Miyagawa I, Matoh T (2002) Purification and cDNA cloning of UDP-D-glucuronate carboxy-lyase (UDP-D-xylose synthase) from pea seedlings. Plant Cell Physiol. **43:** 1259-1265

Kohn R (1975) Ion binding on polyuronates, alginate and pectin. Pure Appl. Chem. **42:** 371-397

Kojima N, Tachida Y, Yoshida Y, Tsuji S (1996) Characterization of mouse ST8Sia II (STX) as a neural cell adhesion molecule-specific polysialic acid synthase. Requirement of core α-1,6-linked fucose and a polypeptide chain for polysialylation. J. Biol. Chem. **271:** 19457-19463

Komalavilas P, Mort A (1989) The acetylation at O-3 of galacturonic acid in the rhamnose-rich portion of pectins. Carbohydr. Res. **189:** 261-272

Konishi T, Mitome T, Hatsushika H, Haque M, Kotake T, Tsumuraya Y (2004) Biosynthesis of pectic galactan by membrane-bound galactosyltransferase from soybean (*Glycine max* Merr.) seedlings. Planta **218:** 833-842

Koplin R, Brisson J, Whitfield C (1997) UDP-galactofuranose precursor required for formation of the lipopolysaccharide O antigen of *Klebsiella pneumoniae* serotype O1 is synthesized by the product of the rfbDKPO1 gene. J. Biol. Chem. **272:** 4121-4128

Kyte J, Doolittle R (1982) A simple method for displaying the hydrophobic character of a protein. J. Mol. Biol. **157:** 105-132

Laemmli U (1970) Cleavage of structural proteins during the assembly of the head of bacteriophage T4. Nature **227:** 680-685

Lake M, Williamson C, Slocurn R (1998) Molecular cloning and characterization of a UDP-glucose-4-epimerase gene (*galE*) and its expression in pea tissues. Plant Physiol. Biochem. **36:** 555-562

Lao N, Long D, Kiang S, Coupland G, Shoue D, Carpita N, Kavanagh T (2003) Mutation of a family 8 glycosyltransferase gene alters cell wall carbohydrate composition and causes a humidity-sensitive semi-sterile dwarf phenotype in *Arabidopsis*. Plant Mol. Biol. **53:** 647-661

Lau J, McNeil M, Darvill A, Albersheim P (1985) Structure of the backbone of rhamnogalacturonan I, a pectic polysaccharides in the primary cell walls of plants. Carbohydr. Res. **137:** 111-125

Lau J, McNeil M, Darvill A, Albersheim P (1987) Treatment of rhamnogalacturonan I with lithium in ethylenediamine. Carbohydr. Res. **168:** 245-274

Le Goff A, Renard C, Bonnin E, Thibault J (2001) Extraction, purification and chemical characterisation of xylogalacturonan from pea hulls. Carbohydr. Polym. **45:** 325–334

Lee C, Wu M, Lee B, Jiang C, Chang H (2003) Changes in molecular weight of transacylated pectin catalyzed by tomato and citrus pectinesterases as determined by gel permeation chromatography. J. Agric. Food Chem. **51:** 5455-5461

Lerouge P, O'Neill M, Darvill A, Albersheim P (1993) Structural characterization of *endo*-glycanase-generated oligoglycosyl side chains of rhamnogalacturonan I. Carbohydr. Res. **243:** 359-371

Li Q, Reeves P (2000) Genetic variation of dTDP-L-rhamnose pathway genes in *Salmonella enterica*. Microbiology **146:** 2291-2307

Liao T, Barber G (1972) Purification of guanosine 5'-diphosphate D-mannose oxidoreductase from *Phaseolus vulgaris*. Biochim. Biophys. Acta. **276:** 85-93

Liljebjelke K, Adolphson R, Baker K, Doong R, Mohnen D (1995) Enzymatic synthesis and purification of uridine diphosphate [^{14}C]galacturonic acid: A substrate for pectin biosynthesis. Anal. Biochem. **225:** 296-304

Lin A, Mu J, Yang J, Roach P (1999) Self-glucosylation of glycogenin, the initiator of glycogen biosynthesis, involves an inter-subunit reaction. Arch. Biochem. Biophys. **363:** 163-170

Lin T, Elbein A, Su J (1966) Substrate specificity in pectin synthesis. Biochem. Biophys. Res. Commun. **22:** 650-657

Liners F, Gaspar T, Van Cutsem P (1994) Acetyl- and methylesterification of pectins of friable and compact sugar-beet calli: Consequences for intercellular adhesion. Planta **192:** 545-556

Loewus F, Kelly S (1963) Inositol metabolism in plants I. Labeling patterns in cell wall polysaccharides from detached plants given *myo*-inositol-2-t or -2-^{14}C. Arch. Biochem. Biophys. **102:** 96-105

Loewus F, Loewus M (1983) *myo*-inositol: Its biosynthesis and metobolism. Ann. Rev. Plant Physiol. **34:** 137-161

Lorence A, Chevone B, Mendes P, Nessler C (2004) *myo*-Inositol oxygenase offers a possible entry point into plant ascorbate biosynthesis. Plant Physiol. **134:** 1200-1205

Lynch M, Staehelin L (1992) Domain-specific and cell type-specific localization of two types of cell wall matrix polysaccharides in the clover root tip. J. Cell Biol. **118:** 467-479

Ma D, Russell D, Beverley S, Turco S (1997) Golgi GDP-mannose uptake requires *Leishmania* LPG2. A member of a eukaryotic family of putative nucleotide-sugar transporters. J. Biol. Chem. **272:** 3799-3805

Majewska-Sawka A, Munster A, Rodriguez-Garcia M (2002) Guard cell wall: Immunocytochemical detection of polysaccharide components. J. Exp. Bot. **53:** 1067-1079

Majewska-Sawka A, Munster A, Wisniewska E (2004) Temporal and spatial distribution of pectin epitopes in differentiating anthers and microspores of fertile and sterile sugar beet. Plant Cell Physiol. **45:** 560-572

Matern U, Grisebach H (1977) UDP-apiose/UDP-xylose synthase. Subunit composition and binding studies. Eur. J. Biochem. **74:** 303-312

Matsunaga T, Ishii T, Matsumoto S, Higuchi M, Darvill A, Albersheim P, O'Neill M (2004) Occurrence of the primary cell wall polysaccharide rhamnogalacturonan II in Pteridophytes, Lycophytes, and Bryophytes. Implications for the evolution of vascular plants. Plant Physiol. **134:** 339-351

Matsuura K, Miyagawa I, Kobayashi M, Ohta D, Matoh T (2003) *Arabidopsis* 3-deoxy-D-*manno*-oct-2-ulosonate-8-phosphate synthase: cDNA cloning and expression analyses. J. Exp. Bot. **54:** 1785-1787

McCann M, Roberts K (1991) Architecture of the primary cell wall. *In* CW Lloyd, ed, The cytoskeletal basis of plant growth and form. Academic Press Ltd., London, pp 109-129

McCartney L, Knox J (2002) Regulation of pectic polysaccharide domains in relation to cell development and cell properties in the pea testa. J. Exp. Bot. **53:** 707-713

McCartney L, Steele-King C, Jordan E, Knox J (2003) Cell wall pectic β-galactan marks the acceleration of cell elongation in the Arabidopsis seedling root meristem. Plant J. **33:** 447-454

McKinney E, Ali N, Traut A, Feldmann K, Belostotsky D, McDowell J, Meagher R (1995) Sequence-based identification of T-DNA insertion mutations in *Arabidopsis* actin mutants *act2-1* and *act4-1*. Plant J. **8:** 613-622

McNab J, Villemez C, Albersheim P (1968) Biosynthesis of galactan by a particulate enzyme preparation from *Phaseolus aureus* seedlings. Biochem. J. **106**

McNeil M, Darvill A, Albersheim P (1980) Structure of plant cell walls: X. Rhamnogalacturonan I. A structurally complex pectic polysaccharide in the walls of suspension-cultured sycamore cells. Plant Physiol. **66:** 1128-1134

McNeil M, Darvill A, Fry S, Albersheim P (1984) Structure and function of the primary cell walls of plants. Annu. Rev. Biochem. **53:** 625-663

Mellerowicz E, Baucher M, Sundberg B, Boerjan W (2001) Unravelling cell wall formation in the woody dicot stem. Plant Mol. Biol. **47:** 239-274

Micheli F (2001) Pectin methylesterases: Cell wall enzymes with important roles in plant physiology. Trends Plant Sci. **6:** 414-419

Mohnen D (1999) Biosynthesis of pectins and galactomannans. *In* D Barton, K Nakanishi, O Meth-Cohn, eds, Comprehensive Natural Products Chemistry, Vol 3. Elsevier Science Ltd., Amsterdam, pp 497-527

Mohnen D (2002) Biosynthesis of pectins. *In* GB Seymour, JP Knox, eds, Pectins and their Manipulation. Blackwell Publishing and CRC Press, Oxford, pp 52-98

Mohnen D, Doong R, Liljebjelke K, Fralish G, Chan J (1996) Cell free synthesis of the pectic polysaccharide homogalacturonan. *In* J Visser, AGJ Voragen, eds, Pectins and Pectinases. Elsevier Science B. V., Amsterdam, pp 109-126

Mohnen D, Hahn M (1993) Cell wall carbohydrates as signals in plants. Semin. Cell Biol. **4:** 93-102

Molhoj M, Verma R, Reiter W (2003) The biosynthesis of the branched-chain sugar D-apiose in plants: Functional cloning and characterization of a UDP-D-apiose/UDP-D-xylose synthase from *Arabidopsis*. Plant J. **35:** 693-703

Molhoj M, Verma R, Reiter W (2004) The biosynthesis of D-galacturonate in plants. Functional cloning and characterization of a membrane-anchored UDP-D-glucuronate 4-epimerase from *Arabidopsis*. Plant Physiol.**:** pp.104.043745

Mollet J, Park S, Nothnagel E, Lord E (2000) A lily stylar pectin is necessary for pollen tube adhesion to an *in vitro* stylar matrix. Plant Cell **12:** 1737-1750

Morre D, Brightman A, Sandelius A (1987) Membrane fractions from plant cells. *In* J Findlay, W Evans, eds, Biological Membranes. IRL Press, Oxford, pp 37-72

Mort A, Moerschbacher B, Pierce M, Maness N (1991) Problems encountered during the extraction, purification, and chromatography of pectic fragments, and some solutions to them. Carbohydr. Res. **215:** 219-227

Mort A, Qui F, Maness N (1993) Determination of the pattern of methy esterification in pectin. Distribution of contiguous nonesterified residues. Carbohydr. Res. **247:** 21-35

Munoz P, Norambuena L, Orellana A (1996) Evidence for a UDP-glucose transporter in Golgi apparatus-derived vesicles from pea and its possible role in polysaccharide biosynthesis. Plant Physiol. **112:** 1585-1594

Munoz R, Lopez R, de Frutos M, Garcia E (1999) First molecular characterization of a uridine diphosphate galacturonate 4-epimerase: An enzyme required for capsular biosynthesis in *Streptococcus pneumoniae* type 1. Mol. Microbiol. **31:** 703-713

Munro S (1995) An investigation of the role of transmembrane domains in Golgi protein retention. EMBO J. **14:** 4695-4704

Nakamura A, Furuta H, Maeda H, Nagamatsu Y, Yoshimoto A (2001) Analysis of structural components and molecular construction of soybean soluble polysaccharides by stepwise enzymatic degradation. Biosci. Biotechnol. Biochem. **65:** 2249-2258

Nakamura A, Furuta H, Maeda H, Takao T, Nagamatsu Y (2002) Analysis of the molecular construction of xylogalacturonan isolated from soluble soybean polysaccharides. Biosci. Biotechnol. Biochem. **66:** 1155-1158

Nakamura A, Furuta H, Maeda H, Takao T, Nagamatsu Y (2002a) Structural studies by stepwise enzymatic degradation of the main backbone of soybean soluble polysaccharides consisting of galacturonan and rhamnogalacturonan. Biosci. Biotechnol. Biochem. **66:** 1301-1313

Neckelmann G, Orellana A (1998) Metabolism of uridine 5'-diphosphate-glucose in Golgi vesicles from pea stems. Plant Physiol. **117:** 1007-1014

Needs P, Rigby N, Colquhoun I, Ring S (1998) Conflicting evidence for non-methyl galacturonoyl esters in *Daucus carota*. Phytochemistry **48:** 71-77

Nelsestuen G, Kirkwood S (1971) The mechanism of action of uridine diphosphoglucose dehydrogenase. Uridine diphosphohexodialdoses as intermediates. J. Biol. Chem. **246:** 3828-3834

Neufeld E, Feingold D, Hassid W (1958) Enzymatic conversion of uridine diphosphate D-glucuronic acid to uridine diphosphate galacturonic acid, uridine diphosphate xylose, and uridine diphosphate arabinose. J. Am. Chem. Soc. **80:** 4430-4431

Neufeld E, Feingold D, Ilves S, Kessler G, Hassid W (1961) Phosphorylation of D-galacturonic acid by extracts from germinating seeds of *Phaseolus aureus*. J. Biol. Chem. **236:** 3102-3105

Norambuena L, Marchant L, Berninsone P, Hirschberg C, Silva H, Orellana A (2002) Transport of UDP-galactose in plants. Identification and functional characterization of AtUTr1, an *Arabidopsis thaliana* UDP-galactose/UDP-glucose transporter. J. Biol. Chem. **277:** 32923-32929

Northcote D, Pickett-Heaps J (1966) A function of the Golgi apparatus in polysaccharide synthesis and transport in the root-cap cells of wheat. Biochem. J. **98:** 159-167

Nothnagel E, McNeil M, Albersheim P, Dell A (1983) Host-pathogen interactions XXII: A galacturonic acid oligosaccharide from plant cell walls elicits phytoalexins. Plant Physiol. **71:** 916-926

Nunan K, Scheller H (2003) Solubilization of an arabinan arabinosyltransferase activity from mung bean hypocotyls. Plant Physiol. **132:** 331-342

Odzuck W, Kauss H (1972) Biosynthesis of pure arabinan and xylan. Phytochemistry **11:** 2489-2494

O'Neill M, Albersheim P, Darvill A (1990) The pectic polysaccharides of primary cell walls. *In* PM Dey, ed, Methods Biochem., Vol 2. Academic Press, London, pp 415-441

O'Neill M, Eberhard S, Albersheim P, Darvill A (2001) Requirement of borate cross-linking of cell wall rhamnogalacturonan II for *Arabidopsis* growth. Science **294:** 846-849

O'Neill M, Ishii T, Albersheim P, Darvill A (2004) Rhamnogalacturonan II: Structure and function of a borate cross-linked cell wall pectic polysaccharide. Ann. Rev. Plant Biol. **55:** 109-139

O'Neill M, Warrenfeltz D, Kates K, Pellerin P, Doco T, Darvill A, Albersheim P (1996) Rhamnogalacturonan-II, a pectic polysaccharide in the walls of growing plant cell, forms a dimer that is covalently cross-linked by a borate ester. *In vitro* conditions for the formation and hydrolysis of the dimer. J. Biol. Chem. **271:** 22923-22930

O'Neill M, Warrenfeltz D, Kates K, Pellerin P, Doco T, Darvill A, Albersheim P (1997) Additions and corrections to rhamnogalacturonan-II, a pectic polysaccharide in the walls

of growing plant cell, forms a dimer that is covalently cross-linked by a borate ester. *In vitro* conditions for the formation and hydrolysis of the dimer. J. Biol. Chem. **272:** 3869-

Oomen R, Doeswijk-Voragen C, Bush M, Vincken J, Borkhardt B, van den Broek L, Corsar J, Ulvskov P, Voragen A, McCann M, Visser R (2002) *In muro* fragmentation of the rhamnogalacturonan I backbone in potato (*Solanum tuberosum* L.) results in a reduction and altered location of the galactan and arabinan side-chains and abnormal periderm development. Plant J **30:** 403-413

Opat A, Houghton F, Gleeson P (2000) Medial Golgi but not late Golgi glycosyltransferases exist as high molecular weight complexes. Role of the luminal domain in complex formation and localization. J. Biol. Chem. **275:** 11836-11845

Orellana A, Neckelmann G, Norambuena L (1997) Topography and function of Golgi uridine-5'-diphosphatase from pea stems. Plant Physiol. **114:** 99-107

Orfila C, Knox J (2000) Spatial regulation of pectic polysaccharides in relation to pit fields in cell walls of tomato fruit pericarp. Plant Physiol. **122:** 775-782

Orfila C, Seymour G, Willats W, Huxham I, Jarvis M, Dover C, Thompson A, Knox J (2001) Altered middle lamella homogalacturonan and disrupted deposition of (1,5)-α-L-arabinan in the pericarp of *cnr*, a ripening mutant of tomato. Plant Physiol. **126:** 210-221

Oxenboll Sorensen S, Pauly M, Bush M, Skjot M, McCann M, Borkhardt B, Ulvskov P (2000) Pectin engineering: Modification of potato pectin by *in vivo* expression of an *endo*-(1,4)-β -D-galactanase. Proc. Natl. Acad. Sci. **97:** 7639-7644

Pan Y, Kindel P (1977) Characterization of particulate D-apiosyl- and D-xylosyltransferase from *Lemna minor*. Arch. Biochem. Biophys. **183:** 131-138

Paulson J, Colley K (1989) Glycosyltransferases. Structure, localization, and control of cell type-specific glycosylation. J. Biol. Chem. **264:** 17615-17618

Pauly M, Scheller H (2000) *O*-Acetylation of plant cell wall polysaccharides: Identification and partial characterization of a rhamnogalacturonan *O*-acetyl-transferase from potato suspension-cultured cells. Planta **210:** 659-667

Pellerin P, Doco T, Vida S, Williams P, Brillouet J, O'Neill M (1996) Structural characterization of red wine rhamnogalacturonan II. Carbohydr. Res. **290:** 183-197

Perrin R, Wilkerson C, Keegstra K (2001) Golgi enzymes that synthesize plant cell wall polysaccharides: finding and evaluating candidates in the genomic era. Plant Mol. Biol. **47:** 115-130

Peugnet I, Goubet F, Bruyant-Vannier M, Thoiron B, Morvan C, Schols H, Voragen A (2001) Solubilization of rhamnogalacturonan I galactosyltransferases from membranes of a flax cell suspension. Planta **213:** 435-445

Popper Z, Sadler I, Fry S (2003) α-D-glucuronosyl-(1,3)-L-galactose, an unusual disaccharide from polysaccharides of the hornwort *Anthoceros caucasicus*. Phytochemistry **64:** 325-335

Puvanesarajah V, Darvill A, Albersheim P (1991) Structural characterization of two oligosaccharide fragments formed by the selective cleavage of rhamnogalacturonan II: Evidence for the anomeric configuration and attachment sites of apiose and 3-deoxy-2-heptulosaric acid. Carbohydr. Res. **218:** 211-222

Ray P (1967) Radioautographic study of cell wall deposition in growing plant cells. J. Cell Biol. **35:** 659-674

Redgwell R, Hansen C (2000) Isolation and characterization of cell wall polysaccharides from cocoa (*Theobroma cacao* L.) beans. Planta **210:** 823-830

Reiter W, Chapple C, Somerville C (1993) Altered growth and cell walls in a fucose-deficient mutant of *Arabidopsis*. Science **261:** 1032-1035

Reiter W, Chapple C, Somerville C (1997) Mutants of *Arabidopsis thaliana* with altered cell wall polysaccharide composition. Plant J. **12:** 335-345

Reiter W, Vanzin G (2001) Molecular genetics of nucleotide sugar interconversion pathways in plants. Plant Mol. Biol. **47:** 95-113

Renard C, Crepeau M, Thibault J (1999) Glucuronic acid directly linked to galacturonic acid in the rhamnogalacturonan backbone of beet pectins. Eur. J. Biochem. **266:** 566-574

Renard C, Jarvis M (1999a) Acetylation and methylation of homogalacturonans I: Optimisation of the reaction and characterisation of the products. Carbohydr. Polymers **39:** 201-207

Reuhs B, Glenn J, Stephens S, Kim J, Christie D, Glushka J, Zablackis E, Albersheim P, Darvill A, O'Neill M (2004) L-galactose replaces L-fucose in the pectic polysaccharide rhamnogalacturonan II synthesized by the L-fucose-deficient *mur1 Arabidopsis* mutant. Planta **219:** 147-157

Rhee S, Somerville C (1998) Tetrad pollen formation in *quartet* mutants of *Arabidopsis thaliana* is associated with persistence of pectic polysaccharides of the pollen mother cell wall. Plant J. **15:** 79-88

Ridley B, O'Neill M, Mohnen D (2001) Pectins: structure, biosynthesis, and oligogalacturonide-related signaling. Phytochemistry **57:** 929-967

Roberts J, Elliott K, Gonzalez-Carranza Z (2002) Abscission, dehiscence, and other cell separation processes. Ann. Rev. Plant Biol. **53:** 131-158

Roberts R (1971) The formation of uridine diphosphate-glucuronic acid in plants. Uridine diphosphate-glucuronic acid pyrophosphorylase from barley seedlings. J. Biol. Chem. **246:** 4995-5002

Robertson D, Smith C, Bolwell G (1996) Inducible UDP-glucose dehydrogenase from French bean (*Phaseolus vulgaris* L.) locates to vascular tissue and has alcohol dehydrogenase activity. Biochem. J. **313:** 311-317

Rodgers M, Bolwell G (1992) Partial purification of Golgi-bound arabinosyltransferase and two isoforms of xylosyltransferase from French bean (*Phaseolus vulgaris* L.). Biochem. J. **288:** 817-822

Rodriguez-Carvajal M, Herve du Penhoat C, Mazeau K, Doco T, Perez S (2003) The three-dimensional structure of the mega-oligosaccharide rhamnogalacturonan II monomer: A combined molecular modeling and NMR investigation. Carbohydr. Res. **338:** 651-671

Ros J, Schols H, Voragen A (1998) Lemon albedo cell walls contain distinct populations of pectic hairy regions. Carbohydr. Polym. **37:** 159-166

Rose J, Hadfield K, Labavitch J, Bennett A (1998) Temporal sequence of cell wall disassembly in rapidly ripening melon fruit. Plant Physiol. **117:** 345-361

Royo J, Gomez E, Hueros G (2000) A maize homologue of the bacterial CMP-3-deoxy-D-*manno*-2-octulosonate (KDO) synthetases. Similar pathways operate in plants and

bacteria for the activation of KDO prior to its incorporation into outer cellular envelopes. J. Biol. Chem. **275:** 24993-24999

Royo J, Gomez E, Hueros G (2000a) CMP-KDO synthetase, a plant gene borrowed from Gram-negative eubacteria. Trends Genet. **16:** 432-433

Ryden P, Sugimoto-Shirasu K, Smith A, Findlay K, Reiter W, McCann M (2003) Tensile properties of Arabidopsis cell walls depend on both a xyloglucan cross-linked microfibrillar network and rhamnogalacturonan II-borate complexes. Plant Physiol. **132:** 1033-1040

Salisbury F, Ross C (1992) The photosynthesis-transpiration compromise. *In* JC Carey, ed, Plant physiology. Wadsworth, Inc., Belmont, pp 66-92

Sandermann HJ, Tisue G, Grisebach H (1968) Biosynthesis of D-apiose IV. Formation of UDP-apiose from UDP-D-glucuronic acid in cell free extracts of parsley (*Apium petroselinum* L.) and *Lemna minor*. Biochim. Biophys. Acta. **165:** 550-552

Saugy M, Farkas V, Maclachlan G (1988) Phosphatases and phosphodiesterases interfere with (1,3)-β-D-glucan synthase activity in pea epicotyl membrane preparations. Eur. J. Biochem. **177:** 135-138

Saxena I, Brown R, Jr, Fevre M, Geremia R, Henrissat B (1995) Multidomain architecture of β-glycosyl transferases: implications for mechanism of action. J. Bacteriol. **177:** 1419-1424

Scheller H, Doong R, Ridley B, Mohnen D (1999) Pectin biosynthesis: A solubilized α-(1,4)-galacturonosyltransferase from tobacco catalyzes the transfer of galacturonic acid from UDP-galacturonic acid onto the non-reducing end of homogalacturonan. Planta **207:** 512-517

Schiefelbein J, Somerville C (1990) Genetic control of root hair development in *Arabidopsis thaliana*. Plant Cell **2:** 235-243

Schols H, Bakx E, Schipper D, Voragen A (1995) A xylogalacturonan subunit present in the modified hairy regions of apple pectin. Carbohydr. Res. **279:** 265-279

Schols H, Geraeds C, Searle-van Leeuwen M, Kormelink F, Voragen A (1990) Rhamnogalacturonase: A novel enzyme that degrades the hairy regions of pectins. Carbohydr. Res. **206:** 105-115

Schols H, Vierhuis E, Bakx E, Voragen A (1995a) Different populations of pectic hairy regions occur in apple cell walls. Carbohydr. Res. **275:** 343-360

Schols H, Voragen A (1994) Occurrence of pectic hairy regions in various plant cell wall materials and their degradability by rhamnogalacturonase. Carbohydr. Res. **256:** 83-95

Schutzbach J, Feingold D (1970) Biosynthesis of uridine diphosphate D-xylose IV. Mechanism of action of uridine diphosphoglucuronate carboxy-lyase. J. Biol. Chem. **245:** 2476-2482

Segawa H, Kawakita M, Ishida N (2002) Human and *Drosophila* UDP-galactose transporters transport UDP-N -acetylgalactosamine in addition to UDP-galactose. Eur. J. Biochem. **269:** 128-138

Seifert G (2004) Nucleotide sugar interconversions and cell wall biosynthesis: How to bring the inside to the outside. Curr. Opin. Plant Biol. **7:** 277-284

Seifert G, Barber C, Wells B, Dolan L, Roberts K (2002) Galactose biosynthesis in *Arabidopsis*: Genetic evidence for substrate channeling from UDP-D-galactose into cell wall polymers. Curr. Biol. **12:** 1840-1845

Seifert G, Barber C, Wells B, Roberts K (2004a) Growth regulators and the control of nucleotide sugar flux. Plant Cell **16:** 723-730

Seitz B, Klos C, Wurm M, Tenhaken R (2000) Matrix polysaccharide precursors in *Arabidopsis* cell walls are synthesized by alternate pathways with organ-specific expression patterns. Plant J. **21:** 537-546

Skjot M, Pauly M, Bush M, Borkhardt B, McCann M, Ulvskov P (2002) Direct interference with rhamnogalacturonan I biosynthesis in Golgi vesicles. Plant Physiol. **129:** 95-102

Smirnoff N, Conklin P, Loewus F (2001) Biosynthesis of ascorbic acid in plants: A Renaissance. Ann. Rev. Plant Physiol. Plant Mol. Biol. **52:** 437-467

Spellman M, McNeil M, Darvill A, Albersheim P, Dell A (1983) Characterization of a structurally complex heptasaccharide isolated from the pectic polysaccharide rhamnogalacturonan II. Carbohydr. Res. **122:** 131-153

Spellman M, McNeil M, Darvill A, Albersheim P, Henrick K (1983a) Isolation and characterization of 3-C-carboxy-5-deoxy-L-xylose, a naturally occurring, branched-chain, acidic monosaccharide. Carbohydr. Res. **122:** 115-129

Spiro M, Kates K, Koller A, O'Neill M, Albersheim P, Darvill A (1993) Purification and characterization of biologically active (1,4)-linked-α-oligogalacturonides after partial digestion of polygalacturonic acid with *endo*polygalacturonase. Carbohydr. Res. **247:** 9-20

Sprong H, Degroote S, Nilsson T, Kawakita M, Ishida N, van der Sluijs P, van Meer G (2003) Association of the Golgi UDP-galactose transporter with UDP-galactose:ceramide galactosyltransferase allows UDP-galactose import in the endoplasmic reticulum. Mol. Biol. Cell **14:** 3482-3493

Staehelin LA, Moore I (1995) The plant Golgi apparatus: Structure, functional organization and trafficking mechanisms. Ann. Rev. Plant Physiol. Plant Mol. Biol. **46:** 261-288

Stephenson M, Hawes M (1994) Correlation of pectin methylesterase activity in root caps of pea with root border cell separation. Plant Physiol. **106:** 739-745

Sterling J, Quigley H, Orellana A, Mohnen D (2001) The catalytic site of the pectin biosynthetic enzyme α-(1,4)-galacturonosyltransferase is located in the lumen of the Golgi. Plant Physiol. **127:** 360-371

Stevenson G, Neal B, Liu D, Hobbs M, Packer N, Batley M, Redmond J, Lindquist L, Reeves P (1994) Structure of the O antigen of *Escherichia coli* K-12 and the sequence of its *rfb* gene cluster. J. Bacteriol. **176:** 4144-4156

Stevenson T, Darvill A, Albersheim P (1988) 3-deoxy-D-lyxo-2-heptulosaric acid, a component of the plant cell-wall polysaccharide rhamnogalacturonan-II. Carbohydr. Res. **179:** 269-288

Stewart D, Copeland L (1998) Uridine 5'-diphosphate-glucose dehydrogenase from soybean nodules. Plant Physiol. **116:** 349-355

Stewart D, Copeland L (1999) Kinetic properties of UDP-glucose dehydrogenase from soybean nodules. Plant Sci. **147:** 119-125

Strominger J, Mapson L (1957) Uridine diphosphoglucose dehydrogenase of pea seedlings. Biochem. J. **66:** 567-572

Swamy N, Salimath P (1991) Arabinans from *Cajanus cajan* cotyledon. Phytochemistry **30:** 263-265

Swofford D (1998) PAUP. Phylogenetic analysis using parsimony and other methods. Sinauer Asso., Sunderland, MA

Takeuchi Y, Tsumuraya Y (2001) In vitro biosynthesis of homogalacturonan by a membrane-bound galacturonosyltransferase from epicotyls of azuki bean. Biosci. Biotechnol. Biochem. **65:** 1519-1527

Tanford C, Reynolds J (1976) Characterization of membrane proteins in detergent solutions. Biochim. Biophys. Acta. **457:** 133-170

Tavares R, Aubourg S, Lecharny A, Kreis M (2000) Organization and structural evolution of four multigene families in *Arabidopsis thaliana*: AtLCAD, AtLGT, AtMYST and AtHD-GL2. Plant Mol. Biol. **42:** 703-717

Tenhaken R, Thulke O (1996) Cloning of an enzyme that synthesizes a key nucleotide-sugar precursor of hemicellulose biosynthesis from soybean: UDP-glucose dehydrogenase. Plant Physiol. **112:** 1127-1134

Thakur B, Singh R, Handa A (1997) Chemistry and uses of pectin - a review. Crit. Rev. Food Sci. Nutr. **37:** 47-73

Thomas J, Darvill A, Albersheim P (1989) Isolation and structural characterization of the pectic polysaccharide rhamnogalacturonan II from walls of suspension-cultured rice cells. Carbohydr. Res. **185:** 261-277

Thompson J, Fry S (2000) Evidence for covalent linkage between xyloglucan and acidic pectins in suspension-cultured rose cells. Planta **211:** 275-286

Tibbits C, MacDougall A, Ring S (1998) Calcium binding and swelling behaviour of a high methoxyl pectin gel. Carbohydr. Res. **310:** 101-107

Tsuji S (1996) Molecular cloning and functional analysis of sialyltransferases. J. Biochem. **120:** 1-13

Turner W, Botha F (2002) Purification and kinetic properties of UDP-glucose dehydrogenase from sugarcane. Arch. Biochem. Biophys. **407:** 209-216

Usadel B, Kuschinsky A, Rosso M, Eckermann N, Pauly M (2004) RHM2 is involved in mucilage pectin synthesis and is required for the development of the seed coat in *Arabidopsis*. Plant Physiol. **134:** 286-295

Vandersall-Nairn A, Merkle R, O'Brien K, Oeltmann T, Moremen K (1998) Cloning, expression, purification, and characterization of the acid α-mannosidase from *Trypanosoma cruzi*. Glycobiology **8:** 1183-1194

Vannier M, Thoiron B, Morvan C, Demarty M (1992) Localization of methyltransferase activities throughout the endomembrane complex system of flaz (*Linum usitatissimum* L) hypocotyls. Biochem. J. **286:** 863-868

Vicre M, Jauneau A, Knox J, Driouich A (1998) Immunolocalization of β-(1,4) and β-(1,6)-D-galactan epitopes in the cell wall and Golgi stacks of developing flax root tissues. Protoplasma **203:** 26-34

Vidal S, Doco T, Williams P, Pellerin P, York W, O'Neill M, Glushka J, Darvill A, Albersheim P (2000) Structural characterization of the pectic polysaccharide rhamnogalacturonan II: Evidence for the backbone location of the aceric acid-containing oligoglycosyl side chain. Carbohydr. Res. **326:** 277-294

Villemez C, Lin T, Hassid W (1965) Biosynthesis of the polygalacturonic acid chain of pectin by a particulate enzyme preparation from *Phaseolus aureus* seedlings. Proc. Natl. Acad. Sci. **54:** 1626-1632

Villemez C, Swanson A, Hassid W (1966) Properties of a polygalacturonic acid-synthesizing enzyme system from *Phaseolus aureus* seedlings. Arch. Biochem. Biophys. **116:** 446-452

Vincken J, Schols H, Oomen R, McCann M, Ulvskov P, Voragen A, Visser R (2003) If homogalacturonan were a side chain of rhamnogalacturonan I. Implications for cell wall architecture. Plant Physiol. **132:** 1781-1789

Watson R, Orenstein N (1975) Chemistry and biochemistry of apiose. Adv. Carbohydr. Chem. Biochem. **31:** 135-184

Watt G, Leoff C, Harper A, Bar-Peled M (2004) A bifunctional 3,5-epimerase/4-keto reductase for nucleotide-rhamnose synthesis in *Arabidopsis*. Plant Physiol. **134:** 1337-1346

Weigel P, Hascal V, Tammi M (1997) Hyaluronan synthases. J. Biol. Chem. **272:** 13997-14000

Wellmann E, Grisebach H (1971) Purification and properties of an enzyme preparation from *Lemna minor* L. catalyzing the synthesis of UDP-apiose and UDP-D-xylose from UDP-glucuronic acid. Biochim. Biophys. Acta. **235:** 389-397

Western T, Burn J, Tan W, Skinner D, Martin-McCaffrey L, Moffatt B, Haughn G (2001) Isolation and characterization of mutants defective in seed coat mucilage secretory cell development in *Arabidopsis*. Plant Physiol. **127:** 998-1011

Western T, Young D, Dean G, Tan W, Samuels A, Haughn G (2004) MUCILAGE-MODIFIED4 encodes a putative pectin biosynthetic enzyme developmentally regulated by APETALA2, TRANSPARENT TESTA GLABRA1, and GLABRA2 in the *Arabidopsis* seed coat. Plant Physiol. **134:** 296-306

Wheeler G, Jones M, Smirnoff N (1998) The biosynthesis pathways of vitamin C in higher plants. Nature **393:** 365-369

Whitcombe A, O'Neill M, Steffan W, Albersheim P, Darvill A (1995) Structural characterization of the pectic polysaccharide, rhamnogalacturonan-II. Carbohydr. Res. **271:** 15-29

Wiggins C, Munro S (1998) Activity of the yeast MNN1 α-(1,3)-mannosyltransferase requires a motif conserved in many other families of glycosyltransferases. Proc. Natl. Acad. Sci. **95:** 7945-7950

Willats W, Gilmartin P, Mikkelsen J, Knox J (1999) Cell wall antibodies without immunization: Generation and use of de-esterified homogalacturonan block-specific antibodies from a naive phage display library. Plant J. **18:** 57-65

Willats W, Knox J (1999a) Immunoprofiling of pectic polysaccharides. Anal. Biochem. **268:** 143-146

Willats W, Limberg G, Bucholt H, van Alebeek G, Benen J, Christensen T (2000) Analysis of pectic epitopes recognised by hybridoma and phage display monoclonal antibodies using defined oligosaccharides, polysaccharides and enzymatic degradation. Carbohydr. Res. **327:** 309-320

Willats W, Marcus S, Knox J (1998) Generation of a monoclonal antibody specific to (1,5)-α-L-arabinan. Carbohydr. Res. **308:** 149-152

Willats W, McCartney L, Mackie W, Knox J (2001) Pectin: Cell biology and prospects for functional analysis. Plant Mol. Biol. **47:** 9-27

Willats W, McCartney L, Steele-King C, Marcus S, Mort A, Huisman M, van Alebeek G, Schols H, Voragen A, Le Goff A, Bonnin E, Thibault J, Knox J (2004) A xylogalacturonan epitope is specifically associated with plant cell detachment. Planta **218:** 673-681

Willats W, Orfila C, Limberg G, Buchholt H, van Alebeek G, Voragen A, Marcus S, Christensen T, Mikkelsen J, Murray B, Knox J (2001a) Modulation of the degree and pattern of methyl-esterification of pectic homogalacturonan in plant cell walls. Implications for pectin methyl esterase action, matrix properties, and cell adhesion. J. Biol. Chem. **276:** 19404-19413

Willats W, Steele-King C, Marcus S, Knox J (1999b) Side chains of pectic polysaccharides are regulated in relation to cell proliferation and cell differentiation. Plant J. **20:** 619-628

Williams M, Freshour G, Darvill A, Albersheim P, Hahn M (1996) An antibody Fab selected from a recombinant phage display library detects deesterified pectic polysaccharide rhamnogalacturonan II in plant cells. Plant Cell **8:** 673-685

Wlasichuk K, Kashem M, Nikrad P, Bird P, Jiang C, Venot A (1993) Determination of the specificities of rat liver Gal(β1,4)GlcNAc alpha 2,6-sialyltransferase and Gal(β1,3/4)GlcNAc α-2,3- sialyltransferase using synthetic modified acceptors. J. Biol. Chem. **268:** 13971-13977

Wolucka B, Persiau G, Van Doorsselaere J, Davey M, Demol H, Vandekerckhove J, Van Montagu M, Zabeau M, Boerjan W (2001) Partial purification and identification of GDP-mannose 3',5'-epimerase of *Arabidopsis thaliana*, a key enzyme of the plant vitamin C pathway. Proc. Natl. Acad. Sci. **98:** 14843-14848

Wolucka B, Van Montagu M (2003) GDP-mannose 3',5'-epimerase forms GDP-L-gulose, a putative intermediate for the *de novo* biosynthesis of vitamin C in plants. J. Biol. Chem. **278:** 47483-47490

Wu J, Woodard R (2003) *Escherichia coli* YrbI Is 3-deoxy-D-*manno*-2-octulosonate 8-phosphate phosphatase. J. Biol. Chem. **278:** 18117-18123

Wulff C, Norambuena L, Orellana A (2000) GDP-fucose uptake in the Golgi apparatus during xyloglucan biosynthesis requires the activity of a transporter-like protein other than the UDP-glucose transporter. Plant Physiol. **122:** 867-878

Yamada K, Lim J, Dale J, Chen H, Shinn P, Palm C, Southwick A, Wu H, Kim C, Nguyen M, Pham P, Cheuk R, Karlin-Newmann G, Liu S, Lam B, Sakano H, Wu T, Yu G, Miranda M, Quach H, Tripp M, Chang C, Lee J, Toriumi M, Chan M, Tang C, Onodera C, Deng J, Akiyama K, Ansari Y, Arakawa T, Banh J, Banno F, Bowser L, Brooks S, Carninci P, Chao Q, Choy N, Enju A, Goldsmith A, Gurjal M, Hansen N, Hayashizaki Y, Johnson-Hopson C, Hsuan V, Iida K, Karnes M, Khan S, Koesema E, Ishida J, Jiang P, Jones T, Kawai J, Kamiya A, Meyers C, Nakajima M, Narusaka M, Seki M, Sakurai T, Satou M, Tamse R, Vaysberg M, Wallender E, Wong C, Yamamura Y, Yuan S, Shinozaki K, Davis R, Theologis A, Ecker J (2003) Empiral analysis of transcriptional activity in the *Arabidopsis* genome. Science **302:** 842-846

York W, Darvill A, McNeil M, Albersheim P (1985) 3-deoxy-D-*manno*-2-octulosonic acid (Kdo) is a component of rhamnogalacturonan II, a pectic polysaccharides in the primary cell walls of plants. Carbohydr. Res. **138:** 109-126

York W, Darvill A, McNeil M, Stevenson T, Albersheim P (1986) Isolation and characterization of plant cell walls and cell wall components. Methods Enzymol. **118:** 3-40

Yu L, Mort A (1996) Partial characterization of xylogalacturonans from cell walls of ripe watermelon fruit: Inhibition of *endo*polygalacturonase activity by xylosylation. *In* J Visser, AGJ Voragen, eds, Pectins and pectinases. Elsevier, Amsterdam, pp 79-88

Zablackis E, Huang J, Muller B, Darvill A, Albersheim P (1995) Characterization of the cell-wall polysaccharides of Arabidopsis thaliana leaves. Plant Physiol. **107:** 1129-1138

Zablackis E, York W, Pauly M, Hantus S, Reiter W, Chapple C, Albersheim P, Darvill A (1996) Substitution of L-fucose by L-galactose in cell walls of *Arabidopsis mur1*. Science **272:** 1808-1810

Zar J (1999) Two-sample hypothesis. *In* T Ryu, ed, Biostatistical analysis, Ed Fourth. Simon and Schuster, New Jersey, pp 122-158

Zhang G, Staehelin L (1992) Functional compartmentation of the Golgi apparatus of plant cells: Immunocytochemical analysis of high-pressure frozen- and freeze-substituted sycamore maple suspension culture cells. Plant Physiol. **99:** 1070-1083

Zhang Q, Liu H (2001) Chemical synthesis of UDP-β-L-arabinofuranose and its turnorver to UDP-β-L-arabinopyranose by UDP-galactopyranose mutase. Bioorg. Med. Chem. Lett. **11:** 145-149